01 Jul 1969

Cold-rolled austenitic stainless steel: materials properties and structural performance

George Winter

S. T. Wang

S.T. Wang George Winter
COLD-ROLLED AUSTENITIC STAINLESS STEEL: MATERIALS PROPERTIES AND STRUCTURAL PERFORMANCE

CCFSS LIBRARY
22 1 * 440
c1

S.T. Wang George Winter
COLD-ROLLED AUSTENITIC STAINLESS STEEL: MATERIALS PROPERTIES AND STRUCTURAL PERFORMANCE

DATE	ISSUED TO

Department of Structural Engineering
School of Civil Engineering
Cornell University

Report No. 334

COLD-ROLLED AUSTENITIC STAINLESS STEEL: MATERIALS PROPERTIES AND STRUCTURAL PERFORMANCE

by
S. T. Wang
Research Associate

George Winter
Project Director

A research project sponsored by the
American Iron and Steel Institute

Ithaca, New York July 1969

PREFACE

This report is a slight modification of a thesis presented to the Faculty of the Graduate School of Cornell University for the degree of Doctor of Philosophy. It constitutes a record of most of the investigation done at Cornell University on materials behavior and structural performance of cold-rolled austenitic stainless steel members. This research project was sponsored by the American Iron and Steel Institute. The only work not included in this report is the investigation on bolted and on welded connections in cold-rolled stainless steel by B. M. Tang and D. W. Popowich, which is reported separately.

The author wishes to thank Professor George Winter for his careful guidance in his joint capacity as the project director and the chairman of the author's special committee, and Messrs. W. G. Kirkland, Vice-President, American Iron and Steel Institute and D. S. Wolford, C. R. Clauer, J. B. Scalzi and R. H. Kaltenhauser of the Institute's Research and Specification Committee for their unfailing cooperation on behalf of the sponsoring organization. He also wishes to acknowledge his indebtedness to Dr. A. L. Johnson whose earlier investigation on annealed austenitic stainless steel (Report No. 327 of November 1966) prepared the ground for much of the present work, and to Prof. S. J. Errera for helpful cooperation.

TABLE OF CONTENTS

ABSTRACT

The cold reduction in thickness of austenitic stainless steel sheet brings about the following significant characteristics of material properties: 1) higher strength with an increasing amount of cold working, 2) more pronounced anisotropic material properties with increasing cold working, 3) stress strain relations different in tension and compression and depending on directions, and 4) nonlinear stress strain curves with relatively low elastic limits, especially in longitudinal compression. In addition, local buckling is encountered in thin walled structural members. These are the problems associated with the structural design of stainless steel members.

The purpose of this investigation is to develop the basic necessary information for design methods for light gage cold formed structural elements and members made of cold rolled austenitic stainless steel.

A detailed investigation of material properties of cold worked stainless steel is made. A statistical approach is introduced to study the variation of yield strength due to cold working so that lower bound values may be established. An affinity approach is introduced to obtain the shear properties from normal stress behavior. Design mechanical properties for tempered Type 301 are obtained.

In order to predict the member behavior, a study of element behavior is essential. The buckling and post buckling

behavior of stiffened and unstiffened elements as a part of the structural member is investigated. The nonlinear and anisotropic material properties are considered in the approximate analyses. Bleich's two-modulus concept of inelastic buckling and Von Karman's effective width concept of post buckling strength were used for predicting the element behavior.

Based on the element behavior, the response of structural members may be predicted in the post buckling domain. A numerical analysis of the inelastic flexural behavior of thin-walled cold formed members with considerations of the unique material properties is made by using a digital computer. The extensive treatment of flexural members is necessary because of its vital importance in light gage steel applications. Simplified methods are also recommended for design purposes. The theoretical predictions agree quite satisfactorily with experimental results.

Design procedures with considerations of strength, local distortion, and deflection are recommended for structural elements and members.

CHAPTER I

INTRODUCTION

1.1 General

The structural behavior of light gage steel members has long been a major topic of investigation. Most of such members are cold formed, in rolls or brakes, from sheet or strip steel. Such members are extensively used alone or in conjunction with hot rolled sections as structural load carrying members, panels and decks. The major reasons for using such members are economy, flexibility of shape, and available useful space considerations. An extensive investigation of the behavior of thin walled cold formed carbon steel members has been made at Cornell University. This is summarized in the American Iron and Steel Institute's Light Gage Cold Formed Steel Design Manual[1-1*] and its commentary by Winter[1-1].

In recent years, stainless steel has gained increasing use in architectural and structural applications. Among the various types of stainless steel sheet and strip developed for different purposes, the most common types are in the austenitic category. They are used in the annealed and strain flattened state or rolled condition. The general applications of austenitic stainless steels are similar to carbon low alloy steels[1-1]. High corrosion resistance, ease of maintenance, and pleasing appearance make them suitable for many special applications[1-2].

---

* Superscripts indicate reference numbers.

Carbon and low alloy steels have relatively high proportional limits and approximately equal mechanical properties in tension and compression. Austenitic stainless steels are highly susceptible to cold working. Cold rolled austenitic stainless steels have much different material properties than the carbon or low alloy steels. In obtaining high strength or a flat surface through the cold working process, certain material characteristics result: (1) anisotropy increasing with the amount of cold work, (2) unsymmetrical stress strain relationships in tension and compression, (3) inelastic stress strain relationships with a low elastic limit, and (4) corner strengthening effect. Therefore, special treatment of these types of material is needed and information on the effects of these factors on the behavior of structural members is required.

1.2 Purpose of Investigation

The purpose of this investigation is to develop the basic, necessary information to prepare a design specification for cold formed structural elements and members made of cold rolled austenitic stainless steel for structural applications. The existing design methods in specification[1-1] for carbon and low alloy steels cannot be applied to cold rolled stainless.

There are a few attempts which have been made to produce design specifications for stainless steel, such as Watter and Lincoln[1-3], research at Franklin Institute[1-4], and a design guide for stainless steel of the State of California[1-5]. They have provided a large amount of information on the design of

stainless steel members. However, the information proposed by them is not complete and some of the methods are either impractical or not theoretically justified. This was discussed in detail in a report by Johnson[1-6].

For the last few years, a research project on stainless steel has been sponsored by AISI at Cornell[1-6]. Based on the extensive experimental information and analysis, a design specification for annealed and strain flattened austenitic stainless has been released recently by AISI[1-7]. However, such information is specifically for annealed and strain flattened stainless steel which undergoes only slight cold reduction in order to have a flattened surface. In contrast, for cold-rolled grades, somewhat more severe cold reduction is involved. The investigation reported here is concerned with cold-rolled austenitic stainless steel, especially Type 301-1/4 and 1/2 hard, as a continuation of the previous investigation on annealed and strain-flattened material.

In order to provide useful information for design, the investigation of the material properties of cold rolled stainless steel is essential. The pronounced anisotropic material properties with the increased amount of cold work must be investigated so that lower bounds of directionally dependent material properties in tension and compression may be established.

In analyzing the structural behavior of elements and members, the inelastic unsymmetrical stress strain relationships in tension and compression as well as the corner strength-

ening effect should be considered. Local buckling phenomena and post buckling strength of plate elements should also be taken into consideration.

The purely mathematical approach in dealing with such a problem is extremely tedious. However, approximate solutions may be obtained by using numerical approaches with simplifying assumptions or semi-experimental analyses. The results from such an approach are not exact, but they may be accurate enough for engineering applications. Experiments are also essential in this type of investigation. They are not only used to verify the analytical results but also constitute a reasonable basis for developing a semi-experimental relationship when the analytical approach is not feasible or is too involved for design purposes.

1.3 Scope of Investigation

The chapters which follow discuss in some detail the most important aspects of the performance of structural members made of cold rolled stainless steel, using 1/2 hard Type 301 and annealed and strain flattened Type 304 as specific examples.

The material properties are described in Chapter 2. The effects of cold working on metals, especially Type 301 austenitic stainless steel, are discussed. A statistical approach is introduced to account for the variations of .2% offset yield strength and to provide lower bound values for the purposes of design. The mechanical properties are

described in general, and then specifically for 1/4 and 1/2 hard Type 301. Analytical stress strain curves are also discussed. The modified Ramberg-Osgood formula is used for analysis and design. Then the mechanical properties in various directions of a cold-rolled austenitic stainless steel sheet are studied.

Local buckling phenomena and out of plane distortions are studied in Chapter 3. Two types of plate structural elements were tested-stiffened and unstiffened elements. Experimental results are presented and discussed. Approximate analysis considering orthotropic material properties and inelastic behavior is briefly discussed. Out of plane waving of the elements in connection with local buckling is also discussed.

Post buckling behavior of stiffened and unstiffened plate structural elements are studied in Chapter 4. Effective width was used to account for the post buckling strength. Experimental results are presented and discussed.

The behavior of structural members is discussed in Chapter 5. An experimental study was made for compression and flexural members. A numerical analysis of flexural strength, curvature, and inelastic deflection of flexural members by using a digital computer (IBM360) is presented. In the analysis, nonlinear and unsymmetrical stress strain relations in tension and compression, post buckling strength, and corner strengthening effects were considered. The ef-

fects of mechanical properties on the behavior of compression and flexural members is described.

Design methods to predict the behavior of structural elements and members are presented in Chapter 6 based on the analytical and experimental evidence in the foregoing chapters. These are the design procedures suggested by the available information; they are not formulated in specification language.

Finally, summary and conclusions are presented in Chapter 7.

CHAPTER 2

MATERIAL PROPERTIES

2.1 General

In this chapter the change of mechanical properties of metals due to cold working will be described with emphasis on austenitic stainless steels especially for Type 301 cold-rolled stainless. The basic austenitic composition is a 17% chromium, 7% nickel alloy. A detailed discussion of chemical composition and influence is outside the scope of this investigation; this is discussed in the literature[1-2, 2-1].

This chapter will constitute the background of basic material properties for this investigation and the typical design material properties for Type 301-1/4 and 1/2 hard stainless steel.

2.2 Effects of Cold Working

2.2.1 Effects of Plastic Deformation on Metals Under Cold Working

The cold working process may be rolling, forging, extrusion or drawing. During any of these processes, the metal undergoes plastic deformation, and the grains change shape. The deformation of single crystals in the metal is under various constraints. Multiple slips occur. Plastic deformation produces an increase in the number of dislocations. The dislocations passing through the grains on intersecting slip systems interact with each other, producing tangled disloca-

tion arrangements. This will increase the resistance to plastic deformation of the polycrystalline metal by the fragmentation of crystals and the rotation, elastic distortion and bending of crystal fragments.

The internal stress distribution is non-uniform because of complex microstructure and plastic deformation. The internal stresses induced are of three kinds. The first, "macroscopic internal stress", is caused by non-uniformity of plastic deformation in different parts of the cross section. The second kind, "micro-structural stress", is due to initial differences in the resistance to plastic deformation of variously oriented grains of a polycrystalline aggregate, and to the differences in the strength of different microconstituents. The third kind of stress is associated with the space lattice expansion changes involved in work-hardening.

The preferred orientation, or texture, in the metals is formed during cold working process. It has been studied by many investigators[2-2,2-3]. A metal which has undergone a severe amount of cold working will develop a preferred orientation, in which certain crystallographic planes tend to orient themselves in a preferred manner with respect to the direction of maximum strain. The preferred orientation is strongly dependent on the slip and twining systems available for deformation. The direction of flow is an important process variable.

The process of work hardening and plastic deformation under cold working not only produces the anisotropic properties of the metal because of non-uniform internal stress dis-

tribution and preferred orientation, but also strengthens the metal sheet to a different extent in the various directions.

The strengthening mechanism of cold working depends on chemical composition and on mechanical as well as thermal processing. However, only the mechanical strengthening mechanism by cold working is considered herein. Strain hardening by plastic deformation is one of the major methods of strengthening a metal.

2.2.2 Strengthening Mechanism

In the austenitic class the effect of the nickel addition is to stabilize the face-centered structure at room temperature. The austenitic stainless steels cannot be hardened to form martensite by quenching. However, austenitic grades are ductile and can suffer considerable cold work without breaking. The alloys are hardened during cold work, and further, many alloys of the class undergo a transformation that is martensitic. Type 301 which has a lower chromium range (and therefore a lower nickel content) is more susceptible than 302 or 304 to cold work. The austenite is less stable in 301. This strengthening mechanism of austenitic stainless steel has been studied and confirmed by many investigators.

Figs. 2-1 and 2-4 show the increase of offset yield strength as a function of the percent of cold reduction for both Type 301 and 302. It is seen that the increase of offset yield strengths for Type 302 is much less than Type 301. In both types of stainless, the anisotropy increases with strength and the range of values of yield strength becomes

more divergent. The rate of increase of yield strength in longitudinal compression is the lowest in both materials. It is also noticed in the same figure that Type 301 can reach higher tensile strength than Type 302 at the same amount of cold reduction.

A thorough investigation of this strengthening mechanism of Type 301 has been reported by Barclay[2-5]. From his test results, Barclay concluded as follows:

(1) The change of the stress-strain relation in the work hardening range has been definitely related to the formation of deformation martensite.

(2) A less stable alloy undergoes transformation sooner, has more martensite formation at a given strain, and reaches a higher tensile strength and more uniform elongation than a more stable alloy.

(3) The deformation of Type 301 has been observed to occur by at least six mechanisms:

(a) Dislocation motion in austenite

(b) Dislocation tangles, cell formation, and formation of stacking faults

(c) Deformation twins in austenite

(d) Martensite formation

(e) Dislocation motion in martensite

(f) Deformation twins in martensite.

The mechanisms are listed in order of appearance with increasing strain, and several mechanisms are operative simultaneously.

(4) The structure suggests that most of the plastic deformation occurs via deformation mechanisms in the austenite stages (a) through (c) plus martensite formation of stage (d).

2.2.3 Cold Forming - Corner Strengthening Effect

Cold working generally increases yield and ultimate strengths and decreases ductility. The nature of these changes depends on the chemical composition of the steel, metallurgical treatment history, prior cold work, and type and magnitude of plastic strain caused by the cold work.

Light gage structural members are cold formed by roll-forming or brake forming. Additional cold work is involved in the corner regions of the structural members through the cold forming process. Forming by press brake is a straight bending and the corners may be either air or coin press braked. In this investigation the corners for the specimens were all air braked. The corners were bent sharper than the desired final angle to allow for springback.

The direction of bending (stretching) of corners related to the rolling direction of the metal sheet is important. However, in general, the yield and ultimate strengths are higher in the corner than in the original sheet (annealed or tempered). The amount of increase in strength depends on the temper, metal, and radius of the corner, etc.

The effects of the additional cold working in corners are the largest in the annealed state and decrease with increasing hardness of the original flat sheet, becoming almost negligible for the full hard grades. An analytical prediction of

the strain hardening effect of cold forming in the corners is a complex problem since there are so many factors involved, especially for the cold-rolled stainless sheet.

Some test results on corners of half hard Type 301 and annealed and skin passed Type 304 will be presented and discussed in 2.3.2.

2.3 Testing Program of Material Properties

In view of the unusual material properties of austenitic stainless steels, especially for the temper rolled grades, an extensive investigation of material properties by tests was necessary, in both longitudinal and transverse directions, and in both tension and compression.

In the following sub-sections, a testing program of coupons will be described briefly. The test results were used to study the stress strain relations and other mechanical properties along with information provided by the steel producers.

2.3.1 Material, Coupon, Instrumentation and Testing Procedure

Material used in this program was 1/4 and 1/2 hard Type 301 stainless of various thickness (0.020" to 0.089", corresponding to 25 to 13 gauge). Duplicate flat coupons were sampled from five 1/2 hard sheets and four 1/4 hard sheets (including the 1/2 hard sheet 301-H-7 used later for flexural members). Mechanical properties obtained from these coupons were used along with additional information from steel producers for statistical analysis of offset yield strength and to

determine the design mechanical properties of these two grades.

Flat coupons from two other sheets 301-H-3 (for flexural and unstiffened compression specimens) and 301-H-2 (for the tests of material properties in different directions) were also tested. One sheet, 304-AS-5 (for flexural specimens), for Type 304 annealed and strain flattened was also tested.

Corner properties were studied for three sheets, i.e. 301-H-3, 301-H-7, and 304-AS-5. The size of corners are the same as for corresponding flexural members tested.

Tension flat coupons were ASTM standard sheet-type coupons. Compression coupons were 0.5" by 2.0". For tension corner coupons, the narrow part was machined to the size of the corner, and the area of the corner was determined by cutting off and weighing the pre-marked portion after test. Compression coupons were cut 2.5" long with about 9/32" from the outer surface of one flange to the tip of the other flange. The area of cross section was determined by weighing and measuring the length of the coupon. The load taken by the corner was obtained by subtracting the load taken by the flat portion from the total load.

The tension tests were conducted according to ASTM Designation E8-61T on "Tension Testing of Metallic Material"[2-6]. An averaging type Tinius-Olsen microformer extensometer was used with an autographic recorder to plot load strain curves.

The compression tests were conducted according to ASTM Designation E9-61 on "Compression Testing of Metallic Mate-

rials"[2-7]. A lateral support jig described in Ref. 2-10 was used for flat compression coupons to prevent buckling of the specimen under load. A Baldwin compressometer of the micro-former type was used with an autographic recorder to plot load strain curves. The corner compression coupons were tested with hydrostone as the lateral support. Strain was measured by a strain gage mounted on the coupon embedded in the hydrostone.

A Tinius-Olsen 30,000 pound capacity screw type testing machine was used for these tests.

2.3.2 Discussion of Test Results

Flats

Stress strain curves can easily be obtained from load strain curves. The initial moduli and 0.2% offset yield strengths were also obtained from the charts. The ultimate strengths of tension coupons were calculated from the maximum loads recorded by the machine. The percentage elongations for tension coupons were obtained by measuring the final length of the pre-marked gage length.

The stress strain curves for the sheets (304-AS-5, 301-H-3, and 301-H-7) from which the compression and flexural specimens were made are presented in Figs. 2-2, 2-4, and 2-6. Some mechanical properties of these three sheets are presented in Table 2-1. The derived quantities, such as tangent and secant moduli, expressed as plasticity reduction factors for longitudinal compression are presented in Figs. 2-3, 2-5 and 2-7 after each graph of the stress strain curves. The tangent moduli were determined from the longitudinal compression

stress strain curve by using a semi-transparent mirror. The method was suggested by Bijlaard and Fisher[2-8]. The plasticity reduction factors will be used in later investigations on local buckling and post buckling behavior analysis. Discussion of other tests will be presented in Sections 2.4, 2.5, and 2.8.

Corners

The stress strain curves of Type 304 corners are shown along with the curves for flat material of the same sheet in Fig. 2-2. The comparison of the mechanical properties of corners and flats is shown in Table 2-1.

The effective stress strain curves of corners for Type 304 annealed and strain flattened stainless steel show a tremendous increase in strength over the original sheet. The initial moduli are usually the same or slightly smaller than in the flat sheet. The yield strength increase is the highest (152%) in longitudinal compression, and in transverse compression (98%) it is also considerable. The net increase in longitudinal (65%) and transverse (63%) tension is smaller than in compression. This is not surprising if one considers the plastic flow during the course of cold working. The cold reduction in thickness is very slight to produce annealed and strain flattened Type 304. The severe cold bending in the corners may wash out the previous cold work effects. The fact that the bending (stretching) direction is perpendicular to the rolling direction of corner specimens in the longitudinal direction is the main cause of such high increase in longitudinal compression strength of corners. The increase in longi-

tudinal and transverse tension is expected to be less pronounced because the bending direction is perpendicular to the coupons. This can be understood if one observes the simple models presented in a study of carbon steel by Chajes, Britvec and Winter[2-9] and by Karren and Winter[2-10].

Similar mechanical properties were also obtained from corner coupon tests of the two sheets of 1/2 hard Type 301. The stress strain curves are shown in the same figure of flats, Figs. 2-4 and 2-6. The mechanical properties are also shown in Table 2-1. The effective yield strength of corners does show an increase as compared to the virgin 1/2 hard flat sheet; however, the percentage of increase is much smaller than for the case of annealed and strain flattened Type 304. The increase of offset yield strength is smallest in transverse compression, being 5% of the original value. This correlates with the fact that the yield strength of the flat sheet is highest in the transverse direction. The initial moduli of corner stress strain curves are usually smaller than for flats. The percentage increase in ultimate strength is about the same (7%) as for Type 304 annealed and strain flattened.

From the comparison of stress strain curves of flats and corners, it is concluded that the strengthening effect of corners may be disregarded within the usual working stress range. In predicting failure, however, neglecting the corner strengthening effect may underestimate the strength of structural members. For accurate calculations, the effective cor-

ner strength should be used.

The applicability of Karren's formula[2-10] for corner strength prediction, which was developed for carbon steel, was checked for austenitic stainless steel. The strengths predicted by Karren's formula for carbon steel exceed the experimental values by an average of 23.4% for stainless steel.

2.4 Statistical Study of Yield Strength of Flat Coupons Under Normal Stress

In the following sections, a brief outline of the statistical analysis is given to deal with the experimental results in order to establish reliable minimum values for purposes of design.

2.4.1 Basis for Statistical Analysis

For a group of observed values, the statistical probability analysis may be achieved by using characteristic statistical parameters or by graphical approach. Such analysis is much simpler if the distribution of observed values may be assumed as normal.

The characteristic statistical parameters can be calculated from a group of observations by means of a simple computer program. For graphical analysis, a fractile diagram may be used. The theoretical basis for the fractile diagram by plotting points of cumulative frequency on the probability paper was discussed in detail by Hald[2-11]. If the points appear to deviate only at random from a fitted straight line, the theoretical distribution is very close to the normal distribution. The values with a certain percentage of probability

can be determined easily from the straight line or by using the characteristic statistical parameters calculated. In this investigation of offset yield strength, the points deviated only at random from the fitted straight line.

Figs. 2-8 and 2-9 show the typical analyses for 1/4 and 1/2 hard Type 301 in transverse tension. If the theoretical distribution is normal, the observed value of cumulative probability deviates at random from the theoretical cumulative probability which is the straight line. The confidence bands for selected percentages of confidence may be calculated. The variance of the fractile corresponding to the cumulative frequency may be found. By considering the variance of a stochastic variable, assuming that the fractile is normally distributed about a theoretical value and that the observed values are stochastically independent, then from the theoretical values the limits may be calculated between which the observations should lie with a certain probability. The formulation of finding the interval of confidence bands is given elsewhere (Hald)[2-11]. For example, for 95% probability, the observed values should be within the interval of $\pm$ 1.96 times the standard deviation from theoretical values.

2.4.2 Data for Statistical Analysis

Based on the approach outlined, a statistical analysis was made for .2% offset yield strength in order to establish the lower bound design values. The statistical population included results from testing program just described and from steel producers. The number of heats and coupons involved in

each analysis is shown in Table 2-2. The range of the population for each group is also listed in the same Table.

2.4.3 Discussion of Statistical Results

Values of the mean, variance, and standard deviation obtained from computer program output are listed in Table 2-2. The cumulative frequency distribution and confidence bands are plotted on arithmetic probability paper. Figs. 2-8 and 2-9 show the typical analysis in transverse tension for both 1/4 and 1/2 hard Type 301 stainless steel. The 90% and 95% probability .2% offset yield strength and 95% with 95% confidence values are listed in Table 2-3 along with the values given in other publications.

It is seen from Table 2-3 that the design compression yield strengths of MIL-HDBK-5[2-12] are lower than the values obtained by this analysis. These values could be raised to give more economical design. Such an increase is also supported by the data shown in Fig. 2-1 if one considers the ASTM[2-13] minimum tensile yield strength as a standard value and obtains the others from the graph.

For tensile yield strengths, the statistical results are quite close to the ASTM[2-13] specification minimum values except in the case of 1/2 hard in the transverse direction. However, the values for 95% probability and 95% confidence are lower than the specification values.

Inspecting the values in Table 2-3, the values for 95% probability can best be used for guidance. On this basis, the specification tension values for 1/4 hard are acceptable,

but the compression values could be raised to 50 ksi longitudinally and to 90 ksi transversely. For 1/2 hard, one finds that instead of the MIL-HDBK-5[2-12] values of 110, 110, 58, and 118 ksi the following values are more realistic: 110, 100, 65, and 120 ksi. These values are recommended as design values which represent the lower bound of these two cold rolled grades.

2.5 Other Mechanical Properties of Flat Material Under Normal Stress

2.5.1 Initial Modulus of Elasticity

The initial modulus of elasticity is one of the most important mechanical properties. In a polycrystalline metal, the value of the modulus is an average since the crystals are randomly oriented. Under cold working the value is expected to change not only depending upon the degree of cold work but also upon the direction of measurement.

Mebs and McAdam[2-14] showed the change of tensile modulus for 18-8 Cr-Ni stainless steel due to cold working. They indicated that the tensile modulus showed an initial slight rise during the first 5% of extension, followed by a steady and somewhat rapid decrease through the remainder of the extension range. The initial rise may be attributed to the predominance of increasing internal stress, the subsequent decrease may be attributed in part to lattice expansion. Some of this decrease, however, may be due to preferred orientation.

The comparison of average values of initial moduli from the author's tests with certain publications and reports from

steel producers is shown in Table 2-4. It shows the usual spread which depends on instrumentation and other testing technique details. Based on the information in the table, it seems that the multiplicity of values of MIL-HDBK-5[2-12] is a superfluous complication. It seems acceptable to specify 27.0×10^3 ksi in the longitudinal direction, for compression and tension and for both 1/4 and 1/2 hard, and to specify 28.0×10^3 in the transverse direction, for both compression and tension and for 1/4 and 1/2 hard.

2.5.2 Proportional Limits

It is quite difficult to determine the stress at which the stress-strain curve starts to deviate from an initial elastic straight line. However, based on the information from individual tests and the variation from one test to the other in the same group, representative values may be obtained.

It is customary to define a small value of inelastic permanent strain for determining an apparent limit of proportionality. This property gives an indication of the shape of the stress strain curve in the working stress range when changing from elastic to inelastic behavior.

The values of noticeable deviation from elastic behavior, and 0.01% offset proportional limits are determined and listed in Table 2-5. The apparent proportional limit values of noticeable deviation from linear behavior are reflected in the plots for secant and tangent moduli, and are taken as the proportional limits for the buckling stress determinations. The effective proportional limits for flexural members are

also suggested in the same table.

The values of proportional limits based on the 0.01% offset are very close to those given in Reference 2-15.

2.5.3 Typical Stress Strain Curves

The recommended 95% probability yield strength and the initial moduli for design were stated above. From the stress strain curves obtained from the coupon tests, the general shape and trend of those curves can be seen. The proposed typical stress strain curves for design can be constructed by following the general shape and using initial modulus and yield strength as controlling values. In Fig. 2-10 four stress strain curves for the design for 1/4 and 1/2 hard Type 301 are shown.

2.5.4 Secant and Tangent Moduli

The secant moduli are used for calculating inelastic deflections of flanged beams and in determining buckling stresses for unstiffened elements. Secant moduli were obtained from the proposed stress strain curves and are presented graphically in Fig. 2-11.

In calculating the buckling strengths of columns and certain compression elements, tangent moduli are used in the analysis of inelastic response. The tangent moduli have been determined from the proposed compression stress strain curves by using a semi-transparant mirror. The values so obtained are plotted in Fig. 2-12.

2.5.5 Ultimate Tensile Strength

The comparison of the average of ultimate tensile strength

from the author's tests in both longitudinal and transverse directions with certain publications and reports from steel producers is shown in Table 2-6. It seems to indicate that for 1/4 hard the ASTM value of 125 ksi could be raised to 130 ksi, for 1/2 hard the ASTM value of 150 is probably satisfactory.

From the values of ultimate tensile strength and yield strength, it can be seen that the ratio of yield strength to the ultimate tensile strength gets closer to one as the prior cold work of the sheet increased.

2.5.6 Ductility

The ductility is greatest in the annealed state and reduces with increasing cold working. The elongation in 2" for the tensile coupons tested is shown in Table 2-6 along with values from certain other publications. Inspection of Table 2-6 shows that the ASTM values could safely be raised. However, since the ASTM values do provide more than ample ductility and are easily met, no change seems to be indicated.

2.5.7 Poisson's Ratio

In the elastic analysis, Poisson's ratio is assumed to be a constant and relates to initial modulus and shear modulus as follows:

$$\nu = \frac{E}{2G} - 1 \qquad 2\text{-}1$$

where E = initial modulus of elasticity

G = Shear modulus

ν = Poisson's ratio

When anisotropy is encountered, Poisson's ratio will vary

in different directions. For cold-rolled austenitic stainless steel, the stress-strain relationship is anisotropic and nonlinear. Therefore, there has been uncertainty as to the constancy of Poisson's ratio with increasing stress.

In a report by Muhlenbruch, Krivobok and Mayne[2-16], a thorough study of Poisson's ratio for austenitic stainless steels was presented. Poisson's ratio in longitudinal and transverse directions for certain austenitic stainless steels as a function of stress was determined by a series of tension specimen tests.

From the work of Muhlenbruch[2-16], Poisson's ratio for annealed Type 301 is almost constant throughout the whole stress range and equal to 0.30. Muhlenbruch[2-16] also showed that for Type 301-1/2 hard sheet, Poisson's ratio remained practically constant throughout the major portion of the structurally significant stress range for tension specimens in the longitudinal direction, while there was a slight increase at higher stresses. From test evidence, a value of 0.31 for Poisson's ratio may be used for both 1/2 and 1/4 hard Type 301. In the transverse direction a value of 0.34 for Poisson's ratio may have to be used since a higher value than in the longitudinal direction was evident from test results.

2.6 Mechanical Properties of Flat Material in Shear

Very little experimental work has been done on the determination of complete shear stress strain curves. The shear stress strain behavior is not a basic independent material property. It may be desirable to derive an estimation of the

shear behavior from the usual tension and compression tests. Probably the most convenient approach available is to determine the stress strain curves of material under tension and compression and then use affinity relationships to establish the shear stress strain curve.

The shear stress strain relationships obtained by this manner are verified by existing test results to ensure the suitability of adopting the approach for material of anisotropic properties with nonlinear stress strain relationships.

2.6.1 Affinity Relationships

In order to establish the relationships between the simple tension and shear stress strain curves, it is assumed that the two curves are related by the following affinity factors:

$$\tau = \alpha\sigma \qquad 2\text{-}2$$

$$\gamma = \beta\varepsilon \qquad 2\text{-}3$$

where τ = shear stress

σ = tension stress, uniaxial

γ = shear strain

ε = tensile strain

α = stress affinity factor

β = strain affinity factor

Values for affinity factors which have been used by other investigators were summarized by Johnson[1-6]. The stress affinity factor α ranges from 0.5 to 0.77, and the strain affinity factor β ranges from 1.3 to 1.732. According to the maximum shear theory the values of affinity factors for stress and

strain are 0.5 and 1.5 respectively, and for the distortion energy theory they are 0.577 and 1.732. Other values used by some investigators were based on experimental evidence for some particular materials.

A thorough study of affinity relationships was made by Stang, Ramberg, and Back[2-17]. The correlation of shear and tensile stress strain relationships is indicated by the similarity in shape of the two sets of curves. The evidence from tests showed that the theoretical affinity ratios 0.577 and 1.5 are fair approximations for a sharp yielding metal; for aluminum-alloys the affinity ratios are closer to 0.5 and 1.3.

The normal stress strain curve used by Gerard[2-18] was taken as the mean of tensile and compressive data at 45 degrees with the rolling direction. The mean curve represents more nearly the properties of the material in the shear field. In Gerard's arguments the directional and unsymmetrical stress strain relationships were somewhat taken care of. Satisfactory prediction of inelastic shear buckling was obtained by Gerard.

In order to take the nonlinear material properties into account, the following approximate relation may be used according to Muhlenbruch et al[2-16].

$$G_s = \frac{E_s}{2(1+\nu)} \qquad 2\text{-}4$$

where E_s = secant modulus

G_s = shear secant modulus

ν = Poisson's ratio

The following ratio of stress and strain affinity factors may be obtained if the definitions of affinity factors, as shown in Eqs. 2-2 and 2-3, are used:

$$\frac{\alpha}{\beta} = \frac{1}{2(1+\nu)} \qquad 2\text{-}5$$

For an elastic Poisson's ratio of 0.31, $\alpha/\beta = 0.382$ is given by the above equation. If the stress affinity factor is chosen, the other may be determined by this ratio up to the proportional limit. Above the yield strength α/β becomes 0.333 if Poisson's ratio is taken as 0.5. This same value is also obtained by using the maximum shear theory or distortion energy theory. Hence, the ratio should vary from 0.382 at the proportional limit to 0.333 at the yield strength.

For simplicity in design it is suggested that a constant affinity factors may be used. Therefore, affinity factors will be chosen which will provide a reasonable prediction of the stress curve in shear, but which will remain constant throughout the stress range.

Three sets of affinity factors were chosen for investigation. The first of these was $\alpha = 0.55$ and $\beta = 1.43$. Next, it was assumed that the stress affinity factor $\alpha = 0.5$ and strain affinity factor was 1.3. The third was $\alpha = 0.577$, and $\beta = 1.5$.

2.6.2 Construction of Normal Stress Strain Curve

A suitable procedure has to be established in order to obtain a representative stress strain curve from which the shear stress strain curve may be derived by using affinity

factors. The average of the curves in the four directions may be used as a representative curve in this connection. The reason for doing so is similar to the argument by Gerard of taking the average stress strain curves in tension and compression in the 45 degree direction. From a study of anisotropy (discussed in 2.8) of a sheet of Type 301 1/2 hard stainless steel, the average value of .2% yield strength in longitudinal and transverse tension and compression is very close to the average value in tension and compression in the 45 degree direction, being 125.17 ksi and 128.64 ksi respectively. This indicates the suitability of using the average curves in the longitudinal and transverse directions and in both tension and compression.

2.6.3 Verification of Proposed Approach by Tests

In order to ensure the applicability of the approach outlined, it is necessary to verify it by test. Three torque twist diagrams of tests on Type 301 1/2 hard stainless reported by Muhlenbruch et al[2-16] were converted into shear stress strain curves by the following equations:

$$\tau = T \frac{5.0929\, d_o}{d_o^4 - d_i^4} \qquad 2\text{-}6$$

$$\gamma = \frac{d_o}{2} \phi \qquad 2\text{-}7$$

where T = torque

ϕ = twist angle

d_o = outside diameter of the tube

d_i = inside diameter of the tube

It should be noted that these equations were derived on the assumption that strain is proportional to the distance from the axis of the tube and stress varies linearly with strain. However, these equations were used by Muhlenbruch et al successfully for the same material.

The four normal stress strain curves of 301-H-3 reported in Fig. 2-4 were chosen for comparison because the material properties of this sheet are very close to the one used by Muhlenbruch et al. The average normal stress strain curve from four curves of 301-H-3 is shown in Fig. 2-13. The reduced shear stress strain curves from the three sets of affinity factors mentioned are shown in the same figure along with the experimental shear stress strain curves reduced from Muhlenbruch's tests. It can be seen that satisfactory agreement exists between the test results and the curves (especially curve c with $\alpha = 0.577$, $\beta = 1.5$) obtained by applying the affinity factors to the average normal stress strain curve. It is also interesting to check the relationship among the initial moduli of the normal and shear stress strain curves and Poisson's ratio by using Eq. 2-1. The initial shear modulus obtained from the equation is 10,760 ksi if the average initial modulus (28,210 ksi) of the four curves and 0.31 for Poisson's ratio are used. This value is very close to the value obtained by Muhlenbruch et al namely 9950 ksi at a shear stress of 12.5 ksi. Based on all this evidence, the approach seems acceptable.

2.6.4 Shear Stress Strain Curve for Design

It can be concluded that the simplest and most reliable way to obtain the shear stress strain curve is from the average normal stress strain curve. In order to provide such a curve for purposes of design, the proposed normal stress strain curves should be used.

From the comparison of calculated and experimental shear stress strain curves in Fig. 2-13, it seems that the shear stress strain curve with $\alpha = 0.577$ and $\beta = 1.5$ may be safely used. Therefore, for design purposes, these values are recommended. Average normal and shear stress strain curves for both 1/4 and 1/2 hard Type 301 are shown in Fig. 2-14.

2.6.5 Proportional Limit and Shear Yield Strength

Using the stress affinity factor $\alpha = 0.577$, the proportional limit in shear is 11.50 ksi for 1/4 hard and 13.30 ksi for 1/2 hard Type 301. The shear yield strengths for 1/4 and 1/2 hard are 41.8 ksi and 56.2 ksi respectively. The proportional limit is 0.577 of the proportional limit of the average normal stress-strain curve. The shear yield strength is 0.577 of the 0.2% offset yield strength of the average normal stress strain curve corresponding to an offset of 0.30% on the shear stress strain curve.

2.6.6 Initial Shear Modulus

Muhlenbruch et al[2-16] have determined the secant shear modulus from tests on tempered Type 301 stainless steel tubes at low shear stresses. The average values of three tests of 1/4 and 1/2 hard Type 301 at shear stress equal to 12.5 ksi

are 10,320 ksi and 9,950 ksi respectively. Based on these tests and those by Mebs et al[2-14], the shear modulus decreases as cold work increases, i.e. hard grades have lower shear moduli than softer grades. The initial shear modulus found from the shear stress-strain curve by applying the affinity factors to the average normal stress strain curve of sheet 301-H-3 is 10,500 ksi, which is close to the experimental value by Muhlenbruch et al[2-16]. If the average initial normal modulus (28.21 ksi) of sheet 301-H-3 and Poisson's ratio 0.31 are used in Eq. 2-4, it gives a value of G = 10,760 ksi, which is also close to the values shown above by various means.

Hence, it seems that the initial shear modulus may be obtained from Eq. 2-1 or 2-4 by using the average normal initial moduli recommended for design, and Poisson's ratio of 0.31. The average normal initial modulus is 27,500 ksi and the G value is 10,500 ksi for both 1/4 and 1/2 hard Type 301. This value is very close to the experimental values and also maintains agreement with Eq. 2-1 or 2-4.

The AISI Steel Products Manual[1-2] and the ASM Metals Handbook[2-19] give 12,500 ksi for the initial shear modulus for annealed Type 301 and indicate that the value decreases with the increase of cold work. MIL-HDBK-5[2-12] gives 12,000 ksi and 11,500 ksi for 1/4 and 1/2 hard respectively, which are slightly higher than the experimental values.

2.6.7 Secant Shear Moduli

Secant shear moduli were obtained from the proposed shear stress strain curves for both 1/4 and 1/2 hard Type 301 and

are presented graphically in Fig. 2-15.

2.7 Analytical Stress Strain Curves

2.7.1 General

The stress strain relationship for cold worked stainless steels is nonlinear and anisotropic. Therefore, an analytical expression is useful to define this relationship so that the behavior of structural elements and members may be calculated.

Simplicity and close agreement to the experimental stress strain data are the basic requirements of such an expression. The elementary requirements are that the curve represented by the equation go through the origin and have a slope equal to the initial modulus. Besides, the equation should be in quite general form so that it will fit different materials by varying the parameters. It is also desirable that the curve be continuous and smooth not only for the stress strain relations but also for its derived values, such as tangent and secant moduli.

A general discussion on stress strain formulas was reported by Osgood[2-20]. Several formulas were suggested to meet various requirements depending upon the characteristics of the material and the type of problem. Practically, any stress strain relation can be closely represented by polynomial approximations if sufficient terms are taken.

In order to satisfy the condition of simplicity, three parameters may be adequate to describe the stress strain relationship. In view of the relevant range of strain (up to 1%)

and the basic requirements outlined, the Ramberg-Osgood formula may be the best to use.

2.7.2 Modified Ramberg-Osgood Formula

The original form of Ramberg-Osgood formula[2-21] involving three parameters is

$$\varepsilon = \frac{\sigma}{E} + K \left(\frac{\sigma}{E}\right)^n \qquad 2\text{-}8$$

where K and n are constants. The applicability of this equation may be tested by plotting a strain deviation-stress curve on a log-log scale. This should lead to a straight line if the equation holds. The values of K and n may also be evaluated by considering two secant yield strengths determined for slopes of 0.7E and 0.85E.

Later the equation was modified by Hill[2-22] by using two offset yield strengths rather than secant yield strengths since yield strength values determined by the offset method are commonly used. It was shown by Hill that by considering the strain deviation from elastic strain at the 0.2% and 0.1% offset stresses and strains, Ramberg and Osgood's formula can readily be reduced to

$$\varepsilon = \frac{\sigma}{E} + 0.002 \left(\frac{\sigma}{\sigma_{.002}}\right)^n \qquad 2\text{-}9$$

where $\sigma_{.002}$ is the .2% offset yield strength, and n is given by

$$n = \frac{0.301}{\log(\sigma_{.002}/\sigma_{.001})} \qquad 2\text{-}10$$

where $\sigma_{.001}$ is the .1% offset yield strength. These offset

strain values and the corresponding offset stresses have been used by Hill and others. The .1% offset value will locate a point in between the elastic range and usual yield strength, and this is the region of importance for inelastic buckling.

From this analytical expression of the stress strain curve, the tangent moduli can easily be obtained by differentiation. The equation for tangent modulus can be expressed as

$$E_t = \frac{\sigma_{.002}\, E}{\sigma_{.002} + 0.002\, nE \left(\frac{\sigma}{\sigma_{.002}}\right)^{n-1}} \qquad 2\text{-}11$$

2.7.3 Fitted Stress Strain Curves for Analysis and Design

The applicability of Eq. 2-9 to the material considered may be tested by plotting the strain deviation vs. the stress ratio ($\sigma/\sigma_{.002}$) on log-log scale. This should lead to a straight line. Such a relation was verified by making plots for stress strain curves in tension and compression, and in both longitudinal and transverse direction for sheets 301-H-3 (half hard) and 304-AS-5 (annealed). The experimental points are very close to a straight line all the way up to the stress slightly beyond the .2% offset yield strength. This simply indicates that the modified Ramberg and Osgood formula is at least applicable up to and slightly beyond the .2% offset yield strength which is adequate for most cases. If the higher stress range is also considered, two straight lines may be needed.

A further modification of the modified Ramberg-Osgood formula is that the .2% and .05% offset strains and stresses were used in this investigation rather than the .2% and .1% offset values usually used. The reason for this is simply because of the consideration of the accuracy of stress strain data in the working stress range and the inelastic buckling in this region. The .1% offset yield strength is close to the .2% offset yield strength and the curves so determined yield stress which are too high in the stress range below the .1% offset strength. The greatest effects due to this fact are on the stress strain curves with the larger n values, which is the measure of the shape of the stress strain curve and is called the shape factor. The curves with sharper yielding have a larger n value than the ones with gradual yielding type. In this case n may be calculated from the following equation.

$$n = \frac{0.602}{\log(\sigma_{.002}/\sigma_{.0005})} \qquad 2\text{-}12$$

The experimental .2% and .05% offset yield strengths for both flat material and corners of 304-AS-5, 301-H-3, and 301-H-7 are shown in Table 2-7. The yield strength ratio and n values along with initial moduli are shown in the same table. The same approach was also applied to the proposed design stress strain curves and the related data is shown in Table 2-8. The .2% and .05% offset yield strengths of averaged normal stress strain curves were used as controlling stresses and strains for the shear stress strain curves by

considering proper multiplication of affinity factors for both strength and strain. This means that the offset values on the shear stress strain curves are .30% and .075%. The expression for n in shear may then be written as

$$n = \frac{0.602}{\log (\tau_{.0030}/\tau_{.00075})} \qquad 2\text{-}13$$

2.7.4 Derived Values From Fitted Curves

The modified Ramberg-Osgood stress strain curves have continuous first derivative so that the tangent moduli may be calculated from Eq. 2-11. The secant moduli can also be obtained readily. The plasticity reduction factors which will be used for inelastic buckling analysis can also be calculated.

2.7.5 Comparison Between Analytical and Experimental Data

The strains can easily be calculated from the analytical stress strain curve if the stresses are known. However, in some cases, the stress is needed from known strain. In this case, an iterative procedure is necessary to obtain the stress from known strain. A computer program has been prepared for the iterative process based on the Newton's tangent method and very fast convergence can be obtained through this process. In general, around 5 cycles result in convergence of .001 ksi of two consecutive values. This iterative process is shown in Fig. 2-16. The program is used as a sub-program for flexural strength and deflection calculation in Chapter 5.

The stress strain data and the derived values from the computer program by using the analytical stress strain curves

presented in Table 2-7 are obtained. The fitted analytical stress strain curves are not distinguishable from the experimental curves for both flat and corner materials up to and slightly higher than the 0.2% offset yield strength. The derived values of secant and tangent moduli for the sheets 301-H-3, 301-H-7, and 304-AS-5 longitudinal compression are plotted in Figs. 2-3, 2-5 and 2-7 along with the experimental data. It can be seen that the analytical results agree with the experiments very well up to and slightly beyond the .2% offset yield strength. However, in the initial stage of stress the predicted values are lower than the experiments. This is the nature of the Modified Ramberg-Osgood formula because it starts to deviate from the elastic portion from the very beginning.

The stress strain data and the values derived from the computer program by using the analytical stress strain curves for design presented in Table 2-8 are also compared with the proposed data for design in Figs. 2-10, 2-11 and 2-12. Similar conclusion may be drawn.

It is believed that the modified Ramberg-Osgood formula can safely be used for the material considered. This will give a designer a choice of working with experimental data or an analytical formula depending upon the nature of the problem.

Although the agreement between analytical and experimental results is very good, the analytical stress strain curves are used herein only for the flexural analysis which

will be presented in Chapter 5. The experimental data are used everywhere else in order to obtain a realistic comparison between analytical and experimental behavior.

2.8 Anisotropy of a Cold Worked Austenitic Stainless Steel Sheet

2.8.1 General

The mechanical properties discussed in the foregoing sections concerning cold worked stainless are mainly in the longitudinal and transverse directions, and intermediate variations between these two directions were not considered. Since cold rolled stainless has different mechanical properties according to the orientation and sense of stressing, it is interesting to look into the directional variations of such properties. Such information is also essential and important when a biaxial stress field exists.

2.8.2 Sampling Scheme

A series of tension and compression coupons of a sheet of 1/2 hard Type 301 was tested to investigate the variations of mechanical properties in various directions. The coupons were cut along radial lines at angles of 22.5 degrees apart from each other and the intersections of these radial lines were at the center of the sheet. The sampling scheme is shown in Fig. 2-17. Two of the radial lines are in the longitudinal and transverse directions.

2.8.3 Discussion of Test Results

The initial moduli, the 0.2% offset yield strength for both tension and compression coupons, the ultimate strength,

and the percent elongation of tension coupons are shown in Table 2-9.

The initial moduli, ultimate strengths, and elongations of tension coupons show the usual spread which depends on instrumentation and other testing technique details, and the influence of anisotropy on these values is small. Regarding 0.2% tensile yield strength, the highest value is in the longitudinal direction (H2T-3600) and the lowest in the transverse direction (H2T-2700).

For compression coupons, the value of initial modulus is higher in the transverse direction and lower in the longitudinal direction. The variation of offset compression yield strength is very obvious from the longitudinal to transverse directions.

From the test results and the variations in 0.2% offset yield strengths for tension and compression, an elliptic distribution of such values is suggested. Fig. 2-18 shows the proposed elliptic curve and the test results. It shows satisfactory agreement between test points and the ellipse. An even better fit may be obtained if an arbitrary elliptical curve is used instead of using test results in longitudinal and transverse directions as the major and minor axis of the ellipse.

The yield strength in any orientation, $\sigma_{y\theta}$, can be obtained by the following simple relationship if the yield strength in the longitudinal (σ_{yL}) and transverse (σ_{yT}) directions are specified. For the purposes of design, such speci

fied yield strengths may be the previously recommended design values. The general equation of an ellipse in polar coordinates can be written as

$$r = ab/ (b^2\cos^2\theta + a^2\sin^2\theta)^{1/2} \qquad 2\text{-}14$$

where r = radius

θ = angle

a = axis of ellipse along longitudinal direction

b = axis of ellipse along transverse direction

therefore,

$$\sigma_{y\theta} = \sigma_{yL}\,\sigma_{yT}/ (\sigma_{yT}^2\cos^2\theta + \sigma_{yL}^2\sin^2\theta)^{1/2} \qquad 2\text{-}15$$

In Eqs. 2-14 and 2-15, θ is measured from the longitudinal direction and the magnitude is less than or equal to 90 degrees. Such a relationship may be considered as a general equation for the limiting stress (0.2% offset yield strength here) in various orientations. In a biaxial stress field, the limiting stress from Eq. 2-15 in the same direction as the principal stress should be used.

2.9 Summary and Conclusions

A general discussion of the effects of cold working on the material properties was presented with emphasis on austenitic stainless steels, especially for cold-rolled Type 301. Test results on flat and corner materials for 1/4 and 1/2 hard Type 301 as well as annealed and strain flattened Type 304 austenitic stainless steels were presented. Design mechanical properties of 1/4 and 1/2 hard Type 301 stainless steel were recommended. An affine relation between normal and shear stress

strain curves was introduced to obtain the design properties in shear. An analytical expression for stress strain curves using the Ramberg Osgood formula was described. The topics presented in this chapter constitute the background of material properties for this investigation and the basic design mechanical properties for 1/4 and 1/2 hard Type 301 austenitic stainless steel. The results are summarized as follows:

(1) the most significant characteristics of cold worked austenitic stainless steel are: (a) high strength with increasing cold work, (b) pronounced anisotropy material properties with increasing cold working, stress strain curves being different in tension and compression and depending on directions, (c) inelastic stress strain curves with relatively low elastic limits especially in longitudinal compression.

(2) The strengthening effect produced by cold forming in the corners is the largest in the annealed state and decreases with increasing hardness of the sheet, becoming almost negligible for the full hard grades. For annealed and strain flattened Type 304, the ratio of .2% offset yield strength in corners to flats is largest in longitudinal compression and lowest in transverse tension being 2.52 and 1.63 respectively. For 1/2 hard Type 301, the ratio is the largest in longitudinal compression and lowest in transverse compression, being 1.33 and 1.05 respectively. The increase in ultimate tensile strength is relatively small for both cases. The corners were air press braked and with R/t ratio approximately equal to 2 (3 for specimens made from sheet 301-H-3).

(3) From a study of directionality of a 1/2 hard Type 301 sheet, an elliptical relationship between offset yield strength and direction was established, in both tension and compression. It is believed that such a relation may hold for other types of austenitic stainless under similar treatment.

(4) Although cold-rolled stainless steels are manufactured to specified minimum values of yield strength, the mechanical properties vary from coil to coil and heat to heat. A statistical approach was presented to account for the variation of offset yield strength in order to determine lower bound values for design. Three reliability criteria were investigated: 90% probability; 95% probability, and 95% probability with 95% confidence.

Based on a statistical evaluation of test results (from author's and three steel producers) and the values given in various specifications (Table 2-3), the following values of yield strengths (which are close to 95% probability statistical values) are recommended.

	1/4 Hard	1/2 Hard
Longitudinal Compression	50 ksi	65 ksi
Londitudinal Tension	75	110
Transverse Tension	75	100
Transverse Compression	90	120

(5) For simplicity, the initial modulus of elasticity may be taken as 27,000 ksi in tension and compression in the longitudinal direction for both 1/4 and 1/2 hard tempers, and

28,000 ksi in the transverse direction (Table 2-4).

(6) From the yield strengths and initial moduli established and the stress-strain curves prepared from author's tests, the typical normal stress-strain curves for design for flat sheet for both 1/4 and 1/2 hard Type 301 were constructed and summarized as shown in Fig. 2-10.

(7) Proportional limits of the typical stress strain curves for both 1/4 and 1/2 hard Type 301 according to different definitions are listed in Table 2-5. Stresses at which inelastic strain begins are used as proportional limits for buckling stress calculations, and slightly higher values are recommended for the case of bending.

(8) Secant and tangent moduli derived from the typical stress-strain curves are presented graphically in Figs. 2-11 and 2-12.

(9) Values of normal tensile ultimate strength from author's tests and certain publications are shown in Table 2-6. The ASTM value of 150 ksi for 1/4 hard is satisfactory, but for 1/4 hard, it may be raised from 125 ksi to 130 ksi.

(10) Ductility is indicated by the percentage of elongation in a two inch gage length; the ASTM values are recommended.

(11) Poisson's ratio may be taken as 0.31 for the structurally significant stress range in the longitudinal direction, and 0.34 in the transverse direction for both 1/4 and 1/2 hard Type 301.

(12) To obtain a shear stress strain curve, an affine relationship between the average normal stress-strain curve and the shear stress-strain curve was assumed. Such an approach was verified by the test results and satisfactory agreement was obtained. Stress affinity factor $\alpha = 0.577$ and strain affinity factor $\beta = 1.5$ are recommended for cold-rolled Type 301 austenitic stainless steel.

(13) The shear stress strain curves obtained by this approach for both 1/4 and 1/2 hard Type 301 are shown in Fig. 2-14. The proportional limits in shear are 11.50 ksi and 13.30 ksi for 1/4 and 1/2 hard respectively; and shear yield strengths are 41.8 ksi and 56.2 ksi.

(14) The initial shear modulus may be taken as 10,500 ksi for both 1/4 and 1/2 hard. The shear secant moduli are shown in Fig. 2-15.

(15) A modified Ramberg Osgood formula was shown to be applicable to cold-rolled Type 301 austenitic stainless as well as to annealed and strain flattened Type 304. Fitted analytical curves from experimental .2% and .05% offset strains and strengths showed satisfactory agreement with experimental data up to and slightly beyond the .2% offset yield strength. Coefficients of the formula were determined from the proposed design stress strain curves, and are shown in Table 2-8.

CHAPTER 3

BUCKLING AND WAVING OF PLATE STRUCTURAL ELEMENTS

3.1 General

The critical and post critical behavior of compression elements is a subject of major importance in thin walled steel where the individual components of the sections are generally very thin with large width to thickness ratios w/t. Therefore, adequate safety against failure by local buckling at the service loads is necessary. A similar situation occurs in aircraft construction in which local buckling is a chief design criterion.

It is universally recognized that the critical stresses determined by classic eigenvalue methods do not indicate the actual strength. Once the critical stress is reached, the plane flat plate merely deforms into a non-developable, wavy surface, but continues to resist increasing stress. In this case incipient buckling creates membrane stresses which are stabilizing and yield so called post buckling strength.

In considering the critical buckling stress of thin compression elements in design, the study of adequate strength reserve is important. Besides, the correlation of buckling stresses and the corresponding plate distortions (out of plane waving) should be studied.

The material considered in this investigation has anisotropic material properties and nonlinear stress strain re-

lations with relatively low elastic limits, especially in longitudinal compression. Therefore, an analytical approach to take inelasticity into account together with anisotropic material properties should be investigated.

In general, for thin walled metal design[1-1 and 1-7], compression elements may be divided into two main groups-stiffened elements and unstiffened elements. Stiffened elements are plates supported along both unloaded edges by thin webs or edge stiffeners. Unstiffened elements are supported along one unloaded edge and the other is free. These are the two types of compression elements considered in this investigation.

Experimental results of extensive test series of compression members and flexural members containing compression elements will be analyzed and compared with the predicted values.

3.2 Theoretical Buckling Stresses for Plate Elements

The elastic theory of isotropic plate buckling is well understood. Most isotropic elastic theories and applications have corresponding anisotropic or orthotropic theories. The elastic theory of anisotropic buckling is also rather well developed.

In taking the non-linear stress strain characteristics into consideration, many investigators have suggested approximate or more exact inelastic theories for the buckling of isotropic plates. For predicting stress for an isotropic

plate in the non-linear range the general equation can be shown as

$$\sigma_{cr} = \frac{k\pi^2 E\eta}{12(1 - \nu^2)\,(w/t)^2} \qquad 3\text{-}1$$

where η is the plasticity reduction factor, k is a coefficient of the boundary conditions, ν is poisson's ratio, and w/t is the width to thickness ratio.

The plasticity reduction factor η has been defined in many ways by various investigators. Bijlaard[3-1] and Ilyushin[3-2] made a rational analysis of stability of plates beyond the elastic limit based on a deformation type stress strain law and the octahedral plasticity law. Stowell[3-3] succeeded in developing a rational theory of inelastic buckling by using Ilyushin's general relations. He suggested different η values to be used for plates with various boundary conditions. Based on his analysis, the η value for a compressed plate is a function of E, E_s, and E_t.

A simpler approach was earlier suggested by Bleich[3-4]. He assumed orthotropic behavior of the plate when the critical stress lies above the elastic limit. This two modulus concept for inelastic buckling may be considered as an approximation of Stowell's[3-3] theory and gives $\eta = \sqrt{E_t/E}$ for stiffened elements. Figs. 2-3, 2-5, and 2-7 show the various η values as a function of stress. The value of η suggested by Stowell is lower than E_s/E and $\sqrt{E_t/E}$, but very close to $\sqrt{E_t/E}$.

On the other hand, the plastic theory for buckling of anisotropic material is only in an early stage of development. This fact was pointed out in a recent paper by Winter [3-5]. In view of the complexity of the inelastic buckling of isotropic plates, a rational inelastic anisotropic plate buckling theory is even more complex. It will be preferable if a simpler approach can be established in parallel with the general development of the inelastic theory of isotropic plates.

Along the same line as the general form of inelastic buckling theory for isotropic plates, the concept of a plasticity reduction factor may also be applied to the orthotropic case in order to obtain an approximate critical buckling stress analogous to the isotropic case.

a. Stiffened Element

For an elastic orthotropic plate with simply supported edges, the critical buckling stress which is derived from the equation in reference [3-6] is given as

$$\sigma_{cr} = \frac{\pi^2 E_1}{12(1-\nu_{21}\nu_{12})(w/t)^2} \left\{2[\sqrt{E_2/E_1} + \nu_{21} + 2\frac{G_{12}}{E_1}(1-\nu_{21}\nu_{12})]\right\} \quad 3\text{-}2$$

or

$$\sigma_{cr} = \frac{\pi^2 E_1 k'}{12(1-\nu_{21}\nu_{12})(w/t)^2} \quad 3\text{-}3$$

where $k' = 2[\sqrt{E_2/E_1} + \nu_{21} + 2(G_{12}/E_1)(1-\nu_{21}\nu_{12})]$

k' couples the effects of boundary conditions of unloaded

edges and the use of E_1 as an effective modulus. In the above equations, subscripts 1 and 2 indicate longitudinal and transverse directions.

E_1, E_2 = initial moduli in longitudinal and transverse directions respectively.

ν_{12}, ν_{21} = Poisson's ratios in longitudinal and transverse directions respectively.

G_{12} = shear modulus

A general form may be written as follows

$$\sigma_{cr} = \frac{\pi^2 E_1 k'' \eta'}{12(1-\nu_{21}\nu_{12})(w/t)^2} \qquad 3\text{-}4$$

where η' is the plasticity reduction factor for the inelastic buckling of orthotropic plates, and

$$k'' = F(E_1, E_2, G_{12}, \nu_{12}, \nu_{21}, \eta') \qquad 3\text{-}5$$

However, it is doubtful whether such equations will be used in design instead of the simpler form by Bleich suggested previously. Since the differences between the elastic constants in the longitudinal and transverse directions are relatively small for the present material at low stresses, the effects of the orthotropic material properties on the buckling stresses of the plate calculated by elastic analysis are not appreciable. This is evident from Eq. 3-2. At higher stress levels, not only the nonlinearity of the stress strain relationships should be considered in the formulation but also the differences of material properties in both the longi-

tudinal and transverse directions. However, it is realized that the tensile stress in the transverse direction of the plate is considerably smaller than that in the longitudinal direction, and in general is still in the elastic range. If the slight difference in initial moduli in the longitudinal and transverse directions is ignored, only the material properties in longitudinal compression need to be considered. Therefore, the Bleich's[3-4] two modulus concept and his inelastic buckling theory for an isotropic plate based on such a concept in the inelastic range is an approximation for stiffened elements. This is supported by the fact that the plasticity reduction factors suggested by Bleich and Stowell respectively, are very close for stiffened elements, as shown in Figs. 2-3, 2-5, and 2-7. The applicability of such an approach to the material considered will be verified later in this Chapter by a series of tests.

b. Unstiffened Element

The general form of Eq. 3-1 is applicable to unstiffened elements provided that proper consideration is given to boundary condition. For the same reason as above, the simplified method for inelastic buckling will be considered here for unstiffened elements. Based on Bijlaard[3-1] and Stowell's[3-3] conclusions, $\eta = E_s/E$ may be used for the case with one unloaded edge simply supported and the other free. This is an approximate value reduced from a more complicated expression which is a function of stress and moduli. The applica-

bility of such an approach to the material considered again will be verified by tests.

3.3 Buckling of Unstiffened Elements

A series of tests on compression members containing unstiffened elements will be presented and the test results will be analyzed and compared with the predicted values. The material was ½ hard Type 301 austenitic stainless steel. Analyses for Type 304 annealed and strain flattened stainless steel were made by Johnson[1-6].

3.3.1 Unstiffened Compression Member Tests

3.3.1.1 Design and Fabrication of Test Specimens

Four short compression members were tested. Local buckling of the unstiffened elements was the primary consideration in their design. The w/t ratios of the unstiffened elements in this series ranged from 11.02 to 49.21. The cross section of the specimen is shown in Fig. 3-1. The dimensions of the cross sections and related properties are shown in Table 3-1.

Each compression member was made by placing two channel sections back to back to form an I section. The dimensions of the outstanding flanges, were determined by w/t ratios. The dimensions of the webs were so chosen that the webs are fully effective throughout the loading range. The length of the specimen was so determined that over all column buckling will not occur. Integrity of the sections was insured by bonding the channels with a structural adhesive.

All specimens were formed on a press brake by a process identified as air forming. The edges were parallel to the rolling direction of the sheet.

The ends were ground flat and parallel to each other, as well as perpendicular to the longitudinal axis. The lapping compound used was 300 grain boron carbide abrasive.

3.3.1.2 Instrumentation

Type A-12 strain gages were used. All gages were paired on both faces of the flange except the ones near the web of specimen H301 UE-1. The gage locations are shown in Fig. 3-1. These gages were placed at mid-length of the specimen.

Eight gages were located at the four free edges of the flanges (unstiffened elements) so that determination of buckling of the unstiffened elements can be made by using these four pairs of gages.

Another four pairs of gages were placed at the inner edges of the unstiffened elements. One additional pair of gages was located at the center of the web. From these the strain (inner edge strain) corresponding to the maximum stress in the section could be determined.

The shortening of the whole compression specimen was measured by a pair of dial gages. The lateral deflection was measured by a dial gage at the mid-length of specimens H301UE-2, 3, and 4.

The out of plane waving was measured by the device shown in Fig. 3-2.

3.3.1.3 Test Set-Up and Testing Procedure

All specimens were loaded in a 30,000 pound screw type testing machine. The loads at the beginning and end of the strain readings were recorded and averaged. The dial gages were read in the middle of the strain readings. The out of plane waving measurements were made after the completion of strain and dial gage readings. Small load increments were used in the neighborhood of the critical buckling load.

The specimens were tested between fixed plates as shown in Fig. 3-1. Hardened and ground flat plates were used in direct bearing on the flat ends of the specimens. Hydrostone was used between these plates and the plates of the testing machine to ensure complete bearing over the entire area of the specimen. During the drying period of the hydrostone, a slight setting load was applied to ensure perfect contact. This procedure will eliminate any deviation from parallel of the two ends of the specimen.

3.3.2 Criteria for Critical Strains and Buckling Stresses

It is difficult to determine the critical buckling strains of thin plate elements in compression experimentally. This is because of the characteristics of the buckling phenomenon of such elements. When the bifurcation load is reached in a compressed thin plate, it continues taking increasing load into the post buckling range and exhibits no clear physical changes such as those observed in the case

of columns. However, such a bifurcation situation may be detected from paired strain gages readings or from out of plane waving measurements.

Three criteria[1-6] were considered and used to determine the buckling strains of unstiffened elements from the strain readings in the paired gages at the free edges of unstiffened flanges. The corresponding critical stresses were determined from the experimental stress strain curves of flat sheet from which the specimens were sampled (301-H-3). The critical strains and corresponding loads determined from these criteria were averaged to give a single value. In general, the buckling load level is the same for four paired gages.

Strain Deviation Method

The critical strain is taken as the strain at which the strain increment for one of a pair of gages begins to decrease. The strain determined from this criterion represents a situation in which the stress distribution across the thickness of the plate element is beginning to change from uniform compressive stress to a state of combined compression and bending. This gives an indication that initiation of buckling is started. The critical strain obtained from this criterion is the lowest among the three criteria.

Maximum Surface Strain Method (Strain Reversal Method)

This method was described by Hu et al[3-7] and was termed strain reversal method. By this method, the critical

strain is taken as the maximum compressive strain on the convex side of the plate element, beyond which this strain begins to decrease. The critical strain obtained from this method is higher than that from the strain deviation method.

Maximum Membrane Strain Method

This method was used by Jombock and Clark[3-8]. The critical strain is taken as the maximum of the average of the strains in the paired gages. It indicates that the increment of compressive membrane strain is zero and the membrane strain has reached its maximum value. At this point, a considerable amount of bending and waving is involved and the direct stretching of the thin plate is beginning. The critical strain from this method is generally the highest among three.

3.3.3 Discussion of Results-Buckling Stresses

The critical strains and corresponding stresses for the specimens tested obtained by applying the criteria in 3.3.2 are shown in Table 3-2. The stresses were determined from critical strains by using the stress strain curve of flat material. In general, the critical strains and stresses are the lowest by strain deviation method, and highest by maximum membrane strain method. The maximum surface strain method yields values somewhere in between these two but close to the maximum membrane strain method.

The theoretical critical stresses may be calculated on the basis of $\eta = E_s/E$; from Eq. 3-1 Poisson's ratio may be

taken as 0.31 in the elastic range. The edge condition varies from simply supported to fixed, which corresponds to 0.425 and 1.28 respectively for k values in Eq. 3-1. Considering the theoretical treatment of unstiffened elements as part of H sections by Stowell[3-9] and Bleich[3-4], the k values evaluated from the specimen dimensions range from 0.88 to 1.16 with an average of 1.03. The individual values are shown in Table 3-3. A single value may be used for this case, taking it as 1.03.

However, another situation should be considered, i.e. the nonhomogeniety of the layer of epoxy in the web and the noncontinuity between two unstiffened elements because of corner radii. Therefore, the actual k value must be smaller than the values calculated from H sections. If the channel alone is considered, the k values obtained by the same method range from 0.44 to 0.89 with an average of 0.67. It seems that the actual boundary condition is between these two extremes (H section and channel section). If the average value of k is taken of these two cases, the k values range from 0.658 to 1.024 with an average of 0.85.

Theoretically, the unstiffened elements will buckle into one half wave if the supported edge is simply supported. However, for the specimens tested, the number of half waves observed was more than one, which indicates that the unstiffened flanges are restrained by the web plate.

In order to determine the amount of edge restraint along the unloaded edge, useful information may be obtained from

the wave number or length. On inspection of the wave form, it appears that differences in the wave length and the location of the nodes can occur in the same specimen for different loads in excess of the buckling load. However, the approximate average wave number and wave length for the unstiffened flanges can be determined from observation. Theoretically, the number of half waves which should occur for the specimens tested, can be calculated. The effects of inelasticity which reduces wave length should be taken into account. The analysis taking inelasticity into account on unstiffened elements was reported by Bleich (Ref. 3-4, p. 329, Eq. 649). The analysis was made for the specimens tested for two extreme cases simply supported and fixed unloaded edge. The number of waves was determined from the limit of transition from m to m+1 waves and the length to width ratio of the unstiffened plate of the specimens.

Table 3-4 shows the experimental number of half waves for each specimen. Table 3-5 shows the comparison between the experimental and the calculated number of half waves. Theoretical number of half waves were calculated for the fixed edge condition, for simply supported edge condition, the number of half waves is 1. It is seen that the observed number of half waves falls between the calculated values for fixed edges and simply supported edges. If one compares the experimental to the calculated half waves in Table 3-5, it seems that the use of averaged k values calculated from H and channels sections in Table 3-3 is reasonable.

Furthermore, a single approximate k value of 0.85 may be used for the specimens tested.

Carbon and annealed stainless steels design specifications[1-1,1-7] take the conservative value as 0.5 for all types of boundary conditions at the supported edge. Theoretical critical stresses were calculated here for k = 0.5, 0.85, and 1.03. The plasticity reduction factor E_s/E for 301-H-3 shown in Fig. 2-5 was used. The calculated and experimental critical stresses are compared in Table 3-6, 3-7, and 3-8.

In Table 3-6, where k = 0.5, the ratio of the calculated to the experimental critical stress averages 1.11 for the strain deviation method, 1.45 for the maximum surface strain method, and 1.64 for the maximum membrane strain method. This indicates that the coefficient of 0.5 is too conservative. In Table 3-7, k = 1.03, the average ratios are 0.614 for strain deviation method, 0.789 for maximum surface strain method, and 0.889 for maximum membrane strain method indicating that k = 1.03 is too high. Using k = 0.85, Table 3-8 shows the average ratios for the calculated to the experimental critical stress of 0.712 for the strain deviation method, 0.912 for the maximum surface strain method, and 1.066 for the maximum membrane strain method, indicating satisfactory agreement.

Fig. 3-2 shows a typical load vs. strain diagram for the paired gages at the free edge of an unstiffened element. In the same figure, the corresponding typical load vs. wave amplitude curve is also presented. In the figure, d is half

the wave amplitude; L is the half wave length; and t is the thickness of the sheet. The determination of buckling load by using a waving parameter $(d/L)^2$ is discussed in the following Section. It appears that the critical load determined by the surface strain method shows a better indication of the bifurcation situation than the other two methods. The critical stresses of the specimens tested by using the maximum surface strain method are compared with the three buckling stress curves based on k = 0.5, 0.85 and 1.03 in Fig. 3-3. Satisfactory agreement is seen between the experimental critical stress and the buckling curve based on k = 0.85 and $\eta = E_s/E$.

In Fig. 3-3, the maximum failure stresses at the supported edge σ_{max}, the average member failure stresses (failure load divided by the full cross sectional area P_f/A), and the average element failure stresses (failure load carried by the unstiffened elements divided by the area of these elements P_{fl}/A_f) are also plotted.

The differences between buckling stress and average stress at failure increases with increasing w/t ratios. It is also seen that the actual maximum edge stress at failure for all members are around the .2% offset yield strength of the longitudinal compression stress strain curve. It seems that there is a close correlation between average failure stresses and the w/t ratio of the unstiffened elements. These failure stresses are listed in Table 3-9. The failure loads and the loads at which local distortion becomes visible are also presented. It is seen that considerable

strength is available beyond the visible waving load. In order to take some of this strength into account, it is necessary to study the correlation between waving and local buckling. This is presented in the next Section.

3.3.4 Waving of Unstiffened Elements

Fig. 3-4 shows the plots of load vs. the ratio of wave amplitude to the thickness of the sheet t of the specimens tested. The amplitude increases appreciably when the critical load is reached. The rate of growth of out of plane waving with load gradually reduces because of stabilizing membrane stress. The rate of growths increases again when the failure is approaching. Slight waving due to initial imperfection can be recognized from the plot at loads below the buckling load. The initial imperfection of the specimens tested is a small amount being around 0.05t where t is the thickness of the sheet. The maximum amplitude of out of plane waving can be as high as 3.8t at failure for specimen H301UE-4 which has the largest w/t ratio, 49.21, among the specimens tested. The plot also shows that the large amount of post buckling strength available is accompanied by relatively sizable out of plane waving.

Based on the curves presented in Fig. 3-4, the load at a specified amount of waving amplitude (for example, thickness of sheet) may be determined.

When the waving of compressed flanges becomes visible, it is a clear indication of buckling. The cccurrence of wav-

ing was carefully observed under reflected light during test. The loads so determined are in general slightly higher than those determined by the strain deviation method, but slightly lower than determined by the maximum surface strain method. These loads are presented in Table 3-9.

The buckling load may also be obtained by considering such out of plane waving by using a similar approach as the Southwell plot[3-10]. The characteristic parameter of waving in the post buckling range is the ratio of waving amplitude to wave length of the buckling pattern, i.e. d/L which will govern the behavior of the plate. Because the load in the plate must be independent from the sign of the waving amplitude, the load in the plate may be expressed by

$$P = P_{cr} (1 + a_2(d/L)^2 + a_2(d/L)^4 + \ldots), \qquad 3\text{-}6$$

where P and P_{cr} are total and critical load respectively, a_i are constant parameters. For loads barely in excess of the buckling load, the contribution from the high power terms is very small. Only the first two terms may be considered and the relation between load, P, and $(d/L)^2$ will be substantially linear and the intersection with the load axis will give the experimental buckling load. The experimental amplitude of waving and half wave length are determined directly from test results which are shown in Fig. 3-4 and Table 3-4 respectively. In this investigation, the waving amplitude and the half wave length are the average measured values

from four unstiffened elements. The critical loads of the specimens tested determined by waving consideration are plotted in Fig. 3-4 and listed in Table 3-10.

The similar method was used by Botman and Besseling[3-11] and by Yoshiki and Fujita[3-12].

In order to relate the stresses which cause waving to the measured critical stresses determined from critical strain, a comparison of loads determined by the various methods are presented in Table 3-10 along with the corresponding average stresses. From this table, correlations between buckling loads determined by strain considerations and waving loads are of interest. The loads at which waving was visible are slightly larger than the loads determined by the strain deviation method but close to the maximum surface strain method. This observation supports the use of the maximum surfaces strain method as the critical strain criterion.

Based on this information, the average stresses obtained from the loads determined by various considerations may be correlated with the calculated critical stresses by using Eq. 3-1 with $k = 0.85$ and $\eta = E_s/E$. Such a comparison is shown in Table 3-11. The average stresses are divided by the calculated critical stresses. The ratio for the maximum surface strain method ranges from 0.932 to 1.102 with an average of 0.987. The ratio of the strain deviation method is 0.716. The waving is visible when the average ratio is 0.892. If slight waving is allowed (thickness of sheet) the allowable stress may be as high as 1.243 times the cal-

culated critical stress. This information is useful for formulating design criteria for allowable stresses related to out of plane waving.

3.3.5 Summary and Conclusions-Unstiffened Elements

The critical buckling phenomena of unstiffened elements have been discussed. Inelastic buckling theories have been described briefly. In order to verify the analytical critical stresses a series of compression members containing unstiffened elements was tested. The waving amplitude of unstiffened elements was also studied experimentally. Although a thin element may buckle at a relatively low stress depending upon the w/t ratio, it merely deforms into a nondevelopable, wavy surface, and continues to resist increasing stress. Due to the pronounced out of plane waving the usefulness of unstiffened elements in the post-buckling range may be limited. In order to take part of the post critical strength into account, a study of correlation between buckling and local distortion was made.

The results of this investigation are summarized as follows:

(1) Three criteria for determining critical strains from the experiment were discussed. Based on test evaluation, the maximum surface strain method was found to be the most reliable to determine critical strains. (The critical strain determined by this method is the maximum strain on the convex side of the thin element.) This method was therefore adopted.

(2) For calculating inelastic critical stresses it was found that the Bleich's two modulus concept and his inelastic buckling theory is a usable approximation.

(3) With proper boundary conditions along the longitudinal edges, the calculated critical stresses showed satisfactory agreement with the experiments. In general, the experimental critical stresses are slightly lower than calculated. It is concluded that Eq. 3-1 may be used for predicting the buckling stresses of unstiffened elements of cold-rolled Type 301 stainless by using $\eta = E_s/E$ as plasticity reduction factor.

(4) Based on the test results, it seems that the effects of anisotropic material properties on the buckling phenomena of unstiffened elements are small.

(5) Based on the comparison between buckling stresses and average element failure stresses in Fig. 3-3, considerable post critical strength is available which is highly dependent upon width to thickness ratio.

(6) For cold-rolled stainless, the ultimate carrying capacity of an element is considerably higher than for annealed grades (comparing Table 3-9 with Table 3-8 of Ref. 1-6), but it is accompanied by a larger amount of local distortion due to the high strain involved. If waving is severely restricted, there is no advantage in using tempered grades for unstiffened elements with large w/t ratios.

(7) Due to a comparatively large amount of local distortion, adequate safety against excessive local distortion at service load must be considered as a design criterion.

(8) Correlation between local buckling and specified amount of waving is shown in Table 3-11. The allowable stress for a specified amuont of local distortion may be expressed as critical stresses multiplied by a factor. If either no visible waving or slight waving (equal to the thickness of the sheet) is permitted, the corresponding allowable stresses can be taken as 0.8 and 1.2 times the calculated buckling stress, respectively.

(9) With the information shown in Tables 3-9 and 3-11, design allowable stresses may be established. This will be discussed in Chapter 6.

3.4 Buckling of Stiffened Elements

Stiffened elements are supported along two unloaded edges by webs or edge stiffeners. The stiffened elements studied herein are compression flanges of flexural members with hat cross-section, and flanges of compression members formed by connecting two hat sections.

3.4.1 Compression Flange of Flexural Members

3.4.1.1 Design and Fabrication of Test Specimens

A series of flexural tests were performed for both Type 301 ¼ hard and Type 304 annealed and strain flattened stainless steels. Similar tests for Type 304 annealed and strain flattened

stainless steel were made by Johnson[1-6] but the critical buckling phenomena of the compression flange were not studied.

Incipient local buckling of the stiffened compression flange was the primary consideration in the specimen design. Four specimens were designed of ½ hard Type 301 stainless with w/t ratios ranging from 24.8 to 150.3. The corresponding critical stresses cover a range from yield strength down to very low stress (4.4 ksi) in the elastic range. Three specimens were designed for Type 304 annealed and strain flattened stainless with w/t ratios ranging from 71.52 to 150.18. Eq. 3-1 was used for critical buckling stress calculation with appropriate plasticity reduction factor.

The remaining dimensions of the specimens were chosen so that the compression yield strength would be reached in the compression flange while the stress in the tension flange was lower than the tensile yield strength. The webs were also checked by approximate method for shear stability and were found to be stable. The span length was taken as 44" based on deflection and web crippling considerations. The dimensions and related information are shown in Table 3-12. The notations of the cross section and the test set-up are shown in Fig. 3-5.

Diaphragms were placed between the webs of the flexural members at supports and loading points to prevent deformations of the cross-section. This also increases the strength against web crippling. Clips were also added to the ten-

sion flange at supports and loading points to maintain the section geometry.

All specimens were formed in the same manner as that for unstiffened compression members.

3.4.1.2 Instrumentation and Testing Procedure

Locations of the strain gages for the specimens are shown in Fig. 3-6. Strains at the edges of the flanges were measured by SR-4 single wire gages, placed in pairs on the top and bottom surfaces of the flanges. Paired small foil strain gages were placed transversely to measure Poisson's effect. The membrane and bending strains in the center portion of the compression flange were measured by paired three-element foil gages forming a rosette. At a distance of 0.8w from midspan along the center line, another two pairs of foil gages were placed perpendicular to each other. For specimen H301F-4, at midspan two extra pairs of foil gages were located in the same direction as the edge gages at a distance of w/3 from the center line in order to measure the longitudinal strains at that location.

Mid-span deflections were measured by a pair of dial gages at the inner edges of the tension flanges. The dial gages were supported by a frame which was fixed to the base beam. The relative movement of the center of the base beam was negligible.

The local waving amplitude of the compression flange was measured by dial gages mounted on a movable bridge which al-

lows measuring the waving amplitude relative to the edges of the flexural specimens. By this arrangement, the local waving amplitude is separated from the deflection of the flexural specimen. Such a device is shown on Fig. 3-7.

The test set-up was shown in Fig. 3-5. The load was applied at the center of the loading beam which transmitted the load through two welded columns to the specimen as quarter points loading. The specimens were loaded in a 60,000 pound BTE universal testing machine.

The loads at the beginning and end of strain readings were recorded and averaged. The dial gage readings were made in the middle of the strain readings. The waving measurements were made after the completion of the strain and deflection readings. The specimen was considered as having failed when the load started to drop off. Small increments were used in the neighborhood of the critical buckling load so that a good determination of experimental buckling load was achieved.

3.4.2 Flanges of Short Columns with Closed Cross-Section

A series of flexural tests have just been described. However, it was realized that these high strength beams develop large curvatures which produce inward deflections of the compression flanges. Under such conditions, the compression flange is actually a doubly curved shell rather than a flat plate. Such a doubly curved shell is stronger than a flat plate.

In order to obtain a better experimental determination of buckling stresses by avoiding the bending deformation involved in the flexural members, a series of short column tests containing stiffened elements was performed. The stiffened elements have the same w/t ratios as the compression flange of the flexural members. Since the curvature induced in the flexural members of low strength annealed and strain flattened Type 304 is much smaller than for cold-rolled grades, only cold-rolled Type 301 are concerned herein. No similar column tests were made on Type 304.

3.4.2.1 Design and Fabrication of Test Specimens

Each column was made by putting two hat sections together to form a closed tube. The dimensions of the cross section were so chosen that the webs and the outstanding lips are fully effective throughout the loading range. The length of the column was so determined that overall column buckling will not occur. Only the stiffened flanges of two hat sections were allowed to buckle locally. The dimensions of the specimens are shown in Table 3-13, and the cross section of the specimen is shown in Fig. 3-8. Integrity of the section was insured by bonding the hat section with the same structural adhesive as for unstiffened elements.

The procedure of preparation of the specimen was the same as for unstiffened elements.

3.4.2.2 Instrumentation and Testing Procedure

SR-4 gages were used. The gage locations are shown in Fig. 3-8. Most of the gages were paired on both faces

of the sheet. Foil type gages, 1/8" long, were used in the middle of the stiffened elements, and 1" long wire gages were used at all other locations.

Gages located at the corners of the stiffened elements and at the parts which are fully effective during loading were used to indicate the strain of the specimen. Gages located in the middle of the stiffened elements were used for buckling determination.

Lateral deflection was measured by using dial gages attached to the edges of the stiffened elements near the mid-length of the specimen.

Out of plane waving measurements were also made by using the described device.

The general testing set-up as well as the testing procedure was similar to that for unstiffened element columns.

3.4.3 Discussion of Results-Buckling Stress

The theoretical critical stresses are calculated from Eq. 3-1 by using $\eta = \sqrt{E_t/E}$ as the plasticity reduction factor. Poisson's ratio is taken as 0.31. The edge condition may vary depending upon the relative dimensions of the cross section. The k values in Eq. 3-1 may vary from 4.0 for simply supported edges to 6.98 for the fixed edges. The exact boundary condition of the unloaded edges of the compression flange is difficult to determine. The amount of restraint given by the webs to the compression flange is uncertain. The upper part of the web is under varying com-

pression stresses and the lower part of the web is under tension which acts stabilizing.

Under these conditions, the actual restraint offered to the compression flange by the web may be close to that of an identical rectangular tube under uniform compression. If this is so, the k value in the buckling equation will be around 5.27 for all specimens (varying from 5.00 to 5.47). There is an exact solution of this problem by Lundquist[3-9] and an approximate solution by Bleich[3-4].

Based on a comparison of theoretical and experimental evidence from waving shown in Tables 3-4 and 3-5, it seems that the actual boundary condition may be close to the simply supported case but with a slight restraint from the webs. Experimental wave length and number of half waves for the stiffened compression flanges of flexural members and short columns are shown in Table 3-4. A comparison between experimental and calculated number of half waves is shown in Table 3-5. The theoretical number of half waves were calculated from Bleich's analysis (Ref. 3-4, p. 322, Eq. 639) considering inelasticity for two cases-simply supported and fixed unloaded edges. It is seen that the observed number of half waves is considerably closer to the simply supported than to the fixed case. It seems that the restraint estimated by considering the section as a rectangular tube under uniform compression is overestimated.

For purposes of comparison, the theoretical critical stresses were calculated from Eq. 3-1, taking k = 4.0 and 5.27.

The critical strains and the corresponding stresses for the specimens tested were obtained from the same critical strain criteria as for unstiffened elements. These critical strains and stresses are presented in Table 3-14 for the compression flanges of flexural members (H301F and AS304F series) and the stiffened flanges of short columns (H301SC series).

By comparing the experimental critical strains and stresses of short columns and the corresponding flexural members (H301SC-2 and H301F-2, H301SC-4 and H301F-4), the values for short columns are seen to be smaller than those for flexural members. As discussed, the compression flange of a strongly deflected beam is actually a doubly curved shell rather than a flat plate. The critical buckling strain and stress will be higher for the shell than for the flat plate. An approximate analysis of such distortion was made by Winter[3-13] for similar flexural members. For short columns, there is no such curling effect. It appears that the curling in the compression flange of a high strength flexural member may be partly responsible for the higher experimental buckling strain and stress than of a short column.

The experimental and theoretical critical stresses for the specimens tested are compared in Tables 3-15 and 3-16. In Table 3-15, the calculated values are based on simply supported edges with $k = 4.0$. The average ratios of exper-

imental to calculated stress for ½ hard Type 301 elements are 0.94, 1.20 and 1.26 by strain deviation, maximum surface strain, and maximum membrane strain methods respectively. For Type 304 elements the ratios are 0.90, 1.03, and 1.30. The experimental buckling stresses by the previously adopted maximum surface strain method are higher than calculated. For Type 304 annealed elements, the corresponding ratio is lower, viz. 1.03. It seems that the high strength, which causes more curling in the compression flange, does increase the buckling stress.

In Table 3-16, the calculated values are based on k = 5.27. The average ratios of experimental to calculated stress for Type 301 ½ hard elements are 0.76, 0.97 and 1.00 by the strain deviation, the maximum surface strain, and the maximum membrane strain method respectively. The corresponding ratios for Type 304 annealed elements are 0.74, 0.83, and 1.06. These low ratios indicated that the edge restraint may be slightly overestimated. The slight curling effect, which has been confirmed by short column tests, does not seem to be shown by these low ratios.

The critical buckling stresses obtained by the maximum surface strain method are plotted in Fig. 3-9 along with the theoretical buckling curve with k = 4.00 and k = 5.27 for comparison purposes. The buckling curve is derived for 301-H-7. The buckling stresses for H301F-3 and H301F-4 are in the elastic range so that the experimental buckling

stresses of these two specimens can also be plotted in the same figure although the specimens were made from another sheet 301-H-3. The longitudinal compressive initial moduli of the two sheets are very close. The buckling curves derived from sheet 304-AS-5 and the experimental buckling stresses are also presented in the same figure.

Based on the foregoing discussion, it appears that the longitudinal edges are close to the simply supported condition. The curling in the stiffened compression flange of the flexural member does increase the buckling stress.

3.4.4 Waving of Stiffened Elements

Measurements of out of plane waving relative to the longitudinal edges were made for the compression flanges of flexural members and short columns. Plots of load vs. the ratio of wave amplitude to sheet thickness were made. The growth of the waving amplitude shows a trend similar to that of the unstiffened elements. However, the rate of growth and the magnitude of waving for stiffened elements are smaller than for unstiffened elements.

The maximum initial imperfection encountered was around 0.9t for one specimen with w/t of 150. The amount is much smaller for lower w/t ratios. This initial imperfection is believed to be partly responsible for low experimental critical stresses for specimens with large width to thickness ratios (H301F-4, H301SC-4, and AS304F-4).

Various characteristic waving loads can also be determined in the same manner as for unstiffened elements. These loads are compared with the loads determined by the critical strain criteria in Table 3-17. The observed waving loads are very close to the loads determined by the maximum surface strain method. For stiffened elements, the local distortion is less pronounced than for unstiffened elements. This explains why the observed waving loads for unstiffened elements are slightly lower than the loads determined by the maximum surface strain method. The critical loads determined by the waving parameter plot agree very well with the critical loads determined by the maximum surface strain method. Again, the same as for unstiffened elements, the load at which wave depth equals thickness is close to the load determined by the maximum membrane strain method. Based on the foregoing comparison between waving loads and buckling loads, the correlation between waving magnitude and the calculated buckling stress (Eq. 3-1 with $k = 4.0$ and $\eta = \sqrt{E_t/E}$) may be established qualitatively by using the information shown in Table 3-15. If either no visible waving or slight waving (equal to the thickness of sheet) is permitted, the corresponding stresses can be taken as 0.9 and 1.2 times the calculated buckling stress, respectively. This information is useful, if local distortion of the stiffened plate element is of major concern in design.

It is mentioned that the local distortion of stiffened elements is less pronounced than for unstiffened elements.

Considerable post critical strength is available and useable. It is of interest to see the comparison between the failure load and the observed waving load of the specimens tested. Such a comparison is shown in Table 3-18. For flexural members, the ratio of failure load to waving load was as high as 6.84 for H301F-4. For short columns, the ratio was high as 9.78 for H301SC-4.

In Table 3-18, it is of interest to notice that the ratio of failure load to waving load for cold-rolled Type 301 specimens is much higher than for Type 304 annealed and strain flattened specimens (with practically the same dimensions, H301F-3 and AS304F-2, H301F-4 and AS304F-4). This indicates that cold-rolled stainless possesses much larger post critical strength although it will be accompanied by larger deformation and local distortion.

3.4.5 Summary and Conclusions-Stiffened Elements

The critical buckling phenomena of stiffened elements have been discussed. Inelastic buckling theories have been described briefly. A series of flexural members containing a stiffened element as the compression flange for both cold-rolled Type 301 and Type 304 annealed and strain flattened was tested to verify the predicted values. Two short columns with stiffened flanges (with a similar w/t ratio as for the flexural members) were also tested to detect any influence of curling of the flexural members on the buckling behavior. The local distortion of stiffened elements is less

pronounced than for unstiffened elements with much larger useable post critical strength.

The results are summarized as follows:

(1) The maximum surface strain method can be applied to stiffened elements for determining experimental critical strains and stresses.

(2) Based on the same reason as for unstiffened elements, Eq. 3-1 was used for predicting the inelastic buckling stress, using $\eta = \sqrt{E_t/E}$ as the plasticity reduction factor.

(3) Considering simply supported boundary conditions, the calculated critical stresses are generally slightly lower than those from the experiments. It is believed that this is due to following reasons: (a) curling in the compression flange of flexural members, (b) slight restraint from the webs, and possibly (c) anisotropic material properties at high stress (longitudinal compression being the weakest). However, Eq. 3-1 with $k = 4.0$ may still be used conservatively for cold-rolled Type 301.

(4) The short column tests confirm that the curling does increase slightly the buckling stress of the stiffened compression flange of a flexural member, especially for cold-rolled stainless with large curvature.

(5) Based on a comparison of critical loads determined by various critical strain and waving considerations, the correlation between waving magnitude and calculated buckling stress may be established. Such information is shown

in Tables 3-15 and 3-17. If either no visible waving or slight waving (equal to the thickness of the sheet) is permitted, the corresponding stresses can be taken as 0.9 and 1.2 times the calculated buckling stress respectively. This is useful, if local distortion of plate is of major concern in design.

(6) The local distortion of stiffened elements is less pronounced than unstiffened elements. Considerable post critical strength is available and usable. This is in contrast to unstiffened elements. An interesting comparison may be made between member carrying capacity and waving load, which will give an indirect indication of post critical strength of stiffened elements. For flexural members, the ratio of failure load to waving load was as high as 6.84 for H301F-4. For short columns, the ratio was as high as 9.78 for H301SC-4.

(7) Comparison of the ratios of failure load to waving load of cold-rolled and annealed flexural members in Table 3-18 indicates that cold-rolled stainless possesses much larger post critical strength although it will be accompanied by larger deformation and local distortion.

CHAPTER 4

POST BUCKLING BEHAVIOR OF PLATE STRUCTURAL ELEMENTS

4.1 General

After the buckling stress is reached, compressed plate elements merely deform into a nondevelopable wavy surface and continue to resist an increasing load. Fig. 4-1 shows the buckled stiffened and unstiffened elements under compression supported by the webs along the unloaded edges. Considerable post buckling strength is available for such elements. The failure of the member may finally be induced by yielding for a sharp yielding material, and by large plastic deformation or by geometrical change for a gradual yielding type material.

Theoretical and semi-empirical methods to predict such post buckling behavior of plate elements will be discussed in this Chapter. Post buckling strength evaluated from the series of experiments presented in Chapter 3 will be used to verify some of the existing theoretical treatments.

4.2 Effective Width Concept

The concept of effective width for the post buckling strength of a buckled plate has long been used in both aircraft and thin walled steel structures. This approach provides a practical method for purposes of design.

Structural members containing buckled compression flanges are shown in Fig. 4-1. Once the plate element buckles, the stresses in the plate elements redistribute across the width;

the stresses along the longitudinal edges are the highest. In order to explain this redistribution of stress explicitly, strain distributions across the width of such plate elements from experiments are shown in Fig. 4-2. The strains at various locations across the width of the plate element were measured at several loading levels. The stresses can easily be obtained from these strains by means of stress strain curves. The distribution is uniform until the local buckling occurs. Under higher load, on the other hand, the membrane strain at the free edge of the unstiffened element and at the center of the stiffened element even turns into tension rather than compression. This tension stress and the membrane tension stress in the transverse direction of the plate influence considerably the post buckling waving patterns and behavior of these elements.

Such a nonuniform stress distribution across the width of the buckled plate elements is commonly replaced by an uniformly distributed stress equal to the maximum edge stress, on the effective part of the plate, as shown in Fig. 4-2(c). The solid lines are the actual stress distribution, while the dashed lines indicate the equivalent uniform stress distribution over an effective width such that

$$\sigma_{max}\, bt = \int_{-\frac{w}{t}}^{\frac{w}{2}} \sigma t \, dy \qquad 4\text{-}1$$

where b is the effective width, σ_{max} is the maximum supported edge stress, σ is the membrane stress, and w is the width of the element.

4.3 Theoretical and Semitheoretical Evaluation of Effective Width

Two theoretical approaches are available for the analysis of the post buckling behavior of flat plates. The first is the general direct energy method. The second is to solve the general Karman's large deflection differential equations. These are two nonlinear differential equations, which may also be obtained from the energy expression as the variational problem. This rigorous solution of Karman's equations is not feasible because of the nonlinear characteristics of the equation, but approximate solutions may be obtained.

Cox[4-1 and 4-2], Marguerre[4-3, 4-4, and 4-5], and Koiter[4-6] approached the problem by using the energy approach. Many other investigators obtained a solution from Karman's large deflection equations, such as Levy[4-7], Hemp[4-8], Coan[4-9], Yamaki[4-10], Stein[4-11]. Most of these solutions are of an approximate nature.

All of the above mentioned investigators assume elastic behavior of the plates. There were only few investigators who considered the inelastic effect on the post buckling behavior of plates. Stowell[4-12] used the deformation theory of plasticity, derived from an expression for the average stress in a buckled plate in the inelastic range. Using a variational approach and deformation theory of plasticity, Mayers and Budiansky[4-13] made an investigation of the elastically buckled plate, which enters into the plastic range. Sujata[4-14] studied stiffened plates at plastic buckling. The anisotropic

material properties in the inelastic range were taken into account. From this work, he concluded that the results obtained by the elastic assumption constitute a lower bound.

As a continuation of Coan's work, Yusuff[4-15] modified Karman's large deflection equations, taking orthotropic material properties and initial deflection into account. Schultz [4-16] showed that the post buckling behavior of orthotropic plates is analogous to isotropic plates.

Because of the rapid development of systematic matrix analysis by using electronic computers the problem under consideration may be solved by the finite element approach. The fundamental formulation of the method is quite well developed. The general approach to deal with a nonlinear problem, caused by either nonlinear material properties or large deformations and geometrical changes, was summarized and outlined by Zienkiewicz[4-17]. A detailed outline of the method was reported recently by Mallett and Marcal[4-18]. The elastic post buckling behavior of a flat plate was investigated by Schmit, Bogner, and Fox[4-19], taking into account geometric nonlinearities, while retaining the flexibility of application characteristic of the discrete element structural analysis method.

From the literature survey just presented, it is concluded that the theoretical treatment of post buckling behavior of anisotropic plates has not yet been investigated extensively, neither has the case with nonlinear stress strain relationships. The problem combining both effects has not yet been considered rigorously in the theoretical treatment.

In order to provide a useful method for design, a simplified approach will be followed. One of the most important studies of post buckling strength and effective width was the semi-theoretical analysis by Karman[4-20]. In his derivation the non-uniform stress distribution in a simply supported buckled plate was replaced by two uniformly loaded effective strips as shown in Fig. 4-2(c). Through his assumption of wave shape and minimization of σ/E with respect to wave length, the following relation of effective width was found,

$$b = [\pi / \sqrt{3(1 - \nu^2)}] \sqrt{E/\sigma}\, t$$

or

$$= C \sqrt{E/\sigma}\, t \qquad 4\text{-}2$$

where σ is the supported edge stress.

Hence the maximum load which may be sustained by the plate is:

$$P_u = [\pi/ \sqrt{3(1 - \nu^2)}] \sqrt{E\sigma_y}\, t^2 \qquad 4\text{-}3$$

Through this derivation, Karman was able to show that the ultimate load is proportional to $\sqrt{E\sigma_y}\, t^2$; the constant is to be found for different boundary conditions. Donnel and Sechler[4-20] rewrote Eq. 4-3 as follows to account for the boundary condition:

$$P_u = C \sqrt{E\sigma_y}\, t^2 \qquad 4\text{-}4$$

for a simply supported case with $\nu = 0.3$ and C equals 1.9. From the experimental results obtained by Schuman and Back[4-21], Donnel and Sechler[4-20] concluded that C should be taken as 1.5. However, from additional tests he performed, Sechler[4-22] concluded that C depends on the material properties and width to

thickness ratio. Therefore, Sechler suggested that C should be a variable rather than a constant.

However, it should be noted that the equations obtained by Karman et al were for ultimate strength calculations. Based on the assumption Karman[4-20] made on the buckling wave form, Winter[4-23 and 4-24] stated that the effective width relation in Eq. 4-2 also holds for the sub-ultimate post buckling range. Eq. 4-2 may then be rewritten as

$$b/t = C\sqrt{\frac{E}{\sigma_{max}}} \qquad 4\text{-}5$$

or

$$b/w = C\sqrt{\frac{E}{\sigma_{max}}}\frac{t}{w} \qquad 4\text{-}6$$

where σ_{max} is the maximum supported edge stress.
At buckling Eq. 3-1 is valid. The width, w, can be expressed in terms of stress and taking the ratio of b and w, the following equation is obtained if $\eta = 1$,

$$b/w = \sqrt{\sigma_{cr}/\sigma_{max}} \qquad 4\text{-}7$$

Furthermore stresses may be replaced by strains as in the following equation,[3-8,1-6]

$$b/w = \sqrt{\varepsilon_{cr}/\varepsilon_{max}} \qquad 4\text{-}8$$

where ε_{max} is the maximum edge strain. These equations are based on elastic material properties. Eqs. 4-7 and 4-8 are independent of boundary condition.

The validity of Karman's equation in the post buckling domain for plates and the effects of the w/t ratio and material

property, i.e. Karman's characteristic parameter $\frac{t}{w}\sqrt{E/\sigma_{max}}$, were investigated by several researchers through experiments. Among these, one of the most influential studies was done by Winter[4-23 and 4-24], based on his extensive tests on carbon steel, a linear function of C in terms of $t/w\sqrt{E/\sigma_{max}}$ was obtained for stiffened element plates. The expression may be written as

$$b/t = 1.9\sqrt{E/\sigma_{max}}\,(1 - 0.475\, t/w\sqrt{E/\sigma_{max}}) \qquad 4\text{-}9$$

when $\frac{w}{t} \geq 0.95\sqrt{\frac{E}{\sigma_{max}}}$. For values of $\frac{w}{t}$ smaller than $0.95\sqrt{\frac{E}{\sigma_{max}}}$, b = w. Eq. 4-9 can also be expressed in terms of critical and maximum edge stresses as follows:

$$b/w = \sqrt{\sigma_{cr}/\sigma_{max}}\,(1 - 0.25\sqrt{\sigma_{cr}/\sigma_{max}}) \qquad 4\text{-}10$$

Eq. 4-9 has been used successfully for many years in the Light Gage Cold-Formed Design Manual[1-1] published by the AISI. Because of accumulated experience and some additional information from Skaloud's[4-25] recent series of careful tests, the original equation which was proposed conservatively has now been revised by Winter[3-5] by changing 0.475 to 0.418 in Eq. 4-9, and 0.25 to 0.22 in Eq. 4-10.

Winter's equations are written in terms of elastic material properties with an experimental modification to account for initial imperfections. Based on the same assumption of elastic material properties, Eq. 4-10 can be expressed in terms of critical and edge strains[1-6] as follows:

$$b/w = \sqrt{\varepsilon_{cr}/\varepsilon_{max}}\,(1 - 0.25\sqrt{\varepsilon_{cr}/\varepsilon_{max}}) \qquad 4\text{-}11$$

4.4 Effective Width With Considerations of Nonlinear and Anisotropic Material Properties

The analyses mentioned mainly considered elastic isotropic material properties. The development of methods for nonlinear or anisotropic, or both, material properties is only in its early stage. In order to yield a useful method which is theoretically justified and verified by experimental results to predict the post buckling strength of the plate elements, it may be possible to modify the equations mentioned to take the material properties into account.

Karman suggested that a reduced modulus may be used in the equation to account for the inelasticity. Eq. 4-5 may be then written as

$$b/t = C\sqrt{E\eta/\sigma_{max}} \qquad 4\text{-}12$$

or

$$b/w = C\sqrt{E\eta/\sigma_{max}}\,t/w \qquad 4\text{-}13$$

Although the formulation may be different, the idea of introducing the plasticity reduction factor to the elastic modulus was also used by Needham[4-26], Jombock and Clark[4-27], and Johnson[1-6].

The original derivation of Karman's effective width relation referred to hinged edge support and showed the effective width proportional to $\sqrt{E/\sigma}$. It was pointed out by Donell and Sechler[4-20] that the relation may be valid for other types of edge conditions but with a different C constant. Based on test results and the similarity in formulation, it seems that the constant C may be modified for the particular

boundary condition and that the relation is applicable to other type of plates. Based on this assumption, the following equation may be written to replace Eq. 4-5.

$$b/t = C' \sqrt{Ek/\sigma_{max}} \qquad 4\text{-}14$$

where $C' = \pi/\sqrt{12\ (1-\nu^2)}$ and k is the buckling coefficient in Eq. 3-1. Eq. 4-14 may be further elaborated in the following form to account for inelasticity.

$$b/t = C' \sqrt{kE\eta/\sigma_{max}} = 0.95 \sqrt{kE\eta/\sigma_{max}} \qquad 4\text{-}15$$

This can also be obtained by substituting the inelastic buckling stress of Eq. 3-1 into Eq. 4-7. Such an approach is logical theoretically; then the same assumption may be applied to Winter's effective width formula which is a conceptual and experimental modification of Karman's relation. If Winter's relations are applicable to other types of plates with different boundary conditions, all such relations for different plates should be reduceable to the same form as Eq. 4-10 with approximately the same coefficient which includes the effects of boundary conditions and the w/t ratio of the plate. Eqs. 4-10 and 4-11 may be written in the general form as,

$$b/w = \sqrt{\sigma_{cr}/\sigma_{max}}(1 - \xi \sqrt{\sigma_{cr}/\sigma_{max}}) \qquad 4\text{-}16$$

$$b/w = \sqrt{\varepsilon_{cr}/\varepsilon_{max}}(1 - \xi \sqrt{\varepsilon_{cr}/\varepsilon_{max}}) \qquad 4\text{-}17$$

where ξ is assumed as a variable which equals 0.25 for simply supported stiffened elements as shown in Eq. 4-10. The rela-

tion reduces to Karman's relation if ξ is assumed as zero.

Now let us consider the unstiffened elements. The original form obtained by Miller[4-28] similar to Winter's for stiffened element was as follows:

$$b/t = 1.25\sqrt{E/\sigma_{max}}\ (1 - 0.333\ t/w\sqrt{E/\sigma_{max}}) \qquad 4\text{-}18$$

It was revised by Winter[4-24] to represent the lower bound values from tests as

$$b/t = 0.8\sqrt{E/\sigma_{max}}\ (1 - 0.202\ t/w\sqrt{E/\sigma_{max}}) \qquad 4\text{-}19$$

These equations may be reduced to the form of Eq. 4-16. If the actual experimental boundary condition is considered the values of ξ calculated from Eqs. 4-18 and 4-19 are 0.266 and 0.252. These values are very close to $\xi = 0.25$, as in Eq. 4-10. It is therefore concluded that Eq. 4-16 with $\xi = 0.25$ may be applied to both stiffened and unstiffened elements. Investigating this in more detail, a somewhat more general form based on Winter's effective width formula may be obtained. By substituting the inelastic buckling stress of Eq. 3-1 into Eq. 4-16, the following equation is obtained.

$$b/t = 0.95\sqrt{kE\eta/\sigma_{max}}\ (1 - 0.95\ \xi\ t/w\sqrt{ke\eta/\sigma_{max}}) \qquad 4\text{-}20$$

By using $\xi = 0.25$, this reduces to

$$b/t = 0.95\sqrt{kE\eta/\sigma_{max}}\ (1-0.2375\ t/w\sqrt{kE\eta/\sigma_{max}}) \qquad 4\text{-}21$$

In this equation, the plasticity reduction factor η for plate buckling is the same as used in Chapter 3, (E_s/E for unstiffened elements and $\sqrt{E_t/E}$ for stiffened elements). A similar

approach was used by Johnson.[1.6]

First let us consider unstiffened elements. If k is assumed as 0.5 (see Chapter 3), $\eta = 1$ and $\xi = 0.25$, Eq. 4-21 reduces to

$$b/t = 0.67 \sqrt{E/\sigma_{max}} \left(1 - 0.164 \frac{t}{w} \sqrt{E/\sigma_{max}}\right) \qquad 4\text{-}22$$

If the edge coefficient k is taken as 0.85, $\eta = 1$, and $\xi = 0.25$, Eq. 4-21 reduces to

$$b/t = 0.875 \sqrt{E/\sigma_{max}} \left(1 - 0.217 \frac{t}{w} \sqrt{E/\sigma_{max}}\right) \qquad 4\text{-}23$$

which is close to Eq. 4-19. Hence, Winter's Eq. 4-19 is seen to follow from Eq. 4-16, for various degree of edge restraint. If inelastic behavior is considered, the variable η will remain in the equations as follows:

$$\text{for } k = 0.5,\ b/t = 0.67 \sqrt{E\eta/\sigma_{max}} \left(1 - 0.164\ t/w \sqrt{E\eta/\sigma_{max}}\right) \qquad 4\text{-}24$$

$$\text{for } k = 0.85,\ b/t = 0.875 \sqrt{E\eta/\sigma_{max}} \left(1 - 0.217\ t/w \sqrt{E\eta/\sigma_{max}}\right) \qquad 4\text{-}25$$

Now, let us consider stiffened elements. If k is assumed as 4.0, which is close to most actual boundary conditions and ξ equals to 0.25, Eq. 4-21 reduces to Eq. 4-9 for $\eta = 1$. Considering inelastic behavior, Eq. 4-21 becomes

$$b/t = 1.9 \sqrt{E\eta/\sigma_{max}} \left(1 - 0.475\ t/w \sqrt{E\eta/\sigma_{max}}\right) \qquad 4\text{-}26$$

As was mentioned, a new development is to change ξ from 0.25 to 0.22, and thus the coefficients in the related equations will be changed accordingly for both stiffened and unstiffened elements. The general equation 4-21 is then

$$b/t = 0.95 \sqrt{kE\eta/\sigma_{max}} \left(1 - 0.209\ t/w \sqrt{kE\eta/\sigma_{max}}\right) \qquad 4\text{-}27$$

In the foregoing treatment, the anisotropic material properties have not yet been considered. However, based on the analogue and similarities of isotropic and orthotropic plates in the formulation of critical and post buckling behavior, a similar treatment may be applicable also to orthotropic plate. Based on Eq. 3-3 in Chapter 3, Karman's formula may be extended to orthotropic plates. For elastic orthotropic plates, the effective width relation may be written as

$$b/t = C'_1 \sqrt{E_1 k'/\sigma_{max}} \qquad 4\text{-}28$$

where $C'_1 = \pi/\sqrt{12\ (1 - \nu_{12}\ \nu_{21})}$

$$k' = 2[\sqrt{E_2/E_1} + \nu_{21} + 2(G_{12}/E_1)(1 - \nu_{21}\ \nu_{12})]$$

For the inelastic case, based on Eq. 3-4, the following equation is obtained.

$$b/t = C'_1 \sqrt{E_1 k''\eta'/\sigma_{max}} \qquad 4\text{-}29$$

where $k'' = F\ (k',\ \eta')$

η' = plasticity reduction factor of orthotropic plates.

This equation can also be obtained by substituting the inelastic critical buckling stress of the orthotropic plate shown in Eq. 3-4 into Eq. 4-7.

If the further assumption is made that the effects of boundary conditions and the w/t ratio on the linear modification term found by Winter for the isotropic plate are

analogous to the present case, then, one may go one step further to obtain an equation similar to Eq. 4-20 for orthotropic plates. By substituting the inelastic critical stress of the orthotropic plate shown in Eq. 3-4, into Eq. 4-16, the following equation is obtained with an open parameter λ,

$$b/t = 0.95\ \sqrt{k''E_1\eta'/\sigma_{max}}(1 - 0.95\ \lambda\ t/w\ \sqrt{k''\ E_1\eta'/\sigma_{max}}) \quad 4\text{-}30$$

Since Winter's coefficient ξ based on carbon steel in Eq. 4-19 was also applicable to annealed stainless,[1-6] and [4-33], it is believed that λ for the present case is very close to ξ. Eq. 4-30 may be written as

$$b/t = 0.95\ \sqrt{k''E_1\eta'/\sigma_{max}}(1 - 0.95\ \xi\ t/w\ \sqrt{k''E_1\eta'/\sigma_{max}}) \quad 4\text{-}31$$

However, in Eqs. 4-30 and 4-31 the effective values of k'' and η' are not known. If anisotropy is not very pronounced, Eq. 4-20 may be used as an approximation for Eq. 4-31.

Another approach to the problem may be through strain analysis. Botman[4-29 and 4-30] and Besseling[3-11 and 4-31] compared their test results on aluminum alloys with Koiter's treatment; an excellent agreement was obtained by using strain parameters (b/w, $\sqrt{\varepsilon_{cr}/\varepsilon_{max}}$). It was concluded by Koiter[4-32] that his theory in terms of strains is applicable in the inelastic range if it is evaluated for the actual value of the ratio $\varepsilon_{cr}/\varepsilon_{max}$. He also concluded that his theoretical treatment of post buckling behavior of plates is applicable to various boundary conditions.

Some other investigators[3-8 and 1-6] have suggested that elastic expressions for effective width are also applicable for inelastic behavior if strains are used instead of stresses. Along this line, Karman's and Winter's equations (Eqs. 4-7 and 4-10) were expressed in terms of critical and edge strains as shown in Eqs. 4-8 and 4-11, assuming elastic material properties. Eqs. 4-8 and 4-11 may also be obtained from Eqs. 4-7 and 4-8 by using E_s/E as plasticity reduction factors to the elastic moduli for isotropic inelastic plates. The use of strains in the formulation for inelastic plates means in fact that the secant modulus is used as an effective modulus. This is reasonable for unstiffened plates since E_s/E is used as plasticity reduction factor for such plates, but may be somewhat dubious for stiffened plates. Based on Koiter's statements, it seems that Eqs. 4-8 and 4-11 are approximately applicable to inelastic post buckling behavior of plates with various boundary conditions.

Although the anisotropic material properties are not directly considered in Eqs. 4-8 and 4-11, it seems that the effect of anisotropy on the inelastic postbuckling behavior might be included implicitly if the actual critical and edge strains are used in the equations.

4.5 Post Buckling Behavior of Unstiffened Elements

In order to investigate the validity of the approach outlined, the effective widths of unstiffened elements were evaluated from the experiments described in Section 3.3. A similar analysis of Type 304 annealed and strain flattened stainless

steel was made by Johnson[1-6]. The present analysis concerns only 1/2 hard Type 301 in order to investigate the effects of high strength and pronounced anisotropic material properties as well as nonlinear stress strain relations.

The compression members shown in Fig. 3-1 responded very satisfactorily throughout the loading range. The specimens were considered failed when the maximum load was reached. The waving pattern of unstiffened elements was very uniform. The buckling pattern changed from time to time. During the loading process some explosive sounds were heard which were thought to be due to changes of the buckling pattern.

Fig. 4-3 shows a series of pictures taken during the test of specimen H301UE-4; the general post buckling behavior of unstiffened elements throughout the loading range can be seen clearly.

4.5.1 Evaluation of Experimental Effective Width

From flat and corner material properties, the geometric dimensions of cross section, and the measured strains the experimental effective width of the unstiffened elements may be determined.

The average strain of the fully effective part of the compression specimen (web and corners) was used to determine the stresses in the web and corner materials separately, by using the appropriate stress strain curves. The portion of the load $P_{f\ell}$ carried by the unstiffened flanges was determined by subtracting the load taken by the effective part of the specimen (including both webs and corners) from the total

experimental load carried by the specimen. Knowing the $P_{f\ell}$ and the measured maximum edge stress σ_{max} the effective area of the unstiffened flanges is $A_{eff} = P_{f\ell}/\sigma_{max}$. The stress strain curves for flat and corner materials used for this procedure were the experimental longitudinal compression curves from sheet 301-H-3 as shown in Fig. 2-4. The compression members were produced from this sheet.

4.5.2 Analysis of Results

In order to evaluate and compare the experimentally determined effective widths to the theoretical analyses in Sections 4.3 and 4.4, three sets of significant parameters will be used. The same type of analysis was used by Johnson for annealed and strain flattened Type 304[1-6].

The first approach is to use the same elastic parameters which were used for carbon steels, viz.

$$b/t\ \sqrt{\sigma_{max}/E} \quad , \quad t/w\ \sqrt{E/\sigma_{max}},$$

where b = effective width

w = actual flat width

t = thickness

E = initial modulus of elasticity

σ_{max} = maximum stress along the edge of compression element

It is evident that the improved approach is to modify these parameters by applying the plasticity reduction factor η to the elastic modulus in order to account for the non-linearity of the stress strain relationship, viz.

$$b/t\ \sqrt{\sigma_{max}/E\eta}\quad ,\quad t/w\ \sqrt{E\eta/\sigma_{max}}$$

where η is plasticity reduction factor.

The other approach is to use strain analysis. The alternative form of Karman's relation of effective width was shown in terms of strains in Eq. 4-8. The experimentally modified formula by Winter can also be shown in terms of strains as in Eq. 4-11. The significance of strain analysis was briefly outlined in 4.4. The strain parameter may be shown as

$$b/w\quad ,\quad \sqrt{\varepsilon_{cr}/\varepsilon_{max}}$$

where ε_{cr} = critical buckling strain

ε_{max} = maximum strain along the edge of the compression element.

For each specimen the test data were reduced at several stress levels according to these characteristic parameters so that a direct comparison may be made between test and theories. Based on the significance of each set of parameters, the effects of tempered material properties on the effective width may be detected.

4.5.2.1 Elastic Parameters

The elastic parameters were evaluated from the inner edge stresses, elastic modulus, w/t ratios, and the experimental effective width. The results are shown in Fig. 4-4. The edge restraint coefficients considered are 0.5 and 0.85. Eqs. 4-22 and 4-23 may be written in the following form and are plotted in the same figure.

$$b/t \sqrt{\sigma_{max}/E} = 0.67 - 0.11\ t/w \sqrt{E/\sigma_{max}} \qquad 4\text{-}32$$

$$b/t \sqrt{\sigma_{max}/E} = 0.875 - 0.19\ t/w \sqrt{E/\sigma_{max}} \qquad 4\text{-}33$$

Eq. 4-33 approximately represents the actual boundary condition, and is close to a lower bound for all test points. On the other hand, Eq. 4-32 represents a conservative lower bound which is purposely devised for design use in order to account for unstiffened elements with small edge restraint.

4.5.2.2 Inelastic Parameters

The inelastic parameters were evaluated with $\eta = E_s/E$ corresponding to the maximum inner edge stress. Eqs. 4-24 and 4-25 may be written in the following form and plotted along with the data points in Fig. 4-5.

$$b/t \sqrt{\sigma_{max}/E\eta} = 0.67 - 0.11\ t/w \sqrt{E\eta/\sigma_{max}} \qquad 4\text{-}34$$

$$b/t \sqrt{\sigma_{max}/E\eta} = 0.875 - 0.19\ t/w \sqrt{E\eta/\sigma_{max}} \qquad 4\text{-}35$$

The scatter of the data points is reduced when the plasticity factors are applied. The data points (except those of H301UE-4) follow the trend indicated by Eq. 4-35.

The higher values for E301UE-4 are mainly due to the restraint along the supported edge. For this specimen, the estimated restraint coefficient is 1.024 which is larger than for the other specimens and larger than 0.85 which was used in Eq. 4-35.

Eq. 4-34 again represents a conservative lower bound, and Eq. 4-35 is close to the lower bound of the scatter of the

test points, except those of H301UE-4.

4.5.2.3 Strain Parameters

The critical strains were obtained from experiments and reported in Table 3-2 by the maximum surface strain method. The maximum edge strains were obtained from tests. The results are plotted in Fig. 4-6 along with theoretical predictions. Eq. 4-11 shows the lower bound of the test results. Karman's relation of effective width also appears conservative for higher strains, but is unconservative for the strains near or below the critical strain. The test results agree very satisfactorily with Koiter's analysis[4-6], except at the strains near or below the critical strain.

4.5.3 Discussion of Results

Based on the qualitative information shown by these analyses in Figs. 4-4, 4-5, and 4-6 the effective widths of unstiffened elements of temper rolled Type 301 stainless are discussed in the following paragraphs.

In Fig. 4-4 it appears that the effective widths of tempered Type 301 are underestimated by the elastic formula (Eq. 4-33). This equation was obtained by using $k = 0.85$, which is the estimated average restraint coefficient for the specimens tested. The deviation between the experimental effective widths and those predicted by the elastic formulation may be due to different restraint conditions and possibly to material properties.

In order to take the nonlinearity into account, inelastic parameters were used. It is noticed in Fig. 4-4 that the

experimental values $\frac{b}{t}\sqrt{\sigma_{max}/E}$ are fairly constant for $\frac{t}{w}\sqrt{E/\sigma_{max}}$ smaller than 1.0. This range corresponds to the higher edge stresses. This failure of the parameter $\frac{b}{t}\sqrt{\sigma_{max}/E}$ to continue increasing with decreasing $\frac{t}{w}\sqrt{E/\sigma_{max}}$ is thought to be due to inelasticity. By applying a plasticity reduction factor to the elastic parameters, the values of $\frac{b}{t}\sqrt{\sigma_{max}/E}$ corresponding to the higher edge stresses (beyond elastic limit) are seen from Fig. 4-5 to increase with decreasing $\frac{t}{w}\sqrt{E/\sigma_{max}}$ and follow the trend indicated by Eq. 4-35. The data points corresponding to the stresses below the elastic limit are not affected since $\eta = 1$. This is seen in Fig. 4-5.

However, it is noticed that considering the inelastic effect increases the spread between the experimental data points and Eq. 4-35. A better agreement between experimental data and Eq. 4-35 could be achieved if a slightly higher plasticity reduction factor were used. This may be justified because the plasticity reduction factor used was from longitudinal compression which is the lowest.

Also, the anisotropic material properties may be responsible for the larger deviation of the experimental values $b/t\sqrt{\sigma_{max}/E\eta}$ from Eq. 4-35 at low $t/w\sqrt{E\eta/\sigma_{max}}$ values (corresponding to higher stresses) than that of annealed and skin passed Type 304[1-6] (Fig. 3-16), since anisotropy of annealed stainless is less pronounced than of cold-rolled stainless.

By using strain analysis, the experimental effective widths show good agreement with the analytical expressions except near or below the critical strain. At high stress (with

small $\sqrt{\varepsilon_{cr}/\varepsilon_{max}}$ values), test results are very close to Koiter's expression for effective width. Karman's expression also shows good agreement with the test results in the initial post buckling range. Eq. 4-11 is the lower bound of the test data.

It was concluded by Koiter[4-32] that his equation is applicable in the inelastic range if it is evaluated for the actual value of the ratio $\varepsilon_{cr}/\varepsilon_{edge}$. He stated that the equation can also be applied to other boundary conditions if the actual experimental critical and edge strains were used. Based on the good agreement between tests and theory shown in Fig. 4-6 by using actual maximum edge strains in the analysis, it seems that Koiter's equation is applicable to the material considered. This indicates that by using experimental critical and edge strains the nonlinearity, the anisotropy, and the boundary conditions of the plate are approximately taken into account automatically. The analysis by using strains probably is the most accurate way to treat the effective width, especially for the material and boundary conditions considered, but because of its reliance on experimental strains and its complex form is not amenable to design use.

4.6 Post Buckling Strength of Stiffened Elements

Stiffened elements possess greater post buckling strength as well as much less pronounced local distortion than unstiffened elements. In order to investigate the validity of the formulations derived for the material considered, the effective widths of stiffened elements were evaluated from experi-

ments which were described in Section 3.4. These stiffened elements were the compression flanges of flexural members or flanges of short compression members.

A similar analysis of Type 304 annealed and strain flattened stainless steel was made by Johnson and Winter[1-6 and 4-33] for a series of flexural member tests. The present analysis concerns tempered Type 301 stainless except that three flexural members made of Type 304 annealed and strain flattened stainless were also tested for comparison.

Since the high strength develops large curvatures which produce inward deflections of the stiffened compression flanges, two short columns were studied to avoid such effect.

Fig. 4-7 shows a sequence of photographs taken during the test of flexural specimen H301F-4; the general post buckling behavior of the stiffened compression flange throughout the loading range can be seen. The waving of the compression flange is only slightly visible when the load on the specimen is about twice of the critical load (797 lbs.). At the final stage, the specimen is seriously buckled in the compression flange and failed by wrinkling at the buckled corners.

4.6.1 Evaluation of Experimental Effective Width

4.6.1.1 Compression Flanges of Flexural Members

In order to determine the effective width of the stiffened compression flange of the flexural member, beam theory and equilibrium requirements were used. The following assumptions are made: 1) planes normal to the axis of the flexural member remain plane after bending, 2) every longitudinal

fiber acts as if separate from the other. The stress strain relations in tension and compression from coupon tests are applicable to these individual fibers. 3) The effects of differences of material properties in the transverse direction are ignored. 4) Geometrical changes of the cross-section are ignored.

At each loading level the strains of the four gages along the edges of the compression flange were averaged to represent the edge membrane strain of the compression flange. The average value of the four gages in the tension flange represents the tension membrane strain. The neutral axis can be located from these averaged strains if the assumption (1) is used. The stresses at each fiber may be determined from corresponding strains from the appropriate stress strain relations. The stress strain relations are nonlinear and unsymmetrical in tension and compression, but the following integral holds for internal equilibrium of forces:

$$\int_A \sigma dA = 0 \qquad 4\text{-}36$$

where σ is a function of strains applicable for both tension and compression. In order to simplify evaluation, a numerical procedure is used by dividing the area of the cross section into m segments.

This may be expressed as,

$$\sum_{i=1}^{m} \sigma_i A_i = 0 \qquad 4\text{-}37$$

where σ_i is the stress at the centroid of segment i and is obtained from proper stress strain relations from the strain at the centroid. A_i is the area of the ith sub-area of the cross section. It may further be simplified by using a straight line stress distribution in the web across the depth as shown dashed in Fig. 4-8. Number and location of the segments are shown. The force to be taken by the compression flange to satisfy the internal force equilibrium can easily be calculated. Based on the experimental edge strain in the compression flange, the effective width can then be obtained. The legitimacy of such a simplified approach may be verified by calculating the internal moment from the effective width so determined. This internal moment should be equal to the external moment at that loading level. The accuracy of the calculation may be seen from the ratio of calculated moment to the experimental moment. Effective widths for the compression flange were calculated at several loading levels for each specimen. Reasonably close agreement between computed and experimental moments indicates that the above procedure is satisfactory. The calculated moment ratios vary from 1.051 to 1.128 with an average of 1.083. This is shown in Table 4-1.

4.6.1.2 Flanges of Short Columns

The procedures to determine the effective width of stiffened elements from short column tests are similar to those followed for unstiffened elements.

The strains of the gages at the edges of stiffened elements, the webs, and the outstanding lips were averaged to

represent the edge strains of the specimen. The load carried by the corners, webs, and the outstanding lips is determined from the measured averaged edge strain and the stress strain curves for flat and corner materials. The load taken by the effective part of the stiffened elements is then obtained, from which the effective width can be calculated.

It is the purpose of this series of tests of short columns to eliminate the effects of member curvature on effective width.

4.6.2 Analysis of Results

The effective widths determined from both flexural and short column member tests are presented herein. The approaches to analysis, presented for unstiffened elements, will also be used for stiffened elements. The edge strains were obtained from tests and corresponding stresses determined from appropriate stress strain curves. The plasticity reduction factor used is the same as for buckling of stiffened elements, i.e. $\sqrt{E_t/E}$.

Eq. 4-9 may be written with elastic parameters as

$$b/t \sqrt{\sigma_{max}/E} = 1.9 - 0.9025 \, t/w \sqrt{E/\sigma_{max}} \qquad 4\text{-}38$$

and Eq. 4-26 may be written with inelastic parameters as

$$b/t \sqrt{\sigma_{max}/E\eta} = 1.9 - 0.9025 \, t/w \sqrt{E\eta/\sigma_{max}} \qquad 4\text{-}39$$

The straight lines of these equations are shown in Figs. 4-9 and 4-10 along with the data points calculated from the experiments. From Figs. 4-9 and 4-10, phenomena similar to those of unstiffened elements are observed, i.e. Winter's equations

with or without inelasticity modification represent lower conservative bound but that the inelasticity modification makes it excessively conservative, similarly as for unstiffened elements. Fig. 4-9 also can be shown alternately as in Fig. 4-11 which contains the earlier and later Winter equations without inelasticity modification.

In Fig. 4-12, the strain parameters are used for analysis. The critical strains were obtained from experiments and reported in Table 3-14 by the maximum surface strain method. Analytical expressions by Koiter and Eqs. 4-8 and 4-11 are also presented along with the experimental effective widths.

4.6.3 Discussion of Results

Several significant phenomena are observed in Fig. 4-9 which refers to the analysis of experimental data by using elastic parameters. (1) The experimental values of $b/t\sqrt{\sigma_{max}/E}$ of the annealed and strain flattened Type 304 element (Series AS304F) are close to those from Winter's formula which was also concluded earlier by Johnson and Winter[1-6 and 4-33]. (2) The experimental values of $b/t\sqrt{\sigma_{max}/E}$ of short column tests are lower than for the corresponding flexural tests (H301F-2 vs. H301 SC-2, H301F-4 vs. H301 SC-4). (3) The experimental values of $b/t\sqrt{\sigma_{max}/E}$ of flexural members of cold-rolled Type 301 are higher than those of annealed and strain flattened Type 304 stainless (H301F-3 vs. AS304F-2, H301F-4 vs. AS304F-4).

Observation (1) further confirms the applicability of Winter's formula to annealed and strain flattened stainless. Observation (2) confirms that the effective widths of flexural

members may be affected by the double curvature in the stiffened compression flange. Since the deformation of cold-rolled stainless is larger than the annealed, the effect of this curling on the effective width may partly explain the observation (3) which indicates higher effective widths of cold-rolled stainless than annealed. However, if one compares the test results of short columns, the effective width of H301SC-4 are higher than those of AS304F-4. These two specimens have about the same w/t ratio. No curling being present in columns this indicates that the stronger anisotropy of tempered 301 than annealed 304 may be partly responsible for this difference.

The effort of inelasticity becomes apparent as follows: For any specimen the data points with the smaller values of $\frac{t}{w}\sqrt{E/\sigma_{max}}$ correspond to the higher edge stresses. It is noted in Fig. 4-9 which is based on elastic parameters that the experimental values $\frac{b}{t}\sqrt{\sigma_{max}/E}$ start to decrease with decreasing $\frac{t}{w}\sqrt{E/\sigma_{max}}$ at certain values of $\frac{t}{w}\sqrt{E/\sigma_{max}}$ for each specimen. This is especially obvious for the two short columns H301SC-2 and H301SC-4. The failure of the parameter $\frac{b}{w}\sqrt{\sigma_{max}/E}$ to continue increasing with decreasing $\frac{t}{w}\sqrt{E/\sigma_{max}}$ is thought to be due to inelasticity. In Fig. 4-10 a plasticity reduction factor was applied to the elastic parameters. It is seen that the value of $\frac{b}{t}\sqrt{\sigma_{max}/E}$ corresponding to the higher edge stresses (beyond elastic limit) now continues to increase with decreasing $\frac{t}{w}\sqrt{E/\sigma_{max}}$ and to follow the trend of Eq. 4-39. The data points corresponding to the edge stresses lower than the elastic limit are not affected.

By using strain analysis, the experimental effective widths show satisfactory agreement with the analytical expression by Koiter. The data points are lower near or below the critical strain. Eq. 4-11 is shown to be the lower bound of the data points. The general behavior is similar to that discussed for unstiffened elements.

4.6.4 Waving Pattern of Buckled Plate Element

In this section, the wave pattern in the longitudinal and transverse directions of the stiffened plate elements will be discussed. The correlation between the experimental wave form and that assumed in the theoretical treatment will also be discussed.

The waving pattern of stiffened elements has been investigated by many researchers, such as Botman and Besseling, Farrar, and Skaloud. The first two were concerned with aluminum alloys, while Skaloud used carbon steel.

The waving amplitude along the center line of the compression flange relative to the edges was measured. The points of peak and valley were obtained by moving the dial gage bridge (Fig. 3-7) along the specimen to obtain the maximum or minimum readings. The measurements were made on the left half of the center half of the span at 16 points along the center line of the compression flange. This coordinate system for waving measurement is shown in Fig. 4-13.

The longitudinal and transverse waving patterns of flexural specimen H301F-4 at various loading levels are shown in Fig. 4-14 a and b. Similar patterns of H301F-3 are shown

in Fig. 4-15 a and b.

The initial imperfections affect the early stage of buckling, when the waving goes in the same direction as the initial imperfection. The compression flange will then buckle gradually in the expected theoretical manner. The waving pattern changes from time to time in order to adjust itself to the instantaneous equilibrium condition. The buckle of the waved compression flange flattens out transversely as the load increases. However, the wave pattern in the longitudinal directions along the center line is still close to the sine wave but with a decreasing increment in amplitude with increasing load. The transverse configuration may be divided into two parts - the central essentially flat region and the curved portions near the edges. Such a phenomenon was also discussed by many other investigators[4-25] and [4-34].

4.7 Summary and Conclusions

In this Chapter the post buckling behavior of stiffened and unstiffened plate compression elements has been discussed. In spite of the fact that the plate elements may buckle at relatively low stresses, these elements can sustain considerable strength after buckling has occurred.

The effective width concept was used for analyzing the behavior of plate elements in the post buckling range. Karman's semi-theoretical treatment of effective widths of plates and Winter's experimental modification and generalization of Karman's equation were discussed. Based on these equations, an attempt was made to take the orthotropic material properties

and inelasticity into account.

In order to verify the applicability of these equations to cold-rolled stainless steel, a detailed analysis of the experimental effective widths of the stiffened and unstiffened elements was made. The experimental widths were obtained from a series of tests described in Sections 3.3.1, 3.4.1, and 3.4.2.

The results of this investigation are summarized as follows:

Theory

(1) Winter's equation (Eq. 4-10) in terms of critical stress and maximum edge stress was shown to be valid for both stiffened and unstiffened elements. This was verified by the ξ values obtained from experimental equations (Eqs. 4-18 and 4-19) for unstiffened elements. In obtaining ξ values from Eqs. 4-18 and 4-19, the actual experimental boundary conditions were considered. It is seen that the effect of boundary condition on the ξ value is small.

(2) By substituting the inelastic buckling stress of Eq. 3-1 into Eq. 4-16, a general equation (Eq. 4-20) was obtained. With $\xi = 0.25$, Eq. 4-20 was reduced to Eq. 4-21. These equations are applicable to both stiffened and unstiffened elements by using the proper restraint coefficient k. The inelastic effect is considered by applying plasticity reduction factors η to the elastic moduli.

(3) By substituting the inelastic critical stress of the orthotropic plate shown in Eq. 3-4 into Eq. 4-16, a general equation (Eq. 4-30) for effective width for inelastic ortho-

tropic plates was obtained. Considering appropriate restraint coefficient k in the equation, Eq. 4-30 is applicable to both stiffened and unstiffened elements. It was concluded that Eq. 4-30 may be approximated by Eq. 4-20 or 4-21 if anisotropy is not very pronounced.

Test Evidence

(4) Based on the theoretical considerations, the experimental effective widths of stiffened and unstiffened elements were analyzed by using elastic parameters ($\frac{b}{t}\sqrt{\sigma_{max}/E}$, $\frac{t}{w}\sqrt{E/\sigma_{max}}$), inelastic parameters ($\frac{b}{t}\sqrt{\sigma_{max}/E\eta}$, $\frac{t}{w}\sqrt{E\eta/\sigma_{max}}$), and strain parameters ($\frac{b}{w}$, $\sqrt{\varepsilon_{cr}/\varepsilon}$). It was qualitatively concluded that the boundary condition and material properties are implicitly taken into account if the experimental critical and maximum edge strains are used.

(5) For unstiffened elements, using elastic parameters, the experimental effective widths are slightly underestimated by Eq. 4-33 which corresponds to an average estimated restraint coefficient k = 0.85 for the tested specimens. This is shown in Fig. 4-4. By applying the plasticity reduction factor ($\eta = E_s/E$) to the experimental effective widths corresponding to higher edge stresses (beyond the elastic limit), the inelastic effect is taken into account as shown in Fig. 4-5. The underestimation of Eqs. 4-33 and 4-35 was concluded to be due to the restraint coefficient and possibly to material properties.

By using strain analysis, test results showed good agreement with Koiter's expression for effective width at high edge

strains. Near and below the critical strain, the experimental effective widths are lower than those from theory. Eq. 4-11 represents a lower bound of the test results.

(6) For stiffened elements, using elastic parameters, the experimental effective widths are underestimated by Winter's equation (Eq. 4-38) which is shown in Fig. 4-9. Comparing test results of short columns and flexural specimens, the latter's higher experimental effective widths was concluded to be partly due to curling induced by the curvature of flexural members. It was also concluded that stronger anisotropy of cold-rolled stainless than for annealed material increased the effective width of stiffened elements.

By applying a plasticity reduction factor ($\eta = \sqrt{E_t/E}$) to the experimental effective widths corresponding to higher edge stresses, the inelastic effect is considered as shown in Fig. 4-10. By using strain analysis, the agreement between test results and the analytical expressions is improved similarly as for unstiffened elements.

(7) It appears that the analysis using strain parameters is the most accurate method to predict effective width for both stiffened and unstiffened elements of tempered Type 301 stainless. However, it is not practical for design purposes. In view of the complications which would be caused in design if plasticity reduction factors were used and the fact that their inclusion does not improve agreement between predicted and experimental values, the following simple effective width formulas are recommended for design:

Stiffened Elements: $\frac{b}{t} = 1.9\sqrt{E/\sigma_{max}}(1-0.418\ \frac{t}{w}\sqrt{E/\sigma_{max}})$

4-40

when $\frac{w}{t} \geq 1.28\sqrt{E/\sigma_{max}}$. For values of $\frac{w}{t}$ smaller than $1.28\sqrt{E/\sigma_{max}}$, b = w.

Unstiffened Elements: $\frac{b}{t} = 0.67\sqrt{E/\sigma_{max}}(1-0.164\ \frac{t}{w}\sqrt{E/\sigma_{max}})$

4-22

CHAPTER 5

STRUCTURAL MEMBER BEHAVIOR

5.1 General

In considering the structural performance of thin walled members made from the material considered, material properties and the local buckling in the compression elements must be considered.

The material properties presented in Chapter 2 as well as the critical and post buckling behavior of stiffened and unstiffened elements presented in Chapters 3 and 4 can serve as the basis for the analysis of the behavior of structural members.

5.2 Flexural Members

5.2.1 General

In view of the described material properties of annealed and cold-rolled austenitic stainless steels, a study of the behavior of flexural members is essential. Methods to account for nonlinear unsymmetrical stress strain relations in tension and compression, low proportional limits, and strengthening of corners and their influence on the flexural behavior will be presented in this section. In addition to material properties, the post buckling strength of the buckled compression flange of flexural members is considered. A series of tests was performed to investigate the flexural behavior of thin walled members made of annealed and cold-rolled austenitic stainless steels. Based on these experimental and theoretical

analyses, design methods for strength and deflection calculations may be formulated.

5.2.2 Experimental Investigation

A series of hat section flexural members of Type 304 annealed and Type 301 half hard stainless, with w/t ratios in the compression flange ranging from 24.82 to 150.34, was tested. The sectional dimensions and other information are presented in Table 3-12. The test set up is shown in Fig. 3-5. Strain in compression and tension flanges, deflection at mid-span, and out of plane wavings were all recorded at each loading level. From the loading scheme, the center half of the span is under pure bending. By using the assumption that "plane sections remain plane", the experimental location of the neutral axis and curvature can easily be determined from measured strains. The actual location of the neutral axis shifts continuously away from the compression flange, due to buckling of the compression flange and the unsymmetrical stress strain relations in tension and compression[5-1]. The load or moment-deflection curve at mid-span can be constructed.

The flexural specimen can take a considerable amount of load beyond the buckling load because of the post-buckling strength of the stiffened compression flange. The ratio of the ultimate load to the buckling load depends upon the w/t ratio of the compression flange of the specimen. Such information is shown in Table 3-18. For large w/t ratios of the compression flange, the ratio of ultimate load to the buckling load was as high as 4.30 for H301F-4. However, for small w/t

ratios the buckling load is very close to the ultimate load; for H301F-1 the ratio is 1.00.

The experimental inelastic deflections of specimens made of cold-rolled Type 301, are much larger than for Type 304 annealed and strain flattened of the same dimensions at the same fractions of their own ultimate loads. This is because of the high strength of Type 301 stainless steel, which is accompanied by high strain. Fig. 5-1 shows the load deflection curves for a pair of flexural members with the same dimensions and loading conditions for these two types of materials.[5-2]

The specimen usually reached failure when the stress along the compression flange edges was at the 0.2% offset yield strength. For specimens with small w/t ratios, failure occurs by gradual yielding with excessive deformation. If the w/t ratio is large, failure occurs by gradual yielding as well as by the formation of kinks at the corners of the seriously bucked square pattern. A somewhat deeper discussion on failure criterion of flexural members will be presented in 5.2.3.3b.

The flexural members behaved satisfactorily throughout the loading range. The webs were flat and unbuckled until serious buckling occurred in the compression flange and the final stage was approaching. During test the tendency of tension flanges to bend outward was partly prevented by stiffeners welded underneath the specimen which served as ties at the loading and supporting points. There was no failure observed by bearing, web crushing or shear buckling of the web.

5.2.3 Theoretical Analysis

In order to predict the structural behavior of flexural members of cold-rolled austenitic stainless, it is necessary to consider the material properties and the local buckling phenomena in the compression flange. A rigorous solution by a purely mathematical approach for this type of problem is complex. In view of this, a numerical approach with simplified assumptions may best be used. Based on this approach, a digital computer program was prepared for calculating sectional properties, moment capacity, and moment curvature data for certain thin walled cross sections as well as inelastic deflections of flexural members with different span length. The nonlinear unsymmetrical stress strain relations and the local buckling of the compression flange as well as the corner strengthening effect were considered. Simplified methods are also investigated with design applications in mind.

5.2.3.1 Stress Strain Relationship

For flexural members, the longitudinal direction of the specimens is in the rolling direction of the sheet; therefore only the stress strain relations in the longitudinal direction will be used. It is assumed that the stress strain relations of the individual fibers of the flexural member are the same as those determined in the uniaxial tests of flat and corner materials in both tension and compression. It was noted from the strain readings of the flexural tests that the effect of the biaxial stress field on the edge strain or stress was negligible.

For the following analyses, the particular sets of stress strain curves in tension and compression, for both flat and corner material from the same sheet of material as the flexural members, were used. The stress strain curves were approximated by the Ramberg-Osgood function. The coefficients of the fitted Ramberg Osgood stress strain functions for the flexural members tested in this investigation are shown in Table 2-7. These functions are valid up to and slightly beyond .2% offset yield strength.

5.2.3.2 Effective Width

It was concluded in the previous chapters that the effective width for stiffened elements may be predicted satisfactorily and slightly conservatively both for annealed and cold-rolled stainless steel by Winter's formula. For the following analyses, the original and the revised Winter's formulas (Eqs. 4-9 and 4-40 respectively) were employed. The intention was to see the difference in member behavior by using the original and revised Winter's formulas for effective width prediction of stiffened elements.

5.2.3.3 Strength of Thin Walled Flexural Members

a. Numerical Procedure in Predicting Flexural Strength

The basic assumptions made for the numerical analysis were the same as stated in 4.6.1.1. In that case the neutral axis was located by the experimentally measured strains in tension and compression flanges of flexural members so that the experimental effective width could be determined from the equilibrium of internal forces. In the present case, the

strain in the compression flange is assumed and the effective width is computed from Winter's formula, but the location of the neutral axis is not known (or the strain in tension flange may be assumed). Therefore, the usual iterative process is necessary to locate the neutral axis in order to satisfy the internal equilibrium. Then the internal moment corresponding to this particularly assumed flange edge strain may be obtained. These conditions can simply be expressed as

$$\int_A \sigma \ dA = 0 \qquad 5\text{-}1$$

$$\int_A \sigma y \ dA = M, \qquad 5\text{-}2$$

where y = the distance from the neutral axis

M = internal moment

A = cross sectional area.

However, due to nonlinear unsymmetrical stress strain relations in tension and compression and the complicated thin walled cross section, the integral is evaluated numerically by dividing the cross section into small straight and curved segments. Theoretically, the value may be very close to the exact solution if the number of segments is very large. Eqs. 5-1 and 5-2 may be rewritten as

$$\sum_{i=1}^{m} \sigma_i A_i = 0 \qquad 5\text{-}3$$

$$\sum_{i=1}^{m} \sigma_i y_i A_i = M, \qquad 5\text{-}4$$

where m = number of segments divided in the cross-section

i = subscript

y_i = distance from the neutral axis to the centroid of segment i

The assumed linear strain distribution and its corresponding stress distribution across the depth of the cross section are shown in Fig. 5-2. The stress at the centroid of each segment is also shown. This centroidal stress is used as the average stress on the particular segment.

The use of the edge strains and stresses for effective width calculations permits the location of the neutral axis by the assumption that plane sections remain plane[5-1, 5-3].

For a given edge strain either in the compression or tension flange, internal equilibrium may be checked by assuming a trial location of the neutral axis. If equilibrium is not satisfied, a new location of neutral axis will be assumed. The process will continue until the unbalanced net force in the cross section is smaller than a predetermined value (EPS2) or the difference in location of neutral axes of two consecutive trials is smaller than a predetermined value (EPS1). In this investigation, these values (EPS2 and EPS1) were taken as 10^{-3} kips and 10^{-3} in. respectively. The convergence criteria of the location of neutral axis is the same as that used by Uribe[5-4] for the case of isotropic elasto-plastic material. The position of the neutral axis of the fully effective section is used as the first approximation. If the net force is larger than the limiting value assigned, a new distance of

the neutral axis is taken as 1.1 or 0.9 times that of the old one depending on the sign of the calculated net force. If the net force is still larger than the limiting value, then successive cycles of iteration are necessary. For these cycles of iteration, a new position of the neutral axis is computed by using the secant method of interpolation, and the computer always keeps the values of the position of the neutral axis corresponding to the minimum absolute values of the net forces of the cross section. Once the internal equilibrium is reached, according to the convergence criteria, the internal moment can easily be calculated from the contributions of each segment.

The computer program for strength calculations is capable of dealing with certain cross sectional shapes as indicated in Uribe's report[5-4]. The form of the program for strength calculations is essentially the same as Uribe's[5-4], but the program has also been modified to account for the unsymmetrical inelastic stress strain relations in tension and compression. The program was written in Fortran 63 for the CDC 1604 computer and was transformed into Fortran IV by a program called "SHIFT" at Cornell. All results which will be presented were obtained from the IBM 360 computer at Cornell.

The formulation of the program follows closely the foregoing numerical procedure. The sequence of calculations is shown by the flow chart of Fig. 5-3.

In this program, the web of the flexural member was divided into 20 segments and the stiffener on the tension side

was divided into 10 segments.

Two iteration processes are involved-stress strain computation and internal equilibrium of force of the cross section. In general the convergence is quite satisfactory for both the stress strain iteration and the internal equilibrium iteration processes. However, the number of cycles needed depends on the type of stress strain curve, the convergence limiting value assigned, and the starting value of stress assigned. In most cases in this investigation six cycles are needed to reach the limiting convergence stress difference of 10^{-5} ksi. For the internal equilibrium iteration process, in general, five cycles are needed to satisfy the limiting convergence force difference of 10^{-3} kips.

Following the procedure outlined, the flexural strength of the section for any assigned strain at either the tension or the compression flange may be determined. The stresses across the depth of the cross section are calculated from appropriate stress strain functions, either corners or flats, in the sub-program.

The maximum moment capacity of the section may be determined if the limiting stress or strain is known. The 0.2% offset yield strength was chosen for this purpose. The limiting strain is the sum of 0.002 in./in. plus the elastic strain corresponding to the yield strength. Then the limiting flexural strength of the section can be calculated as that producing this limiting strain at the extreme fiber along the edge of the compression flange. The computed results will be

discussed in d. The suitability of using the 0.2% offset yield strength as the limiting stress for the material is discussed in the following.

b. Failure Criterion

The maximum moment capacity is defined as the moment at which the flexural member can no longer sustain an additional increment of load. The experimental maximum moment capacity of a flexural member can easily be determined by the peak of a load-deformation (strain, curvature, or deflection) plot or directly from a test machine.

For hot rolled sections with sharp yielding stress strain relations, the maximum moment capacity can be predicted accurately. For thin walled sections with sharp yielding stress strain relations, the maximum moment capacity can be predicted accurately. For thin walled sections with sharp yielding stress strain relations, it can also be reasonably predicted by considering the effective width in the buckled compression flange[1-1].

For the present case, the prediction of the maximum moment capacity is complicated by the inelastic unsymmetrical stress strain relationship in tension and compression without an obvious yield plateau. This situation was also encountered in the earlier investigation on annealed and strain flattened Type 304 stainless[1-6]. For cold-rolled stainless steel, the effects of high strength (accompanied by large deformation) and the pronounced difference of stress strain relations in tension and compression must be considered.

For the specimens tested, the following modes of failure were observed. For specimens with a large w/t ratio in the compression flange there is a tendency to fail by wrinkling at the junction of the nodal line (between the buckles) and the edge. For compact specimens (with small w/t ratio) the member will fail by excessive deformation. In both modes, considerable inelastic strain and distortion is involved.

Table 5-1 shows that the ratio of maximum edge stress in the compression flange to the .2% offset yield strength at failure ranged from 0.95 to 1.05 with an average of 1.00 for series H301F. Therefore it appears that the .2% offset yield strength may be used as a limiting value to predict the maximum moment capacity of flexural members of cold-rolled Type 301 stainless. These flexural members were all designed to fail in the compression flange rather than tension, i.e. the edge stress in the compression flange was able to reach the .2% offset yield strength in longitudinal compression before the edge stress in the tension flange could reach the 0.2% offset yield strength in longitudinal tension.

In the following, an approximate theoretical reasoning is given to support such a criterion. The ultimate strength of a stiffened plate element can be approximated by Karman's Eq. 4-4. This equation may be written as follows to be applicable in the inelastic case.

$$P_u = Ct^2 \sqrt{E\eta\sigma} \qquad 5\text{-}5$$

The maximum load which the plate element can sustain appears

to be governed by the maximum value of the product of $\eta\sigma$. Based on this simple reasoning, the maximum stress of the stiffened plate may be approximated from the curves in Figs. 2-3, 2-5, and 5-7 showing the relationship between stress and plasticity reduction factors. Using $\eta = \sqrt{\frac{E_t}{E}}$, the maximum stresses so obtained for the three sheets (301-H-3, 301-H-7, and 304-AS-5) are 110.0,95.0 and 29.0 ksi respectively. The experimental 0.2% offset yield strengths for the three sheets are 89.90,100.50, and 34.09 ksi respectively. The ratios of the calculated limiting stresses to the experimental offset yield strengths are 1.22, 0.95, and 0.85 respectively with an average of 1.01. From this simple calculation, it appears that the 0.2% offset yield strength may have some intrinsic justification as a limiting stress for predicting the ultimate load of a stiffened plate element.

However, from the stress strain curves shown in Figs. 2-4 and 2-6, it is evident that considerable material strength is available beyond the 0.2% offset yield stress. However, it seems that the large amount of inelastic deformation and distortion at high stresses is responsible for the fact that in these structural members failure occurs before the highest portions of the stress-strain curve are reached. Based on this reasoning and on the experimental evidence, the .2% offset yield stress can be reasonably used as the limiting stress for defining failure of structural members.

Consequently the 0.2% offset yield strengths in compression and tension are used as limiting stresses for predicting

the maximum moment capacity of the flexural members of cold-rolled Type 301 stainless steel.

c. Simplified Methods for Flexural Strength Predictions

Although the developed numerical method yields satisfactory results for flexural strength predictions, which will be cited in d, a considerable amount of machine computation is needed and can not be used for routine design procedure. If possible, the designer should be able to predict the flexural strength and deflection with no more information than the geometry of the member and its material properties. Several methods[1-1,1-6, and 1-7] are developed with various simplifications to treat the present problem.

Simplified Numerical Method

Based on the numerical approach outlined in a., a simplified numerical method suggests itself. The approach is the same as before except that the web is divided into only two parts, tension and compression. The strains and corresponding stresses at the center of these two segments under tension and compression are used as average values for these parts. This implies that the strains and stresses across the depth of the cross section (between the inner edges of the corners of the web) are assumed to be linearly distributed. The stress and strain distributions are the same as described in 4.6.1.1 for effective width evaluation (Fig. 4-8) except in this case the location of the neutral axis is not known.

This simplifies computation although an iterative process is still needed. The location of the neutral axis is

assumed and the contribution of each segment is calculated. The moment capacity is obtained when the internal force balance condition is satisfied. Otherwise, the process is repeated by assuming a new location of the neutral axis until this condition is fulfilled.

Elastic Method

This method has long been used successfully for light gage cold formed carbon steel flexural members[1-1]. It is also applied to annealed and strain flattened Type 304 stainless[1-6, 1-7].

The maximum moment can be calculated easily by the following equation

$$M_y = \sigma_y \frac{I_{eff}}{c} = \sigma_y S_{eff}, \qquad 5\text{-}6$$

where M_y = yield moment

c = distance from neutral axis to the extreme tension or compression fiber

S_{eff} = effective section modulus

σ_y = 0.2% offset yield strength in tension for the tension flange or in compression for the compression flange

In this equation, local buckling of the compression flange is considered by using the effective section modulus as for carbon steel members. The stress is assumed again as linearly distributed.

The effect of corner strengthening is ignored. It is to be expected that the flexural strength calculated from

this method is underestimated.

Plastic Method I

In this alternative method, the stress distribution is assumed to be fully plastic. The stress magnitude is the compressive .2% offset yield strength throughout the entire section. The effective width is calculated and the neutral axis is located by considering internal equilibrium. The moment capacity can then be calculated easily.

The plastic stress distribution, of course, overestimates the strength. However, it should be noted that the method does give a simple way to calculate flexural strength. Also, since the tensile strength is higher than the compression strength, the use of the compressive yield strength as the limiting strength will reduce the overestimation.

Plastic Method II

This method is the same as plastic method I except that the compressive yield strength is used only above the neutral axis and the tensile yield strength is used below the neutral axis.

d. Discussion of Results

Using the computer program, and the .2% offset yield strength as the limiting stress, the flexural strength capacities of the specimens were calculated by the Numerical Procedure of a., above. Both Winter's original and revised formulas were used to account for the postbuckling strength of the compression flange. The corner strengthening effect was either considered or ignored.

Table 5-2 shows the computed moment capacities and the experimental failure moments of the specimens. From the percent deviation of calculated moment from experimental moment, it seems that the use of the .2% offset yield strength as a limiting stress yields reasonable predictions of moment capacity. In general, the analytical predicted values for 1/2 hard Type 301 stainless steel are somewhat lower than the experimental values even when corner strengthening effect is included. Only for H301F-2 are the analytical values higher than the test values. For annealed and strain flattened 304, the predicted values without considering corner strengthening effect are very close to the experiments, but with corner effect the predicted values are somewhat too high.

The increase of moment capacity for flexural members due to the revised Winter's formula is comparatively small. The largest effect is for compact sections which have a slightly larger effective width increase. The amount of increase for H301F-1 (w/t = 24.82) and H301F-4 (w/t = 150.34) are 3% and .3% respectively. In general the revised Winter's formula somewhat improves the deviation from experiments for 1/2 hard 301.

The effect of corner strengthening is shown in Table 5-3. The effect on the strength capacity is larger for annealed and strain flattened Type 304 than for 1/2 hard Type 301. If the corner strengthening effect is ignored in the calculations, the average predicted values are -7.36% and -3.72% lower for annealed and strain flattened and 1/2 hard 301 respectively than

when the corner effect is considered.

This verifies the use of .2% yield strengths as limiting stress and Winter's formulas for effective width calculations.

Moment capacities calculated by simplified methods, using Winter's original formula, are shown in Table 5-4 along with the experimental values. The values calculated by the simplified numerical method are very close to the computer results though slightly higher because of the linear approximation of the stress distribution in the web.

Moment capacities determined by the simplified numerical method deviate from the experimental ultimate moment by from +6.94% to -12.13% with an average value of -4.30%.

The elastic method for calculating the moment capacity for the H301F series gives moments which underestimate the test failure moments by from +1.31% to -22.84% with an average of -12.49%. For series AS304F, the percentages of deviations ranges from -18.10% to -14.48% with an average of -15.70. Generally, this method underestimates the flexural capacity of the sections considered except for H301F-2, but is better for cold-rolled than for annealed grades because of the more gradual yielding type of stress strain curve.

If plastic methods I and II are used for the H301F series, the deviations from the experimental values range from +12.14% to -0.82% with an average of +3.65% and from +22.3% to +8.43% with an average of +13.69% respectively. For series AS304F, the average deviations by using plastic methods I and II are

2.40% and 10.45% respectively. In general plastic method II overestimates unduly the flexural capacity for the sections considered. Plastic method I gives values close to the experimental failure moments.

In general the deviations from the experimental ultimate strengths calculated by these suggested methods are of the same order of magnitude for carbon steel tests[4-24] or Type 304 annealed and strain flattened[1-7]. This verifies Winter's effective width formula for effective width calculations for Type 301- 1/2 hard stainless. It is suggested that the elastic method may be used for design because of its simplicity and not unduly conservative prediction of moment capacity.

5.2.3.4 Moment Curvature Relationship

a. Analytical Moment Curvature Relationship

Once the internal equilibrium is established, the effective cross section, moment capacity and location of the neutral axis are determined. With known strains in the compression and tension flanges and the depth of the member, the curvature can be calculated from the following equation,

$$\Phi = \frac{\varepsilon_{mt} + \varepsilon_{mc}}{D'} \qquad 5\text{-}7$$

where ε_{mt} = edge membrane strain in tension flange

ε_{mc} = edge membrane strain in compression flange

D' = distance between the mid-thickness of tension and compression flanges

If a series of strains at the edge of the compression flange is assigned, the moments and the corresponding curva-

tures can be calculated by repeating the process discussed in 5.2.3.3 a., using a do loop in the program. In this manner the moment-curvature relationship of a particular section may be represented by a series of discrete points on a moment-curvature plot. The number of points and the strain increment are controlled by the input data.

b. Discussion of Results

Moment curvature data were calculated for strain increments at the extreme fiber in the compression flange of the section. This strain increment was taken as 0.0001 in./in. for the series H301F and AS304F.

Moment curvature relations can easily be obtained by test. Fig. 5-4 shows the comparison of moment curvature data from numerical computations and experiments for Type 301 1/2 stainless flexural members. In general, the agreement between numerical and experimental results is very satisfactory. There are two reasons for the deviations at near failure loads: 1) the method cannot predict performance when large deformations and cross-sectional geometrical changes are involved, 2) the analytical stress strain functions are valid only slightly beyond the .2% offset yield strength.

The calculated curvatures are overestimated for H301F-4 and underestimated for H301F-1. For H301F-2 and 3, the theoretical curvatures are very close to the experimental results. Better agreement was obtained between theory and experiments if the corner strengthening effect is considered. The corner effect becomes important only when the stress level is high.

Fig. 5-5 shows the same comparison for annealed and strain flattened Type 304 specimens. The general behavior is similar to that just discussed for cold-rolled Type 301.

It appears that the present numerical method can calculate satisfactorily the moment curvature relation of the flexural members of tempered Type 301 and annealed and skin passed Type 304 stainless. Based on this information, the deflection of flexural members may be calculated.

5.2.3.5 Deflections of Thin Walled Flexural Members

a. Numerical Procedure in Predicting Deflections

Since the stress strain relations are nonlinear, unsymmetrical in tension and compression and since there is local buckling in the compression flange, the load-deflection relation is nonlinear. The effective moment of inertia of the section, I_{eff} changes along the flexural member depending upon the magnitude of the moment at the section. The effective modulus, E_{eff} at any section, is unknown because of the shape of the stress strain relations. In view of the difficulties involved in taking these factors into account, an alternative approach is taken as follows:

In the basic beam theory for elastic material properties the following equations are valid:

$$\text{Curvature} = \frac{d^2y}{dx^2} = \frac{M}{EI} \qquad 5\text{-}8$$

$$\text{Slope} = \frac{dy}{dx} = \int \frac{M}{EI}\, dx \qquad 5\text{-}9$$

$$\text{Deflection} = y = \iint \frac{M}{EI}\, dx\, dx \qquad 5\text{-}10$$

However, the more direct and general approach is to use curvature directly. These more general equations are:

$$\text{Curvature} = \Phi \tag{5-11}$$

$$\text{Slope} = \int \Phi \, dx \tag{5-12}$$

$$\text{Deflection} = \iint \Phi \, dx \, dx \tag{5-13}$$

These equations are valid regardless of material properties provided the moment curvature relations are known so that curvature may be calculated for a given moment for the section.

In order to perform the integration in Eqs. 5-12 and 5-13 a numerical procedure is employed. The approach is the same as Newmark's method[5-5,5-6]. This is to replace the continuously flexible system by a system with a finite number of rigid segments connected by flexible joints at which the continuously varied curvature is lumped. The original system and the reduced system are shown in Fig. 5-6. The varied curvature is lumped at the node point by using parabolic formulae for numerical integration. These formulae are:

$$\psi_i = \frac{h}{12} (\Phi_{i-1} + 10\Phi_i + \Phi_{i+1}) \tag{5-14}$$

$$\psi_{i,i-1} = \frac{h}{24} (3\Phi_{i-1} + 10\Phi_i - \Phi_{i+1}) \tag{5-15}$$

$$\psi_{i-1,i} = \frac{h}{24} (7\Phi_{i-1} + 6\Phi_i - \Phi_{i+1}) \tag{5-16}$$

where h is the length of the segment, Φ_A, Φ_B, Φ_C are the curvatures at points i-1, i, i+1, ψ_i is the central concentration, $\psi_{i,i-1}$ is the one side central concentration, and $\psi_{i-1,i}$ is the more remote forward concentration. The error of central

concentration ψ_B is to the order of magnitude of h^4, and for forward or backward concentration and one central concentration it is of the order of h^3. It is obvious that the size of the segments is important.

The numerical approach for the solution of the representative system is straight forward and may be summarized briefly as follows: (1) the moment at each node point is calculated, and the corresponding curvature is obtained from the stored pre-calculated moment-curvature data through the linear interpolation sub-program. (2) by using parabolic numerical integration formulae, the curvature is concentrated at node points and the rotation at the joint calculated. (3) The increment of deflection at each node point may then be obtained. (4) By assuming a trial slope at one support the deflection at each node point may be obtained. (5) Considering the boundary condition at the other support, by a linear correction the final inelastic deflection at each node point is then obtained. The detailed sequence of computations is shown in flow chart in Fig. 5-7.

In the flow chart, the moment curvature data computation is similar to the flow chart shown in Fig. 5-3 for the maximum moment capacity of the flexural member except that a repeating process is employed for successive strain increments. A series of moment curvature data is computed and stored in the machine. The second part is the numerical procedure for deflection calculations by using the stored moment curvature data points to obtain the curvature from the moment through

a linear interpolation sub-program.

In this program, the flexural member was divided into 8, 20, and 40 rigid chords along the span. The computed moment curvature data points exceeded 80, which include a limited range beyond the yield moment (Moment at which the outmost fiber of the compression flange reaches the .2% offset yield strength).

Based on this approach, the inelastic deflection at mid-span from the computer output agrees satisfactorily with the experimental measurements. This will be discussed in c.

b. Simplified Methods for Deflection Predictions at Service Loads

The basic equation relating curvature and deflection was shown in Eq. 5-13. An approximate form of Eq. 5-13 was shown in Eq. 5-10. Based on this equation, the deflection for different loadings of flexural members can easily be evaluated by a number of methods. For instance, the elastic deflection at midspan for a simply supported beam loaded at the quarter points, considering bending deflection only, is

$$\delta = \frac{P\,a}{48\,EI}\,(3L^2 - 4a^2) \qquad 5\text{-}17$$

or

$$\delta = \frac{11}{768}\,\frac{PL^3}{EI} \qquad 5\text{-}18$$

where P = load on the beam

a = distance of symmetrical loading point to support

L = span length

δ = mid-span deflection

Eq. 5-17 can be generalized as

$$\delta = c \frac{P}{EI} \qquad 5\text{-}19$$

where c is a function of the loading conditions and span length. In order to apply the equation to thin walled steel design a drastic assumption is usually made, i.e. the effective section at the point of the maximum moment is considered as constant for the entire length of the beam. This assumption is used in the AISI design Manuals[1-1,1-7] for carbon and stainless steels to take the local buckling in the compression flange into account. In addition to local buckling, the non-linear unsymmetrical stress strain relationships should also be considered. This is achieved by introducing a reduced effective modulus in the formulation[4-33]. Eq. 5-19 is then rewritten as follows:

$$\delta = c \frac{P}{E_r I_{eff}} \qquad 5\text{-}20$$

where δ = deflection

c = expression depending upon loading and support conditions

P = equivalent load term

I_{eff} = moment of inertia of the effective section

E_r = effective reduced modulus

The reduced effective modulus used in the investigation was the averaged secant modulus[1-7 and 4-33],

$$E_{sa} = \frac{E_{st} + E_{sc}}{2} \qquad 5\text{-}21$$

where E_{st} = the secant modulus corresponding to the stress in the tension flange at location of maximum moment

E_{sc} = the secant modulus corresponding to the stress in the compression flange at location of maximum moment

As shown by Wolford[5-7], the secant modulus is exact for a two-flange beam with equal flanges (neglecting the web) and with equal material properties in tension and compression. While these conditions are not met in the case at hand, it is believed that the effect of the web of a light gage flexural member is comparatively small and that the averaged secant moduli[1-7,4-33] in tension and compression will adequately take care of the effect of nonlinear unsymmetrical stress strain relationships. Eq. 5-20 can then be written as

$$\delta = c \frac{P}{E_{sa} I_{eff}} \qquad 5\text{-}22$$

E_r varies with the inelastic stress strain relationship and the effective reduced section changes because of local buckling; hence the combined effect of these two factors may be considered as a reduced rigidity of the section expressed as $(EI)_r$. If $(EI)_r$ is substituted for (EI), Eqs. 5-8 and 5-19 becomes:

$$\frac{1}{\rho} = \frac{M}{(EI)_r} = \Phi \qquad 5\text{-}23$$

$$\delta = c \frac{P}{(EI)_r} \qquad 5\text{-}24$$

Therefore, as a result of the analysis outlined in a., the deflection can simply be expressed in terms of curvature from Eq. 5-24 as

$$\delta = c \frac{P\Phi}{M} \qquad 5\text{-}25$$

since

$$(EI)_r = M/\Phi \qquad 5\text{-}26$$

then

$$\delta = c' \Phi \qquad 5\text{-}27$$

where c' is a function of c and of the ratio of the load term P to the maximum moment, while M is a function of P.

$$\Phi = \frac{|\varepsilon_t| + |\varepsilon_c|}{D} \qquad 5\text{-}28$$

Therefore deflection can also be expressed in terms of extreme fiber strains as follows:

$$\delta = c' \frac{|\varepsilon_t| + |\varepsilon_c|}{D} \qquad 5\text{-}29$$

Thus, as an approximation, it appears that the deflection of the flexural member may be considered as directly proportional to the maximum curvature. c' can be evaluated numerically, and the deflection can then be computed from curvature. Such an approximate correlation between curvature and deflection is evident if one compares the moment-curvature diagrams in Figs. 5-4 and 5-5 to the corresponding moment deflection diagrams in Figs. 5-8 and 5-9.

c. Discussion of Results

Fig. 5-8 shows the comparison of the experimental and analytical deflections at mid-span of the flexural members of 1/2 hard Type 301. The analytical deflections were computed

by dividing the flexural member into 8, 20, and 40 rigid chords. Since the differences in resulting deflection are small in the case of quarter point loading of the member (the center half being under pure bending), only the results from the 40 segments model are presented. Twelve points were computed along the moment deflection curve.

The effect of using the original and the revised Winter's formulas for effective width is again small. The deflections are overestimated for H301F-4 and underestimated for H301F-2 and 3;the theoretical deflections are very close to the experimental results. Again, at the final stage approaching failure, the experimental deflection is larger than the predicted values. The effect of corner strength becomes important only at higher stresses. In general, the behavior of the predicted values as compared to the experimental deflections is similar to that of the curvature values.

Fig. 5-9 shows a similar comparison between analytical and experimental deflection for annealed and strain flattened Type 304 specimens. The general behavior is similar to that of cold-rolled Type 301 specimens.

For design the two essential considerations are strength at overload and deflection at the service load. The strength can be determined by the methods discussed in 5.2.3.3. The service load is defined as the ultimate load divided by the safety factor. A safety factor of 1.85 was used for the numerical analysis and for the approximate elastic method, while 2.0 was used for plastic methods of moment calculation.

Table 5-5 shows the service moments for specimens tested, obtained by dividing numerically the calculated maximum moments by the safety factor. The corresponding calculated (by numerical method) and experimental deflections were obtained from Figs. 5-8 and 5-9. In most cases, the calculated deflections are slightly smaller than the experimental values especially for the compact sections (H301F-1). The average percentage of deviation of the analytical deflection from the experimental deflection is -2.6% and -1.8% for Series H301F and AS304F respectively. This may be considered as satisfactory.

Table 5-6 shows a similar analysis for H301F series. The service moments and deflections were determined from the discussed simplified method (Eq. 5-22); the corresponding experimental deflections are again determined from Figs. 5-8 and 5-9. The results show that the agreement between calculated and experimental values is satisfactory. In most cases, the calculated deflections underestimate the test data except for H301F-4 which has the largest w/t ratio among the specimens tested. This agrees with the analytical results just discussed.

Using the elastic method for calculating ultimate moment capacity and a safety factor of 1.85 the deviations of calculated from the experimental deflections range from 5.50% to -7.8% with an average value of -0.72%. Using a safety factor of 2.00 for the moment capacity calculated by plastic method I and II, the deviations of calculated deflection from experi-

ments range from 8.08% to -7.82% with an average of -1.08% and 11.37% to -7.56% with an average of -1.51% respectively.

From these results, it is clear that the approximate method for predicting the deflections at service loads is quite satisfactory. This constitutes further indirect support for using Winter's effective width formulas for cold-rolled Type 301 stainless steel. In sum, it is suggested to use the elastic method for moment determination and to obtain the deflection by using average secant moduli formula (Eq. 5-22) for design purposes.

5.3 Compression Members

Compact and noncompact compression members are the two types of members encountered in light gage steel structures. A compact compression member is that in which only overall column buckling is involved and the section is so compact that no local buckling occurs. Noncompact compression member, containing plate elements which have large w/t ratios, will buckle locally or by interaction of local and column buckling. Only compact compression members with overall column buckling and non-compact compression members without overall column buckling are discussed briefly herein.

5.3.1 Compact Compression Members

The behavior of compact columns with ordinary material properties is well understood. Shanley's tangent modulus theory for column strength in the inelastic range is generally accepted. This amounts to substituting the tangent modulus, E_t, in the classical Euler formula,

$$\sigma_{cr} = \frac{\pi^2 E_t}{(L/r)^2} \qquad 5\text{-}30$$

where L = effective length of the column

r = radius of gyration in the plane of bending

Various theoretical and experimental methods of verification on inelastic buckling of columns were reviewed briefly by Karren[5-8].

It is realized that material properties and the cold forming process of light gage cold formed stainless columns create some difficulties in predicting the critical column buckling stress. Since there have been some prior investigations by others on this subject, the purpose here is to survey the literature in order to recommend a suitable method to calculate buckling stresses of columns.

An extensive experimental investigation on column curves for Type 301 stainless steel was made by Hammer and Petersen.[5-9] The specimens consisted of two hat sections spot welded together to form a closed column. It was concluded by the authors that column curves based on reduced modulus theory agree with the test data for the 1/4, 1/2, full hard columns formed in the longitudinal sheet direction. For columns formed in the transverse sheet direction, the column curves based on tangent modulus theory agree with the test data. In the short column region, the experimental values are generally higher than by the tangent modulus. It was also noticed that this deviation decreases for harder material. This phenomenon is mainly due to the effect of cold forming in the corners

which was neglected by the authors. The better agreement for harder tempers simply indicates that the cold forming effect is smaller for harder material. For short columns the effect of cold forming is more pronounced than for the long ones which buckle at relatively low stress and in which, therefore, the corner strengthening effect is negligible. It was stated in 2.3.2 that the increase in corner strength is more pronounced in longitudinal compression than in transverse compression. Hence, with less corner effect in transverse than in longitudinal compression, the test results of transverse direction columns agree better with the tangent modulus theory than the test results of the columns in the longitudinal direction.

Dubec, Krivobok, and Welter[5-10] also claimed that their test results agreed with the reduced modulus theory for columns made of 1/4 and 1/2 hard Type 301.

Some compact columns made of annealed and strain flattened Type 304 reported by Johnson and Winter[(1-6 and 4-33)] show similar behavior. Barlow[5-11] used tangent moduli obtained from the average stress strain curve of a stub column to predict the 18-8 stainless steel column buckling stress. Johnson[1-6] also used Barlow's approach. Such column curves based on stub column stress strain curves show better agreement with the test results. It should be noted that this approach does account for the amount of corner material in the column section, but does not account for the distribution of the corner material. If the corners are located close to

the buckling axis, the column curve based on the average stress strain curve may overestimate the column strength.

Anisotropic material properties may also affect the strength of columns. Since the longitudinal compression stress strain curve is the lowest among the four, it is to be expected that the tangent moduli derived from this curve may somewhat underestimate the column strength.

In the analysis by Duberg and Wilder[5-12] which considered the curvature of the stress strain curve, it was concluded that the column strength should lie between the tangent and reduced modulus values depending upon the shape of the stress strain curves. The larger the value of the exponent n in the Ramberg Osgood formula the less the column strength exceeds that given by the tangent modulus theory. Based on their analysis, the strength of stainless columns should lie somewhere between the two theories.

In an analysis by Osgood[5-13], the tangent modulus theory was extended to account for stress strain characteristics which are not constant throughout the cross sectional area of the column. Peterson and Bergholm[5-14] applied Osgood's approach to doubly symmetrical members. By assuming variations of the tangent modulus over the cross section, the column load may be expressed as

$$P = \frac{\pi^2}{L^2} \int_A E_t \, y^2 \, dA \qquad 5\text{-}31$$

where E_t = changeable tangent modulus

y = distance from neutral axis to the centroid of dA

Considering the different tangent moduli in different parts of the cross section, the column load may be expressed as

$$P = \frac{\pi^2}{L^2} \sum_{i=1}^{j} E_{ti} I_i \qquad 5\text{-}32$$

and the critical stress as

$$\sigma_{cr} = \frac{\pi^2}{AL^2} \sum_{i=1}^{j} E_{ti} I_i \qquad 5\text{-}33$$

where E_{ti} = tangent modulus of ith sub-area at a particular strain

I_i = moment of inertia of ith sub-area about the neutral axis of total cross section.

This approach is theoretically justified to account for the different material properties in the cross section. By applying it to annealed, 1/4 and 1/2 hard Type 301 stainless steel, Peterson and Bergholm obtained excellent agreement between test results and theory. Karren[5-8] used the same approach for cold formed carbon steel columns, and quite satisfactory results were also obtained. Based on the analytical results, it seems that the effect of anisotropic material properties is quite small.

Based on this experimental and theoretical evidence, it is concluded that the strength of cold formed cold-rolled austenitic stainless steel columns may be calculated by the tangent modulus theory somewhat conservatively. A better prediction may be obtained by using Eq. 5-33 with proper material properties. However, the effective corner stress strain relation for stainless is not known. Until a rigorous theoretical

treatment is available, it may be necessary to determine the effective corner strength and derive the tangent moduli from experiments, or to neglect the corner strengthening.

5.3.2 Noncompact Compression Members

A series of short compression members containing stiffened and unstiffened elements was tested. The short compression members with unstiffened elements were discussed in 3.3.1. Specimens were designed so that only the unstiffened elements were subject to local buckling and overall column buckling did not occur. Short compression members with stiffened elements were discussed in 3.4.2; only the stiffened elements were allowed to buckle locally. Therefore, the behavior of slender compression members with the combined action of local and overall column buckling is not discussed herein.

The general response of these compression members through the loading range up to the failure was described in Chapters 3 and 4 along with the behavior of stiffened and unstiffened elements. Despite local buckling in part of the member, the compression member can develop considerable post buckling strength.

However, the most important aspect is to calculate the maximum carrying capacity of the compression members. Eqs. 4-9 and 4-22 were used to account for the post buckling strength of stiffened and unstiffened elements. It was assumed that the maximum edge stress of the compression member, i.e. of the fully effective part, at failure was equal to the .2% offset yield strength of the compressive stress strain curve of the

sheet from which the members were formed. The justification of using this value as a limiting stress for the failure of flexural members was discussed briefly in 5.2.3.3 b.

The specimens, in general, failed by yielding or excessive local distortion. Around the offset yield strength, a considerable amount of plastic deformation is involved and serious out of plane waving in the locally buckled plate elements penetrates to the other part of the member. When some wrinkling occurs at the root of the buckles, the specimen has failed. The experimental maximum edge stresses at failure of these specimens are shown in Table 5-1. It is seen that the ratio of the maximum failure edge stress to the .2% offset yield strength averages 1.00 and 1.10 for short compression members containing unstiffened elements and stiffened elements, respectively.

This indicates that compression members with closed shape (containing stiffened elements) can sustain a load which causes a failure edge stress slightly higher than the .2% offset yield strength. For the open section (containing unstiffened elements) the 0.2% yield strength is essentially equal to the limiting stress. Thus, using the .2% offset yield strength may somewhat underestimate the carrying capacity of the closed section compression member. This fact is shown in Table 5-7 for Series H301SC.

It should be noted that in Table 5-7 the underestimation of the carrying capacity of noncompact compression members with unstiffened elements is mainly due to the slightly conservative

equation (Eq. 4-22) used for effective width calculations. This equation uses a buckling coefficient k = 0.5 which is conservative for a design specification[1-1] and 1.7. As discussed in Chapter 3 the average buckling coefficient for the H301UE series is k = 0.85 which explains the underestimation of Eq. 4-22. The data shown in Table 5-7 is merely a demonstration of the applicability of Eq. 4-22. A better agreement might be obtained if Eq. 4-23 were used for effective width calculations.

It is also noted in the same Table that the predicted carrying capacity agrees better with the experimental value if the corner strengthening effect is considered. For example, for H301UE series, the average percentages of deviation of calculated values from the experimental failure loads are -7.8% and -12.9% respectively, if the corner strengthening effect is considered or ignored.

It appears that it is possible to evaluate conservatively the failure loads of noncompact compression members (without column buckling) by using the effective width formulas and flat and corner material properties.

5.4 Summary and Conclusions

The structural performance of thin walled cold formed austenitic stainless steel flexural and compression members has been discussed. Based on the element behavior in the post buckling range, the structural behavior of thin walled members may be calculated. Methods for predicting member behavior, considering the material properties and local buckling

in the compression flange, have been presented. The significant results are summarized as follows:

(1) In order to investigate structural performance experimentally, a series of flexural members with hat cross-section (with w/t ratios ranging from 24.82 to 150.34 in the compression flange) for Type 301 1/2 hard and Type 304 annealed and strain flattened stainless was tested.

(2) A numerical iterative procedure was presented for predicting the maximum moment capacity of flexural members. The computer results based on a limiting stress equal to the .2% offset yield strength show satisfactory agreement with experiments. The comparison of computed and experimental results is shown in Table 5-2.

(3) The increase of the moment capacity for flexural members due to the revised Winter's formula (Eq. 4-40) for effective width, is comparatively small. The largest effect was for relatively compact section, H301F-1 with an increase of 3%, while for H301F-4 only with an increase of 0.3%.

(4) The effect of corner strengthening on the maximum moment capacity of the cold-rolled Type 301 flexural members is smaller than for the annealed Type 304. If the corner strengthening effect is ignored in the calculation, the computed moment capacities were -7.36% and 3.72% lower for Type 304 annealed and strain flattened and Type 301 1/2 hard respectively than when the corner effect is considered.

(5) Moment capacities calculated by simplified methods were obtained for design application. Moment capacities deter-

mined by the simplified numerical method deviated from the experimental ultimate moment by an average of -4.30% for the H301F series.

The elastic method generally underestimated the flexural capacity, and gave moments which deviated from the test by an average of -12.49%.

If plastic methods I and II are used, the deviations from the experimental ultimate moments averaged 3.65% and 13.69% respectively.

The deviations from the experimental ultimate moments calculated by these methods are of the same order of magnitude as for carbon steel tests and Type 304 annealed and strain flattened.

(6) Based on the results of the maximum moment capacity calculations for flexural members by using the numerical method or approximate methods, it appears that the use of effective width formulas (Eqs. 4-9 and 4-40) to account for the post buckling strength and the use of the .2% offset yield strength as a limiting stress are adequate and slightly on the conservative side.

(7) The calculated moment curvature data were in satisfactory agreement with the experimental values up to near-failure loads. There are two reasons to explain the deviation of the predicted and the experimental moments at near failure loads: (a) the method presented does not consider the large deformations and the change of cross sectional geometry, (b) the analytical stress strain functions are valid only slight-

ly beyond the .2% offset yield strength.

(8) The effect of Winter's original and revised formulas on the moment curvature relationship of the flexural members tested was very small, but the revised formula did improve the prediction slightly.

(9) The corner strengthening effect became important only when the stress level was high (at least 60% of the yield strength). Better agreement between calculated and experimental curvatures was obtained if the corner effective strength was considered. This was not true for the compact section tested (H301F-1, w/t ratio 24.82). The computed curvature, in this case, was lower than the experimental value.

(10) A numerical approach has been presented for inelastic deflection prediction. The actual continuous flexibility system is represented by a system with a finite number of rigid segments connected by flexible joints at which the continuously varied curvature is lumped. Newmark's procedure was used for deflection computation.

(11) The effect of using Winter's original and revised formulas on the deflection calculation was very small, but the revised formula did yield better results.

(12) The effect of the corner effective strength on the deflections of flexural members is similar to that discussed for curvatures in (7). The deflections were also underestimated at the final stage approaching failure as were curvatures, since there is a close direct correlation between curvature and deflection.

(13) The average percentages of the deviations of the analytical service load deflections from the experimental deflections were -2.6% and -1.8% for the H301F and the AS304F series respectively. The method showed satisfactory prediction of the deflection at the service load for both annealed and cold-rolled stainless.

(14) It must be emphasized that the service load deflection of Type 301 1/2 hard flexural member is considerably larger than for annealed stainless as a result of the high strength and strain. The service load deflections (either analytical or experimental) of the 1/2 hard flexural member exceed twice that of annealed stainless (H301F-4 and AS304F-4, H301F-3 and AS304F-2 practically have the same cross sectional dimensions and span).

(15) The simplified method for inelastic deflection calculations (used in the design specification for annealed Type 304 stainless) yields very satisfactory results when compared to the experimental deflections or computer results using Newmark's method. Based on the service moments determined by the elastic method and the plastic methods I and II the average deviations of the calculated from the experimental deflections were -0.72%, -1.08% and 1.51% respectively for H301F series. In Eq. 5-22, local buckling is considered by using the effective section moment of inertia, and the nonlinear unsymmetrical stress strain relationship in tension and compression is taken into consideration by using the averaged secant moduli. The equation appears to be adequate for

the service load deflection prediction for cold-rolled Type 301.

(16) Based on a survey of analytical and experimental evidence, for stainless column behavior, the tangent modulus theory for compact column buckling may be conservatively used for cold-rolled Type 301 stainless in both longitudinal and transverse directions. The corner strengthening effect on the column strength becomes less important with increasing hardness of cold-rolled stainless.

(17) The maximum carrying capacity of noncompact short columns may be predicted conservatively by using the effective width formulas for post buckling strength and the .2% offset yield strength as a limiting edge stress. A series of noncompact compression members containing stiffened and unstiffened elements was tested.

It was noted that the short columns with closed sectional shape (with less distortion) and compact sections could sustain larger load than that estimated by using the .2% offset yield strength as the limiting stress of the fully effective part of the section. The corner effective strength might be considered especially for the compact cross sections with large ratio of corner area to flat area.

(18) Based on the results in this Chapter, the following are the recommendations for the design of structural members of cold rolled Type 301 austenitic stainless steel. The methods and formulas recommended are simple and straightforward, but slightly on the conservative side.

(a) The revised Winter's formula is recommended for an

effective width prediction of the stiffened compression flange (Eq. 4-40)

$$\frac{b}{t} = 1.9\sqrt{E/\sigma_{max}}\ (1-0.418\ \frac{t}{w}\sqrt{E/\sigma_{max}})$$

(b) The 0.2% offset yield strengths in tension and compression are recommended as the limiting stresses for ultimate strength calculation.

(c) The elastic method (Eq. 5-6) is recommended for the maximum moment capacity calculation.

$$M_y = \sigma_y \frac{I_{eff}}{c} = \sigma_y S_{eff}$$

(d) The average secant moduli formula (Eq. 5-22) is recommended for the deflection calculation at service loads. The internal equilibrium is achieved by using the elastic method as in (c)

$$\delta = c \frac{P}{E_{sa} I_{eff}}$$

(e) Column curves based on tangent modulus theory are recommended.

(f) The corner strengthening effect may be neglected for harder tempers.

(g) The carrying capacity of noncompact compression member without column buckling may be calculated by using the effective width formulas, Eqs. 4-40 and 4-22, for stiffened and unstiffened components.

CHAPTER 6

DESIGN CONSIDERATIONS

6.1 General

Based on the results of this investigation, methods and procedures for design of similar types of elements and members made of Type 301 1/4 and 1/2 hard stainless steel considered may be recommended. It is not intended to formulate the findings in this investigation in design specification language. However, alternative procedures of design, based on rational and practical methods, will be outlined.

Design procedures for 1/4 and 1/2 hard Type 301 austenitic stainless steels will be emphasized. Since design methods exist for light gage construction using carbon and annealed austenitic stainless steels, the basic questions are concerned with the differences which arise from the mechanical behavior of cold-rolled austenitic stainless steel.

6.2 Material Properties

Mechanical properties of Type 301 1/4 and 1/2 hard austenitic stainless steel were studied in detail and presented in Chapter 2. For other cold-rolled austenitic stainless steels, a separate study on material properties is necessary.

Since tempered Type 301 is more strongly anisotropic than annealed Type 304 stainless, separate values of the .2% yield strength in tension and compression, for both longitud-

inal and transverse directions are recommended. The recommended values are shown in Table 2-3 based on a statistical study. For the tensile strength for ¼ and ½ hard stainless, recommended values are given in Table 2-6.

The initial moduli of elasticity for Type 301 ¼ and ½ hard are smaller than for Type 304 annealed and strain flattened stainless. In order to avoid superfluous complication, 27.0 $x10^3$ ksi is recommended in the longitudinal direction for compression and tension for both ¼ and ½ hard, and $28.0x10^3$ ksi is recommended in the transverse direction for both compression and tension for both ¼ and ½ hard.

Typical design stress strain curves for ¼ and ½ hard Type 301 were developed and are shown in Fig. 2-10. Their derived quantities, such as secant and tangent moduli are shown in Figs. 2-11 and 2-12. The values of the proportional limits of these typical stress strain curves are given in Table 2-5.

A value of 0.31 for Poisson's ratio is recommended for both ¼ and ½ hard Type 301. Information on mechanical properties in shear for Type 301 stainless steel ¼ and ½ can be found in Section 2.6. The coefficients of the analytical expression of the typical stress strain curves and the shear stress strain curves were presented in Table 2-8. This will give designers a choice to work with an analytical function or experimental data depending upon the nature of the problem.

6.3 Safety Factors

A safety factor of 1.85 is assumed in the following discussion of the structural performance of cold-rolled austenitic stainless steel. This value is used in the design specification of annealed and strain flattened austenitic stainless[1-7].

If the basic working stress is taken as $\sigma_y/1.85$, the working stress is 0.54 of the yield strength. If one compares this ratio with the ratios of the .01% offset effective proportional limits to the corresponding 0.2% yield strengths, one finds that 0.54 is very close to those ratios shown in Table 2-5. These ratios are listed as follows:

	¼ Hard	½ Hard
Longitudinal Compression	0.520	0.492
Longitudinal Tension	0.520	0.491
Transverse Tension	0.573	0.640
Transverse Compression	0.533	0.517

Hence, using 1.85 as a safety factor, the effective proportional limits in longitudinal compression, longitudinal tension, and transverse compression are slightly lower than the working stresses (allowable stresses) for both ¼ and ½ hard Type 301. Therefore, member design based on this safety factor may cause very slight inelastic deformations at design loads, especially for ½ hard.

In Type 304 annealed and strain flattened stainless (Ref. 1-6, Table 2-4), the ratios of effective proportional limits to the corresponding strengths of cold-rolled 301 are smaller than those

of Type 304 annealed stainless. This indicates that if the same safety factor is used, the cold-rolled grades may slightly enter into the inelastic range, while annealed Type 304 is still in the elastic range at design loads.

In order to avoid inelastic strain, a higher safety factor may be necessary (2.0). In this case, the ratio of allowable stress to the yield strength is 0.5. With this ratio, there will be no significant inelastic strain for ¼ hard or for ½ hard. Using a larger safety factor may also be appropriate because the deformation at design loads of structural members of cold-rolled 301 is larger than for annealed stainless because of the high strength. Deflection may control more often for tempered stainless than for annealed stainless or carbon steel.

6.4 Design Criteria for Plate Structural Elements

The critical and post buckling behavior of structural elements was discussed in Chapter 3 and 4. Criteria for local buckling, limitations of local distortion, and post buckling strength of the cold-rolled stainless stiffened and unstiffened thin elements will be discussed.

6.4.1 Local Distortions

Although plate elements possess considerable post buckling strength, at the same time out of plane waving is involved. The waving amplitude in the post buckling range for tempered stainless is more pronounced than for the annealed grades because high strength is accompanied by large strain.

Similar to annealed stainless, the cold-rolled stainless unstiffened elements exhibit extreme out of plane waving at higher stresses, while local distortion is less pronounced for stiffened elements. Due to large local distortion, the utility of the post buckling strength of unstiffened elements is restricted. On the other hand, local distortion for stiffened elements must be considered only when limitations on waving apply.

In general, the calculated buckling stress (Eq. 3-1) may be used as an index of local distortion. Based on this index and the experimental waving observation, criteria for stresses to limit the local distortion have been formulated in Chapter 3.

It is suggested that for design purposes Eq. 3-1 be used with $k = 4.0$, $\eta = \sqrt{E_t/E}$, and $k = 0.5$, $\eta = E_s/E$ for stiffened and unstiffened elements, respectively. If either no waving or slight waving (equal to the thickness of sheet) is permitted, the corresponding allowable stresses for unstiffened elements can be taken as 0.8 and 1.2 times the calculated critical buckling stress respectively. For stiffened elements, the corresponding ratios are 0.9 and 1.2.

6.4.2 Ultimate Strength

Various formulations were discussed in Chapter 4 to account for the post buckling strength of cold-rolled stainless stiffened and unstiffened elements, using effeciive widths. Based on the experimental evidence and simplicity for design,

Eqs. 4-40 and 4-22 with elastic parameters are recommended for calculating the post buckling strength of stiffened and unstiffened elements respectively. The reason for using the revised Winter's formula, Eq. 4-40, for stiffened elements is to account for the higher effective width for tempered Type 301 than for the annealed grades.

6.4.2.1 Unstiffened Elements.

The post buckling strength of unstiffened elements was demonstrated by the series of cold-rolled stainless unstiffened compression member tests described in Sections 3.3 and 4.5. Due to a large amount of out of plane waving, the post buckling strength of unstiffened elements can best be utilized as a strength reserve in connection with an allowable stress approach. This is similar to the approach for carbon steel[1-1] and annealed stainless[1-6,1-7].

Four practical qualitative conclusions are drawn from the findings in Chapter 3. (1) The edge failure stresses of the elements are close to the .2% offset yield strength as shown in Fig. 3-3 and Tables 3-9 and 5-1. (2) Unstiffened elements with w/t equal to 11.02 buckled at a stress very close to the .2% offset yield strength although it appears that the elements with w/t ratios lower than this value may not buckle at the limiting stress of the .2% offset yield strength. (3) There is a close relationship between the w/t ratio and the average element failure stress or the average member failure stress as shown in Fig. 3-3. The failure

stress decreases rapidly with an increasing w/t ratio, and is close to the buckling stress. A slight local distortion was observed for the specimens with intermediate w/t ratios (10 to 25). (4) Considerable post buckling strength is available for the specimens with higher w/t ratios (>25), but it is accompanied by a large amount of out of plane waving.

Based on these observations, an approach similar to that used for carbon steel[1-1] and annealed stainless steel[1-6 and 1-7] may be considered. As a consequence of the first conclusion, the .2% offset yield stress may be used as a limiting stress. This was also discussed in detail in Sections 5.2.3.3 b and 5.3.2. The consequence of the second observation is that the elements with small w/t ratios can be designed by the ultimate strength consideration. The limiting w/t ratio $(w/t)_1$ must be smaller than 11 from the experimental evidence. Based on the third observation, the allowable stress from the limiting w/t ratio $(w/t)_1$ to some intermediate value of w/t ratio $(w/t)_2$ can be determined by the element strength consideration. For larger w/t ($>(w/t)_2$) ratios, the stress must be based on local distortion.

With these considerations in mind, typical design allowable stress curves for ½ hard Type 301 are shown in Fig. 6-1. The buckling curves for $k = 0.5$ and $\eta = E_s/E$ as well as $\eta = 1$ are shown in the figure. By using the .2% offset yield strength (65 ksi) as a limiting edge stress, the average element failure stress is determined by the effective

width formula, Eq. 4-22. The element failure stresses and the values of these stresses divided by the safety factor (1.85) are plotted in Fig. 6-1. The .2% offset yield strength and the value of this strength divided by the safety factor (1.85) are used as the cut off strength for the curves.

In order to determine the value of $(w/t)_1$, the following equations in the carbon steel design specifications[1-1] and the annealed stainless specifications[1-7] respectively were used:

$$(w/t)_1 = 1820/\sqrt{\sigma_y} \qquad \text{or} \qquad 1340/\sqrt{f_b} \qquad 6\text{-}1$$

From this equation, the value of $(w/t)_1$ is 7.15. By setting b/t equal to w/t in the effective width formula, Eq. 4-22, the calculated value of $(w/t)_1$ is 7.69. It appears that $(w/t)_1$ may be reasonably taken as 7.0. The value of $(w/t)_1$ is smaller for the cold-rolled grades than for the annealed stainless.

The ratio $(w/t)_2$ is the transition value from strength consideration to distortion considerations. The value of $(w/t)_2$ should be so determined so that the corresponding stress is less than the proportional limit (to simplify the critical stress calculation), small enough to cause no visible waving, and adequate for the strength reserve against element failure. Based on the conclusion (8) of unstiffened elements of Section 3.3.5 and the data shown in Table 3-11, the stress at which no waving is observed may be taken as 0.8 of the calculated buckling stress. The value of $(w/t)_2$ is

taken as 25, which meets all the requirements mentioned. The allowable stress for the range between w/t = 7 and 25 may be represented by a straight line which is close to the element failure stress divided by the safety factor. For cold-rolled grades, the value of $(w/t)_2$ is smaller than for the annealed grades because of the effects of high strength.

Beyond $(w/t)_2$, adequate strength reserve is evident and the local distortion must be considered. The no waving allowable stress is represented by the following stress.

$$\sigma_{all} = 0.8\sigma_{cr} = 0.8\frac{k\pi^2 E}{12(1-\nu^2)\ (\frac{w}{t})^2} \qquad 6\text{-}2$$

where k is taken as 0.5. It is suggested that the upper limit of the w/t ratio, $(w/t)_3$, may be taken as 50 for the following reasons: (1) it is not economical to use unstiffened elements with large w/t ratios since the buckling stresses are so low, (2) there is no advantage to use cold-rolled stainless at the buckling stress lower than the proportional limit of annealed stainless.

If slight waving is permitted (equal to the thickness of the sheet), the allowable stress may be made higher than the critical stress, and may be represented by a straight line connecting $(w/t)_2$ and the buckling stress at w/t = 50. This is based on the information shown in Table 3-11.

Based on the foregoing discussion, the allowable design stress for ½ hard Type 301 stainless unstiffened elements may be easily established by knowing the values of $(w/t)_1$,

$(w/t)_2$, and $(w/t)_3$, and their corresponding stresses. The allowable design stresses may be summarized as follows:

$$0 < w/t < (w/t)_1 \qquad \sigma_{all} = \sigma_y/S.F. \quad \text{or } 35.10 \text{ ksi} \qquad 6\text{-}3$$

$$(w/t)_1 < w/t < (w/t)_2 \qquad \sigma_{all} = 35.10 - 1.07(\frac{w}{t} - 7) \qquad 6\text{-}4$$

$$(w/t)_2 < w/t < (w/t)_3 \qquad \sigma_{all} = \frac{0.4\pi^2 E}{12(1-\nu^2)(\frac{w}{t})^2} \quad \text{(no waving)} \qquad 6\text{-}5$$

$$\sigma_{all} = 15.77 - 0.43(\frac{w}{t} - 25) \qquad 6\text{-}6$$

(slight waving)

The same approach may be applied to the other tempers. The values of $(w/t)_1$ and $(w/t)_2$ decrease with increasing of hardness.

6.4.2.2 Stiffened Elements

Stiffened elements possess considerably more post buckling strength with less pronounced out of plane waving than unstiffened elements. In general, the usual factor of safety (1.85) against failure by reaching yield strength along the edges is adequate because of comparatively small distortion.

The ultimate strength of stiffened elements may be computed from Eq. 4-40 for effective width. The equation was shown to be valid for cold-rolled austenitic stainless steel as described an Section 4.6.3.

For stiffened elements of cold-rolled grades, there are two factors which are different from annealed stainless,

i.e., higher post buckling strength (especially for elements with large w/t ratios) and larger local distortion (due to high strength, service stress and strain). In some cases when the local distortion is of major concern, the allowable stress based on waving consideration other than strength may have to be used to limit the distortion. This is mainly for large w/t ratios of the stiffened elements. In order to utilize the high post buckling strength of cold-rolled stainless and to avoid waving in the post buckling range, stiffened elements with somewhat small w/t ratios should be used for major load carrying members.

From the correlation between waving observations and measurements and the critical buckling stress, the allowable stresses when considering distortion may be determined in a similar manner to that for unstiffened elements. Because of the much less pronounced waving encountered in stiffened elements, the restrictions of allowable stress need not be as rigid as for unstiffened elements. Thus, the major restriction for stiffened elements is that in no cases should the allowable edge stress be larger than the strength divided by a factor of safety (1.85). This is to maintain the necessary strength reserve.

Based on the correlation of waving and critical buckling stresses and loads in Tables 3-15 and 3-17, the allowable stress for design may be recommended in terms of the theoretical buckling stress σ_{cr}. The allowable stress is summarized as follows:

For small w/t ratios, the full section will be effective and no buckling is involved up to the 0.2% offset yield strength, which is used as a limiting stress. By dividing the yield strength by a safety factor of 1.85, the maximum allowable stress is obtained.

For members in which no visible local distortion at service loads is permissible, the stress in the stiffened compression elements shall not be larger than 0.9 of the theoretical critical buckling stresses σ_{cr}.

For members in which local distortions at service loads are limited to a slight visible amounts (the thickness of the sheet), the allowable stress in stiffened compression elements may be up to $1.2\sigma_{cr}$ but not larger than the yield strength/1.85.

If local distortion is of no concern, the allowable stress in the effective section of stiffened compression elements may be up to the maximum allowable stress.

The critical buckling stress may be determined from Eq. 3-1 by using $k = 4.0$ and $\eta = \sqrt{E_t/E}$.

6.5 Design Criteria for Structural Members

With the design procedure for element behavior and simplified methods for predicting member behavior, the member response under loading can be analyzed. Based on the methods of analyzing member behavior presented in Chapter 5 and information on element behavior presented in Chapters 3 and 4,

design procedures for structural members are presented in the following sub-sections.

6.5.1 Flexural Members

For flexural member design the two essential considerations are strength at overloads and deflections at service loads. For design purposes, the designer should be able to predict the flexural capacity and deflection with no more information than the geometry of the member and its material properties. In connection with this, simplified methods with acceptable accuracy are needed.

6.5.1.1 Flexural Strength

Two alternative methods for the calculation of flexural strength of stiffened elements are recommended herein. The basic assumptions and procedures were outlined in 5.2.3.3 c. These two methods are the "elastic" and the "plastic" methods. Both of these approximate methods are relatively simple and are familiar to the designers. With the aid of Winter's formula (Eq. 4-40) to account for post buckling strength of the compression flange, the flexural strength can easily be obtained for given limiting stresses.

It is obvious that the actual stress distribution falls between the two methods assumed. It is expected, in general, that the flexural strength is underestimated by the elastic method and overestimated by the plastic method. The elastic method approach is straight forward and is well defined in

the light gage cold formed steel design manual for carbon steel[1-1]. The location of the neutral axis is obtained by an iterative process of checking internal force equilibrium; then flexural strength can be calculated from Eq. 5-6.

The elastic method for calculating the moment capacity for series H301F and AS304F gives moments which underestimate the test failure moments by an average of -12.46% and -15.70% respectively. The method is somewhat better for cold-rolled grades because of the more gradual yielding type of stress strain curves than for the annealed stainless. This simple method may best be used for design purposes. The corner strengthening effect is neglected in the formulation.

The plastic method is the easiest to apply since no iteration is needed. The location of the neutral axis can be determined from the geometry of the cross section and the effective width in the compression flange. In general, the method overestimates the actual flexural strength because of the fully plastic assumption of stress distribution (see below). The range of overestimation is reduced by using the compression yield strength as the limiting value for tension and compression.

In order to determine the allowable moment at service loads from flexural capacity, it is necessary to use the appropriate factor of safety. For the elastic method, a factor of safety of 1.85 is recommended as mentioned in 6.3. A factor of safety of 2.0 is suggested for obtaining service

load moments from flexural moment capacities by the plastic method. It is of interest to compare the experimental failure moment to the calculated service load moment, indicating the actual strength reserve is thus obtained. Such a comparison is shown in Table 6-1. The strength reserve for the allowable moment by the elastic method, with a safety factor of 1.85 averages 117%. For the allowable moment by plastic method I with a safety factor of 2.00, the strength reserve averages 79%.

6.5.1.2 Deflections at Service Loads

The deflection can be determined from Eq. 5-22[1-7 and 4-33] by using the information obtained from the elastic method for flexural strength calculation. This method is consistent with the elastic method for flexural strength computation. Since the stress distribution at the service moment is not known, an iterative process must be used to determine the location of neutral axis, the secant moduli at extreme fibers, the effective moment of inertia, and the corresponding moment. The procedure is similar to that of the elastic method for flexural strength calculation. The service load deflection can be obtained from two consistent calculations of deflection in the vicinity of the service load by interpolation or extrapolation.

The agreement between calculated and experimental deflections is very satisfactory, as shown in Table 5-6. Bas-

ed on the deviation of the computed deflection at the service load from the test data, the method yields better results for cold-rolled grades than for the annealed stainless. This again is due to the more gradual yielding type of stress strain relation for the cold-rolled grades than for the annealed stainless.

Due to the high yield strength, the low proportional limit, and local buckling, the deflection at service load will frequently be excessive when compared to the usual requirements in specifications. In view of this situation, deflection rather than strength of the cold-rolled stainless flexural members will frequently govern.

6.5.2 Compression Members

It is proposed that the tangent modulus formula be used to predict the strength of compact columns. A flat cut off is suggested at the .2% offset yield strength. The allowable design stress is obtained by dividing the values from Eq. 5-30 by a safety factor. Typical column curves derived from the typical longitudinal compression stress strain curves for annealed and strain flattened Type 304 and ¼ and ½ hard Type 301 from Fig. 2-10 are presented in Fig. 6-2. A safety factor of 2.15[1-7] was used.

The tangent modulus formula underestimates the compact column strength at lower values of the slenderness ratios; however, this deficiency becomes smaller with the increasing hardness of the cold worked stainless sheets. Experi-

ments by others[5-9] and [5-14] showed that the test data of columns with small L/r slenderness ratios were closer to the values predicted by the reduced modulus theory.

A more accurate method to take corner effective moduli into account was proposed by Peterson and Bergholm[5-14]. However, the usefulness of the approach to account for the cold forming effect depends upon the availability of an expression for the corner effective stress strain relation and its derived values. Column curves in other specifications are not applicable to the material under consideration in the inelastic range. The tangent modulus formula without corner effects is also used in the specifications for annealed and strain flattened Type 304[1-7]. Except for low w/t ratios of stiffened and unstiffened elements contained in the compression member, the possibility of local buckling in these elements should be recognized. The case of very short columns where only local buckling is involved was discussed in Section 5.3.2. For such short columns the strength can be predicted by using the effective section (Eq. 4-22 and 4-40) and the .2% offset yield strength as the limiting stress.

However, for cases intermediate between the above mentioned situations, interaction between local buckling and over all column buckling must be considered. There is no simple method to account for this interaction to predict the column strength. In connection with this, the "Q" fac-

tor approach, which is used in the light gage cold formed design manuals for carbon steel[1-1] and annealed stainless[1-7], is recommended for design.

6.6 Effects of Cold Forming

The strengthening effect of cold forming of corners was discussed in 2.2.3 and 2.3.4. The effect of corners on the member behavior was described in 5.3 for compression members and in 5.2.3 for flexural members.

The effect is more pronounced on the member behavior if the section contains a large percentage of corner area. The distribution of these deformed corners is also a factor important to the member behavior. The strengthening effect of corners decreases with increasing hardness, the effect being the largest for annealed material and almost negligible for full hard temper.

From Table 2-1, it can be seen that the strength increase in corners over flats is more pronounced for annealed Type 304 than 1/2 hard Type 301 stainless. The percent of increase in flexural strength of the specimens tested are 7.36% for annealed stainless and 3.72% for 1/2 hard Type 301 from a numerical analysis, as shown in Table 5-3. Based on the data of strength increase either for corners or for structural members, it appears that the amount of increase for cold-rolled austenitic stainless is not appreciable.

It should be realized that a simple design method cannot easily account for the cold forming effect. Besides,

there is no analytical method to predict the strength increase in the corners for cold-rolled austenitic stainless steel. The Karren formulas for carbon steel are not applicable to cold-rolled stainless.

In view of the foregoing discussion, it is suggested that the corner strengthening effect may be neglected in design.

6.7 Summary and Conclusions

Based on the findings of this investigation, simplified methods for the design of elements and members of cold-rolled stainless steel have been described in this Chapter. Satisfactory agreement was obtained between the predicted values and the experimentally determined data. It was found that in most of the cases the design approach and formulas for annealed stainless steel[1-6, 1-7, and 4-33] are applicable to the cold-rolled stainless with due account being taken of the considerably higher strength of the latter.

The recommendations on material properties, design methods for structural elements and members, and other related topics are summarized as follows:

(1) Design material properties for Type 301 stainless steel 1/4 and 1/2 hard are summarized in Section 6.2. The detailed information on the typical material properties was given in Chapter 2 in tables and figures. Due to the variation of material properties as a result of cold working reducing, the design mechanical properties for other types or tempers of austenitic stainless steels should be investigated

individually. It is believed that the same procedure as described in Chapter 2 can be reliably used.

(2) The basic safety factor used in this investigation was 1.85 which is the same as that used in the design specification[1-7] for annealed and strain flattened Type 304 stainless. The ratios of the effective proportional limits to the corresponding yield strengths for cold-rolled Type 301 are smaller than those of Type 304 annealed stainless. A slightly higher safety factor (2.0) may be necessary in order to avoid inelastic deformation at service loads.

(3) Due to large local distortions, the usefulness of the post buckling strength of unstiffened elements is restricted. Therefore, the post buckling strength of unstiffened elements can only be utilized as a strength reserve in connection with an allowable stress approach similar to that which has been used for both carbon steel[1-1] and annealed stainless steel[1-7].

For small w/t ratios ($< (w/t)_1$), the allowable stress is based on the yield strength. For intermediate w/t ratios ($(w/t)_1 < w/t < (w/t)_2$), the allowable stress is based on the average element failure stress. For large w/t ratios ($(w/t)_2 < w/t < (w/t)_3$), the allowable stress is based on local distortion considerations. The limiting values of w/t ratios for $(w/t)_1$ $(w/t)_2$, and $(w/t)_3$ were taken as 7, 25, and 50 respectively for Type 301 1/2 hard stainless steel. The values of $(w/t)_1$ and $(w/t)_2$ decrease with increasing hardness of the material. Typical design allowable stress for 1/2 hard Type 301 is shown in Fig. 6-1.

(4) The stiffened elements of cold-rolled grades possess higher post buckling strength (with larger local distortion) than annealed stainless. When compared to unstiffened elements, stiffened elements possess relatively greater post buckling strengths with less pronounced local distortions. Because of this, the usual factor of safety (1.85) against failure by reaching yield strength along the edges is generally adequate. The design approach for stiffened elements is then based on the element ultimate strength in the post buckling range which may be determined from the effective width calculated from Eq. 4-40.

However, in cases when the local distortion is of major concern, the allowable stress based on waving consideration may have to be used to limit distortion. For elements with small w/t ratios, the allowable stress is then yield strength/ 1.85. For elements with large w/t ratios, the allowable stress is based on local distortion using the buckling stress as an index. If no waving is permissible, the allowable stress is taken as $0.9\ \sigma_{cr}$. If slight waving (thickness of the sheet) is permissible, the allowable stress is taken as $1.2\ \sigma_{cr}$. In no case should the stress be larger than yield strength/1.85.

(5) The buckling stress for (3) and (4) may be computed from Eq. 3-1 by using $k = 4.0, \eta = \sqrt{E_t/E}$ and $k = 0.5$, $\eta = E_s/E$ for stiffened and unstiffened elements respectively.

(6) The elastic method is recommended for design purposes in calculating the strength of flexural members. The design

procedure of the method was outlined in 6.5.1.1 and 5.2.3.3. c. Winter's formula for effective width (Eq. 4-40) is used to account for the post buckling strength of the compression flange. The .2% offset yield strengths in longitudinal compression and tension are used as limiting stresses. The method yields better results for cold-rolled grades than for the annealed stainless because of the more gradual yielding type of stress strain curves of cold-rolled grades

(7) Eq. 5-22 is recommended for deflection calculations at service loads. This is the same equation as that used in the design specifications for annealed stainless steel [1-7] and [4-33]. Again the method yields better results for cold-rolled grades than for the annealed stainless steel.

Due to the high yield strength, the low proportional limits (comparing to the corresponding yield strength), and local buckling in the compression flange, the deflections at the service loads will frequently govern the design rather than strength.

(8) The tangent modulus formula is recommended for predicting the compact column strength, although the formula slightly underestimates the column strength at low values. of the slenderness ratios because of neglecting the cold forming effects in corners.. However, this deficiency becomes smaller with increasing hardness of the stainless sheets. Typical column design curves for 1/4 and 1/2 hard Type 301 are shown in Fig. 6-2.

The ultimate strength of short noncompact columns (without column buckling) may be predicted by using the effective width formulas (Eqs. 4-22 and 4-40) and the .2% offset yield strength as a limiting stress.

The usual "Q" factor approach[1-1 and 1-7] may be used for columns with both local and over all column buckling.

(9) The strengthening effect of corners decreases with increasing hardness of stainless sheets. For cold-rolled gra it is suggested that the cold forming effect be neglected in design.

CHAPTER 7

SUMMARY AND CONCLUSIONS

The purpose of this investigation was to develop basic information for design methods of light gage cold formed structural elements and members made of cold worked austenitic stainless steel. Such stainless steels have much different material properties than carbon steel. In obtaining high strength through cold reducing, certain material characteristics result: (a) increasing strength and anisotropy with amount of cold work, (b) unsymmetrical stress strain relations in tension and compression, (c) inelastic stress strain relations with low elastic limit. In addition corner strain hardening and local buckling are also encountered in thin walled members.

The investigation concerns cold-rolled austenitic stainless steel, especially Type 301 1/4 and 1/2 hard, as the second phase in an investigation on the structural performance of austenitic stainless steel members, the first phase having dealt with annealed steels. The topics investigated herein are: (1) Material properties, (2) Buckling and waving of plate structural elements, (3) Post buckling behavior of plate structural elements, (4) Structural member behavior, and (5) Design considerations.

Although these topics are related to each other, they may be considered seperately if the sequence is followed. It is more logical and convenient to conclude each phase before entering on the next topic. For this reason, detailed

summaries and conclusions were given at the end of each Chapter. Therefore, the following is only a brief summary, and the reader is referred to the summary of each chapter for more detailed information.

(1) Material Properties

Due to the severe plastic deformation from cold rolling, the internal stress distribution is nonuniform in the complex microstructure of the stainless steel sheet. The sheet is strain hardened and a preferred orientation of microstructure is developed. The microstructure of the austenitic stainless steel is transformed from austenite into martensite during severe cold working. Due to these changes, the cold worked material characteristics (a), (b), and (c) result. The strength and the anisotropy of the cold worked sheet increase with the increasing amount of cold working.

No theoretical method is available to predict the mechanical changes due to cold working. An experimental study was made, and the data were analyzed on a statistical basis. Based on this analysis, typical mechanical properties for 1/4 and 1/2 hard Type 301 stainless steel were obtained. The typical lower bound .2% offset yield strengths in tension and compression for both longitudinal and transverse directions were established. Typical design minimum stress strain curves under normal and shear stresses were constructed. Analytical expressions of these stress strain curves by using the Ramberg Osgood function were obtained. These typical material properties are ready to be used in design specifications.

(2) Buckling and Waving of Plate Structural Elements

In order to study member behavior, the understanding of element behavior is essential. Two types of plate structural elements were investigated - stiffened and unstiffened. These are the usual plate elements encountered in light gage steel members.

An approximate analysis considering orthotropic material properties and the inelastic behavior was briefly discussed. By considering the appropriate boundary condition and the plasticity reduction factor, the oritical buckling stresses for stiffened and unstiffened elements can be predicted by Eq. 3-1. For stiffened and unstiffened elements, the plasticity reduction factor may be taken as $\sqrt{E_t/E}$ and E_s/E, respectively.

A series of tests of compression members containing stiffened and unstiffened elements and a series of tests of flexural members containing compression flanges as stiffened element were performed. Fair agreement was obtained between the analytical and the experimental critical buckling stresses. Based on the results, it seems that the effect of anisotropic material properties on the buckling stress is small.

For cold-rolled grades, it was concluded that a large amount of local distortion due to the high strain involved severely limited the usefulness of unstiffened elements.

(3) Post Buckling Behavior of Plate Structural Elements

The post buckling behavior of stiffened and unstiffened elements was investigated. The effective width concept was utilized for analyzing the behavior of plate elements in

the post buckling range. Karman's semi-theoretical treatment of effective width of plates and Winter's experimental modification of Karman's equation were discussed. Based on these fundamental equations, an attempt was made to include the orthotropic material properties and inelasticity into account.

A detailed analysis of experimental effective widths of stiffened and unstiffened elements was made. The experimental effective widths reduced from the series of tests mentioned in (2) were compared with the analytical expressions. By using strain analysis, the experimental effective widths showed very satisfactory agreement with Koiter's equation at higher edge strains. Near and below the critical strain, the experimental effective widths were lower than those from the theory. Winter's formula was shown to be the lower bound for the experimental data.

Based on the experimental evidence, it seems that the effective widths of cold-rolled stainless may be higher than of annealed stainless because of the anisotropic material properties (longitudinal compression being the weakest).

Eqs. 4-22 and 4-40 were recommended for design purposes for unstiffened and stiffened elements, respectively.

(4) Structural Member Behavior

Based on the material properties and the element behavior in the post buckling range, the structural behavior of thin walled members may be predicted. Methods for predicting member behavior, considering the peculiar material

properties and local buckling in the compression flange, were presented in Chapter 5. The effects of the material properties, the cold forming process, and the post buckling strength on the structural member behavior were studied.

A numerical iterative procedure was presented for predicting the maximum moment capacity, moment curvature relation, and the service load deflection of flexural members. The .2% offset yield strength was used as a limiting edge stress for computing the maximum moment capacity. Satisfactory agreement was obtained between the calculated and the experimental results.

If the corner strengthening effect is ignored, the calculated maximum capacities were 7.3% and 3.72% lower than the experimental values for Type 304 annealed and Type 301 1/2 hard stainless respectively.

Simplified methods for strength and service load deflection predictions were also presented. The comparison between the calculated and the experimental results showed an acceptable accuracy for design purposes.

The service load deflection of Type 301 1/2 hard flexural members is considerably larger than for annealed stainless because of the high strength and strain. Deflections may frequently govern the design for cold-rolled stainless rather than strength.

A brief study was made of compact and noncompact columns of cold-rolled stainless. It was concluded that the tangent modulus formula may be conservatively used for compact columns;

and the strength of the short noncompact columns may be predicted by using the effective section and the .2% offset yield strength.

(5) Design Considerations

Based on the results of this investigation, methods for design of similar types of elements and members with the material properties considered are recommended in Chapter 6. In general, most of the design methods and formulas for annealed and strain flattened Type 304 stainless are applicable to the cold-rolled grades, with appropriate modifications.

REFERENCES

1-1 Anon., Light Gage Cold-Formed Steel Design Manual, American Iron and Steel Institute, New York, N.Y., 1962, and Winter, G., "Commentary on Light Gage Cold-Formed Steel Design Manual", 1962.

1-2 Anon., "Steel Products Manual: Stainless and Heat Resisting Steels", American Iron and Steel Institute, New York, N. Y., April 1963.

1-3 Watter, M. and Lincoln, R. A., Strength of Stainless Steel Structural Members as Function of Design, Allegheny Ludlum Steel Corp., Pittsburgh, Pa., 1950.

1-4 Hammer, E. W. and Peterson, R. E., "Design Specifications for Stainless Steel, Type 301", Presented at Philadelphia Regional Technical Meeting of American Iron and Steel Institute, October 6, 1954.

1-5 Gilbert, P. H. and Griffith, A. R., "A Guide to the Structural Considerations for Design in Stainless Steel", State of California, The Resources Agency, Department of Water Resources, Technical Memorandum No. 15, June 1965.

1-6 Johnson, A. L., "The Structural Performance of Austenitic Stainless Steel Members", Ph.D. Thesis, Department of Structural Engineering, Cornell University, Ithaca, N. Y., 1967. Also in Cornell University Department of Structural Engineering Report No. 327.

1-7 Anon., Design of Light Gage Cold-Formed Stainless Steel Structural Members, American Iron and Steel Institute, New York, N. Y., 1968.

2-1 Parr, J. G., and Hanson, A., An Introduction to Stainless Steel, American Society for Metals, Metals Park, Ohio, 1965.

2-2 Rosenfield, A. R., "Development of Preferred Orientations", Metal Deformation Processing - Vol. 1, Battelle Memorial Institute, Columbus, Ohio, August 1964.

2-3 Smallman, R. E., "Textures in Face-Centered Cubic Metals and Alloys", The Journal of the Institute of Metals, Vol. LXXXIV, London, 1956.

2-4 Franks, R. and Binder, W. O., "Tension and Compression Stress-Strain Characteristics of Cold-Rolled Austenitic Chromium-Nickel and Chromium-Manganese-Nickel Stainless Steels", Journal of the Aeronautical Sciences, Vol. 9, pp. 419-438, 1942.

2-5 Barclay, W. F., "The Mechanisms of Deformation and Work Hardening in AISI Type 301 Stainless Steel", Advances in the Technology of Stainless Steels and Related Alloys, ASTM STP 369, 1965.

2-6 "Tension Testing of Metallic Materials", ASTM Designation: E 8-61 T, 1965.

2-7 "Compression Testing of Metallic Materials", ASTM Designation: E 9-61, 1965.

2-8 Bijlaard, P. P. and Fisher, G. P., "Interaction of Column and Local Buckling in Compression Members", NACA Tech. Note 2640, March 1952.

2-9 Chajes, A., Britvec, S. J., and Winter, G., "Effects of Cold-Straining on Structural Sheet Steels", Journal of the Structural Division, ASCE, Vol. 89, No. ST2, April 1963.

2-10 Karren, K. W., and Winter, G., "The Effects of Cold-Forming on the Mechanical Properties of Structural Sheet Steel", Report No. 317, Department of Structural Engineering, Cornell University, Ithaca, N. Y., September 1964.

2-11 Hald, A., Statistical Theory with Engineering Applications, John Wiley and Sons, New York, 1952.

2-12 Anon., Metallic Materials and Elements for Flight Vehicle Structures, MIL-HDBK-5, Washington, D. C.: Department of Defense, August 1962.

2-13 "Standard Specification for High-Strength Corrosion-Resisting Chromium-Nickel Steel Sheet and Strip", ASTM Designation: A177-58, 1965.

2-14 Mebs, R. W., and McAdam, D. J., Jr., "Elastic Properties in Tension and Shear of High Strength Nonferrous Metals and Stainless Steel-Effect of Previous Deformation and Heat Treatment", NACA Tech. Note 1100, 1947.

2-15 "Design Data on High Tensile Stainless Steel Sheets for Structural Purposes", Armco, Middletown, Ohio 1944.

2-16 Muhlenbruch, C. W., Krivobok, V. N., and Mayne, C. R., "Mechanical Properties in Torsion and Poisson's Ratio for Certain Stainless Steels", Proceedings, ASTM, 51 832-856, 1951.

2-17 Stang, A. H., Ramberg, W. and Back, G.,"Torsion Tests of Tubes", NACA Report No. 601, 1937.

2-18 Gerard, G., "Critical Shear Stress of Plates Above the Proportional Limit", Journal of Applied Mechanics, 15 7-12, 1948.

2-19 ASM Metals Handbook, Volume I: Properties and Selection of Metals, American Society for Metals, Novelty, Ohio. 8th Ed., 1961.

2-20 Osgood, W. R., "Stress Strain Formulas", Journal of the Aeronautical Sciences, Vol.13, No. 1, pp. 45-48, January 1946.

2-21 Ramberg, W., and Osgood, W. R., "Description of Stress Strain Curves by Three Parameters", NACA Tech. Note No. 902, July 1943.

2-22 Hill, H. N., "Determination of Stress Strain Relations from Offset Yield Strength Values", MACA Tech. Note No. 927, February 1944.

3-1 Bijlaard, P. P., "Theory of the Plastic Stability of Thin Plates", Pubs. International Association of Bridge and Structural Engineering, Vol. VI, p. 45, 1940-1941.

3-2 Ilyushin, A. A., "Stability of Plates and Shells Beyond the Proportional Limit", NACA Trans., Tech. Memo. No. 1116, October 1947.

3-3 Stowell, E. Z., "A Unified Theory of Plastic Buckling of Columns and Plates", NACA Tech. Note 1556, April 1948.

3-4 Bleich, F., Buckling Strength of Metal Structures, McGraw-Hill, New York, N.Y., 1952.

3-5 Winter, G., "Thin-Walled, Gold-Formed Steel Structures: Theory and Tests", Report on Theme II, a, Preliminary Publication, I.A.B.S.E. Congress, 1968.

3-6 Hearmon, R. F. S., An Introduction to Applied Anisotropic Elasticity, Oxford University Press, London, 1961.

3-7 Hu, P.C., Lundquist, E. E. and Batdorf, S. B., "Effect of Small Deviations from Flatness on Effective Width and Buckling of Plates in Compression", NACA Tech. Note 1124, September 1946.

3-8 Jombock, J. R., and Clark, J. W., "Postbuckling Behavior of Flat Plates", Trans. ASCE, Vol. 127, Part II, p. 227, 1962.

3-9 Stowell, E. Z. and Lundquist, E. E., "Local Instability of Columns with I-, Z-, Channel-, and Rectangular - Tube Sections", NACA Tech. Note 743, December 1939.

3-10 Southwell, R. V., "On the Analysis of Experimental Observations in Problems of Elastic Stability," Proc. Roy. Soc. (London). Ser. A. Vol. 135, pp. 601-616, April 1932.

3-11 Botman, M. and Besseling, J. F., "The Effective Width in the Plastic Range of Flat Plates Under Compression", National Luchtvaartlaboratorium (NLL), Amsterdam, Report S. 445 September 1954.

3-12 Yoshiki, M., and Fujita, Y., "Determination of Plastic Buckling Load for Axially Compressed Plates from Experimental Data", Test Method for Compression Members, ASTM STP 419, Am. Soc. Testing Mats., pp. 47-59, 1967.

3-13 Winter, G., "Performance of Thin Steel Compression Flanges", International Association for Bridge and Structural Engineers, Third Congress, Liege, Preliminary Publication, p. 317, 1948.

4-1 Cox, H. L., "The Buckling of a Flat Rectangular Plate Under Axial Compression and its Behavior After Buckling", Aeronautical Research Committee Reports and Memoranda No. 2041, 1945.

4-2 Cox, H. L., "The Buckling of a Flat Rectangular Plate Under Axial Compression and Its Behavior After Buckling, II: Conditions for Permanent Buckles", Aeronautical Research Council Reports and Memoranda No. 2175, 1945.

4-3 Marguerre, K., "Die uber die Ausbeulgrenze belastete Platte", Zeitschrift fur angewandte Mathematik und Mechanik, Band 16, s. 353, October 1936.

4-4 Marguerre, K. and Trefftz, E., "Uber Die Tragfahigkeit eines Langsbelasteten Plattenstreifens nach Uberschreiten der Beullast", Zeitschrift fur angewandte Mathematik und Mechanik, Band 17, s 85-100, April 1937.

4-5 Marguerre, K., "Zur Theorie der gekrummten Platte grosser Formanderung", Proceedings of the Fifth International Congress for Applied Mechanics, Cambridge, pp. 93-101, 1938.

4-6 Koiter, W. T., "De meedragende breedth bij groote overschri jding der knikspanning voor verschillende inklemming der plaatranden", National Luchtvaartlaboratorium (NLL), Amsterdam, Report S. 287, 1943.

4-7 Levy, S. and Krupen, Ph., "Large-Deflection Theory for End Compression of Long Rectangular Plates Rigidly Clamped Along Two Edges", NACA Tech. Note 884, 1943.

4-8 Hemp. W. S., "The Theory of Flat Panels Buckled in Compression", Aeronautical Research Council Reports and Memoranda No. 2178, 1945.

4-9 Coan, J. M., "Large Deflection Theory for Plates with Small Initial Curvature Loaded in Edge Compression", Journal of Applied Mechanics, Vol. 18, Trans. ASME, Vol. 73, pp. 143-151, 1951.

4-10 Yamaki, N., "Postbuckling Behavior of Rectangular Plates with Small Initial Curvature Loaded in Edge Compression", Journal of Applied Mechanics, Vol. 26, pp. 407-414, 1959 and Vol. 27, pp. 335-342, 1960.

4-11 Stein, M., "Loads and Deformations of Buckled Rectangular Plates", National Aeronautics and Space Administration Technical Report R-40, 1959.

4-12 Stowell, E. Z., "Compressive Strength of Flanges", NACA Report 1029, 1951.

4-13 Mayers, J. and Budiansky, B., "Analysis of Behavior of Simply Supported Flat Plates Compressed Beyond the Buckling Load into the Plastic Range", NACA Tech. Note 3368 February 1955.

4-14 Sujata, H. L., "The Effective Width of Longitudinally Stiffened Plates at Plastic Buckling", Journal of the Aerospace Sciences, Vol. 29, pp. 269-274 and p. 283, 1962.

4-15 Yusuff, S., "Large Deflection Theory for Orthotropic Rectangular Plates Subjected to Edge Compression", Journal of Applied Mechanics,Vol. 19, Trans. ASME, Vol. 74, 1952.

4-16 Schultz, H. G., "Buckling and Post Buckling Behavior of a Transversely Stiffened Ship Hull Model", Journal of Ship Research, Vol. 8, n. 2, pp. 6-21, 1964.

4-17 Zienkiewicz, O. C., The Finite Element Method in Structural and Continuum Mechanics, McGraw Hill Ltd., London, England.

4-18 Mallett, R. H., and Marcal, P. V., "Finite Element Analysis of Nonlinear Structures," Journal of the Structural Division, Proc. of the ASCE, Vol. 94, No. ST9, September 1968.

4-19 Schmit, L. A., Bogner, F.K., and Fox, R. L., "Finite Deflection Structural Analysis Using Plate and Shell Discrete Elements", AIAA Journal, Vol. 6, No. 5, May 1968. Also in Proceedings AIAA/ASME Eighth Structures, Structural Dynamics and Materials Conference, 1967.

4-20 Von Karman, T., Sechler, E. E., and Donnell, L. H., "The Strength of Thin Plates in Compression", Trans. ASME, Vol. 54, p. 53, 1932.

4-21 Schuman, L. and Back, G., "Strength of Rectangular Flat Plates Under Edge Compression", NACA Report 356, 1930.

4-22 Sechler, E. E., "The Ultimate Strength of Thin Flat Sheet in Compression", Publication No. 27, Guggenheim Aeronautics Laboratory, California Institute of Technology, Pasadena, California, 1933.

4-23 Winter, G., Lansing, W., and McCalley, R. B., Jr., "Four Papers on the Performance of Thin Walled Steel Structures", Eng. Exp. Sta. Cornell University, Ithaca, New York, Reprint No. 33, November 1950.

4-24 Winter, G., "Strength of Thin Steel Compression Flanges", Trans. ASCE, Vol. 112, 1947. Also in Cornell University Engineering Experimental Station, Reprint No. 32, October 1947.

4-25 Skaloud, M., "Grenzzustand Gedruckter Gurtplatten dunnwandiger Trager", Acta Technica Csav, Vol. 10, pp. 724-751, 1965.

4-26 Needham, R. A., "The Ultimate Strength of Multiweb Box Beams in Pure Bending", Journal of the Aeronautical Sciences, Vol. 22, pp. 781-786, 1955.

4-27 Jombock, J. R., and Clark, J. W., "Bending Strength of Aluminum Formed Sheet Members", Journal of the Structual Division, ASCE, Vol. 94, No. ST2, February 1968.

4-28 Miller, E. A., "A Study of the Strength of Short, Thin-Walled Steel Studs", MCE Thesis, Cornell University, October 1943.

4-29 Botman, M., "The Experimental Determination of the Effective Width of Flat Plates in the Elastic and Plastic Range", Part II, (in Dutch), National Luchvaart Laboratorium (NLL), Amsterdam, Report S. 438, January 1954.

4-30 Botman, M., "The Effective Width in the Plastic Range of Flat Plates Under Compression, III", Nationaal Luchtvaartlaboratorium (NLL), Amsterdam, Report S, 465 June 1955.

4-31 Besseling, J. F., "Experimental Determination of the Effective Width of Flat Plates in the Elastic and Plastic Range", (in Dutch), Nationaal Luchtvaartlaboratorium (NLL), Amsterdam, Report S. 414, February 1953.

4-32 Koiter, W. T., "Introduction to the Post Buckling Behavior of Flat Plates", Societe Royale des Sciences de Liedge Memoires, V. 8, 1963.

4-33 Johnson, A.L., and Winter, G., "Behavior of Stainless Steel Columns and Beams", Journal of Structural Division, ASCE, Vol. 92, No. ST5, October 1966.

4-34 Farrar, D. J., "Investigation of Skin Buckling", R. and M. No. 2652, A. R. C. Tech. Rep., London, 1953.

5-1 Johnson, A.L., and Wang, S. T., "Discussion of Bending Strength of Aluminum Formed Sheet Members", Journal of the Structural Division, ASCE, Vol. 94, No. ST2, February 1968, by Jombock, J.R., and Clark, J.W., "Journal of Structural Division, ASCE, Vol. 95, No. ST1, January 1969.

5-2 Wang, S. T., and Errera S.J., "Current Research on Type 301- 1/4 and 1/2 Hard Stainless Steel", Presented at the ASCE Annual Meeting and National Meeting on Structural Engineering, Pittsburgh, Pa., September 30-October 4, 1968.

5-3 Karren, K. W., and Winter G., Closure to "Effect of Cold-Forming on Light-Gage Steel Members", Journal of the Structural Division, ASCE, Vol. 94, No. ST6, pp. 1607-1610, June 1968.

5-4 Uribe, Jairo, "Effects of Cold Forming on the Flexural Behavior of Light-Gage Steel Members", M. S. Essay, Cornell University, February 1966.

5-5 Newmark, N. M., "Numerical Procedure for Computing Deflections, Moments, and Buckling Loads", Proceeding ASCE, Vol. 68, pp. 691-718, 1942.

5-6 Godden, W. G., Numerical Analysis of Beam and Column Structures, Prentice-Hall, Inc., Englewood, N.J., 1965.

5-7 Wolford, D. S., "Significance of the Secant and Tangent moduli of Elasticity in Structural Design", Journal of the Aeronautical Sciences, Vol. 10, pp. 169-179, 1943.

5-8 Karren, K.W., "Effects of Cold Forming on Light-Gage Steel Members", Report No. 318, Department of Structural Engineering, Cornell University, Ithaca, New York, June 1965.

5-9 Hammer, E. W., Jr., and Peterson, R. E., "Column Curves for Type 301 Stainless Steel", Aeronautical Engineering Review, December 1955.

5-10 Dubec, J., Krivobok, V. N., and Welter, G., "Studies of Type 301 Stainless Steel Columns", American Society for Testing Materials, Special Technical Publication No. 196, 1957.

5-11 Barlow, H. W., "The Column Strength of Thin-Walled Sections of 18-8 Stainless Steel", Journal of the Aeronautical Sciences, Vol. 8, pp. 151-161, 1941.

5-12 Duberg, J. E., and Wilder, T. W., "Inelastic Column Behavior", NACA Tech. Note 2267, January 1951.

5-13 Osgood, W. R., "The Effect of Residual Stresses on Column Strength", Proceedings of the First National Congress of Applied Mechanics, June 1951.

5-14 Peterson, R. E., and Bergholm, A. O., "Effect of Forming and Welding on Stainless Columns", Aerospace Engineering, Vol. 20, No. 4, April 1961.

Table 2-1

COMPARISON OF MECHANICAL PROPERTIES-CORNERS AND FLATS
TYPE 301 1/2 HARD AND TYPE 304 ANNEALED AND STRAIN FLATTENED STAINLESS STEELS

Sheet	Sense and** Direction of Stressing	Yield Strength ksi			Initial Modulus ksi		Ultimate Tensile Strength ksi		
		Flats	Corners*	Ratio	Flats	Corners*	Flats	Corners*	Ratio
301-H-3†	LC	89.90	157.50	1.75	26,880	26,250			
	LT	128.30	146.37	1.14	28,850	25,830	189.38	204.49	1.08
	TT	111.52	141.44	1.27	28,780	26,160	191.79	197.90	1.03
	TC	152.44	159.50	1.05	28,320	27,250			
301-H-7††	LC	100.50	134.00	1.33	26,460	26,620			
	LT	125.80	140.62	1.12	28,830	27,060	165.80	177.06	1.07
	TT	139.00	156.70	1.13	28,760	26,220	167.34	185.66	1.11
	TC	152.70	162.00	1.05	28,240	27,050			
304-AS-5†††	LC	34.09	86.00	2.52	29,120	29,120			
	LT	41.07	67.90	1.65	30,070	29,120	99.17	106.69	1.08
	TT	39.73	64.50	1.63	30,200	29,170	91.86	98.65	1.07
	TC	40.87	81.00	1.98	29,920	29,120			

* Inner radius to thickness ratios are shown in Table 3-12.

** LC = Longitudinal Compression LT = Longitudinal Tension
TT = Transverse Tension TC = Transverse Compression

† = Type 301, Half Hard, Sheet No. 3

†† = Type 301, Half Hard, Sheet No. 7

††† = Type 304, Annealed and Strain Flattened, Sheet No. 5

Table 2-2

TYPE 301 STAINLESS STEEL - 1/4 AND 1/2 HARD
STATISTICAL INFERENCES FOR 0.2% OFFSET YIELD STRENGTH

Temper	Sense and Direction	Number of Heats	Number of Coupons	Mean ksi	Variance	Standard Deviation ksi	Range of Values ksi
1/4 Hard	LT*	6	17	85.92	35.04	5.92	74.8 - 97.0
	TT*	37	81	88.26	40.79	6.39	73.0 - 104.0
	LC*	6	17	59.74	18.15	4.26	55.0 - 70.3
	TC*	6	17	100.03	28.17	5.31	87.5 - 108.4
1/2 Hard	LT	10	29	121.06	74.98	8.66	109.0 - 143.8
	TT	42	93	113.91	73.69	8.58	95.0 - 138.5
	LC	10	29	82.11	83.42	9.13	62.2 - 101.9
	TC	10	29	136.69	87.49	9.35	122.6 - 153.9

*LT = Longitudinal Tension
TT = Transverse Tension
LC = Longitudinal Compression
TC = Transverse Compression

Table 2-3

TYPE 301 STAINLESS STEEL - 1/4 AND 1/2 HARD
0.2% OFFSET YIELD STRENGTH, KSI

Temper	Source	Tension Longitudinal	Tension Transverse	Compression Longitudinal	Compression Transverse	Remark
1/4 Hard	Statistical Analysis†	79.2	80.2	54.0	96.2	90% probability
		77.5	78.0	52.5	94.5	95% "
		72.3	75.0	48.0	91.3	95% probability with 95% confidence
	Armco**	75	75	62	75	
	MIL-HDBK-5*	75	75	43	80	design values
	ASTM ∞ & ASM Metals Handbook§	75		--	--	minimum
	Recommended	75	75	50	90	
1/2 Hard	Statistical Analysis†	111.0	103.0	73.0	124.7	90% probability
		108.2	100.0	70.5	121.3	95% "
		103.5	96.2	65.0	114.5	95% probability with 95% confidence
	Armco**	117	110	83	123	
	MIL-HDBK-5*	110	110	58	118	design values
	ASTM ∞ & ASM Metals Handbook§	110		--	--	minimum
	Recommended	110	100	65	120	

† Statistical inferences are shown in Table 2-2
** From Ref. 2-15
∞ From Ref. 2-13
* From Ref. 2-12
§ From Ref. 2-19

Table 2-4

TYPE 301 STAINLESS STEEL - 1/4 AND 1/2 HARD
INITIAL MODULUS, $x10^3$ KSI

Temper	Source	Tension		Compression	
		Longitudinal	Transverse	Longitudinal	Transverse
1/4 Hard	Cornell Test†	29.5	29.7	27.8	28.4
	Producer II*	26.3	28.4	29.3	30.7
	Armco∞	27.0	28.5	27.0	27.0
	MIL-HDBK-5∞	27.0	28.0	26.0	27.0
	Recommended	27.0	28.0	27.0	28.0
1/2 Hard	Cornell Test†	29.1	29.3	26.7	28.6
	Producer II*	26.8	28.3	30.2	31.8
	Producer I**	27.3	28.0	28.0	31.2
	Armco∞	27.5	28.5	28.0	28.5
	MIL-HDBK-5∞	26.0	28.0	26.0	27.0
	Recommended	27.0	28.0	27.0	28.0

* From reports from steel producer II
** " " " " " I
† From author's tests
∞ See footnote of Table 2-3

Table 2-5

PROPORTIONAL LIMIT
TYPE 301 STAINLESS STEEL - 1/4 AND 1/2 HARD

Sense and Direction of Stress	Yield Strength σ_y ksi	Criterion A σ_{pl} ksi	Criterion A $\frac{\sigma_{pl}}{\sigma_y}$	Criterion B σ_{pl} ksi	Criterion B $\frac{\sigma_{pl}}{\sigma_y}$	Recommended Design value for Bending σ_{pl} ksi	Recommended Design value for Bending $\frac{\sigma_{pl}}{\sigma_y}$
Type 301-1/4 Hard							
Longitudinal Compression	50	20.0	0.400	26.0	0.520	25.0	0.50
Longitudinal Tension	75	30.0	0.400	39.0	0.520	37.5	0.50
Transverse Tension	75	36.0	0.480	43.0	0.573	41.3	0.55
Transverse Compression	90	38.0	0.422	48.0	0.533	45.0	0.50
Type 301-1/2 Hard							
Longitudinal Compression	65	23.0	0.354	32.0	0.492	31.5	0.50
Longitudinal Tension	110	42.0	0.382	54.0	0.491	49.5	0.50
Transverse Tension	100	53.0	0.530	64.0	0.640	60.0	0.60
Transverse Compression	120	53.0	0.442	62.0	0.517	60.0	0.50

Criterion A: Stress at which stress-strain curve deviates from initial elastic straight line.

Criterion B: Stress at which there is 0.01% inelastic strain.

Table 2-6

TYPE 301 STAINLESS STEEL - 1/4 AND 1/2 HARD
TENSILE STRENGTH AND PERCENTAGE OF ELONGATION IN 2" GAGE LENGTH

Temper	Source	Tensile Strength, ksi		Elongation,%	
		Longitudinal	Transverse	Longitudinal	Transverse
1/4 Hard	Cornell Test†	137.9	137.0	39.4	35.8
	Producer II***	136.1	145.0	35.8	32.4
	ASTM 2-13 & MIL-HDBK-5 2-12	125*		25*	
	ASM Metals 2-19 Handbook	125*		25*	
	Recommended	130		25	
1/2 Hard	Cornell Test†	167.0	168.1	26.4	23.8
	Producer II***	157.4	163.0	28.1	21.5
	Producer I***	176.5	176.9	28.3	24.7
	ASTM 2-13 & MIL-HDBK-5 2-12	150*		**	
	ASM Metals 2-19 Handbook	150*		15*	
	Recommended	150		ASTM Values	

* Minimum values (ASTM, ASM); design values (MIL-HDBK-5)
** Depending upon thickness of the sheet
*** See footnotes of Table 2-4
† From author's tests

Table 2-7

COEFFICIENTS OF MODIFIED RAMBERG OSGOOD STRESS STRAIN CURVES
EXPERIMENTAL STRESS STRAIN CURVES

Sheet No.†	Sense & Direction of Stress	Initial Modulus $x10^3$ ksi	.2% Offset Yield Strength ksi	.05% Offset Strength ksi	Ratio of .2% & .05% Offset Strengths	n
			Flat Material			
301-H-3	LT*	28.85	128.30	80.00	1.604	2.934
	TT	28.78	111.52	81.50	1.368	4.423
	LC	26.88	89.90	58.50	1.537	3.224
	TC	28.32	152.44	109.20	1.396	4.155
301-H-7	LT	28.83	125.80	80.90	1.555	3.140
	TT	28.76	139.00	107.00	1.299	5.295
	LC	26.46	100.50	69.20	1.452	3.716
	TC	28.24	152.70	112.50	1.357	4.540
304-AS-5	LT	30.07	41.07	38.20	1.075	19.111
	TT	30.20	39.73	32.50	1.222	6.912
	LC	29.12	34.09	22.60	1.508	3.376
	TC	29.92	40.87	34.55	1.182	8.281
			Corners			
301-H-3	LT	25.83	146.37	106.20	1.378	4.322
	TT	26.16	141.44	109.20	1.295	5.361
	LC	26.25	157.50	97.80	1.610	2.911
	TC	27.25	159.50	106.00	1.505	3.392
301-H-7	LT	27.06	140.62	100.50	1.399	4.126
	TT	26.22	156.70	127.00	1.234	6.594
	LC	26.62	134.00	96.00	1.396	4.155
	TC	27.05	162.00	106.00	1.528	3.272
304-AS-5	LT	29.12	67.90	50.20	1.352	4.599
	TT	29.17	64.50	47.25	1.365	4.456
	LC	29.12	86.00	59.60	1.443	3.779
	TC	29.12	81.00	62.00	1.306	5.199

* LT Longitudinal Tension
TT Transverse Tension
LC Longitudinal Compression
TC Transverse Compression

† See Table 2-1 for sheet temper

Table 2-8

COEFFICIENTS OF MODIFIED RAMBERG OSGOOD STRESS STRAIN CURVES
DESIGN STRESS STRAIN CURVES

Temper	Sense & Direction of Stress	Initial Modulus $x10^3$ ksi	.2% Offset Yield Strength ksi	.05% Offset Strength ksi	Ratio of .2% & .05% Offset Strengths	n
			Direct Stress			
301-1/2 Hard	LT	27.00	110.00	83.00	1.325	4.922
	TT	28.00	100.00	81.00	1.235	6.572
	LC	27.00	65.00	45.00	1.444	3.765
	TC	28.00	120.00	89.00	1.348	4.636
301-1/4 Hard	LT	27.00	75.00	56.80	1.320	4.983
	TT	28.00	75.00	60.00	1.250	6.213
	LC	27.00	50.00	35.50	1.409	4.043
	TC	28.00	90.00	68.50	1.314	5.076
			Shear Stress			
301-1/2 Hard	Shear	10.50	56.20*	41.60#	1.353	4.585
301-1/4 Hard	Shear	10.50	41.80*	30.80#	1.356	4.554

* Corresponding to 0.30% offset yield strength in shear

\# Corresponding to 0.075% offset yield strength in shear

Table 2-9

MECHANICAL ANISOTROPY OF AUSTENITIC STAINLESS STEEL
SHEET 301-H-2 - TYPE 301-1/2 HARD

(a) Mechanical Properties in Tension

Coupon*	E ksi	$\sigma_{ult.}$ ksi	σ_y ksi	Elongation %
H2T-2700	29,430	191.60	116.49	21.88
H2T-2925	28,230	193.33	119.83	21.09
H2T-3150	28,160	191.31	128.16	17.97
H2T-3375	28,430	188.50	125.46	20.31
H2T-3600	28,430	191.59	134.12	20.31

(b) Mechanical Properties in Compression

Coupon*	E ksi	σ_y ksi
H2C-0900	28,200	158.15
H2C-1125	28,560	151.00
H2C-1350	27,714	129.13
H2C-2025	26,514	91.91
H2C-1800	26,780	91.91

* See Fig. 2-17.

Table 3-1

UNSTIFFENED ELEMENT COMPRESSION SPECIMEN DIMENSIONS* AND PROPERTIES - TYPE 301 STAINLESS STEEL -1/2 HARD

Specimen	H301UE-1	H301UE-2	H301UE-3	H301UE-4
D, in.	1.5784	1.6019	1.5995	1.5682
B, in.	0.5158	0.7325	1.1165	1.7519
t, in.	0.0325	0.0326	0.0324	0.0324
w, in.	0.3583	0.5749	0.9591	1.5945
w/t	11.02	17.63	29.60	49.21
D'	1.2634	1.2867	1.2847	1.2534
D'/2t	9.72	9.86	10.23	9.67
R, in.	0.125	0.123	0.125	0.125
R/t	3.85	3.83	3.86	3.86
L, in.	3.555	5.939	9.910	11.630
L/w	9.92	10.33	10.33	7.29
A_c, in.^{2}	0.02886	0.02895	0.02875	0.02875
A_w, in.^{2}	0.08212	0.08390	0.08324	0.08122
A_f, in.^{2}	0.04660	0.07496	0.12428	0.20664
A, in.^{2}	0.1576	0.1878	0.2363	0.3166
Sheet No.	301-H-3	301-H-3	301-H-3	301-H-3

* See Fig. 3-1.

Table 3-2

EXPERIMENTAL CRITICAL STRAINS AND STRESSES
UNSTIFFENED ELEMENTS
TYPE 301 STAINLESS STEEL-1/2 HARD

Specimen	w/t	Strain Deviation Method		Maximum Surface Strain Method		Maximum Membrane Strain Method	
		ε_{cr} μ in/in	σ_{cr} ksi	ε_{cr} μ in/in	σ_{cr} ksi	ε_{cr} μ in/in	σ_{cr} ksi
H301UE-1	11.02	4214	77.90	5211	88.20	5558	91.40
H301UE-2	17.63	1770	42.70	2061	48.30	2328	53.10
H301UE-3	29.60	550	14.78	794	21.40	899	23.90
H301UE-4	49.21	211	5.67	320	10.70	398	6.98

Table 3-3

CALCULATED BUCKLING COEFFICIENT
UNSTIFFENED ELEMENTS

Specimen	w/t	Buckling Coefficient k		
		H Section*	Channel**	Average
H301UE-1	11.02	0.880	0.436	0.658
H301UE-2	17.63	0.986	0.595	0.790
H301UE-3	29.60	1.084	0.748	0.916
H301UE-4	49.21	1.162	0.886	1.024
Average		1.03	0.67	0.85

* Calculated k values based on H section

** Calculated k values based on channel section

Table 3-4

EXPERIMENTAL HALF WAVE LENGTH
STIFFENED AND UNSTIFFENED ELEMENTS

Specimen	Aspect Ratio	Length of Plate in.	Width of Plate in.	No. of Half Waves Observed	Half Wave Length L in.
		Flexural Members - Type 301 1/2 Hard			
H301F-1	14.20	22	1.5490	16	1.375
H301F-2	9.29	22	2.3675	10	2.200
H301F-3	9.44	22	2.5506	10	2.200
H301F-4	4.46	22	5.1844	4	5.500
		Stiffened Element Compression Members Type 301 1/2 Hard			
H301SC-2	4.86	12	2.4669	6	2.000
H301SC-4	3.00	15	5.0060	3	5.000
		Flexural Members - Type 304 A & S			
AS304F-2	9.95	22	2.2099	12	1.833
AS304F-3	6.28	22	3.5060	8	2.750
AS304F-4	4.65	22	4.7308	6	3.667
		Unstiffened Element Compression Members Type 301 1/2 Hard			
H301UE-1	9.92	3.555	0.3583	3	1.185
H301UE-2	10.33	5.939	0.5749	4	1.485
H301UE-3	10.33	9.910	0.9591	4	2.478
H301UE-4	7.29	11.630	1.5945	5	2.326

Table 3-5

CALCULATED AND EXPERIMENTAL NUMBER OF HALF WAVES
STIFFENED AND UNSTIFFENED ELEMENTS

Specimen	w/t	Theoretical* Critical Stress		Plasticity** Reduction Factor		Aspect Ratio	No. of Half Waves Observed	Calculated Limiting Aspect Ratio		No. of Half Waves Calculated	
		S.S.	Fixed	S.S.	Fixed			S.S.	Fixed	S.S.	Fixed
Flexural Members - Type 301 1/2 Hard											
H301F-1	24.82	94.42	116.60	0.600	0.427	14.20	16	14.49	14.31	16	26
H301F-2	37.94	56.45	81.10	0.838	0.697	9.29	10	9.07	9.44	10	15
H301F-3	71.04	19.25	31.10	0.987	0.921	9.44	10	9.46	9.49	9	14
H301F-4	150.34	4.36	7.54	1.000	1.000	4.46	4	4.47	4.33	4	6
Stiffened Element Compression Members - Type 301 1/2 Hard											
H301SC-2	39.85	52.10	76.70	0.859	0.725	4.86	6	5.27	4.61	5	6
H301SC-4	154.51	4.10	7.14	1.000	1.000	3.00	3	3.46	2.99	3	4
Flexural Members - Type 304 Annealed and Strain Flattened											
AS304F-2	71.52	15.25	21.15	0.741	0.590	9.95	12	9.72	9.66	11	17
AS304F-3	113.02	8.24	12.35	1.000	0.860	6.28	8	6.48	6.10	6	10
AS304F-4	150.18	4.66	8.13	1.000	1.000	4.65	6	4.47	4.33	5	7
Unstiffened Element Compression Members - Type 301 1/2 Hard											
H301UE-1	11.02	-	122.70	-	0.478	9.92	3	-	12.09	1	7
H301UE-2	17.63	-	72.60	-	0.723	10.33	4	-	10.07	1	7
H301UE-3	29.60	-	33.70	-	0.947	10.33	4	-	10.74	1	6
H301UE-4	49.21	-	12.88	-	1.000	7.29	5	-	7.52	1	4

* Calculated from Eq. 3-1

** $\eta = \sqrt{E_t/E}$ and E_s/E were used for stiffened and unstiffened elements, respectively.

Table 3-6

COMPARISON OF CALCULATED AND EXPERIMENTAL CRITICAL STRESSES
UNSTIFFENED ELEMENTS
k = 0.5
Type 301 Stainless Steel - 1/2 Hard

Specimen	Calc. k=0.5	Strain Deviation Method		Maximum Surface Strain Method		Maximum Membrane Strain Method	
	σ_{cr} ksi	σ_{cr} ksi	$\frac{\sigma_{cr\ exp.}}{\sigma_{cr\ calc.}}$	σ_{cr} ksi	$\frac{\sigma_{cr\ exp.}}{\sigma_{cr\ calc.}}$	σ_{cr} ksi	$\frac{\sigma_{cr\ exp.}}{\sigma_{cr\ calc.}}$
H301UE-1	72.65	77.90	1.07	88.20	1.21	91.40	1.26
H301UE-2	36.70	42.70	1.16	48.30	1.32	53.10	1.45
H301UE-3	13.96	14.78	1.06	21.40	1.53	23.90	1.71
H301UE-4	4.99	5.67	1.14	8.60	1.72	10.70	2.14
Average			1.11		1.45		1.64

Table 3-7

COMPARISON OF CALCULATED AND EXPERIMENTAL CRITICAL STRESSES
UNSTIFFENED ELEMENTS
k = 1.03
Type 301 Stainless Steel - 1/2 Hard

Specimen	Calc. k=1.03	Strain Deviation Method		Maximum Surface Strain Method		Maximum Membrane Strain Method	
	σ_{cr} ksi	σ_{cr} ksi	$\frac{\sigma_{cr\ exp.}}{\sigma_{cr\ calc.}}$	σ_{cr} ksi	$\frac{\sigma_{cr\ exp.}}{\sigma_{cr\ calc.}}$	σ_{cr} ksi	$\frac{\sigma_{cr\ exp.}}{\sigma_{cr\ calc.}}$
H301UE-1	110.00	77.90	0.708	88.20	0.802	91.40	0.831
H301UE-2	63.20	42.70	0.676	48.30	0.764	53.10	0.840
H301UE-3	28.00	14.78	0.528	21.40	0.764	23.90	0.853
H301UE-4	10.40	5.67	0.545	8.60	0.827	10.70	1.030
Average			0.614		0.789		0.889

Table 3-8

COMPARISON OF CALCULATED AND EXPERIMENTAL CRITICAL STRESSES
UNSTIFFENED ELEMENTS
k = 0.85
Type 301 Stainless Steel - 1/2 Hard

Specimen	Calc. k=0.85	Strain Deviation Method		Maximum Surface Strain Method		Maximum Membrane Strain Method	
	σ_{cr} ksi	σ_{cr} ksi	$\frac{\sigma_{cr\ exp.}}{\sigma_{cr\ calc.}}$	σ_{cr} ksi	$\frac{\sigma_{cr\ exp.}}{\sigma_{cr\ calc.}}$	σ_{cr} ksi	$\frac{\sigma_{cr\ exp.}}{\sigma_{cr,calc.}}$
H301UE-1	98.80	77.90	0.788	88.20	0.893	91.40	1.039
H301UE-2	55.40	42.70	0.771	48.30	0.872	53.10	0.958
H301UE-3	23.50	14.78	0.629	21.40	0.911	23.90	1.017
H301UE-4	8.58	5.67	0.661	8.60	1.002	10.70	1.248
Average			0.712		0.920		1.066

Table 3-9

COMPARISON OF FAILURE LOADS AND OBSERVED WAVING LOADS
UNSTIFFENED ELEMENT COMPRESSION MEMBERS
Type 301 Stainless Steel - 1/2 Hard

Specimen	w/t	Failure Load P_f lb	Observed Waving P_w lb	$\frac{P_f}{P_w}$	Average Member Stress at Failure σ_a ksi	Maximum Edge Stress at Failure σ_{max} ksi	Average Element Stress at Failure σ_a ksi
H301UE-1	11.02	15800	13875	1.14	100.25	96.10	89.40
H301UE-2	17.63	14550	8938	1.63	77.48	89.00	55.00
H301UE-3	29.60	15000	4488	3.34	63.48	87.20	41.00
H301UE-4	49.21	15800	3000	5.26	49.91	86.20	22.75

Table 3-10

COMPARISON OF CRITICAL LOADS AND WAVING LOADS
UNSTIFFENED ELEMENTS
Type 301 Stainless Steel - 1/2 Hard

Specimen	Strain Deviation Method		Maximum Surface Strain Method		Maximum Membrane Strain Method		Waving Observed		Waving Parameter Plot		Wave Depth Equals Thickness	
	P lb	σ_a ksi	P lb	σ_a ksi	P lb	σ_a ksi	P lb	σ_a ksi	P lb	σ_a ksi	P lb	σ_a ksi
H301UE-1	12888	81.78	15319	97.20	15560	98.73	13875	88.40	-	-	-	-
H301UE-2	7938	42.27	9697	51.64	9950	52.98	8938	47.59	9560	50.91	11300	60.17
H301UE-3	3489	14.77	5363	22.70	5738	24.28	4488	18.99	5780	24.46	6498	27.50
H301UE-4	1750	5.33	3000	9.48	3625	11.45	3000	9.48	3600	11.37	4000	12.63

Table 3-11

COMPARISON OF VARIOUS CRITICAL STRESS CRITERIA AND WAVING OBSERVATIONS
UNSTIFFENED ELEMENTS
Type 301 Stainless Steel - 1/2 Hard

Specimen	Calc. k=0.85 σ_{cr} ksi	Strain Deviation Method $\frac{\sigma_a}{\sigma_{cr}}$	Maximum Surface Strain Method $\frac{\sigma_a}{\sigma_{cr}}$	Maximum Membrane Strain Method $\frac{\sigma_a}{\sigma_{cr}}$	Waving Observed $\frac{\sigma_a}{\sigma_{cr}}$	Wave Depth Equals Thickness $\frac{\sigma_a}{\sigma_{cr}}$	Waving Parameter Plot $\frac{\sigma_a}{\sigma_{cr}}$
H301UE-1	98.80	0.828	0.946	0.998	--	--	--
H301UE-2	55.40	0.763	0.932	0.956	0.859	1.086	0.918
H301UE-3	23.50	0.629	0.967	1.033	0.809	1.170	1.041
H 301UE-4	8.58	0.645	1.102	1.335	1.102	1.472	1.324
Average		0.716	0.987	1.081	0.892	1.243	1.094

Table 3-12

FLEXURAL SPECIMEN DIMENSIONS* AND PROPERTIES

Specimen	H301F-1	H301F-2	H301F-3	H301F-4	AS304F-2	AS304F-3	AS304F-4
B, in.	1.9238	2.7424	2.5834	5.1844	2.3968	3.6940	4.9188
D, in.	0.9892	0.9934	1.4919	1.4914	1.5081	1.5005	1.5054
F, in.	0.9055	0.8165	0.8008	1.0061	0.7525	0.8777	1.0033
d, in.	------	0.3718	0.2958	0.2941	0.3070	0.3004	0.3009
R, in.	0.1250	0.1250	0.0938	0.0938	0.0625	0.0625	0.0625
t, in.	0.0624	0.0624	0.0328	0.0328	0.0309	0.0315	0.0315
R/t	2.00	2.00	2.86	2.86	2.023	1.984	1.984
w/t	24.82	37.94	71.04	150.34	71.52	113.02	150.18
Sheet No.	301-H-7	301-H-7	301-H-3	301-H-3	304-AS-5	304-AS-5	304-AS-5
Type	301-¼ Hard	301-½ Hard	301-½ Hard	301-½ Hard	304 A&S**	304 A&S**	304 A&S**

* See Fig. 3-5

** Type 304 annealed and strain flattened stainless steel

Table 3-13

STIFFENED ELEMENT COMPRESSION SPECIMEN
DIMENSIONS* AND PROPERTIES
Type 301 Stainless Steel - 1/2 Hard

Specimen	H301SC-2	H301SC-4
B, in.	2.8407	5.2894
D, in.	0.9926	0.8427
F, in.	0.6790	0.3867
R, in.	0.125	0.109
t, in.	0.619	0.324
R/t	2.02	3.38
w, in.	2.4669	5.0060
w/t	39.85	154.51
D', in.	0.6188	0.5593
D'/t	10.00	17.26
F', in.	0.4921	0.2450
F'/t	7.95	7.56
L, in.	12.00	15.00
L/w	4.86	3.00
A_c, in.^{2}	0.1213	0.0511
A_w, in.^{2}	0.2751	0.1042
A_f, in.^{2}	0.3054	0.3244
A, in.^{2}	0.7018	0.4797
Sheet No.	301-H-7	301-H-3

* See Fig. 3-8.

Table 3-14

EXPERIMENTAL CRITICAL STRAINS AND STRESSES
STIFFENED ELEMENTS

Specimen	w/t	Strain Deviation Method		Maximum Surface Strain Method		Maximum Membrane Strain Method	
		μ in./in.	ksi	μ in./in.	ksi	μ in./in.	ksi
Flexural Members - Type 301 1/2 Hard							
H301F-1	24.82	5453	97.40	7575	112.40	-	-
H301F-2	37.94	3489	74.80	3534	75.30	4113	83.20
H301F-3	71.04	578	15.54	718	19.30	821	22.30
H301F-4	150.34	149	4.01	257	6.91	231	6.22
Stiffened Element Compression Members - Type 301 1/2 Hard							
H301SC-2	39.85	2308	54.80	2813	64.20	3214	70.50
H301SC-4	154.51	73	1.96	132	3.55	138	3.71
Flexural Members - Type 304 A & S							
AS304F-2	71.52	818	17.60	955	19.30	1356	23.40
AS304F-3	113.02	276	8.04	303	8.82	405	10.80
AS304F-4	150.18	92	2.68	118	3.44	172	5.01

Table 3-15

COMPARISON OF CALCULATED AND EXPERIMENTAL CRITICAL STRESSES
STIFFENED ELEMENTS
k = 4.0

Specimen	Calc. k=4.0	Strain Deviation Method		Maximum Surface Strain Method		Maximum Membrane Strain Method	
	σ_{cr} ksi	σ_{cr} ksi	$\frac{\sigma_{cr\ exp.}}{\sigma_{cr\ calc.}}$	σ_{cr} ksi	$\frac{\sigma_{cr\ exp.}}{\sigma_{cr\ calc.}}$	σ_{cr} ksi	$\frac{\sigma_{cr\ exp.}}{\sigma_{cr\ calc.}}$
Flexural Members - Type 301 1/2 Hard							
H301F-1	94.42	97.40	1.03	112.40	1.19	-	-
H301F-2	56.45	74.80	1.33	75.30	1.33	83.20	1.47
H301F-3	19.25	15.54	0.81	19.30	1.00	22.30	1.16
H301F-4	4.36	4.01	0.92	6.91	1.58	6.22	1.42
Stiffened Element Compression Members - Type 301 1/2 Hard							
H301SC-2	52.00	54.80	1.05	64.20	1.23	70.50	1.35
H301SC-4	4.10	1.96	0.48	3.55	0.87	3.71	0.91
Average			0.94		1.20		1.26
Flexural Members - Type 304 A & S							
AS304F-2	15.25	17.60	1.15	19.30	1.27	23.40	1.53
AS304F-3	8.24	8.04	0.98	8.82	1.07	10.80	1.31
AS304F-4	4.67	2.68	0.57	3.44	0.74	5.01	1.07
Average			0.90		1.03		1.30

Table 3-16

COMPARISON OF CALCULATED AND EXPERIMENTAL CRITICAL STRESS
STIFFENED ELEMENTS
k = 5.27

Specimen	Calc. k=5.27	Strain Deviation Method		Maximum Surface Strain Method		Maximum Membrane Strain Method	
	σ_{cr} ksi	σ_{cr} ksi	$\frac{\sigma_{cr\ exp.}}{\sigma_{cr\ calc.}}$	σ_{cr} ksi	$\frac{\sigma_{cr\ exp.}}{\sigma_{cr\ calc.}}$	σ_{cr} ksi	$\frac{\sigma_{cr\ exp.}}{\sigma_{cr\ calc.}}$
Flexural Members - Type 301 1/2 Hard							
H301F-1	105.84	97.40	0.92	112.40	1.06	-	-
H301F-2	68.78	74.80	1.09	75.30	1.09	83.20	1.21
H301F-3	24.60	15.54	0.63	19.30	0.78	22.30	0.91
H301F-4	5.74	4.01	0.70	6.91	1.20	6.22	1.08
Stiffened Element Compression Members - Type 301 1/2 Hard							
H301SC-2	64.00	54.80	0.86	64.20	1.00	70.50	1.10
H301SC-4	5.40	1.96	0.36	3.55	0.66	3.71	0.69
Average			0.76		0.97		1.00
Flexural Members - Type 304 A & S							
AS304F-2	17.95	17.60	0.98	19.30	1.08	23.40	1.30
AS304F-3	10.23	8.04	0.79	8.82	0.86	10.80	1.06
AS304F-4	6.15	2.68	0.44	3.44	0.56	5.01	0.81
Average			0.74		0.83		1.06

Table 3-17

COMPARISON OF CRITICAL LOADS AND WAVING LOADS
FLEXURAL MEMBERS AND STIFFENED ELEMENT COMPRESSION MEMBERS

Specimen	Strain Deviation Method	Maximum Surface Strain Method	Maximum Membrane Strain Method	Observed Waving	Wave Depth Equals Thickness	Waving Parameter Plot
	lb.	lb.	lb.	lb.	lb.	lb.
			Flexural Members - Type 301 1/2 Hard			
H301F-1	1987	2076	-	1987	-	-
H301F-2	1884	1931	2026	1884	1842	1638
H301F-3	374	473	523	498	537	495
H301F-4	200	398	398	250	210	135
			Stiffened Element Compression Members - Type 301 1/2 Hard			
H301SC-2	35950	42950	46925	42950	50800	44300
H301SC-4	942	1490	3980	2460	2970	-
			Flexural Members - Type 304 Annealed & Strain Flattened			
AS304F-2	379	436	553	440	472	462
AS304F-3	235	274	361	295	307	290
AS304F-4	139	200	229	200	230	227

Table 3-18

COMPARISON OF FAILURE LOADS AND OBSERVED WAVING LOADS OR BUCKLING LOADS
FLEXURAL AND STIFFENED ELEMENT COMPRESSION MEMBERS

Specimen	w/t	Failure Load P_f lb.	Observed Waving P_w lb.	$\frac{P_f}{P_w}$	Buckling Load* P_{cr} lb.	$\frac{P_f}{P_{cr}}$	Maximum Edge Stress at Failure σ_{max} ksi
			Flexural Members - Type 301 1/2 Hard				
H301F-1	24.82	2085.5	1987	1.05	2076	1.00	105.10
H301F-2	37.94	2026.0	1884	1.08	1931	1.05	95.20
H301F-3	71.04	1664.0	498	3.34	473	3.52	34.80
H301F-4	150.34	1709.0	250	6.84	398	4.30	85.20
			Stiffened Element Compression Members - Type 301 1/2 Hard				
H301SC-2	39.85	72700.0	42950	1.69	43450	1.67	117.10
H301SC-4	154.51	23050.0	2460	9.78	1490	1.54	93.60
			Flexural Members - Type 304 Annealed & Strain Flattened				
AS304F-2	71.52	647.5	440	1.47	436	1.49	35.70
AS304F-3	113.02	699.0	295	2.37	274	2.55	39.25
AS304F-4	150.18	761.0	200	3.81	200	3.81	38.80

* Determined by the Maximum Surface Strain Method

Table 4-1

COMPARISON OF EXPERIMENTAL CALCULATED MOMENT AND TEST MOMENT
TYPE 301 STAINLESS STEEL - 1/2 HARD

Specimen	Load	Experimental* Moment	Effective Width¢	Calculated Moment@	$\frac{M_{calc}}{M_{test}}$
	P lb.	M_{test} in-lb.	$b_{(exp.)}$ in.	M_{calc} in-lb.	
H301F-1	1888	10384	1.4723	11164	1.0751
	1987	10929	1.5312	12184	1.1149
	2085.5	11470	1.5510	12946	1.1284
H301F-2	1592	8756	2.2913	9501	1.0851
	1689	9290	2.2752	10145	1.0921
	1884	10362	2.3134	11688	1.1280
	2026	11143	2.1788	14061	1.2617
H301F-3	598	3289	1.9768	3507	1.0662
	795	4373	1.5700	4597	1.0514
	994.5	5470	1.3658	5747	1.0513
	1382	7601	1.1381	7357	1.0647
	1535	8443	1.0922	9001	1.0661
H301F-4	498.5	2742	4.0776	3076	1.1218
	599	3295	3.2338	3649	1.1077
	797	4384	2.5904	4743	1.0821
	1191	6551	2.0074	6941	1.0597
	1381.5	7598	1.6654	8016	1.0550
	1583.5	8709	1.3868	9249	1.0654
				Average	1.083

*Moment from tests

¢Experimentally calculated effective width

@Experimentally calculated moment by using experimentally calculated effective width and the simplified numerical method

Table 5-1

MEASURED MAXIMUM EDGE FAILURE STRESSES AND STRAINS
FLEXURAL AND COMPRESSION MEMBERS

Specimen	w/t	Compression			Tension			Curvature
		Edge Strain ϵ_{max} μ in./in.	Stress σ_{max} ksi	σ_{max}/σ_y	Edge Strain ϵ_{max} μ in./in.	Stress σ_{max} ksi	σ_{max}/σ_y	Φ μ rad./in.
Flexural Members - Type 301 1/2 Hard								
H301F-1	24.82	6447	105.10	1.05	5672	117.00	0.93	11828
H301F-2	37.94	5230	95.30	0.95	5828	118.90	0.95	11057
H301F-3*	71.04	5904	94.80	1.05	3857	92.80	0.72	6690
H301F-4*	150.34	4922	85.20	0.95	3274	79.70	0.62	5619
Average				1.00			0.81	
Stiffened Element Compression Members - Type 301 1/2 Hard								
H301SC-2	39.85	8475	117.10	1.16				
H301SC-4	154.51	5786	93.60	1.04				
Average				1.10				
Unstiffened Element Compression Members - Type 301 1/2 Hard								
H301UE-1	11.02	6059	96.10	1.07				
H301UE-2	17.63	5317	89.00	0.99				
H301UE-3	29.60	5114	87.20	0.97				
H301UE-4	49.21	4899	86.20	0.96				
Average				1.00				
Flexural Members - Type 304 Annealed & Skin Passed								
AS304F-2	71.52	3531	35.70	1.05	2032	39.25	0.96	3766
AS304F-3	113.02	4801	39.25	1.15	2303	39.90	0.97	4836
AS304F-4	150.18	4596	38.80	1.14	1770	38.20	0.93	4413
Average				1.11			0.95	
Overall Average				1.03			0.87	

* Strains corresponding to the load level before failure.

Table 5-2

THEORETICALLY COMPUTED MOMENT CAPACITY
BASED ON .2% OFFSET YIELD STRENGTH
(Numerical Method)

Temper	Specimen	Maximum Exp. Moment $M_{exp.}$ in.-lb.	Winter's Formula†				Revised Winter's Formula†			
			M_y Corners and Flats* in.-lb.	%**	M_y Flats Only in.-lb.	%**	M_y Corners and Flats* in.-lb.	%**	M_y Flats Only in.-lb.	%**
Type 301-1/2 Hard	H301F-1	11470.0	11084.7	-3.36	10705.0	-6.67	11431.5	-0.34	11052.1	-3.64
	H301F-2	11143.0	11868.6	+6.51	11492.5	+3.14	12089.0	+8.49	11713.1	+5.12
	H301F-3	9152.0	8022.5	-12.34	7684.3	-16.04	8076.0	-11.76	7737.8	-15.45
	H301F-4	9400.0	8500.9	-9.56	8155.2	-13.24	8526.9	-9.29	8181.2	-12.97
			Average	-4.69		-8.20		-3.23		-6.74
Type Annealed & Skin Passed	AS304F-2	3562.0	3838.0	+7.75	3540.2	-0.61	3886.4	+9.11	3587.8	+0.72
	AS304F-3	3844.0	4162.0	+8.27	3859.5	+0.40	4194.7	+9.12	3892.0	+1.25
	AS304F-4	4185.5	4337.9	+3.64	4032.7	-3.65	4363.0	+4.24	4057.9	-3.05
			Average	+6.55		-1.29		+7.49		-0.36

* Considering both corner and flat material properties.
** Percentage of deviation of calculated values from experimental values.
† Using Winter's formulas for effective width calculations
Winter's Formula: Eq. 4-9; Revised Winter's Formula: Eq. 4-40.

Table 5-3

EFFECT OF CORNER STRENGTHENING ON THE THEORETICALLY COMPUTED MOMENT CAPACITY BASED ON .2% OFFSET YIELD STRENGTH

Temper	Specimen	Winter's Formula†			Revised Winter's Formula†		
		M_y Corners and Flats* in.-lb.	M_y Flats Only in.-lb.	%**	M_y Corners and Flats* in.-lb.	M_y Flats Only in.-lb.	%**
Type 301 1/2 Hard	H301F-1	11084.7	10705.0	-3.43	11431.5	11052.1	-3.32
	H301F-2	11868.6	11492.5	-3.17	12089.0	11713.1	-3.11
	H301F-3	8022.5	7684.3	-4.22	8076.0	7737.8	-4.19
	H301F-4	8500.9	8155.2	-4.07	8526.9	8181.2	-4.05
	Average			-3.72			-3.67
Type 304 Annealed & Skin Passed	AS304F-2	3838.0	3540.2	-7.76	3886.4	3587.8	-7.68
	AS304F-3	4162.0	3859.5	-7.27	4194.7	3892.0	-7.22
	AS304F-4	4337.9	4032.7	-7.04	4363.0	4057.9	-6.99
	Average			-7.36			-7.30

* Considering both corner and flat material properties.
** Deviation from computed moments considering corner strengthening effects.
† See footnote in Table 5-2.

Table 5-4

COMPARISON OF CALCULATED AND EXPERIMENTAL FLEXURAL STRENGTH
TYPE 301 STAINLESS STEEL - 1/2 HARD (SIMPLIFIED METHODS)

Specimen	w/t	Maximum Exp. Moment M_f in-lb.	Simplified Numerical Method		Design Method@					
					Elastic Method		Plastic Method Method I		Plastic Method Method II	
			M_{calc} in-lb.	%	M_{calc} in-lb.	%	M_{calc} in-lb.	%	M_{calc} in-lb.	%
H301F-1	24.82	11470	11240	-2.01	10540	-8.10	11375	-0.82	12437	8.43
H301F-2	37.94	11143	11916	6.94	11289	1.31	12495	12.14	13629	22.30
H301F-3	71.04	9152	8042	-12.13	7059	-22.84	9061	-0.99	10077	10.10
H301F-4a	150.34	9400	8460	-10.00	7489	-20.33	9800	4.25	10709	13.93
Average				-4.30		-12.49		3.65		13.69

*Percentage of deviation of calculated flexural strength from experimental values.

@The stress distribution of these methods across the depth of the cross-section is shown in the following sketches,

Elastic Method

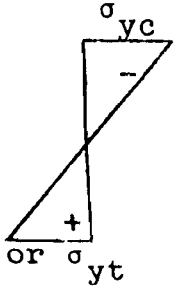

Plastic Method I

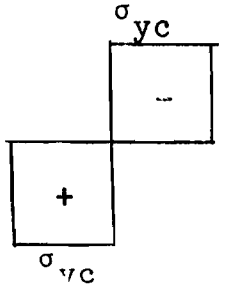

Plastic Method II

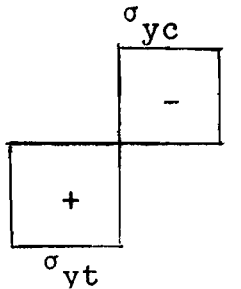

Table 5-5

COMPARISON OF THEORETICAL AND EXPERIMENTAL DEFLECTIONS AT SERVICE LOADS

Temper	Specimen	Moment at Service Load* $M_y/S.F.$ in.-lb.	Deflections at Service Loads: Defl.† (Theor.) in.	Defl. (Exp.) in.	%#
Type 301 1/2 Hard	H301F-1	5991.7	0.995	1.080	-7.8
	H301F-2	6415.5	0.955	1.005	-5.0
	H301F-3	4336.5	0.530	0.535	-0.9
	H301F-4	4595.1	0.495	0.480	+3.1
				Average	-2.6
Type 304 Annealed & Skin Passed	AS304F-2	2074.6	0.242	0.250	-3.1
	AS304F-3	2249.7	0.225	0.238	-5.4
	AS304F-4	2344.8	0.218	0.211	+3.2
				Average	-1.8

† Calculated by numerical integration, Sec. 5.2.3.5.a.

* Moment at service load is equal to $M_y/1.85$; the values of M_y are shown in Table 5-3 considering original Winter's formula and both corners and flats.

\# Percentage of deviation of theoretical deflection from experimental deflection.

Table 5-6

COMPARISON OF CALCULATED AND EXPERIMENTAL DEFLECTIONS AT SERVICE LOADS
TYPE 301 STAINLESS STEEL - 1/2 HARD

Specimen	w/t	Deflections at Service Loads											
		Elastic Method				Plastic Method I				Plastic Method II			
		$\frac{M_{calc}}{1.85}$*	Defl.@ (calc)	Defl.@ (exp)	%**	$\frac{M_{calc}}{2.00}$*	Defl.@ (calc)	Defl.@ (exp)	%	$\frac{M_{calc}}{2.00}$*	Defl.@ (calc)	Defl.@ (exp)	%
H301F-1	24.82	5697	0.9491	1.030	-7.85	5688	0.9467	1.027	-7.82	6219	1.0584	1.145	-7.56
H301F-2	37.94	6102	0.9212	0.950	-2.52	6248	0.9401	0.980	-4.07	6815	1.0664	1.095	-2.61
H301F-3	71.04	3815	0.4570	0.448	2.01	4531	0.5771	0.580	-0.50	5039	0.6810	0.734	-7.22
H301F-4a	150.34	4043	0.4241	0.402	5.50	4900	0.5620	0.520	8.08	5355	0.6426	0.586	11.37
Average					-0.72				-1.08				-1.51

*Flexural strength calculated by Elastic Method, Plastic Method I or II.

**Percentage of deviation of calculated deflection from experimental deflection.

@. Deflections calculated by the simplified method suggested in 5.2.3.5.b

Table 5-7

COMPARISON OF CALCULATED AND EXPERIMENTAL ULTIMATE STRENGTHS
OF NONCOMPACT COMPRESSION MEMBERS
TYPE 301 STAINLESS STEEL - 1/2 HARD

Specimen	Maximum Experimental Load P_f lb.	Stress¢ ksi	Effective Area* A_{eff} $in.^2$	Corner Area A_c $in.^2$	Calculated Load Capacity P_{calc}# (Flats & Corners) lb.	%	P_{calc}@ (Flats only) lb.	%
			Unstiffened Element Compression Members					
H301UE-1	16850	89.90	0.1190	0.0289	14106	-16.3	13295	-21.1
H301UE-2	15000	89.90	0.1253	0.0290	14677	-2.2	13863	-7.6
H301UE-3	15500	89.90	0.1272	0.0288	14832	-4.3	14024	-9.5
H301UE-4	16150	89.90	0.1271	0.0288	14819	-8.2	14011	-13.2
Average						-7.8		-12.9
			Stiffened Element Compression Members					
H301SC-2	72700	100.50	0.4657	0.1213	61353	-15.60	59000	-18.80
H301SC-4	23050	89.90	0.1695	0.0511	21120	-8.35	19650	-14.70
Average						-12.02		-16.75

¢ .2% Offset yield strength of flat material

* Total effective area excluding corner area
(Eqs. 4-22 and 4-9 were used for effective width calculations for unstiffened and stiffened elements, respectively.)

@ Flat Material yield strength for both flats and corners

\# Considering both flat and corner strengths;
Corner strength corresponding to the strain of the .2% offset yield strength of flats was used for corners.

Table 6-1

ACTUAL SAFETY FACTORS OF CALCULATED SERVICE MOMENT AND FAILURE MOMENT FROM EXPERIMENTS
TYPE 301 STAINLESS STEEL - 1/2 HARD

Specimen	Max. Exp. Moment M_f	Elastic Method Service Moment $M_s = M_{ult}^*/1.85$	$\frac{M_f}{M_s}$	Plastic Method I Service Moment $M_s = M_{ult}^*/2.00$	$\frac{M_f}{M_s}$	Plastic Method II Service Moment $M_s = M_{ult}^*/2.00$	$\frac{M_f}{M_s}$
	in.-lb.	in.-lb.		in.-lb.		in.-lb.	
H301F-1	11470	5697	2.01	5688	2.02	6219	1.84
H301F-2	11143	6102	1.83	6248	1.78	6815	1.64
H301F-3	9152	3815	2.40	4531	2.02	5039	1.82
H301F-4a	9400	4043	2.33	4900	1.92	5355	1.76
Average			2.14		1.94		1.77

*Calculated flexural strength by Elastic Method, plastic method I or II.

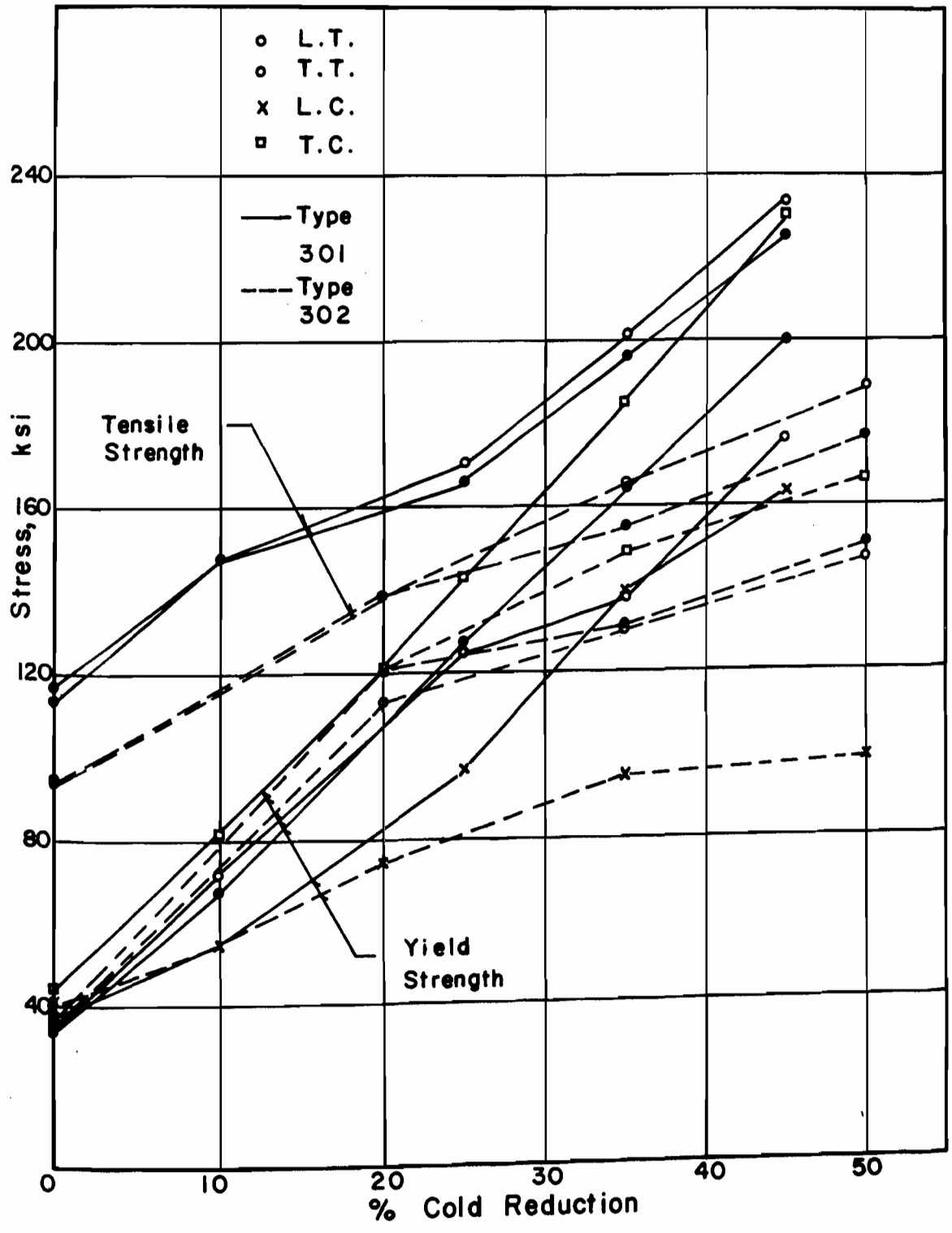

Fig. 2-1 EFFECT OF COLD ROLLING ON YIELD AND TENSILE STRENGTHS, TYPE 301 AND 302 AUSTENITIC STAINLESS STEELS (Adapted from Refs. 2-4 and 2-19)

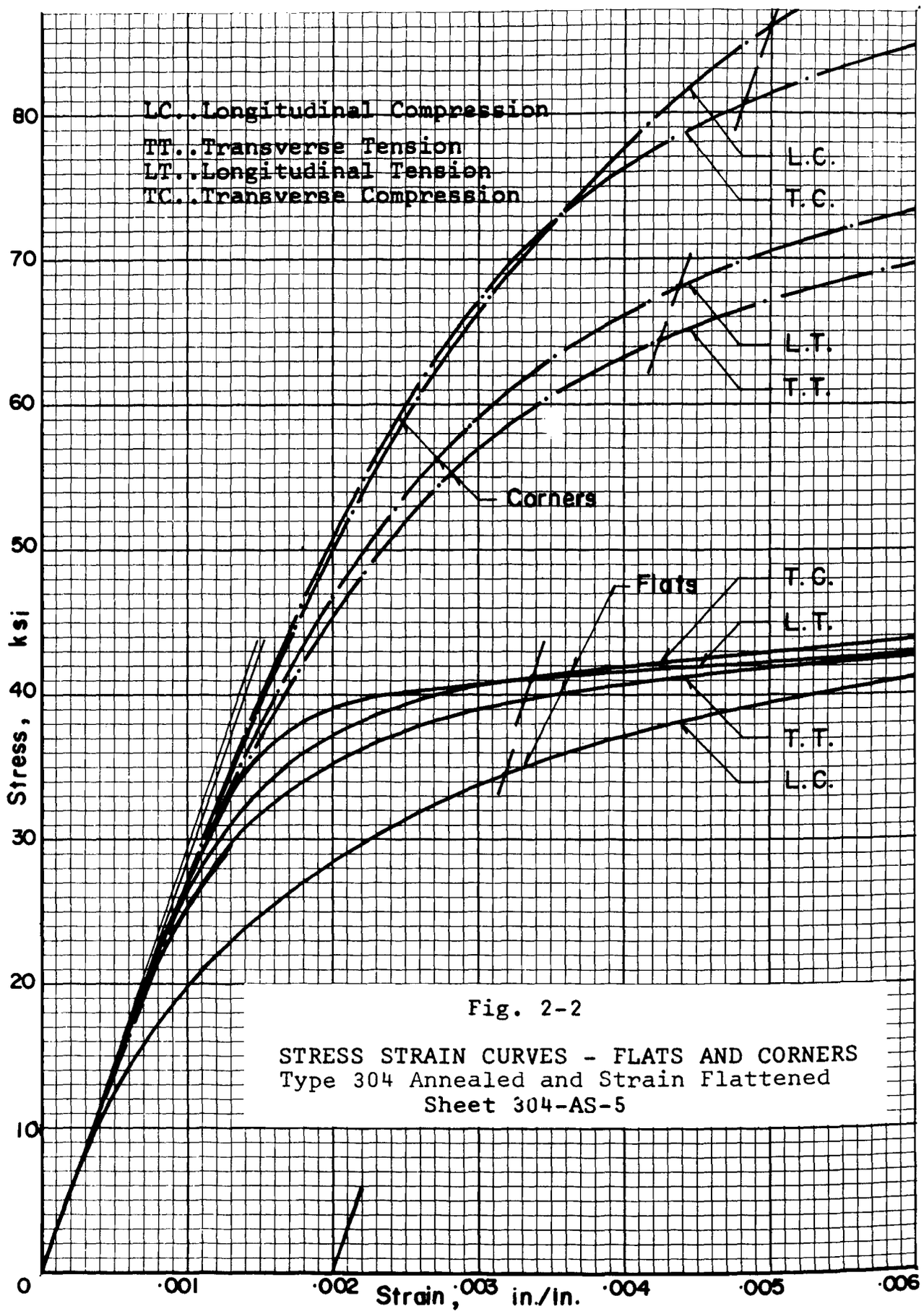

Fig. 2-2

STRESS STRAIN CURVES - FLATS AND CORNERS
Type 304 Annealed and Strain Flattened
Sheet 304-AS-5

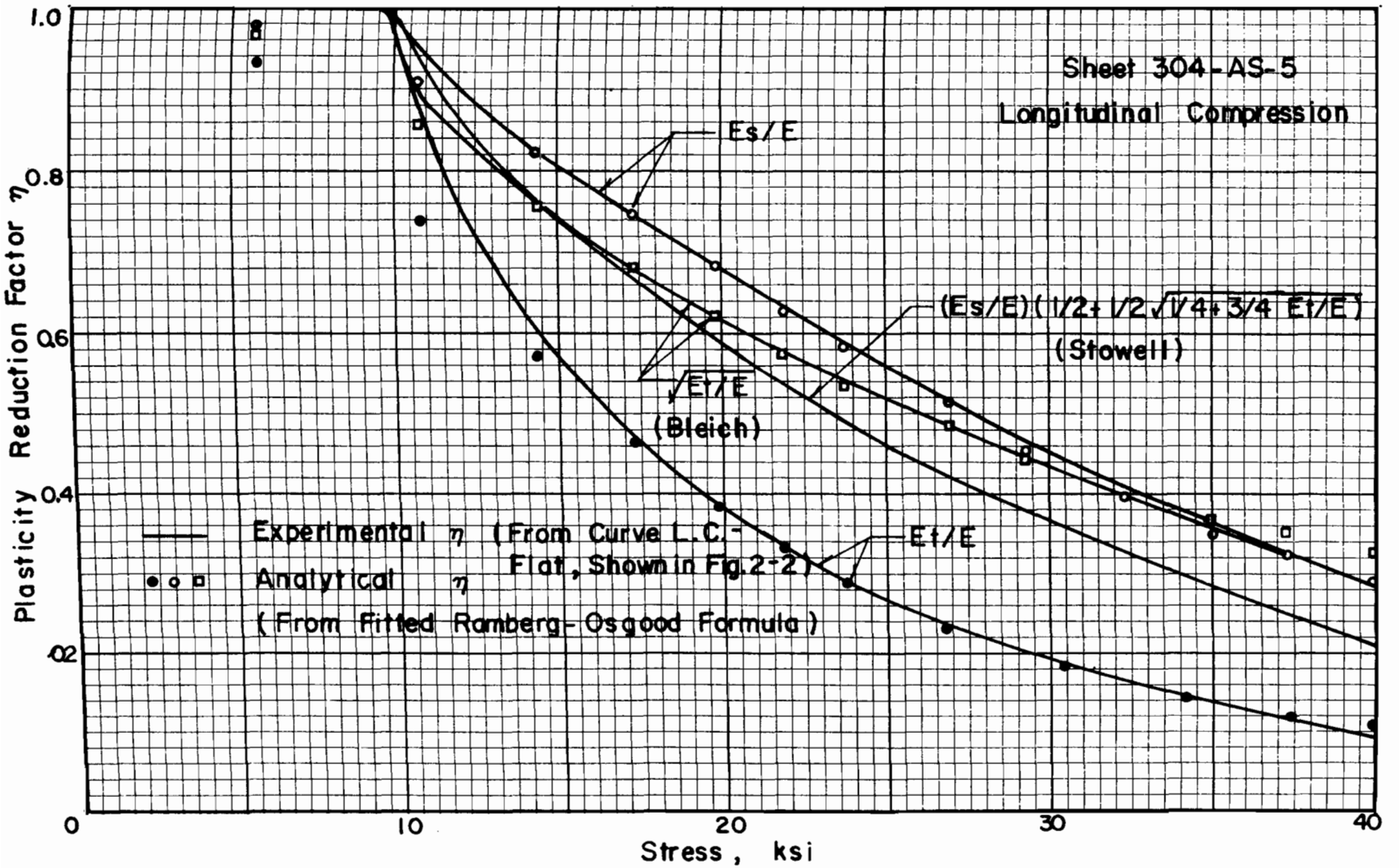

Fig. 2-3 PLASTICITY REDUCTION FACTOR VS. STRESS, TYPE 304 ANNEALED AND STRAIN FLATTENED STAINLESS STEEL

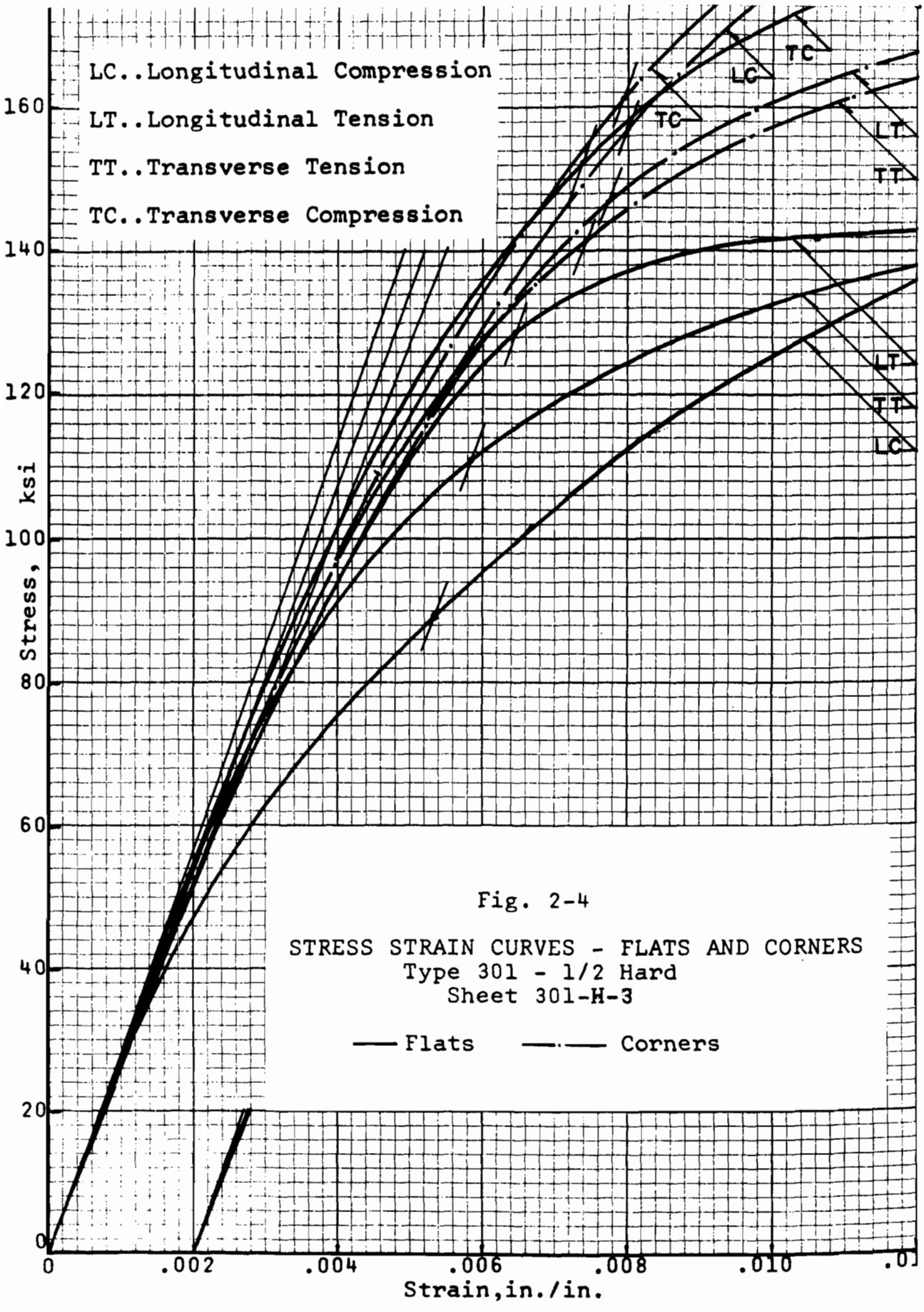

Fig. 2-4

STRESS STRAIN CURVES - FLATS AND CORNERS
Type 301 - 1/2 Hard
Sheet 301-H-3

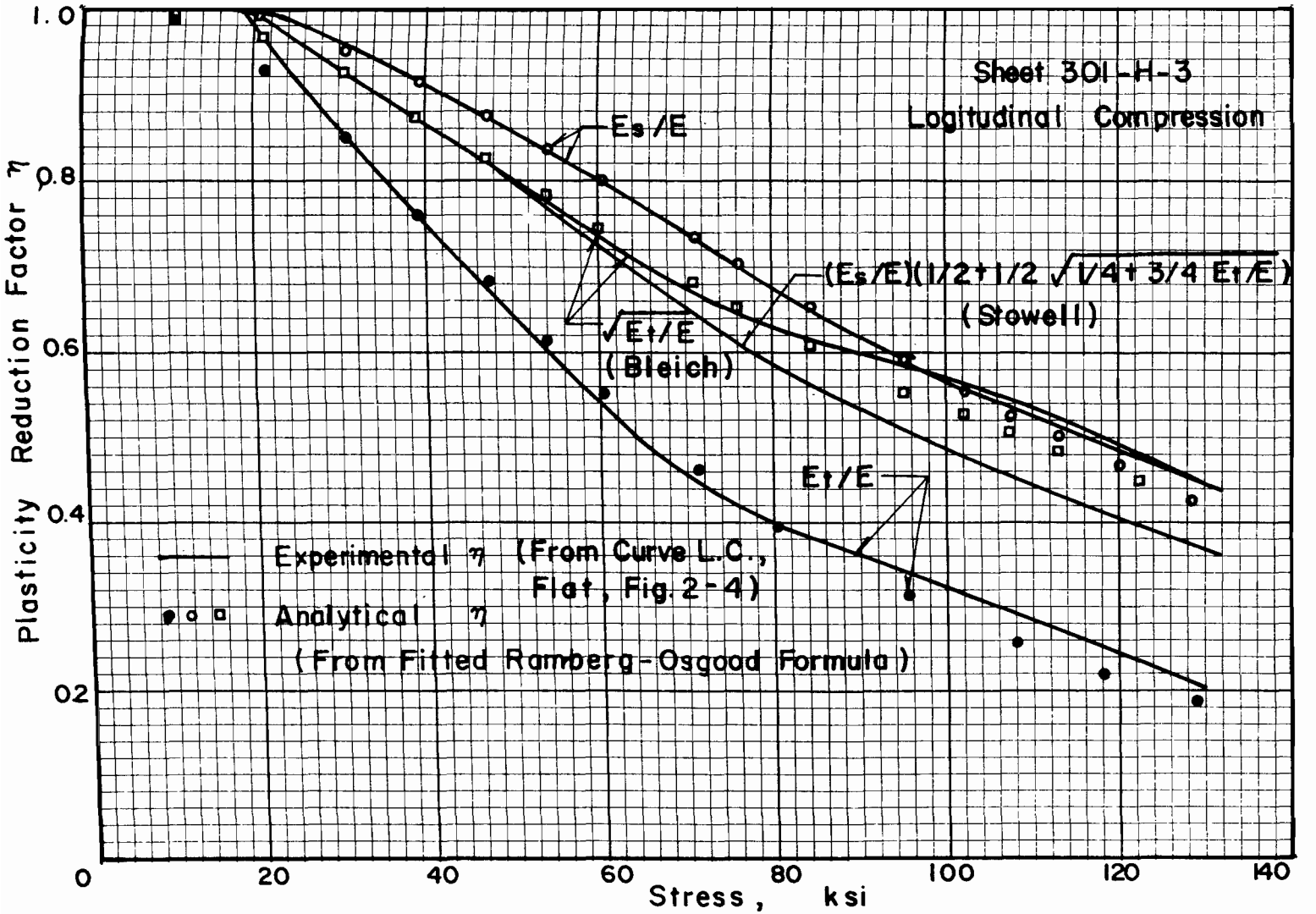

Fig. 2-5 PLASTICITY REDUCTION FACTOR VS. STRESS, TYPE 301 STAINLESS STEEL-1/2 HARD

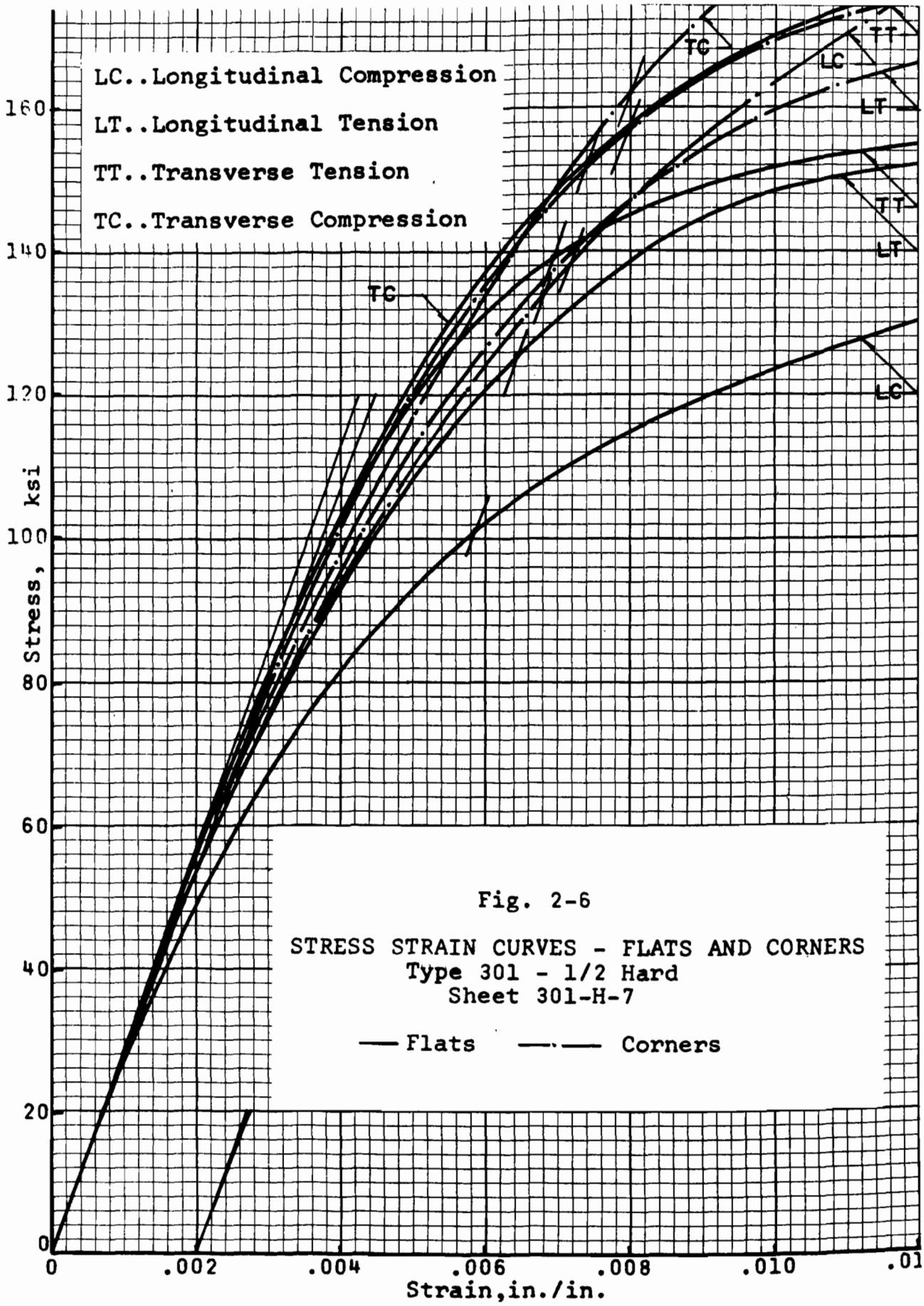

Fig. 2-6

STRESS STRAIN CURVES - FLATS AND CORNERS
Type 301 - 1/2 Hard
Sheet 301-H-7

—— Flats —·—·— Corners

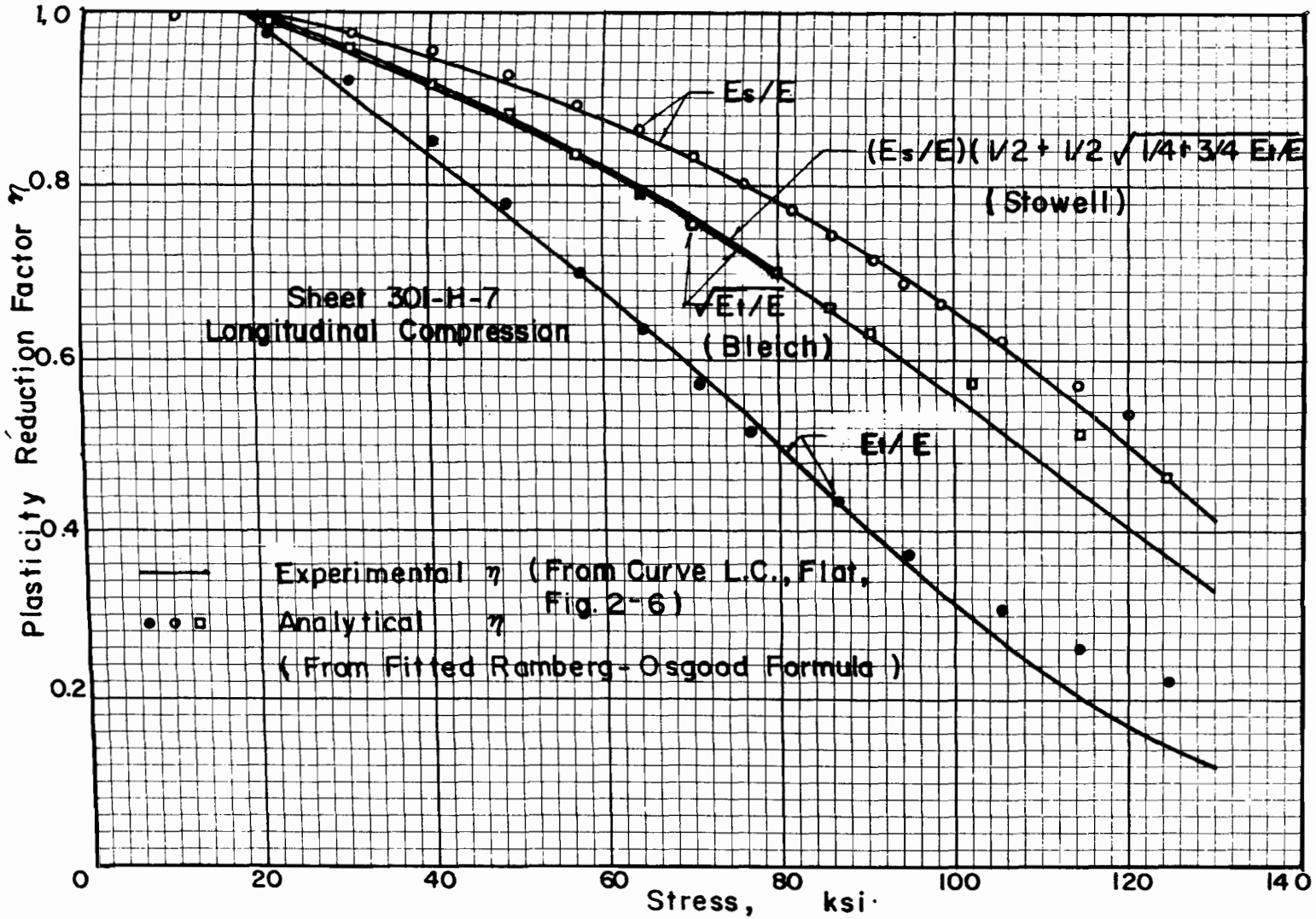

Fig. 2-7 PLASTICITY REDUCTION FACTOR VS. STRESS, TYPE 301 STAINLESS STEEL - 1/2 HARD

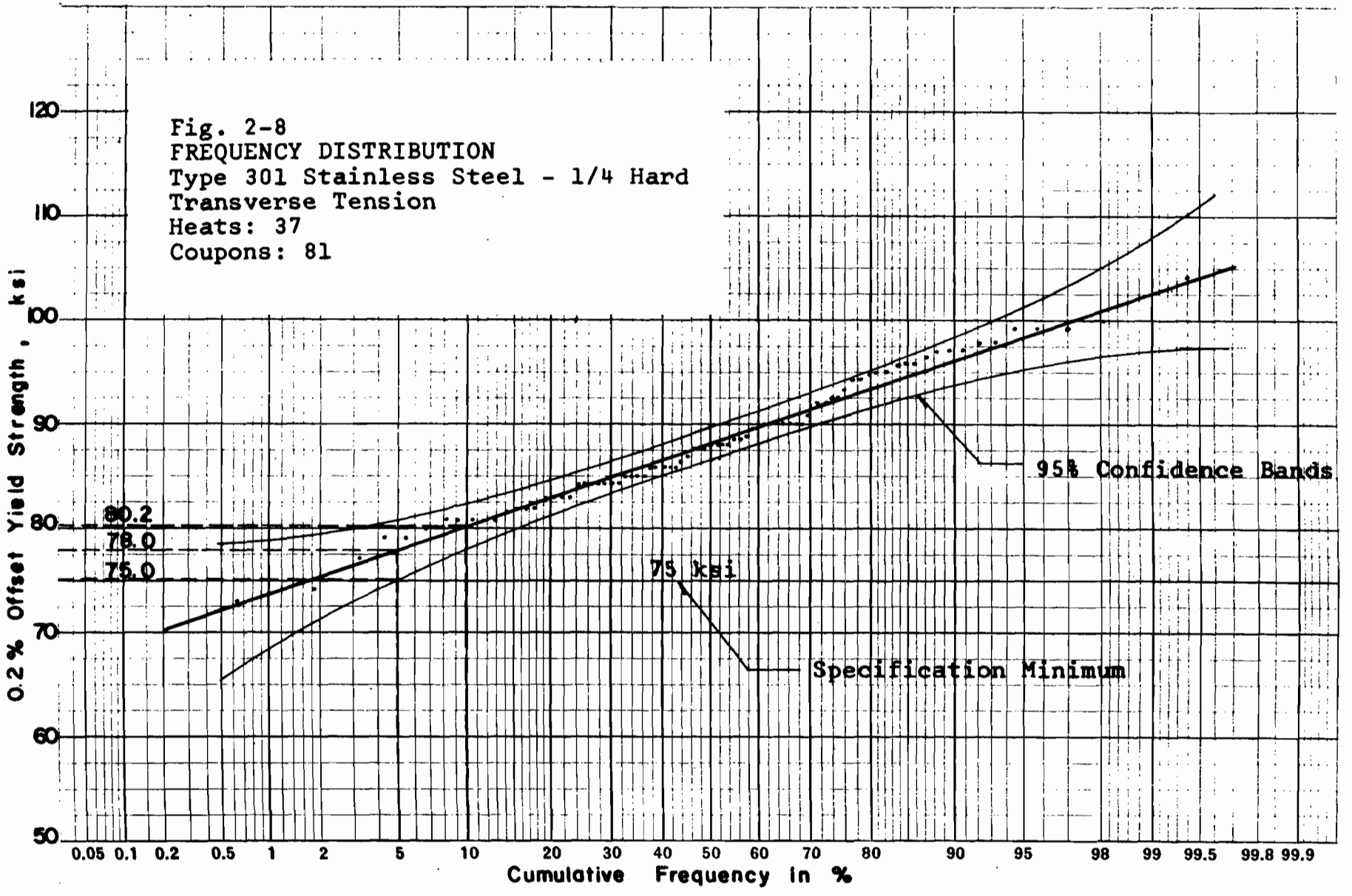
Fig. 2-8
FREQUENCY DISTRIBUTION
Type 301 Stainless Steel - 1/4 Hard
Transverse Tension
Heats: 37
Coupons: 81
0.2% Offset Yield Strength, ksi
120
110
100
90
80
70
60
50
80.2
78.0
75.0
75 ksi
95% Confidence Bands
Specification Minimum
0.05 0.1 0.2 0.5 1 2 5 10 20 30 40 50 60 70 80 90 95 98 99 99.5 99.8 99.9
Cumulative Frequency in %

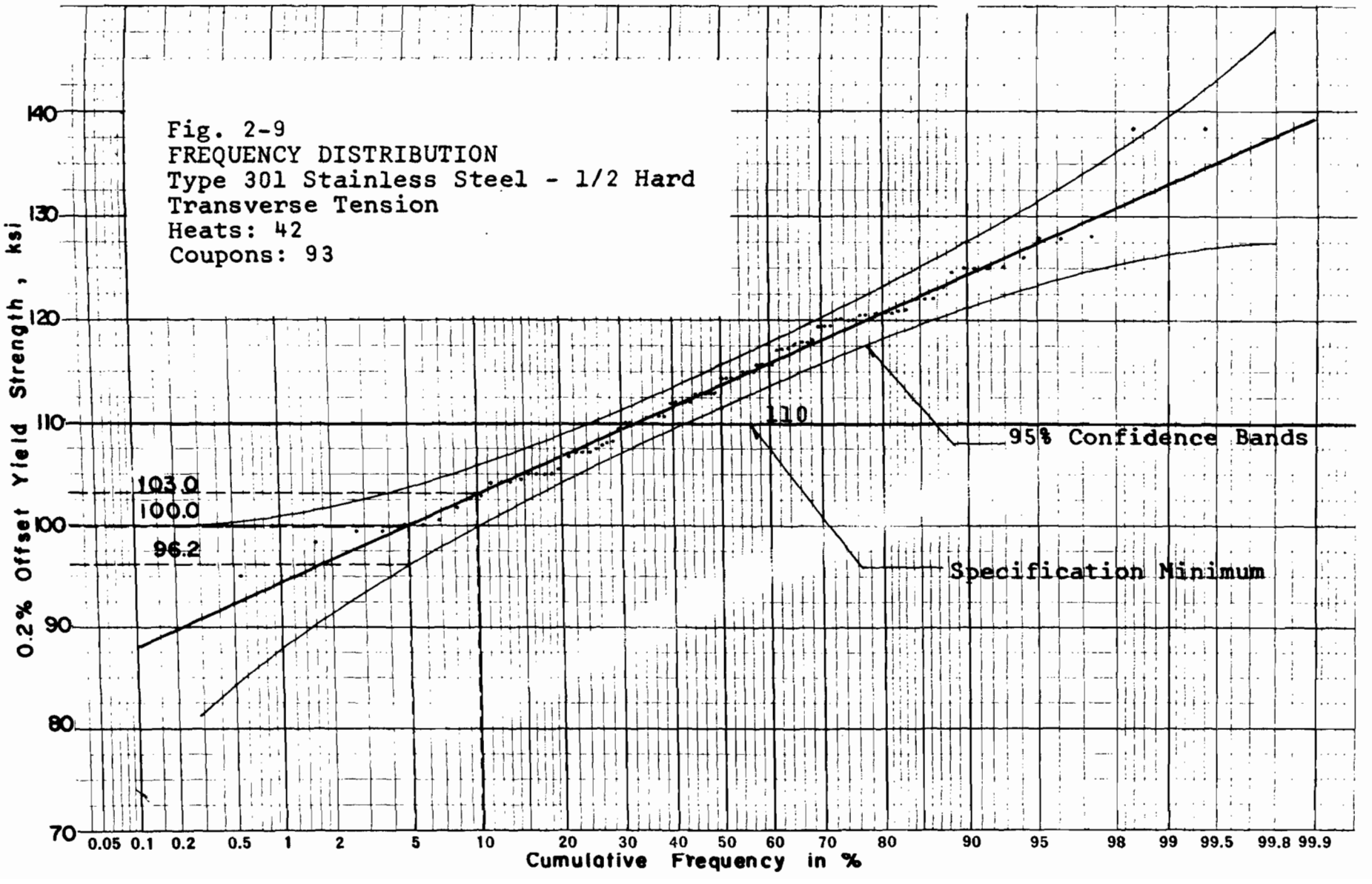
Fig. 2-9
FREQUENCY DISTRIBUTION
Type 301 Stainless Steel - 1/2 Hard
Transverse Tension
Heats: 42
Coupons: 93
0.2% Offset Yield Strength, ksi
140
130
120
110
100
90
80
70
103.0
100.0
96.2
110
95% Confidence Bands
Specification Minimum
0.05 0.1 0.2 0.5 1 2 5 10 20 30 40 50 60 70 80 90 95 98 99 99.5 99.8 99.9
Cumulative Frequency in %

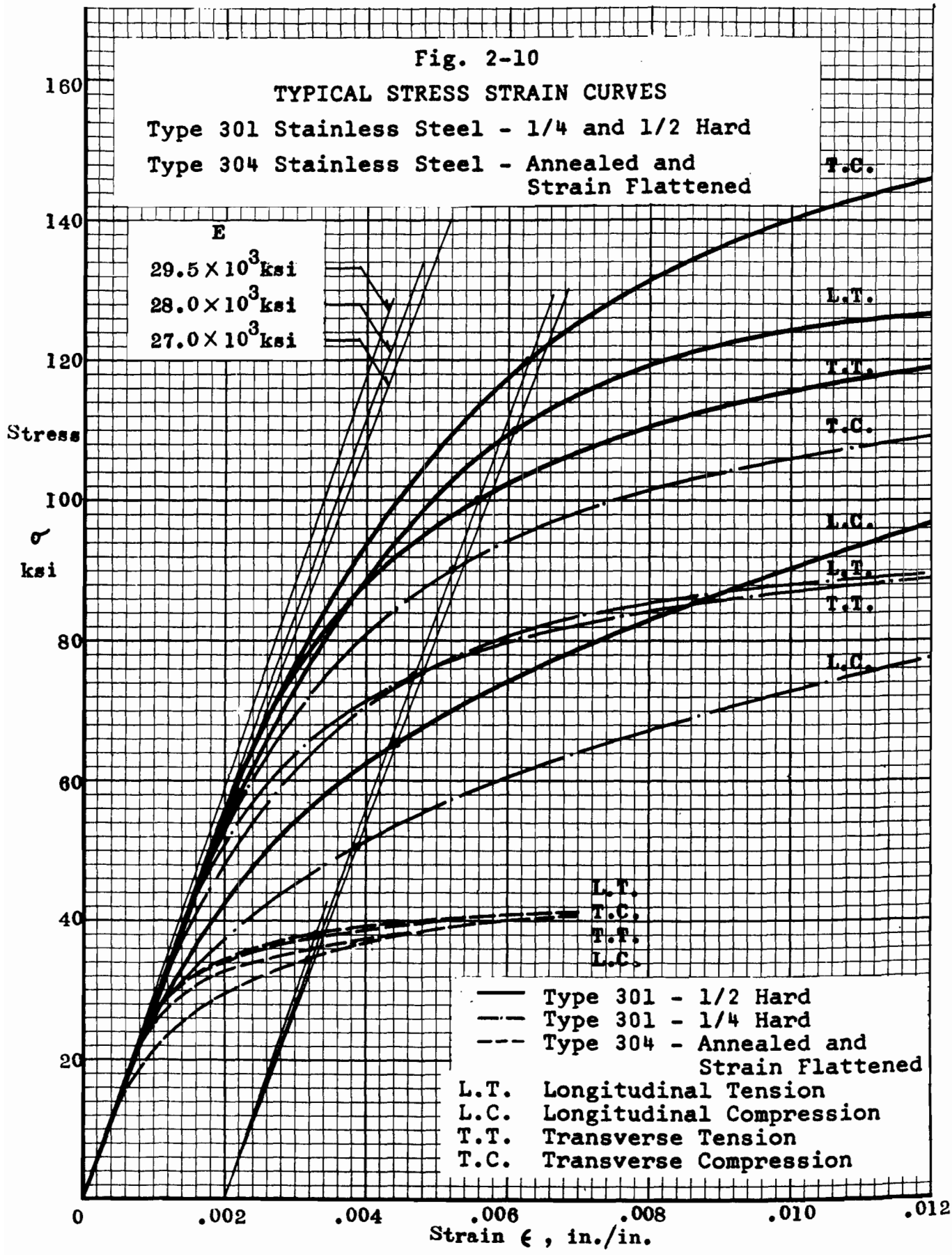
Fig. 2-10
TYPICAL STRESS STRAIN CURVES
Type 301 Stainless Steel - 1/4 and 1/2 Hard
Type 304 Stainless Steel - Annealed and Strain Flattened
E
29.5 × 10³ ksi
28.0 × 10³ ksi
27.0 × 10³ ksi
T.C.
L.T.
T.T.
T.C.
L.C.
L.T.
T.T.
L.C.
L.T.
T.C.
T.T.
L.C.
Type 301 - 1/2 Hard
Type 301 - 1/4 Hard
Type 304 - Annealed and Strain Flattened
L.T. Longitudinal Tension
L.C. Longitudinal Compression
T.T. Transverse Tension
T.C. Transverse Compression
Stress σ ksi
160
140
120
100
80
60
40
20
0
.002
.004
.006
.008
.010
.012
Strain ϵ , in./in.

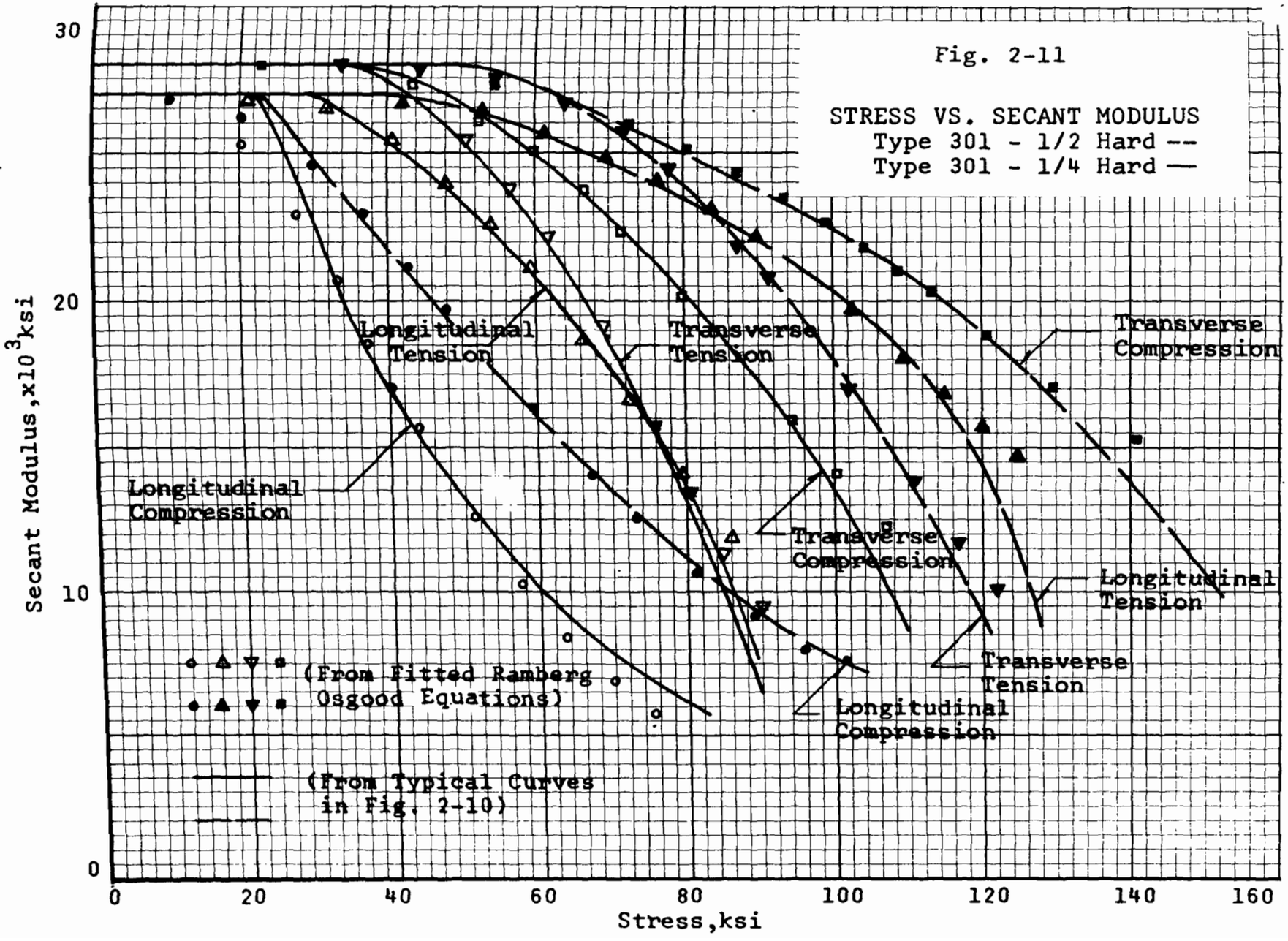
Fig. 2-11
STRESS VS. SECANT MODULUS
Type 301 - 1/2 Hard --
Type 301 - 1/4 Hard —
Secant Modulus, x10^3 ksi
Stress, ksi
0
10
20
30
0
20
40
60
80
100
120
140
160
Longitudinal Tension
Transverse Tension
Transverse Compression
Longitudinal Compression
Transverse Compression
Longitudinal Tension
Transverse Tension
Longitudinal Compression
(From Fitted Ramberg Osgood Equations)
(From Typical Curves in Fig. 2-10)

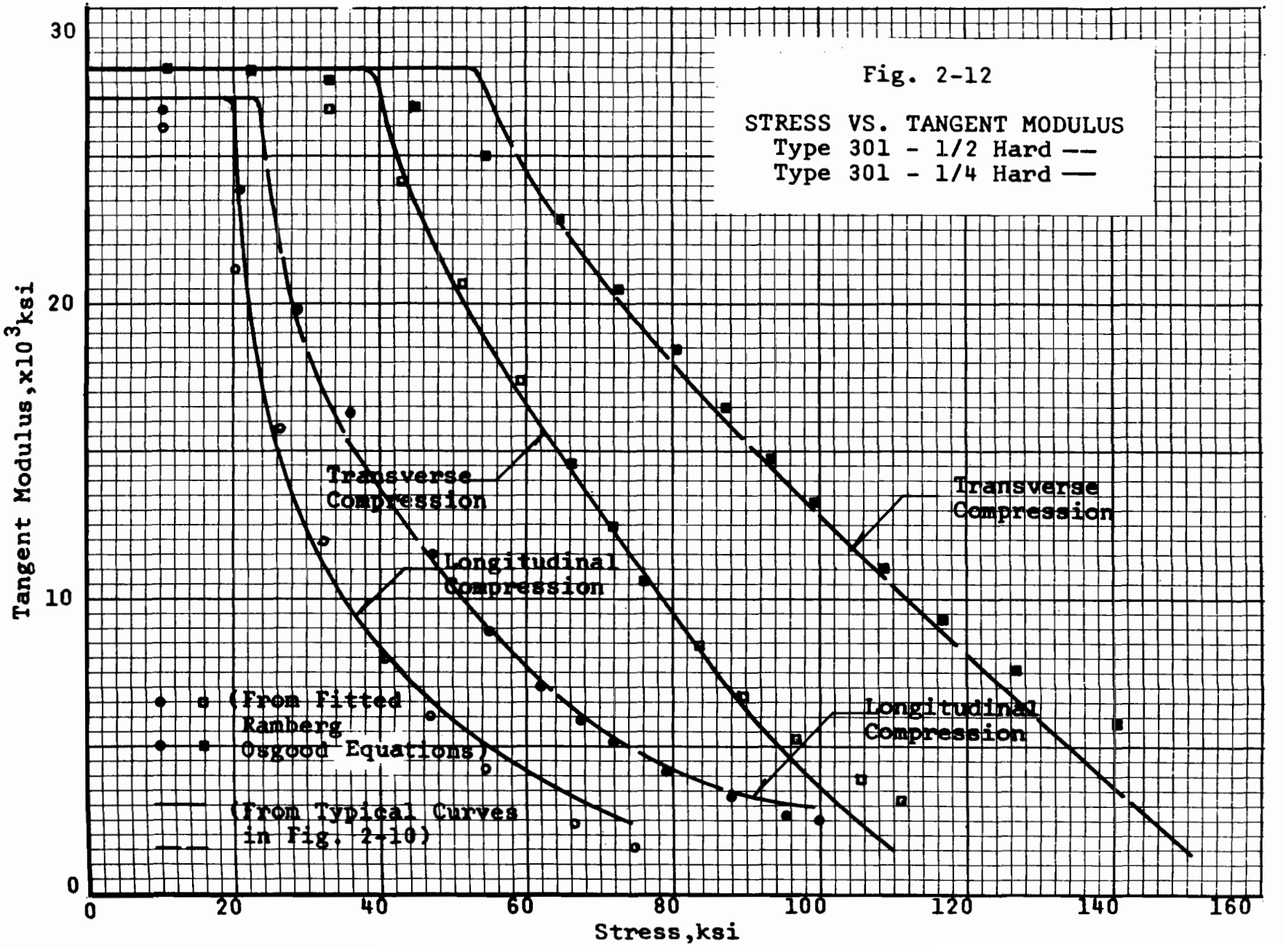
Fig. 2-12
STRESS VS. TANGENT MODULUS
Type 301 - 1/2 Hard --
Type 301 - 1/4 Hard ——
Tangent Modulus, x10³ksi
Stress, ksi
0
10
20
30
0
20
40
60
80
100
120
140
160
Transverse Compression
Longitudinal Compression
Transverse Compression
Longitudinal Compression
(From Fitted Ramberg Osgood Equations)
(From Typical Curves in Fig. 2-10)

Fig. 2-13

AVERAGE NORMAL STRESS STRAIN CURVE
AND
SHEAR STRESS STRAIN CURVES

(Sheet 301-H-3)

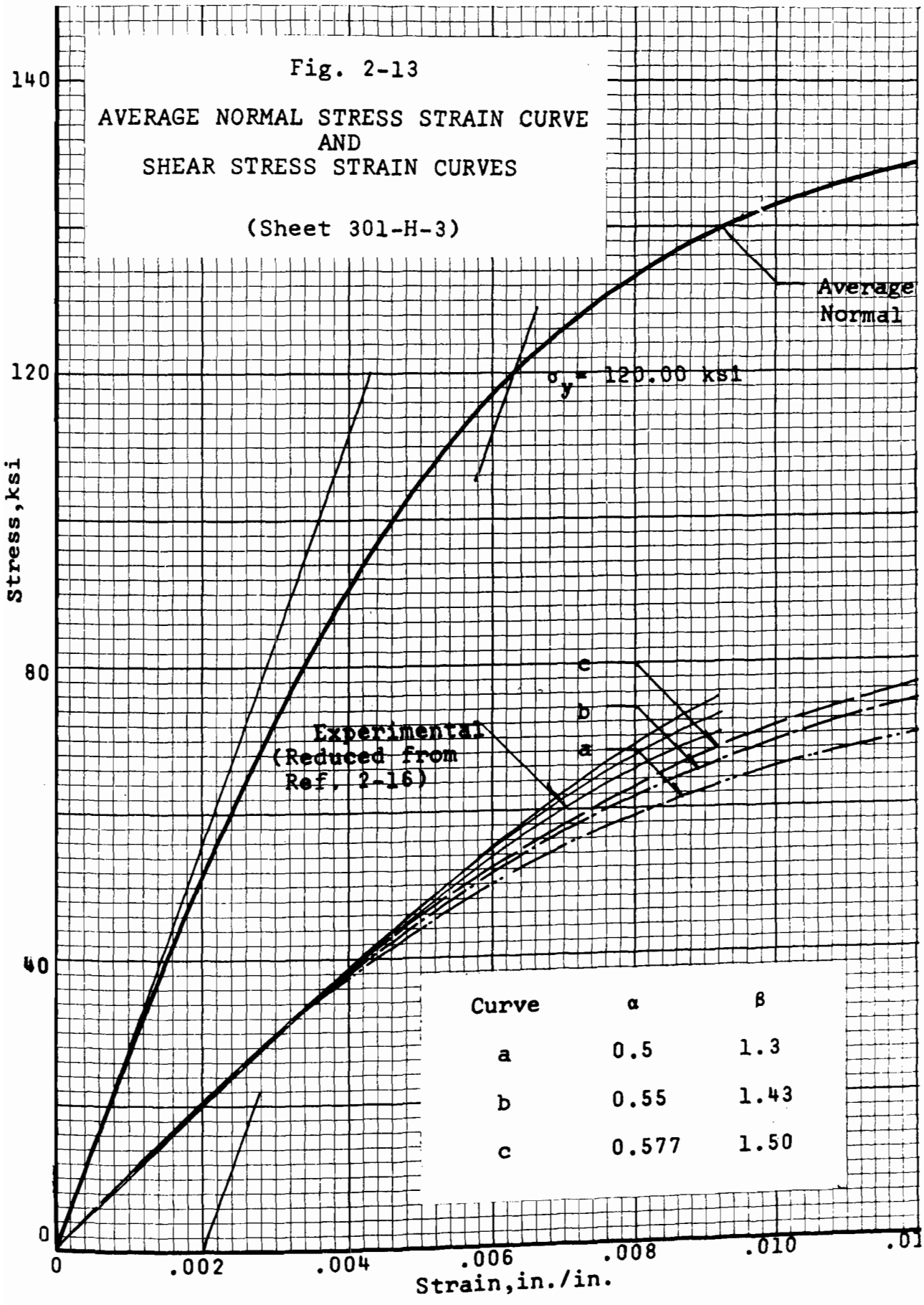

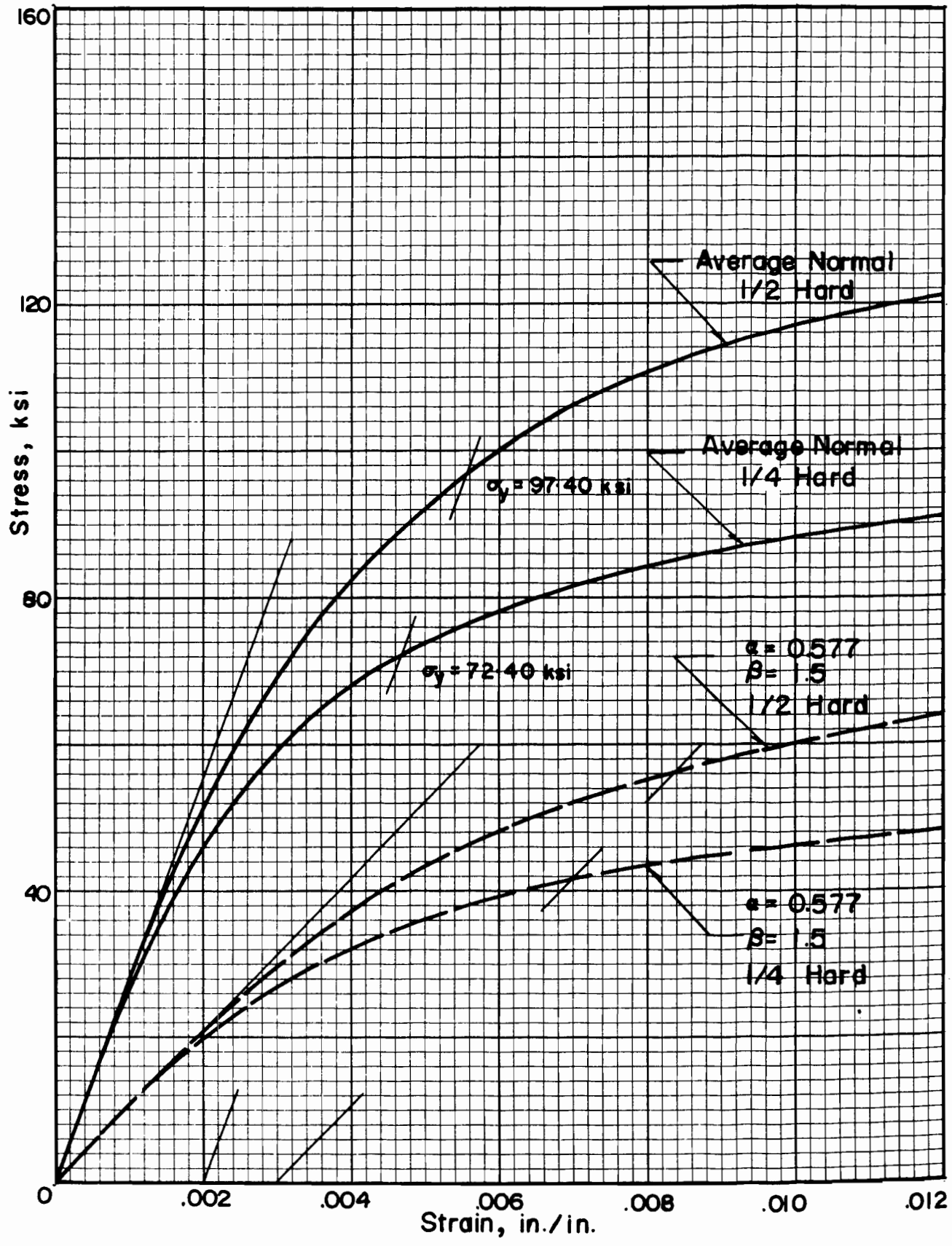

Fig. 2-14 TYPICAL AVERAGE NORMAL STRESS STRAIN CURVES AND SHEAR STRESS STRAIN CURVES - TYPE 301 STAINLESS STEEL-1/4 AND 1/2 HARD

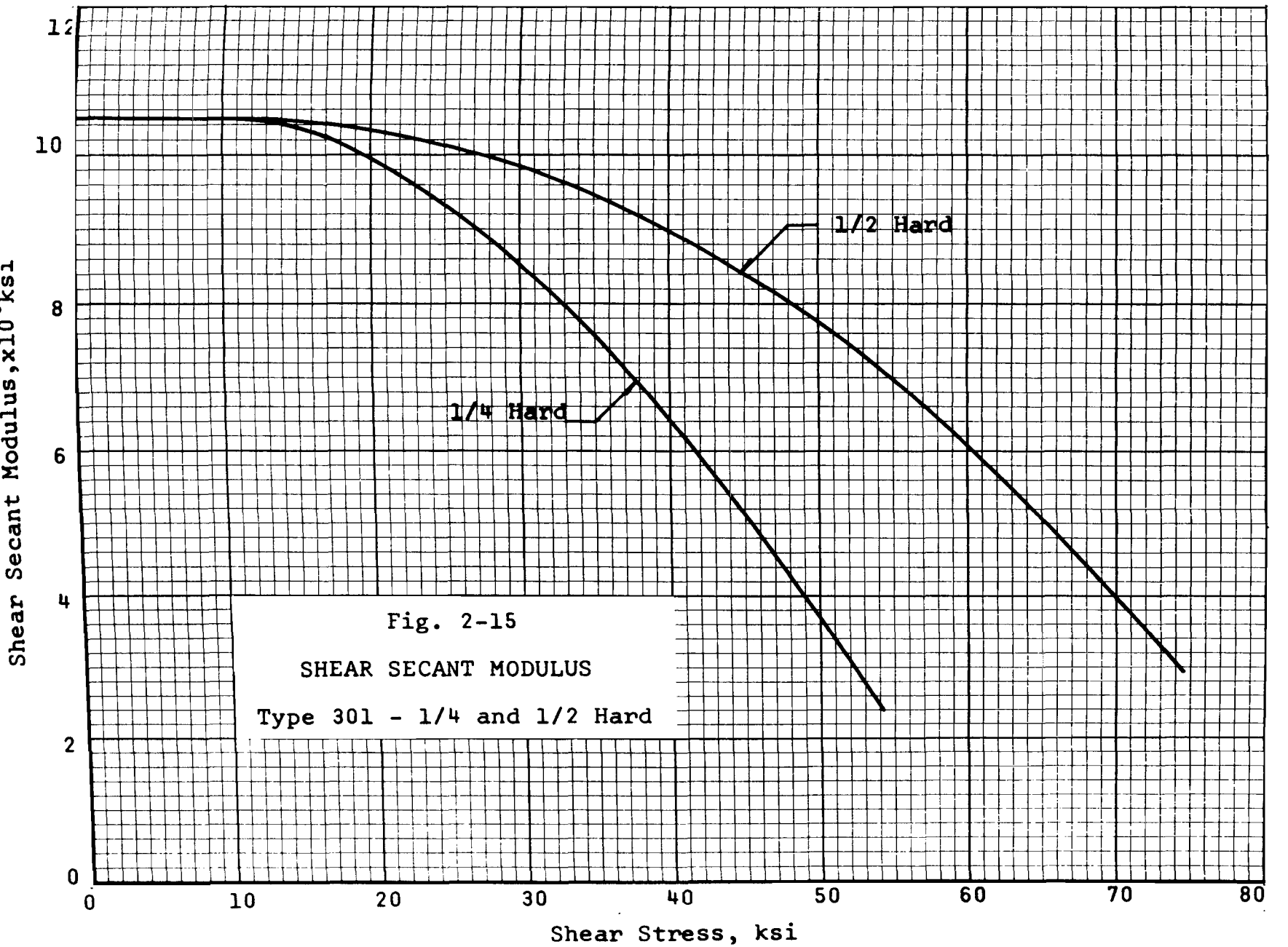

Fig. 2-15

SHEAR SECANT MODULUS

Type 301 - 1/4 and 1/2 Hard

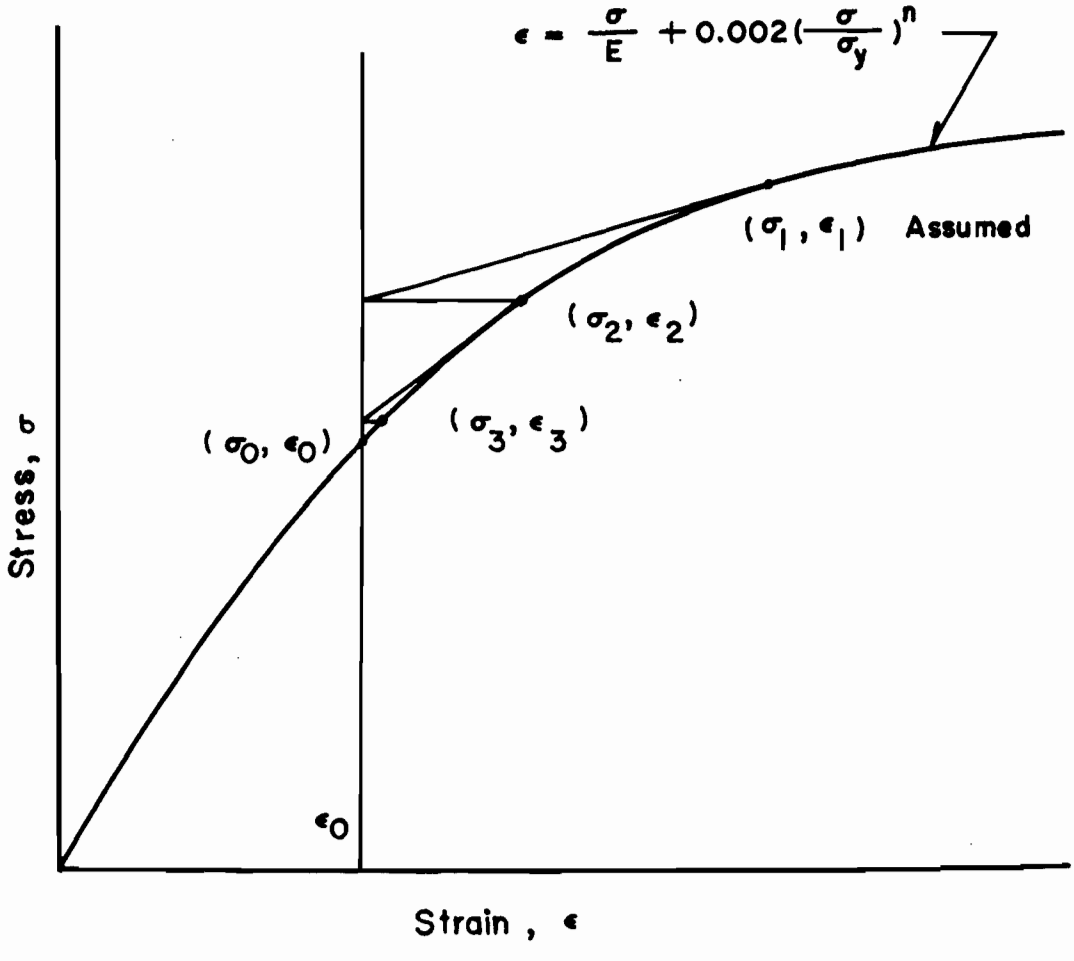

Fig. 2-16 CONVERGENCE SCHEME OF STRESS STRAIN ITERATION - NEWTON'S TANGENT METHOD

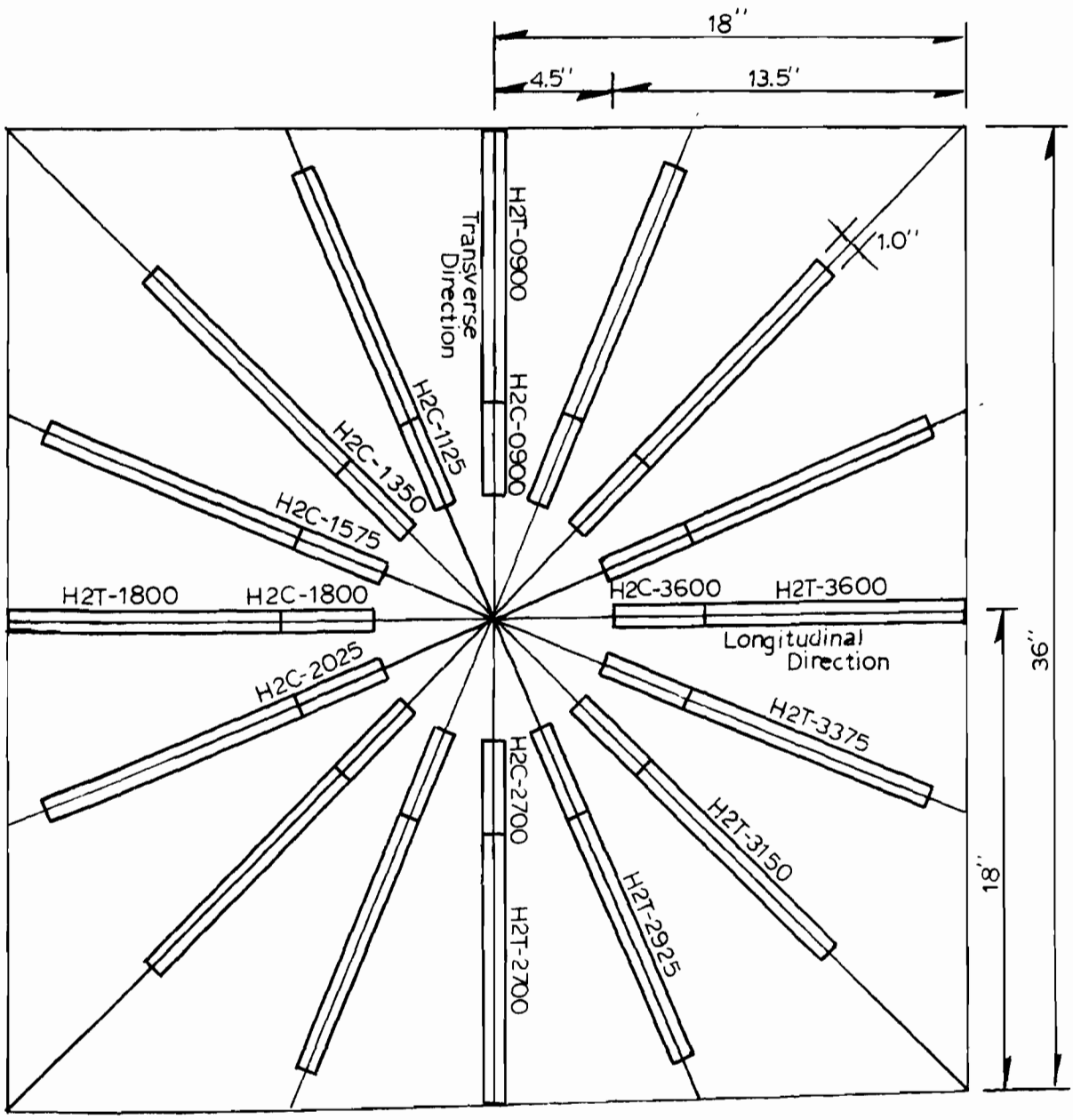

Fig. 2-17 SAMPLING SCHEME FOR ANISOTROPIC PROPERTIES TESTS OF A STAINLESS SHEET - TYPE 301-1/2 HARD

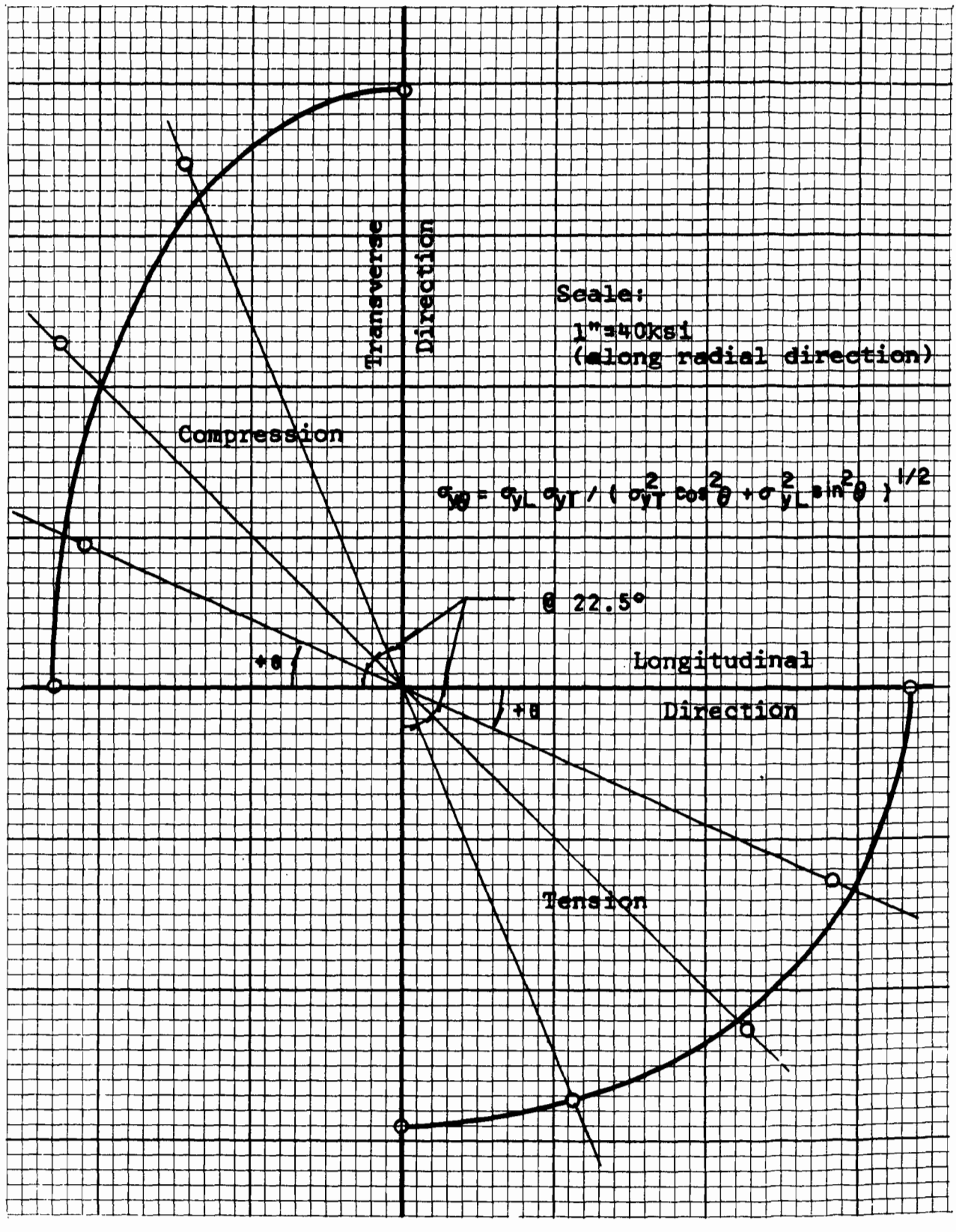

Fig. 2-18 DIRECTIONAL VARIATION OF TENSILE AND COMPRESSIVE YIELD STRENGTHS

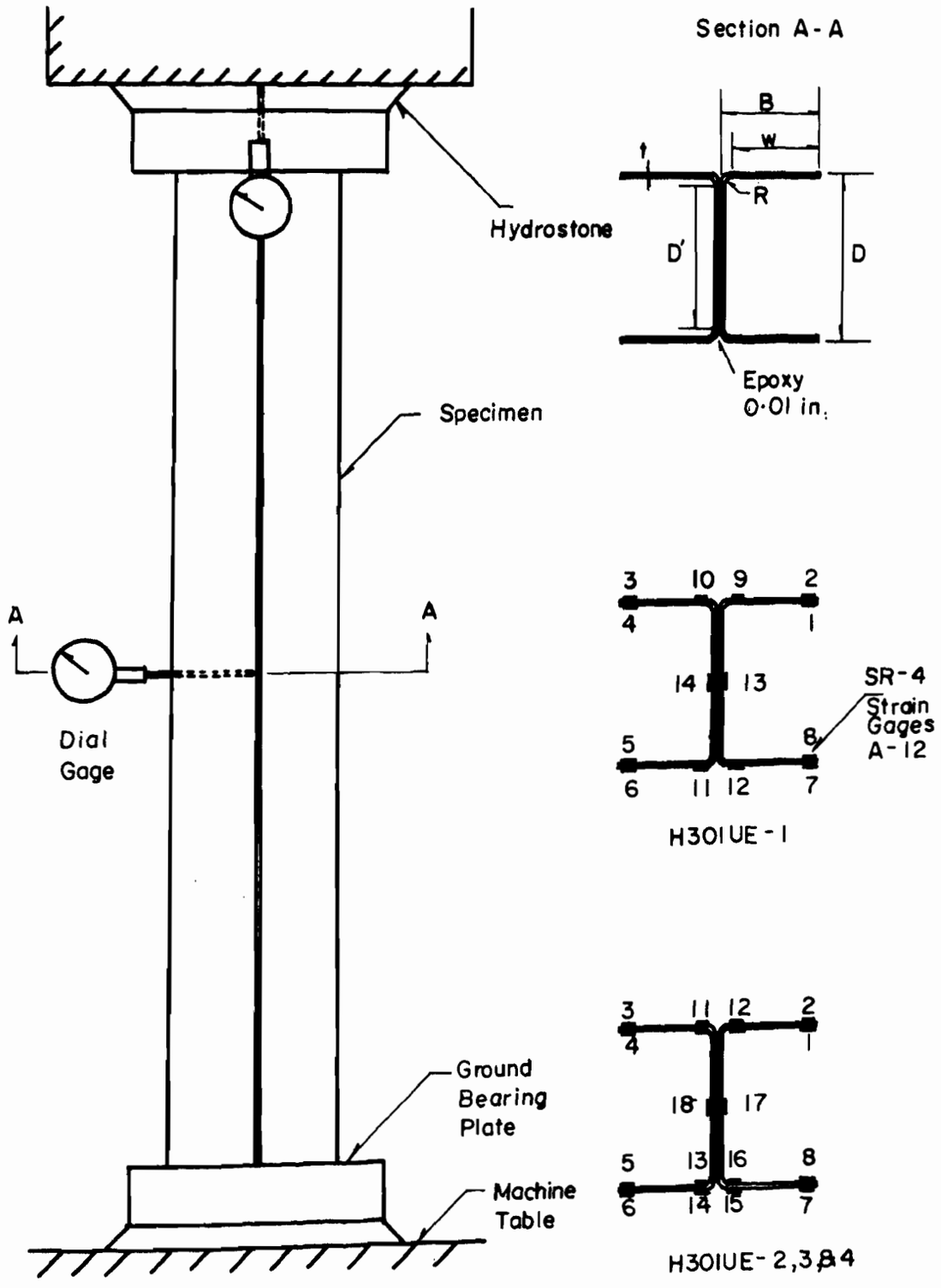

Fig. 3-1 COMPRESSION SPECIMEN LOADING, CROSS SECTION, AND GAGING - UNSTIFFENED ELEMENTS, SERIES H301UE

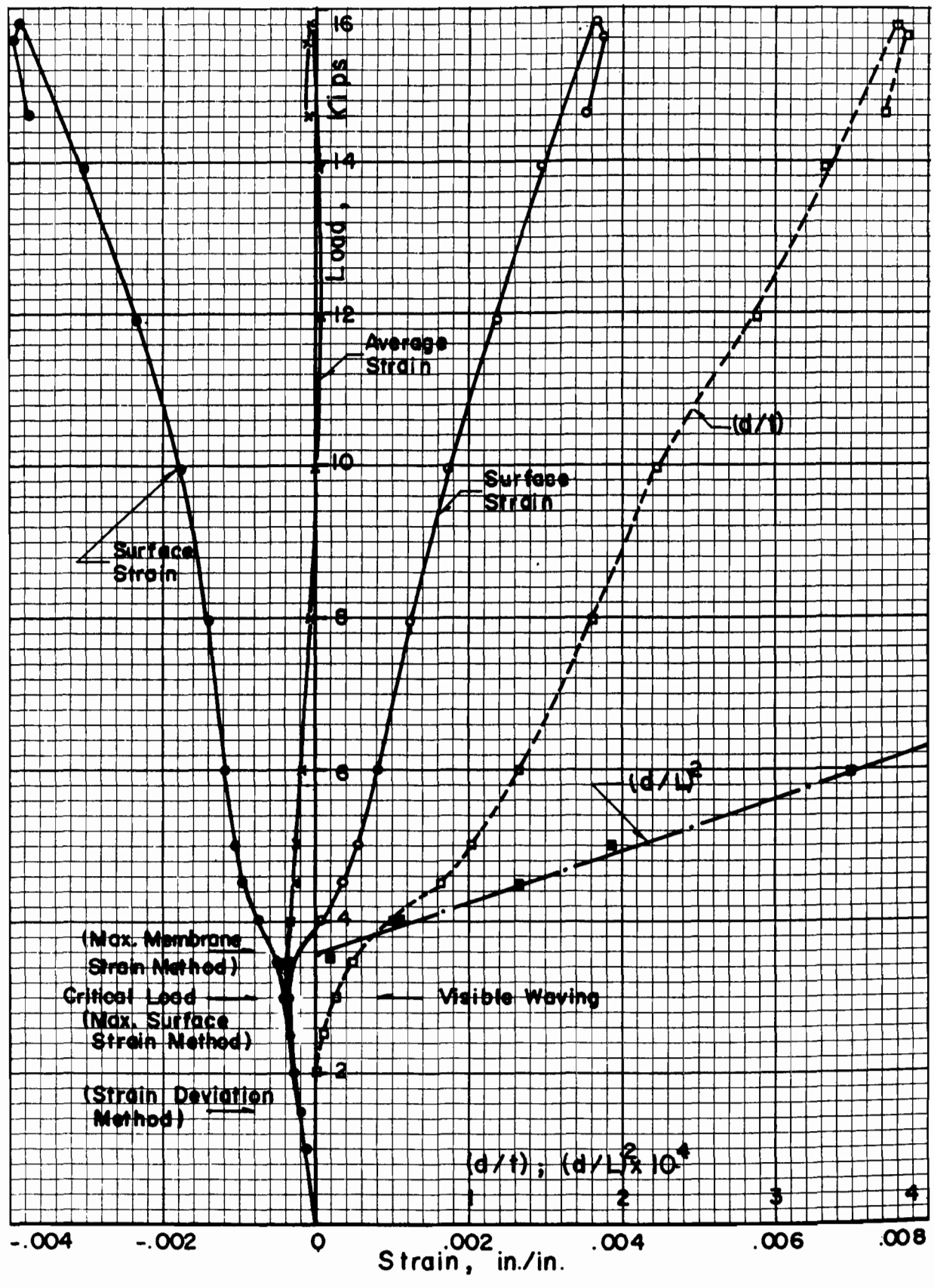

Fig. 3-2 TYPICAL FREE EDGE STRAINS AND WAVING AMPLITUDE - Specimen H301UE-4

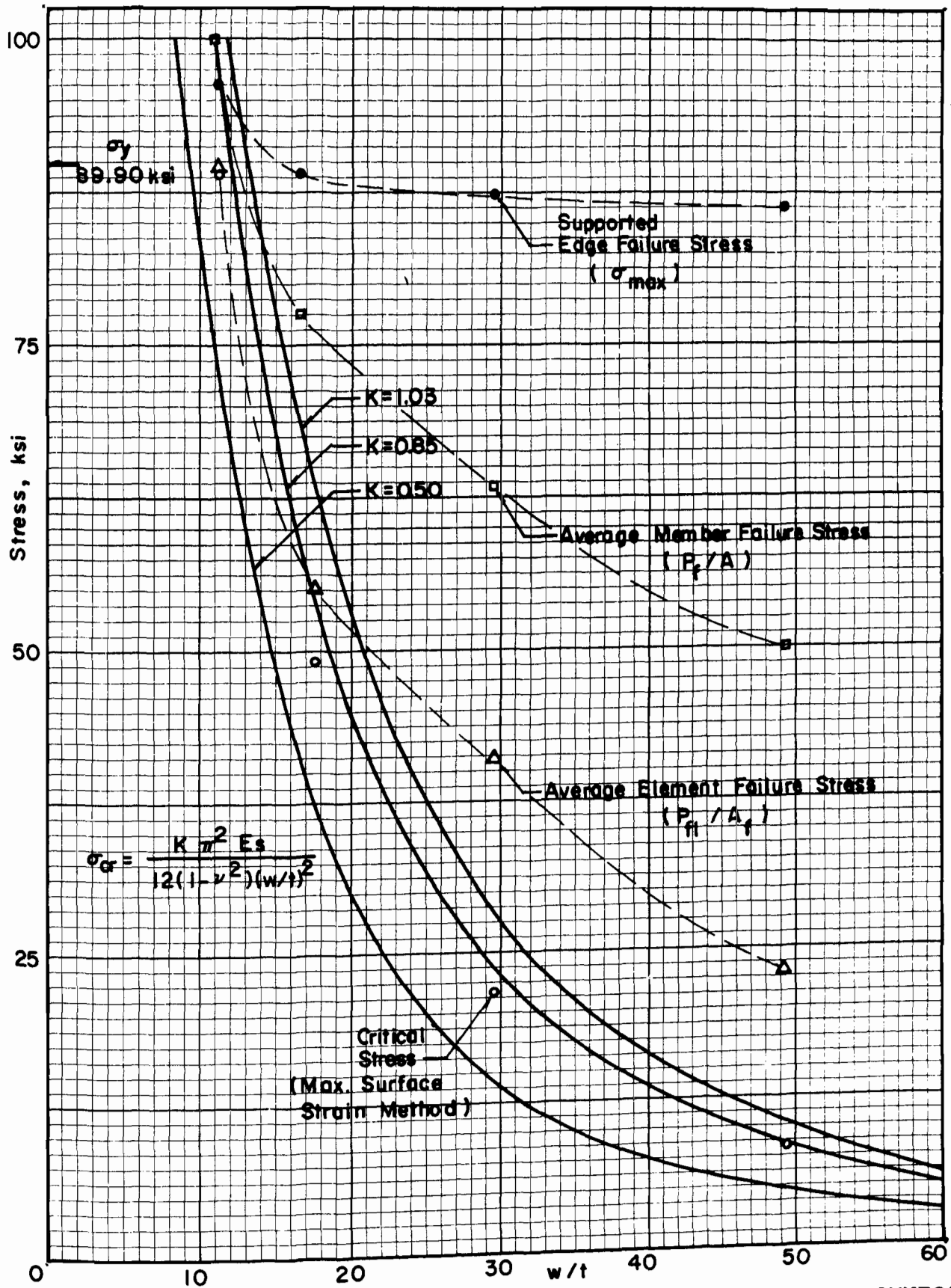

Fig. 3-3 CRITICAL AND FAILURE STRESSES VS. WIDTH TO THICKNESS RATIO - UNSTIFFENED ELEMENTS, TYPE 301 STAINLESS STEEL-1/2 HARD

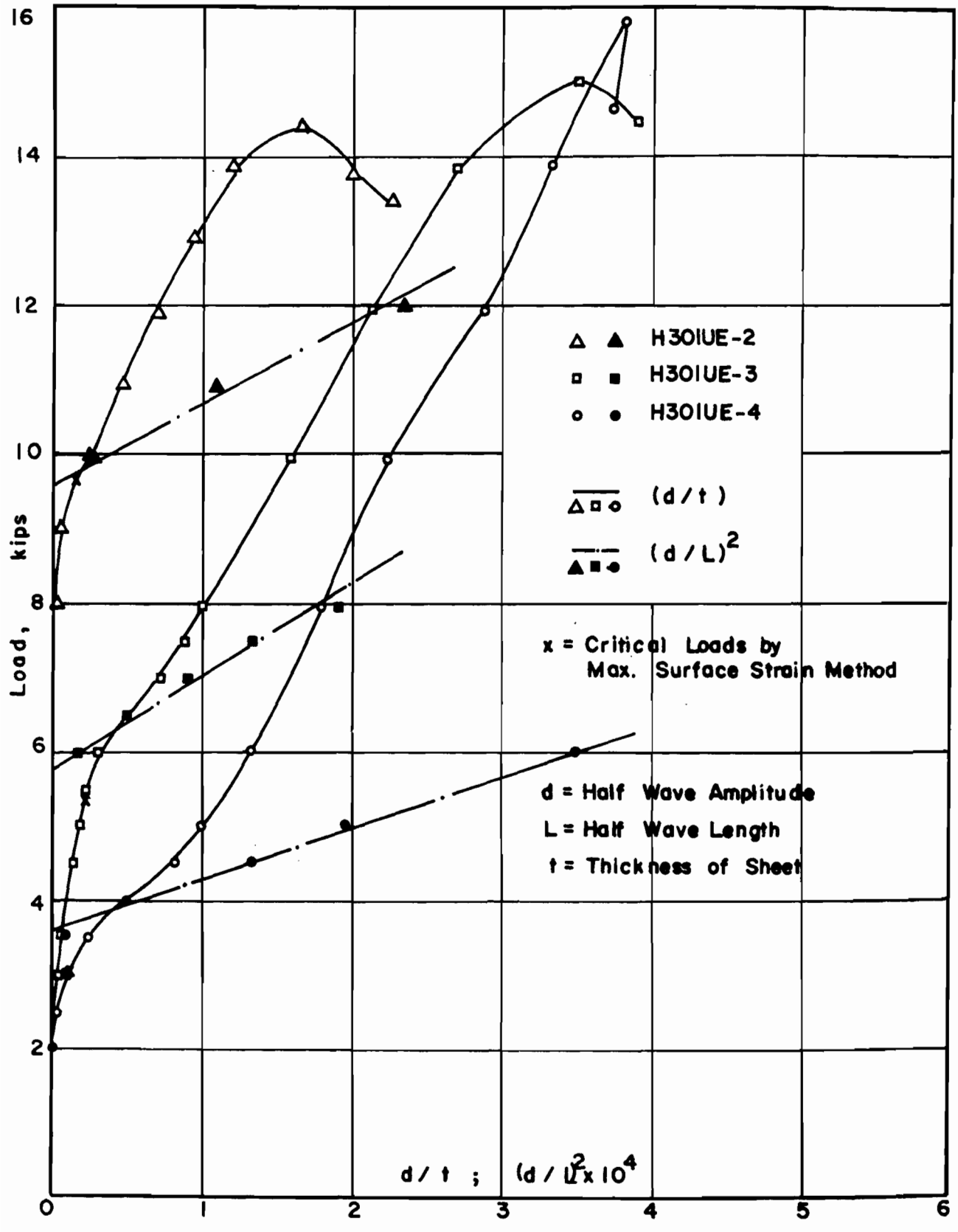

Fig. 3-4 LOAD VS. WAVING AMPLITUDE - SERIES H301UE

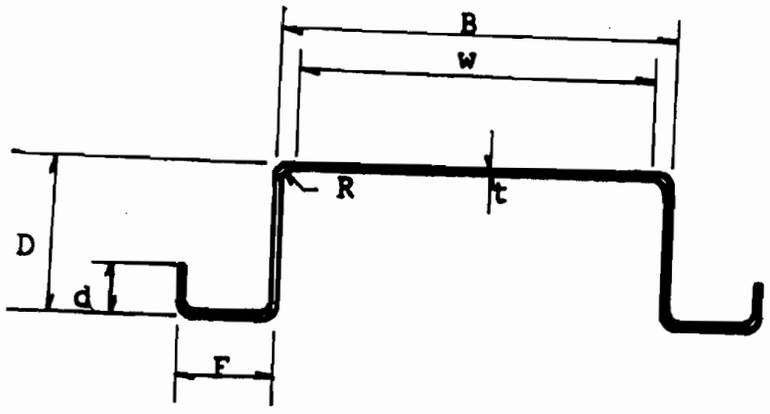

Flexural Specimen Cross-Section

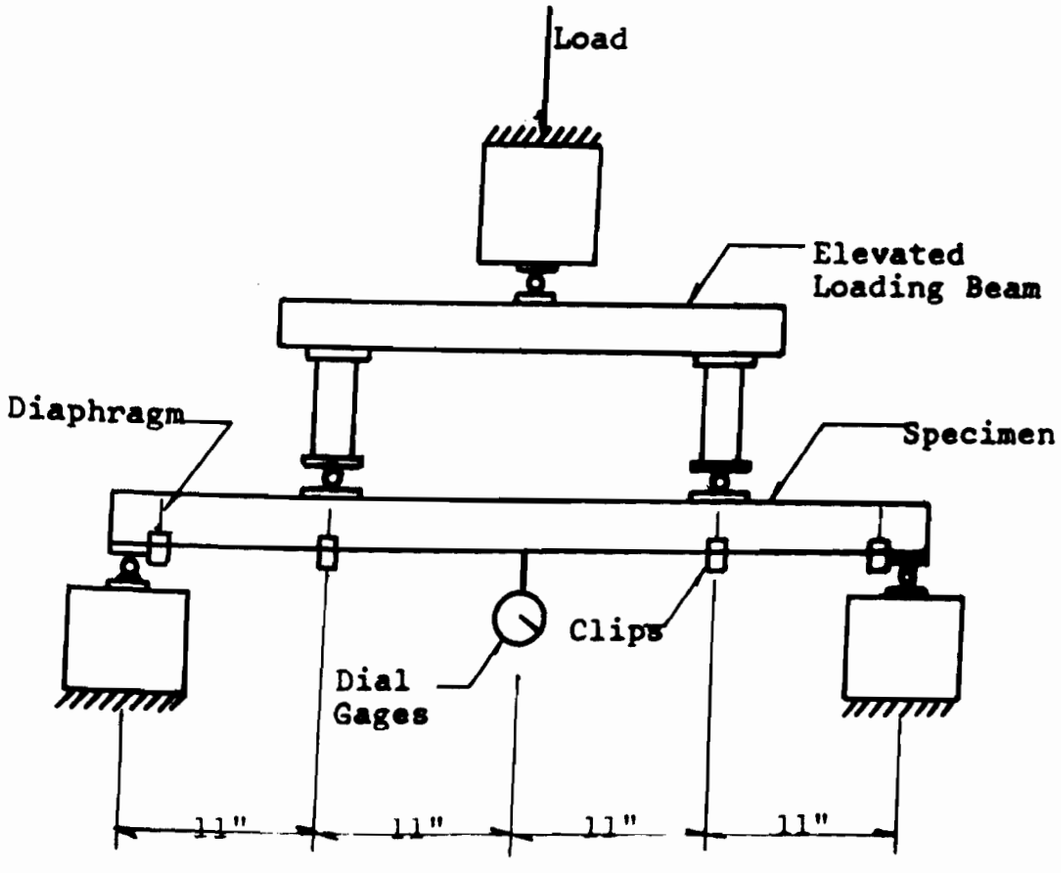

Fig. 3-5 FLEXURAL SPECIMEN LOADING SCHEME AND CROSS SECTION

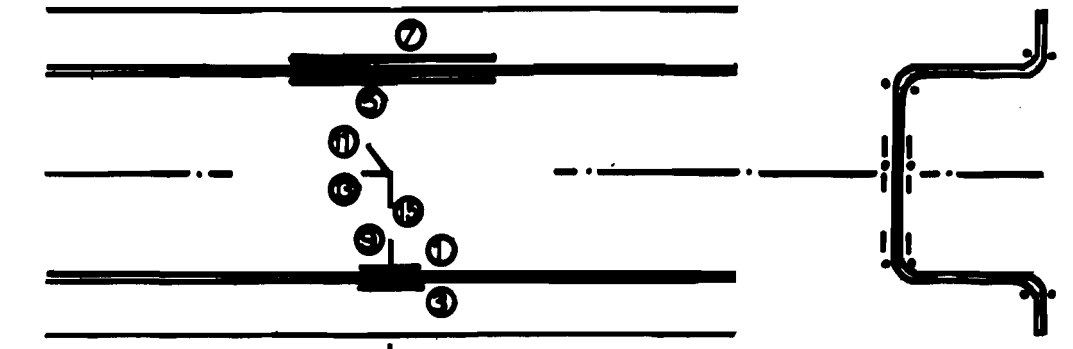

H301F-1

Gages ① - ④ A-12-2
Gages ⑤ - ⑧ A-9-3
Gages ⑨ - ㉕ FAP-12-12

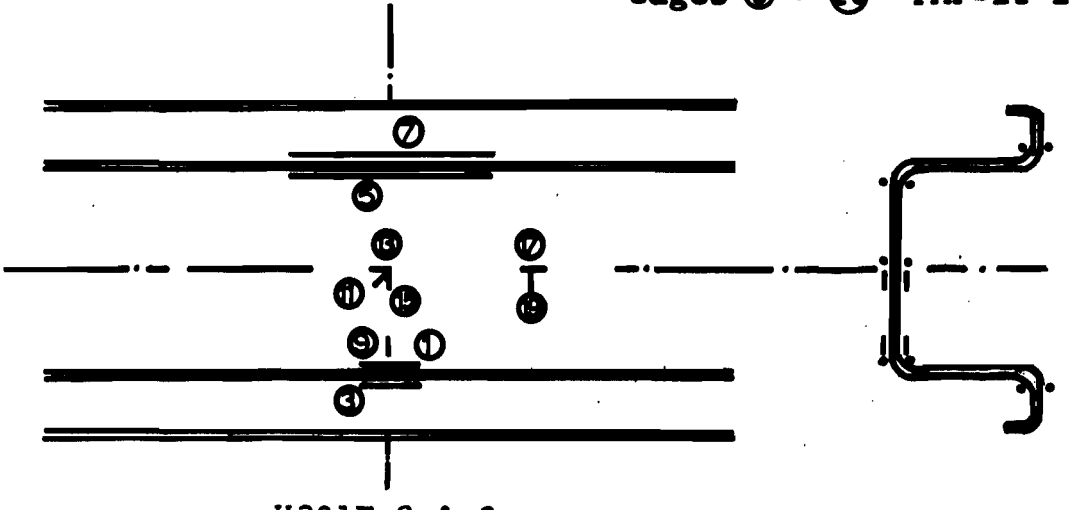

H301F-2 & 3

AS304F-2, 3, & 4(without strain gages 11 & 12)

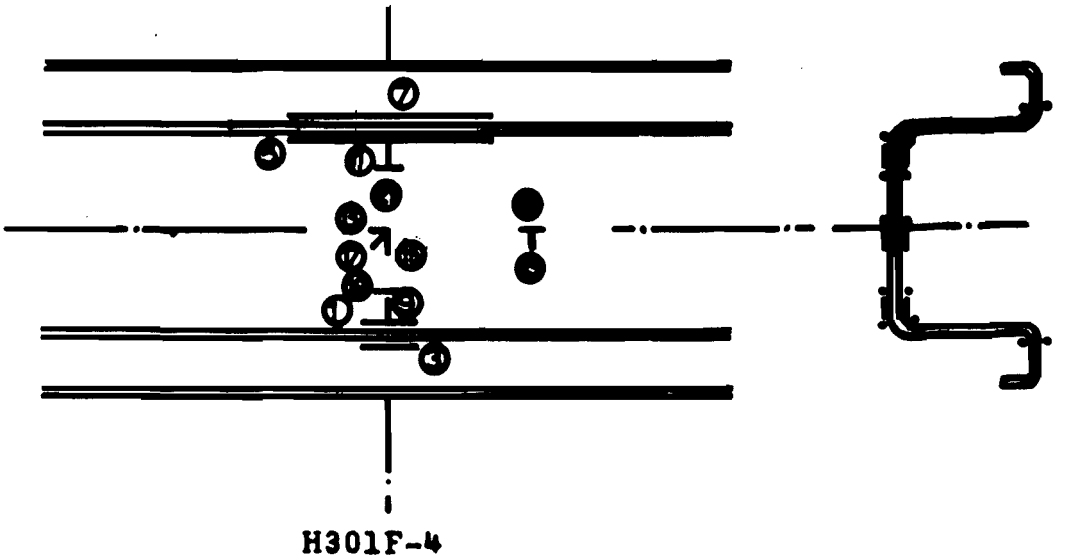

H301F-4

Note: Paired gages on the opposite side are of even numbers and in a consecutive order to the gages shown on the top side.

Fig. 3-6 STRAIN INSTRUMENTATION OF FLEXURAL SPECIMENS

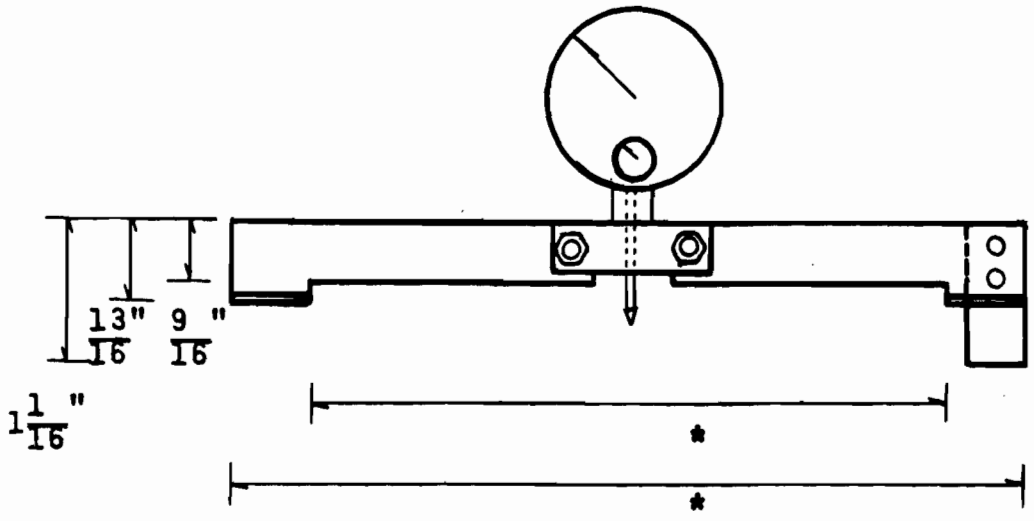

* depending upon the width of flange and $\frac{R}{t}$ ratio for corners

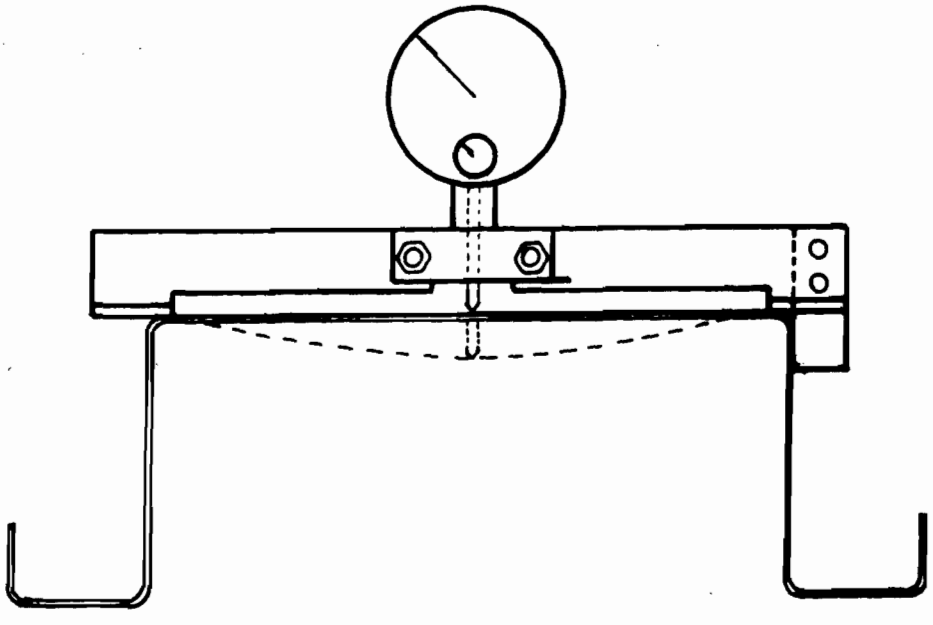

Fig. 3-7 WAVING AMPLITUDE MEASURING DEVICE

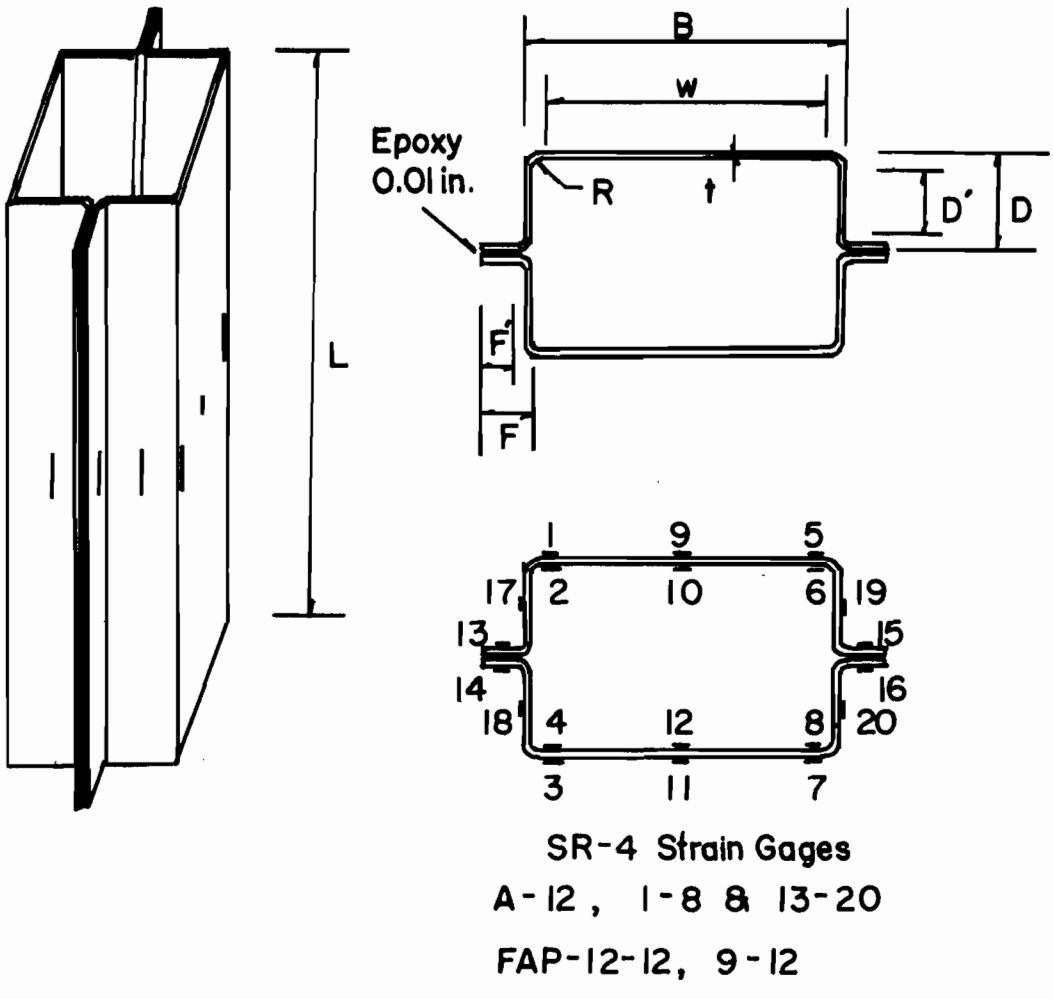

Fig. 3-8 COMPRESSION SPECIMEN CROSS SECTION AND GAGING - STIFFENED ELEMENTS, SERIES H301SC

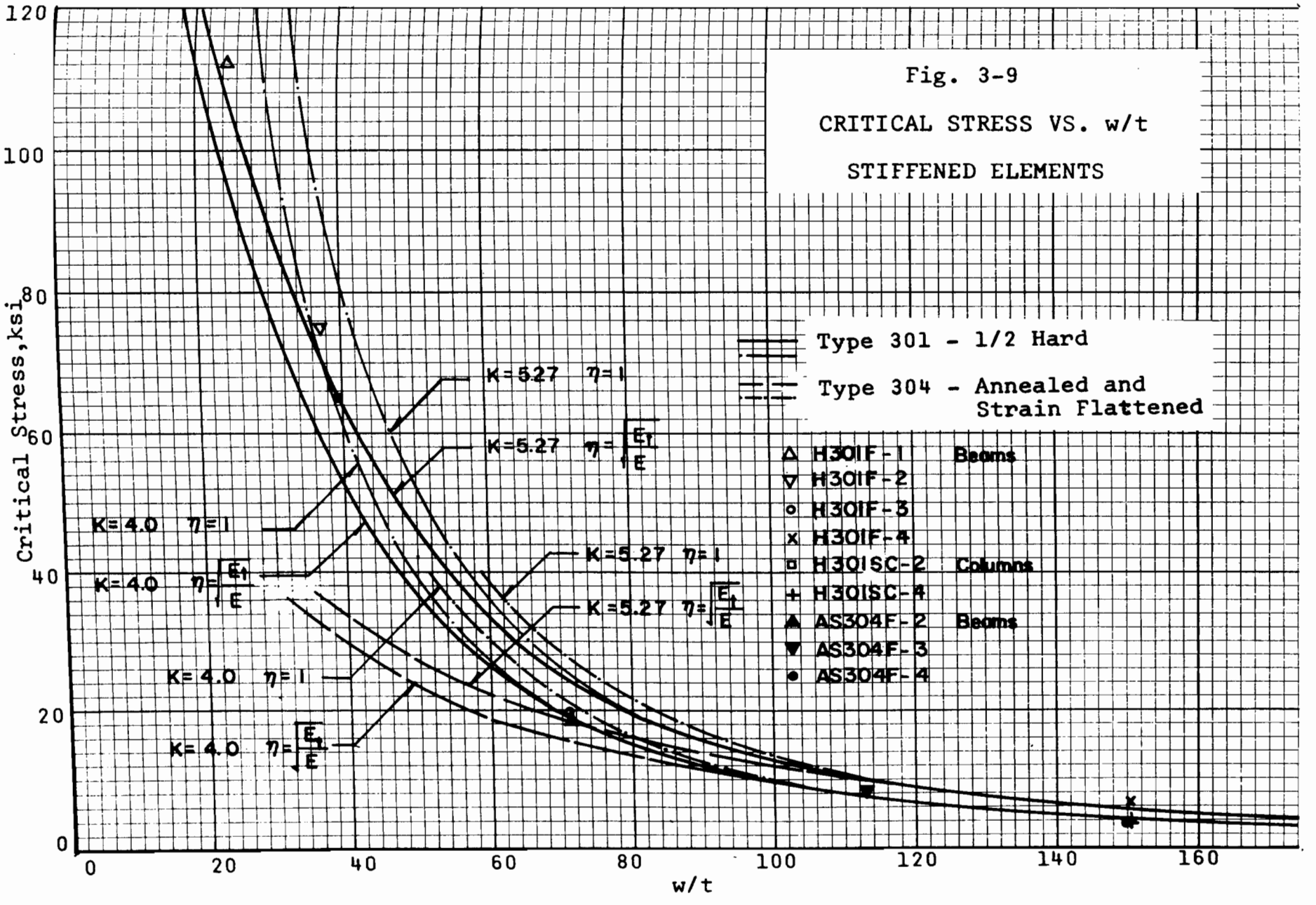
Fig. 3-9
CRITICAL STRESS VS. w/t
STIFFENED ELEMENTS
Type 301 - 1/2 Hard
Type 304 - Annealed and Strain Flattened
H301F-1 Beams
H301F-2
H301F-3
H301F-4
H301SC-2 Columns
H301SC-4
AS304F-2 Beams
AS304F-3
AS304F-4
K=5.27 η=1
K=5.27 η=√(Et/E)
K=4.0 η=1
K=4.0 η=√(Et/E)
K=5.27 η=1
K=5.27 η=√(Et/E)
K=4.0 η=1
K=4.0 η=√(Et/E)
Critical Stress, ksi
w/t
0
20
40
60
80
100
120
140
160

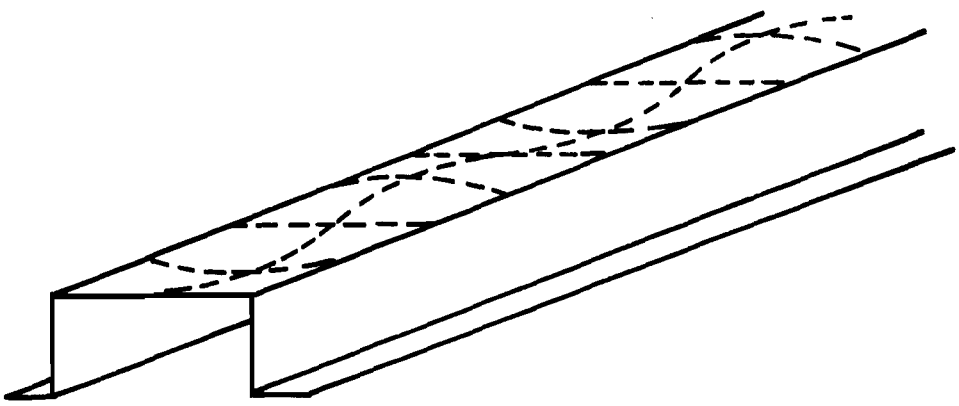

Flexural Member

with Stiffened Compression Flange

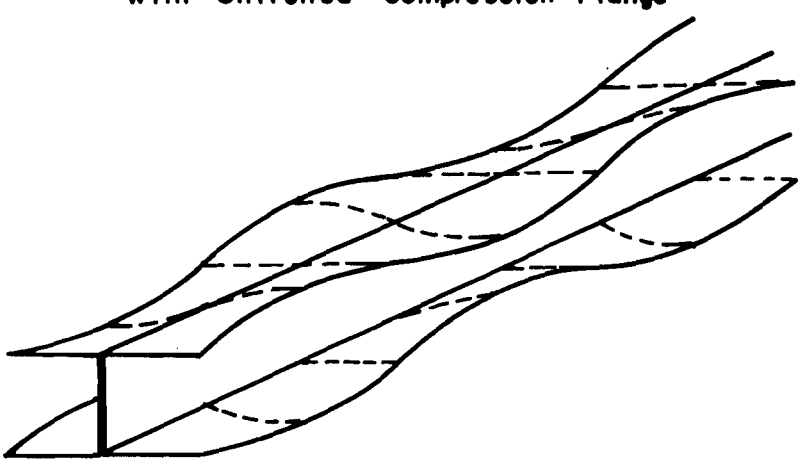

Compression Member

with Unstiffened Flanges

Fig. 4-1 BUCKLED STIFFENED AND UNSTIFFENED ELEMENTS IN STRUCTURAL MEMBERS

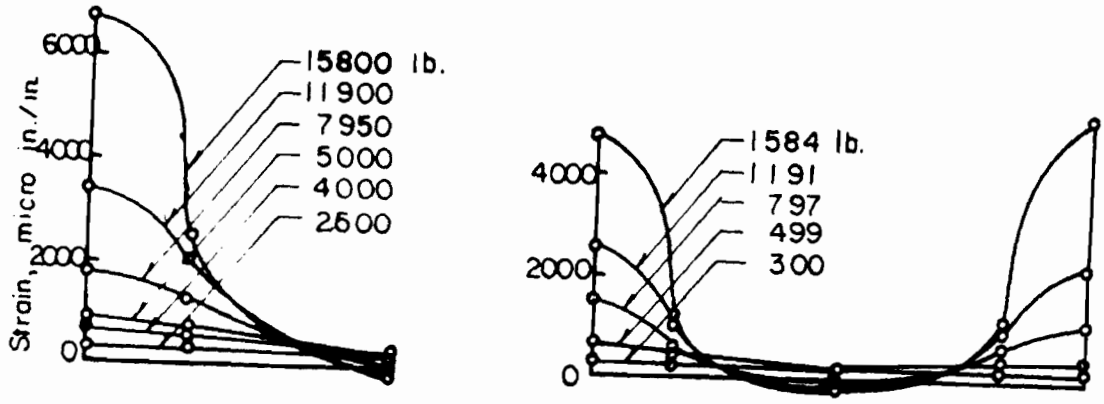

(a) Membrane Strain Distribution

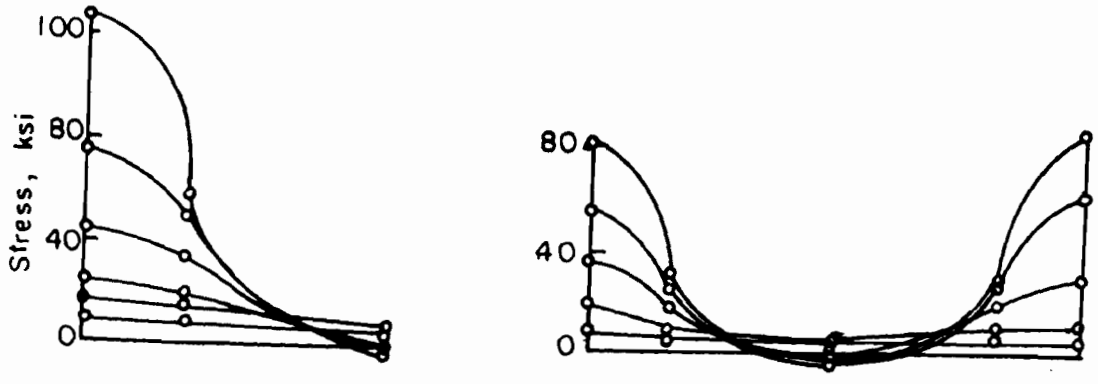

(b) Membrane Stress Distribution

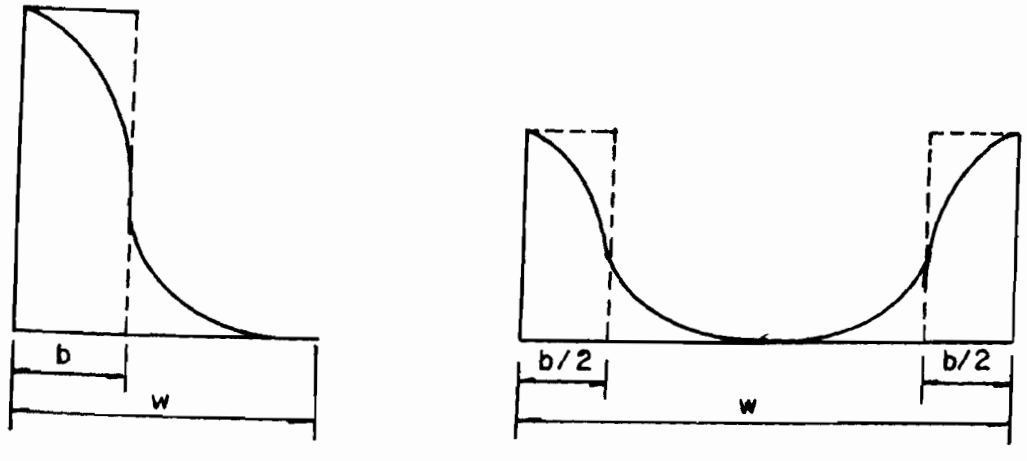

(c) Effective Width Distribution

Unstiffened Element H301UE-4

Stiffened Element H301F-4

Fig. 4-2 POST BUCKLING BEHAVIOR AND EFFECTIVE WIDTH CONCEPT - STIFFENED AND UNSTIFFENED ELEMENTS

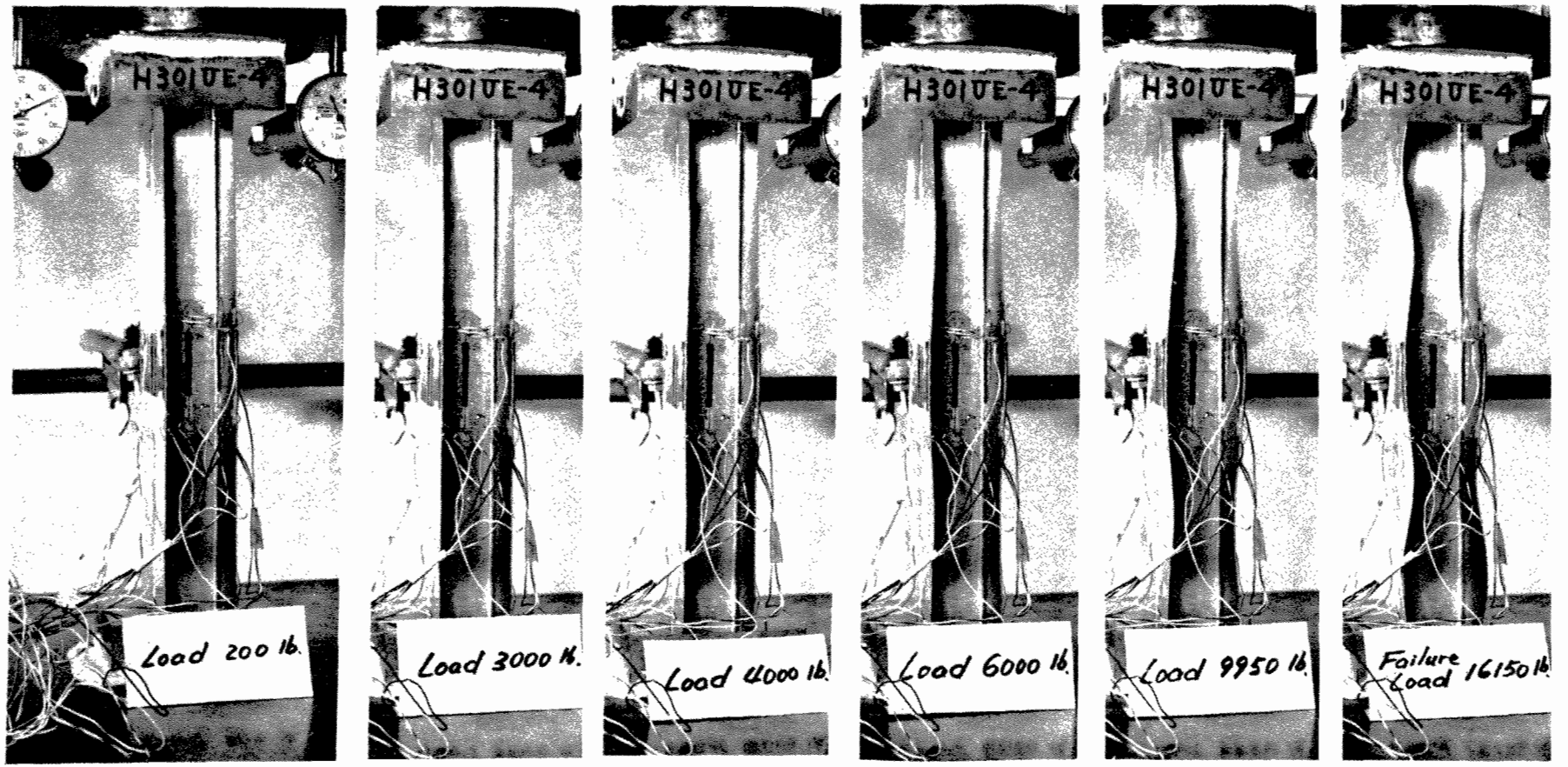

Setting Load | Critical Load P_{cr} | 1.33 P_{cr} | 2.00 P_{cr} | 3.32 P_{cr} | Failure Load 5.38 P_{cr}

Fig. 4-3 UNSTIFFENED ELEMENTS - H301UE-4

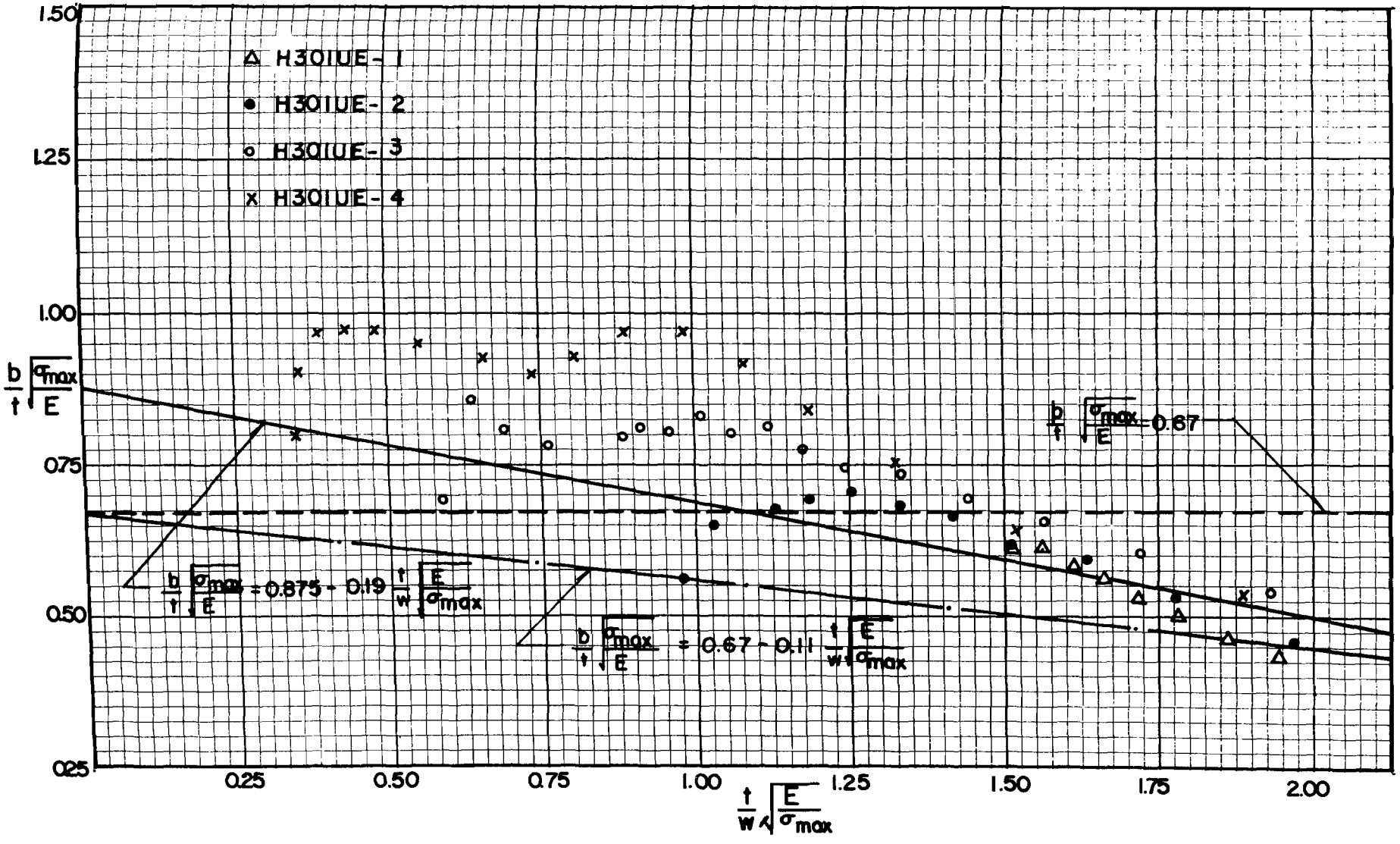

Fig. 4-4 EFFECTIVE WIDTHS OF UNSTIFFENED ELEMENTS - ELASTIC PARAMETERS, SERIES H301UE

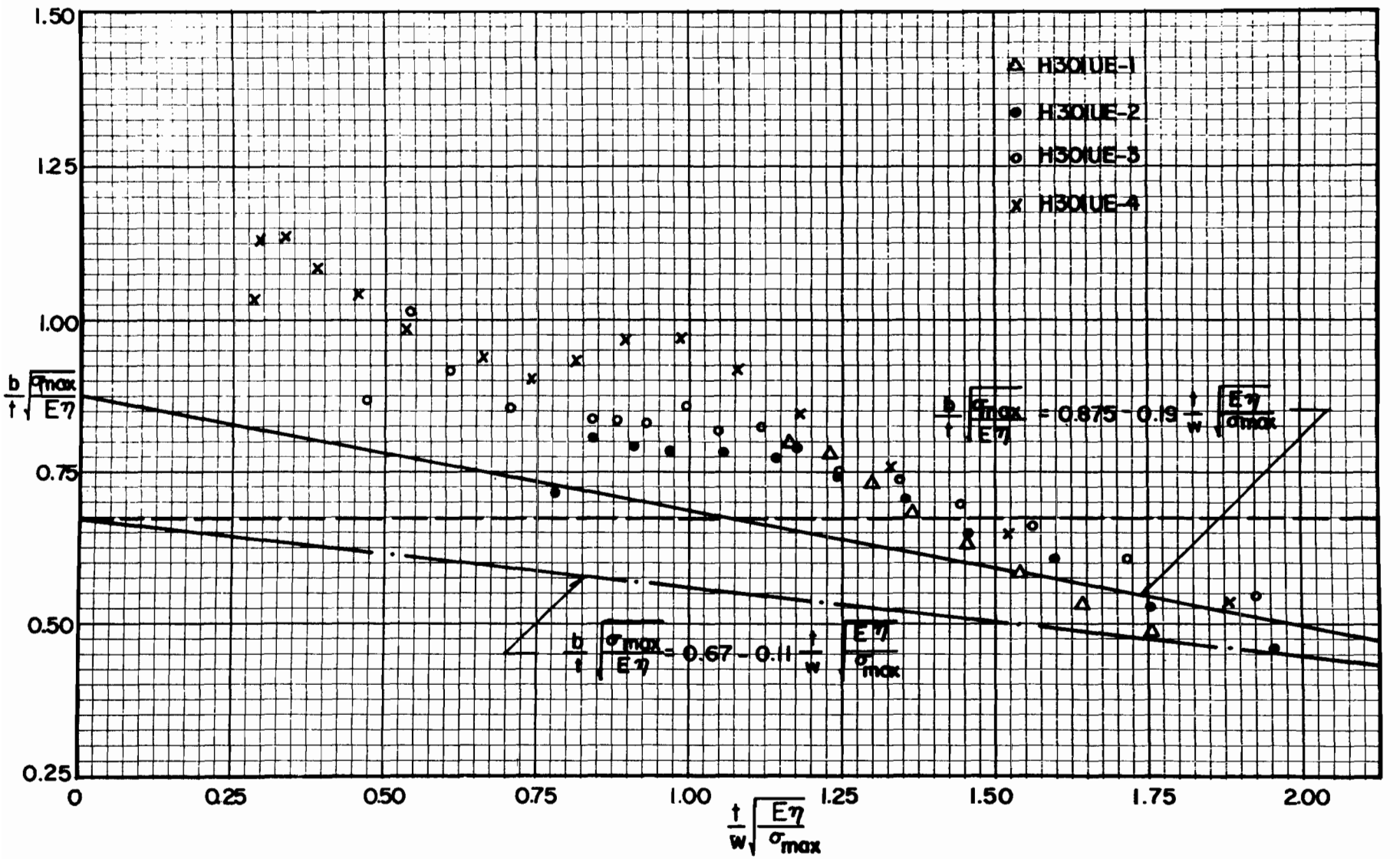

Fig. 4-5 EFFECTIVE WIDTHS OF UNSTIFFENED ELEMENTS - INELASTIC PARAMETERS, SERIES H301UE

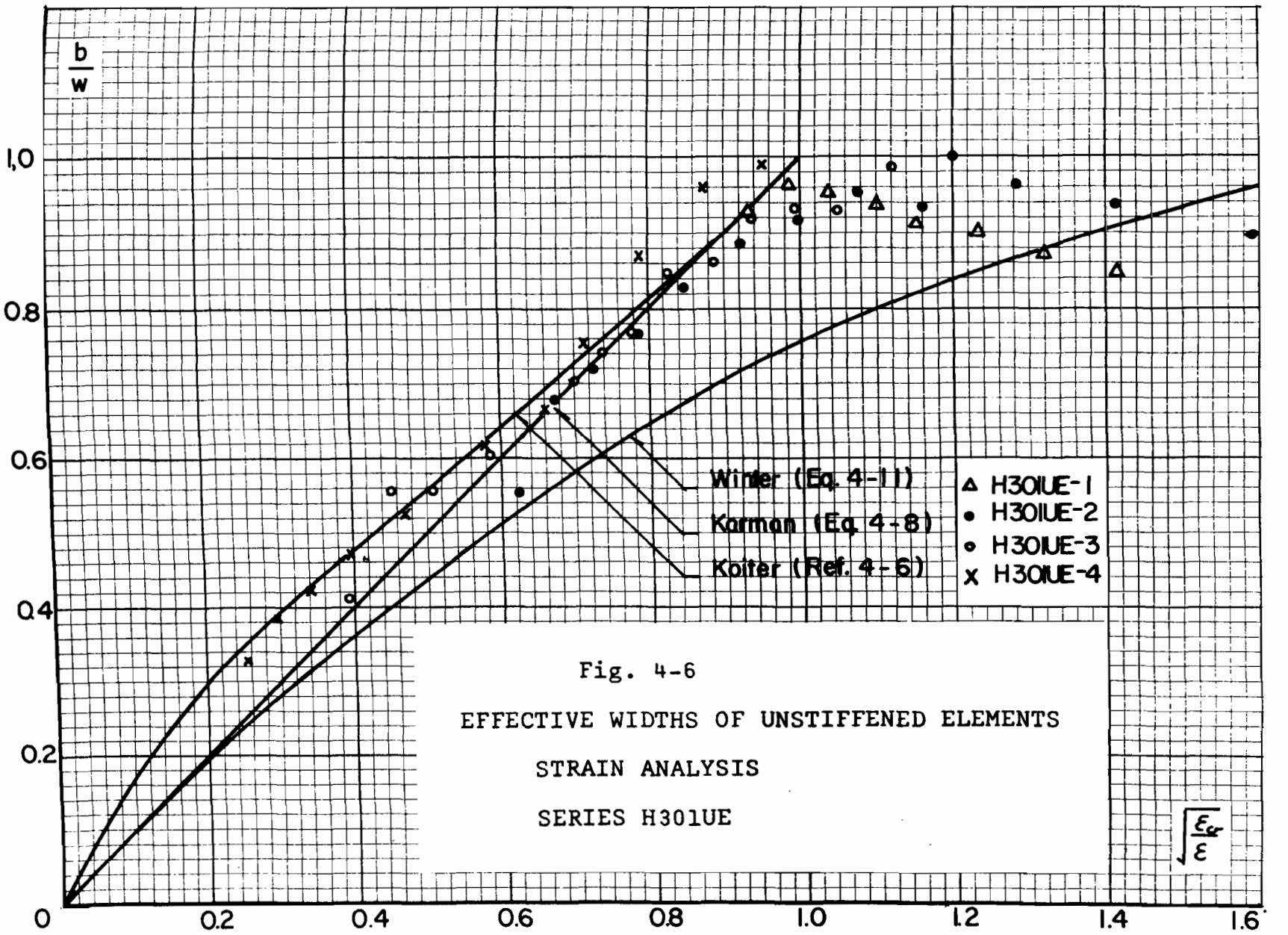

Fig. 4-6

EFFECTIVE WIDTHS OF UNSTIFFENED ELEMENTS

STRAIN ANALYSIS

SERIES H301UE

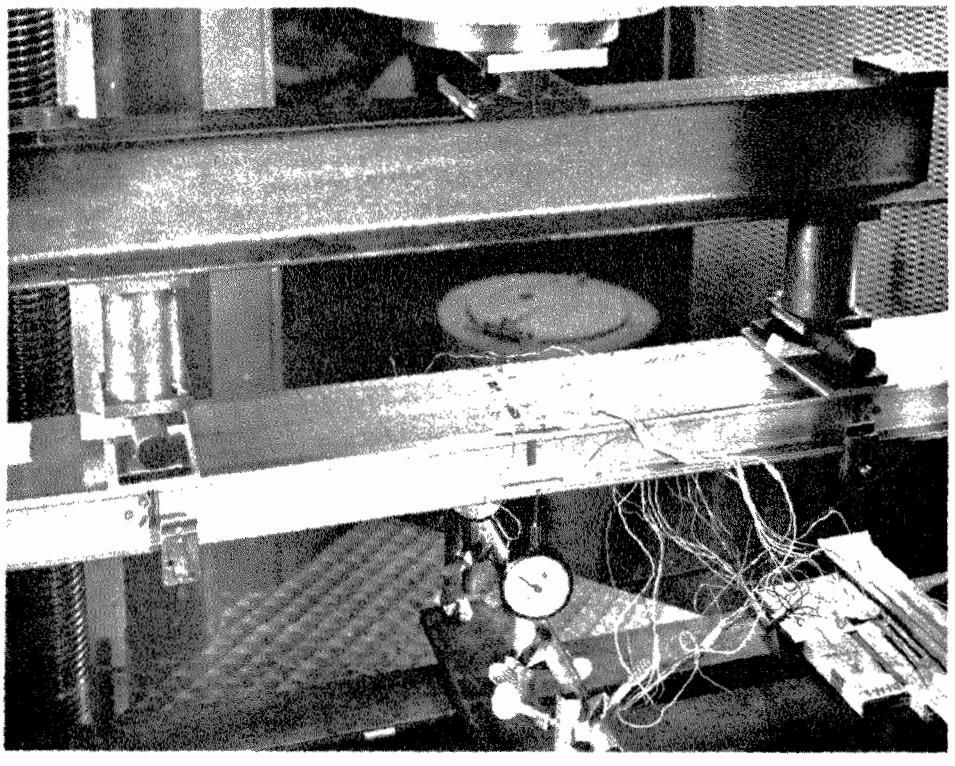

Fig. 4-7a FLEXURAL SPECIMEN H301F-4 AT LOAD=35 lb.

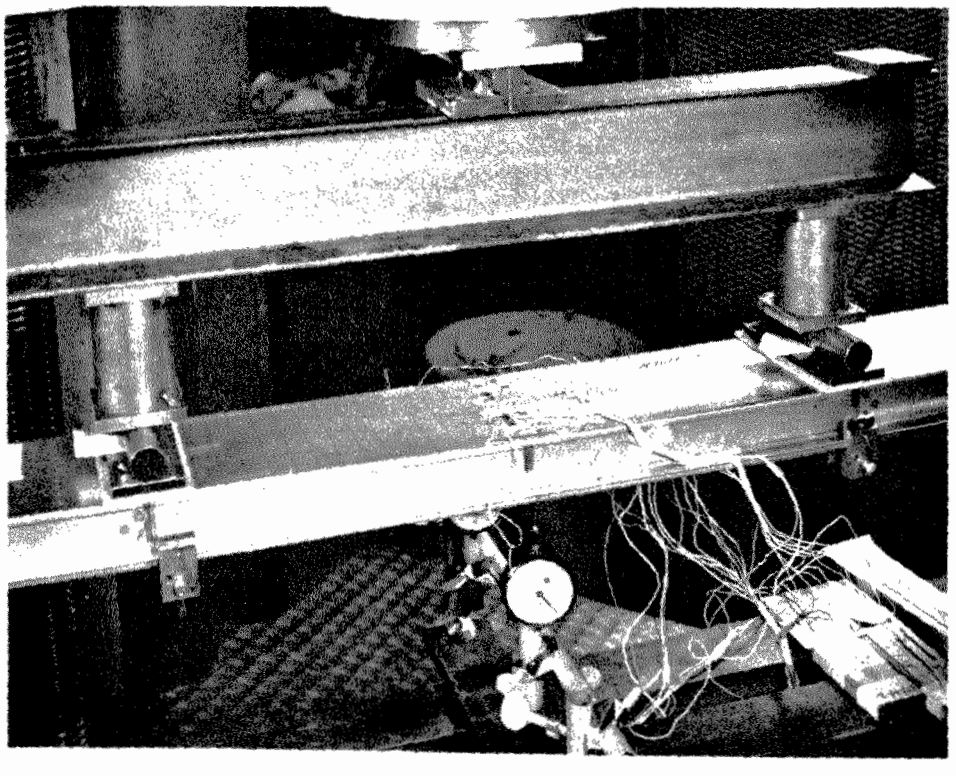

Fig. 4-7b FLEXURAL SPECIMEN H301F-4 AT LOAD=300 lb., 3/4 P_{cr}

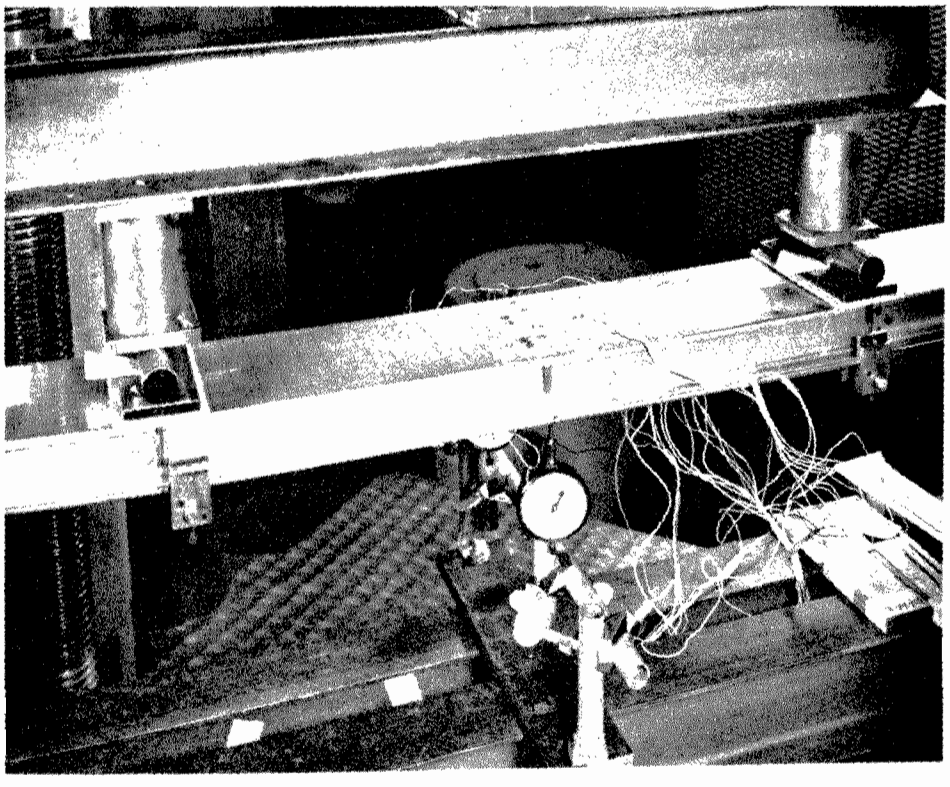

Fig. 4-7c FLEXURAL SPECIMEN H301F-4 AT LOAD=797 lb., $2P_{cr}$

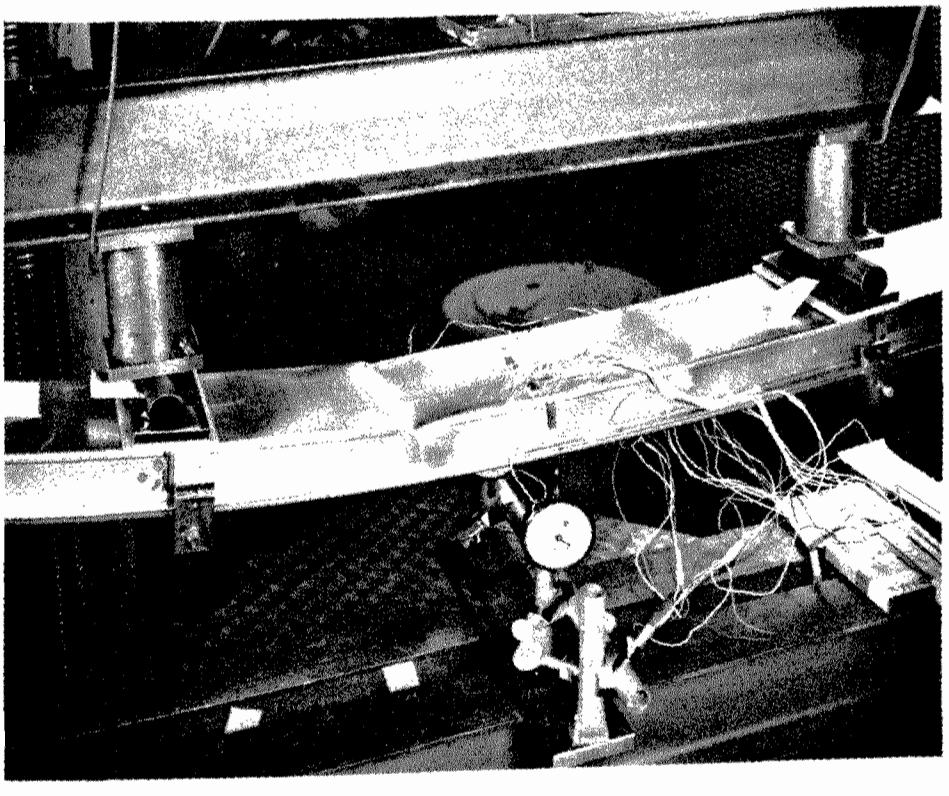

Fig. 4-7d FLEXURAL SPECIMEN H301F-4 AT FAILURE LOAD =1709 lb., 4.30 P_{cr}

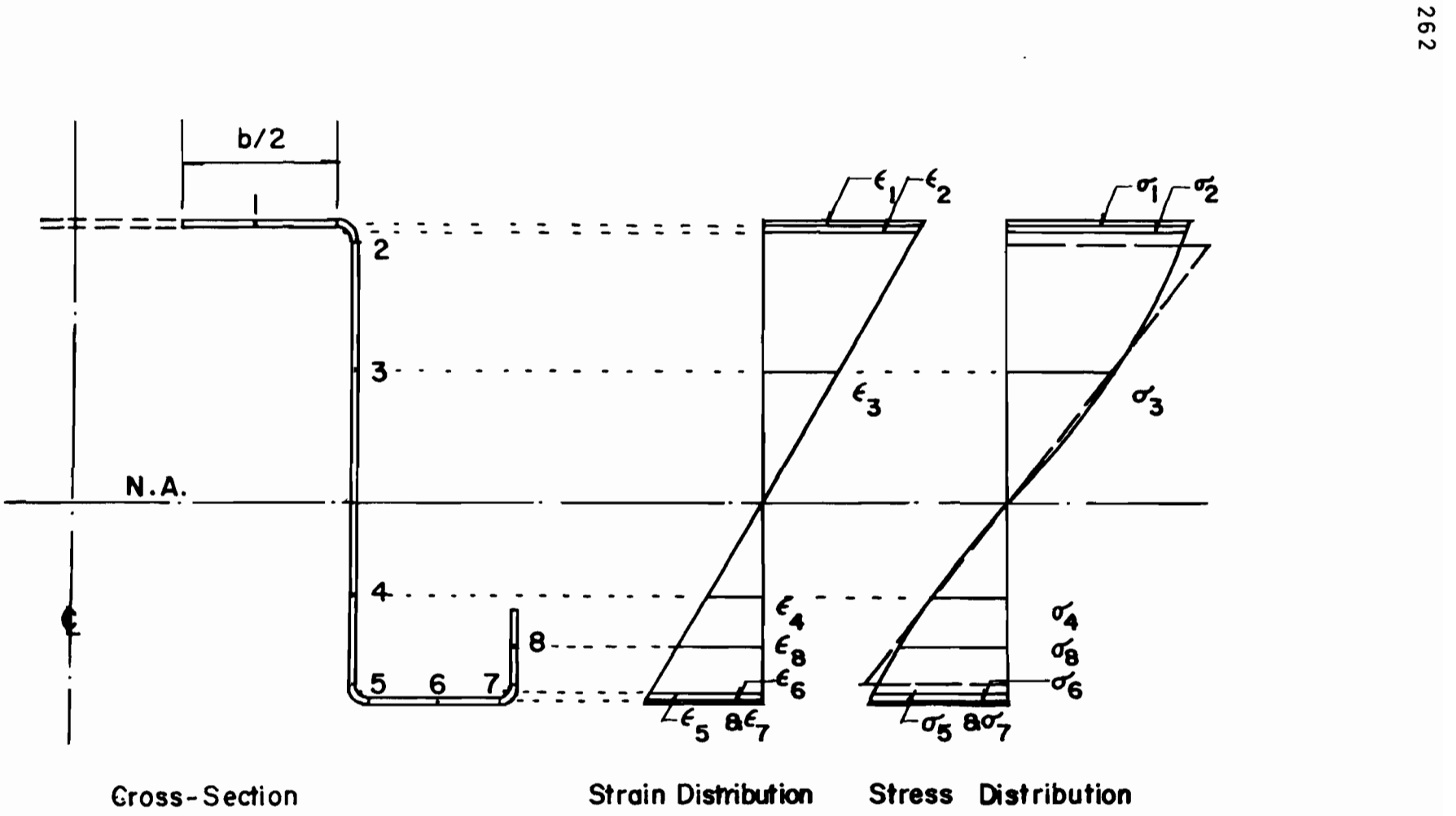

Fig. 4-8 STRAIN AND STRESS DISTRIBUTIONS

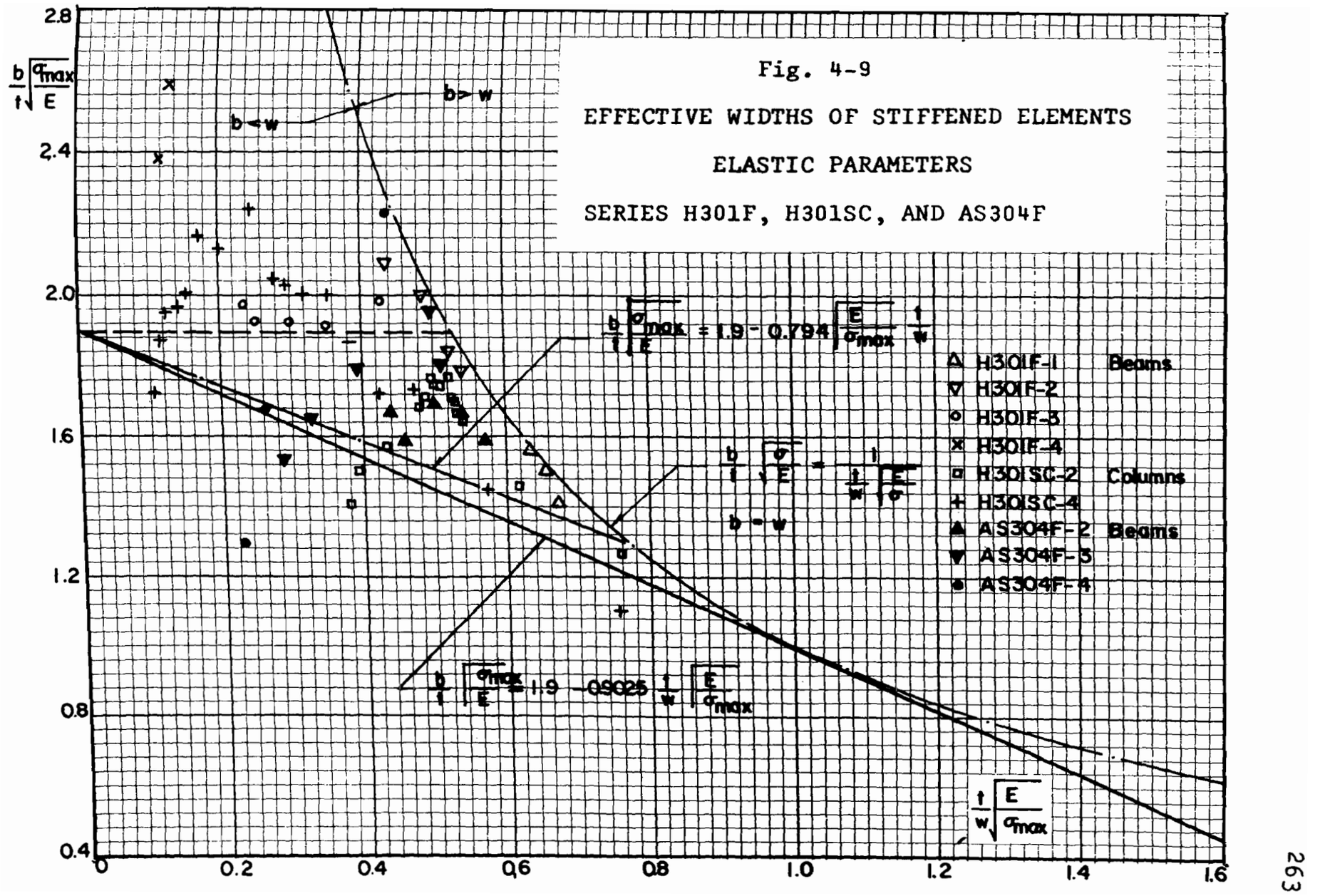
Fig. 4-9
EFFECTIVE WIDTHS OF STIFFENED ELEMENTS
ELASTIC PARAMETERS
SERIES H301F, H301SC, AND AS304F
b/t √(σmax/E)
2.8
2.4
2.0
1.6
1.2
0.8
0.4
0
0.2
0.4
0.6
0.8
1.0
1.2
1.4
1.6
b > w
b < w
b/t √(σmax/E) = 1.9 - 0.794 √(E/σmax) 1/w
b/t √(σ/E) = 1/(1/w √(E/σ))
b = w
b/t √(σmax/E) = 1.9 - 0.9025 1/w √(E/σmax)
1/w √(E/σmax)
H301F-1 Beams
H301F-2
H301F-3
H301F-4
H301SC-2 Columns
H301SC-4
AS304F-2 Beams
AS304F-3
AS304F-4

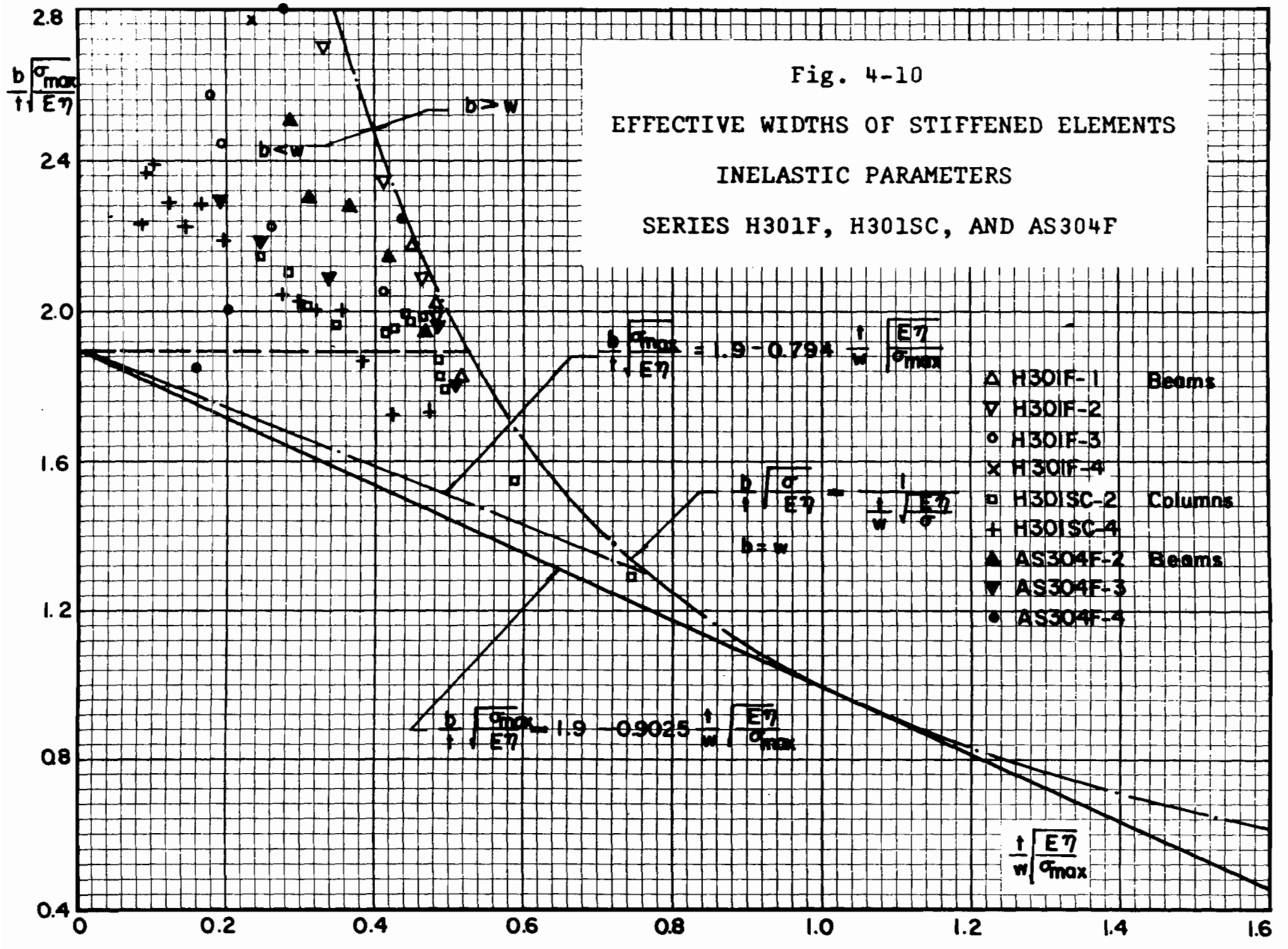
Fig. 4-10
EFFECTIVE WIDTHS OF STIFFENED ELEMENTS
INELASTIC PARAMETERS
SERIES H301F, H301SC, AND AS304F
b/t √(σmax/Eη)
t/w √(Eη/σmax)
b>w
b<w
b=w
b/t √(σmax/Eη) = 1.9 - 0.79 t/w √(Eη/σmax)
b/t √(σ/Eη) = t/w √(Eη/σ)
b/t √(σmax/Eη) = 1.9 - 0.9025 t/w √(Eη/σmax)
H301F-1 Beams
H301F-2
H301F-3
H301F-4
H301SC-2 Columns
H301SC-4
AS304F-2 Beams
AS304F-3
AS304F-4
2.8
2.4
2.0
1.6
1.2
0.8
0.4
0
0.2
0.4
0.6
0.8
1.0
1.2
1.4
1.6

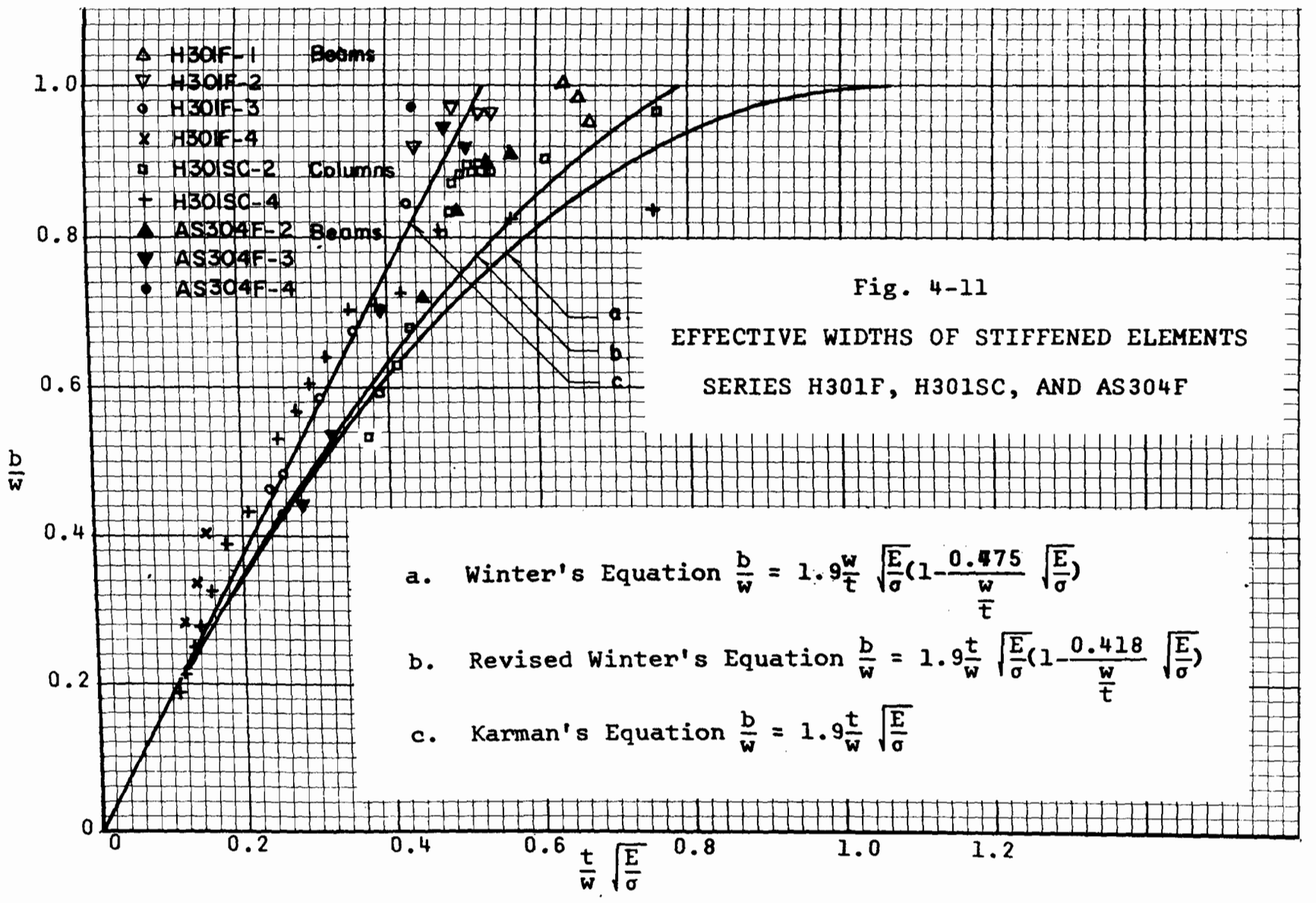

Fig. 4-11

EFFECTIVE WIDTHS OF STIFFENED ELEMENTS

SERIES H301F, H301SC, AND AS304F

a. Winter's Equation $\frac{b}{w} = 1.9\frac{w}{t}\sqrt{\frac{E}{\sigma}}\left(1-\frac{0.475}{\frac{w}{t}}\sqrt{\frac{E}{\sigma}}\right)$

b. Revised Winter's Equation $\frac{b}{w} = 1.9\frac{t}{w}\sqrt{\frac{E}{\sigma}}\left(1-\frac{0.418}{\frac{w}{t}}\sqrt{\frac{E}{\sigma}}\right)$

c. Karman's Equation $\frac{b}{w} = 1.9\frac{t}{w}\sqrt{\frac{E}{\sigma}}$

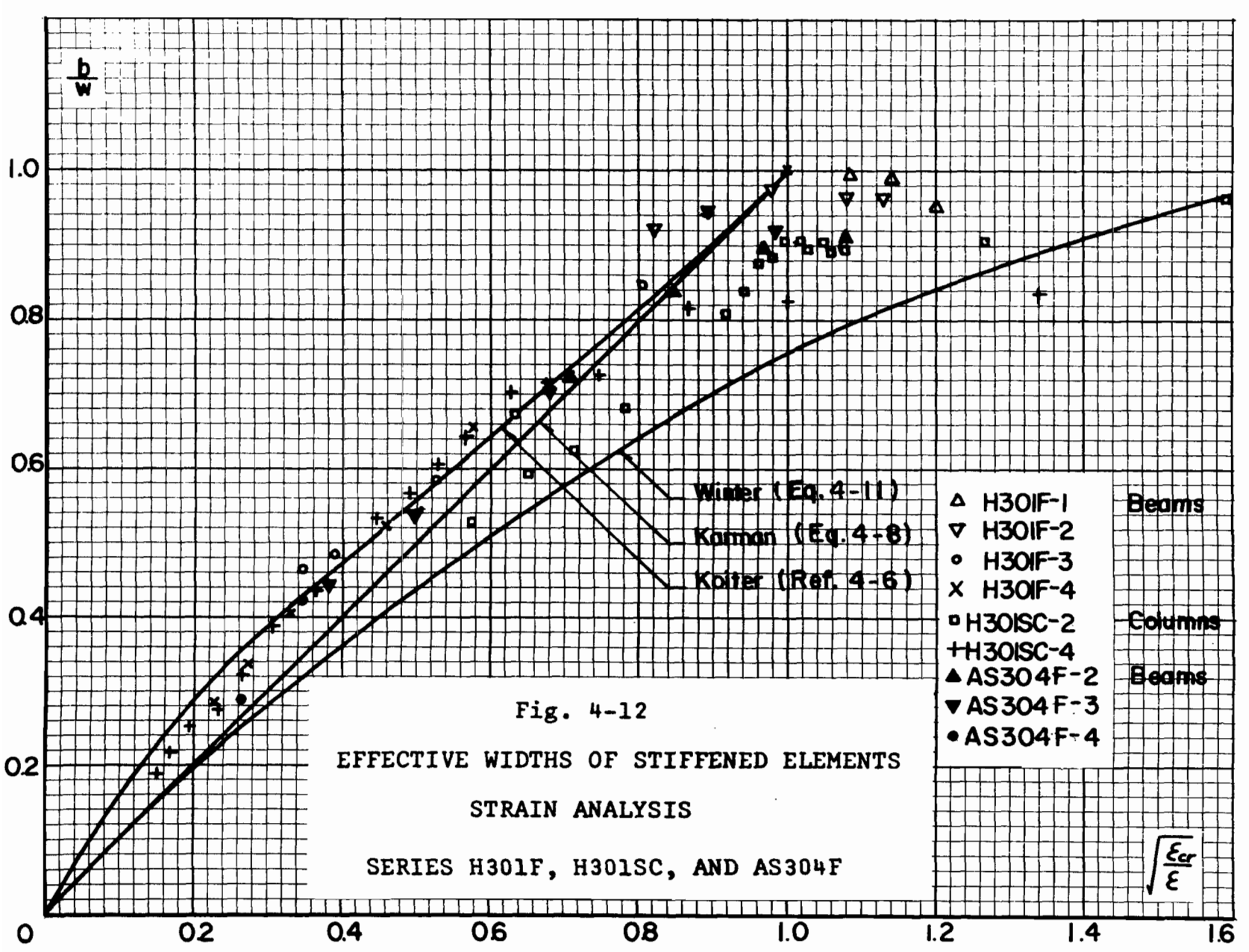

Fig. 4-12

EFFECTIVE WIDTHS OF STIFFENED ELEMENTS

STRAIN ANALYSIS

SERIES H301F, H301SC, AND AS304F

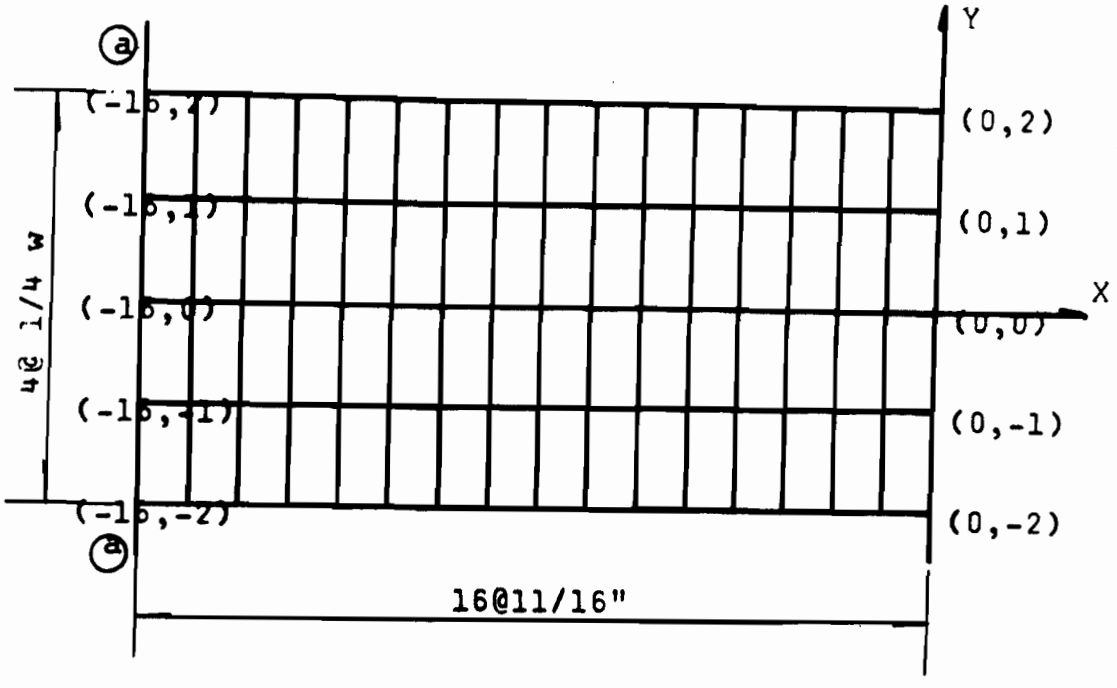

Grids and Nodal Points in Compression Flange

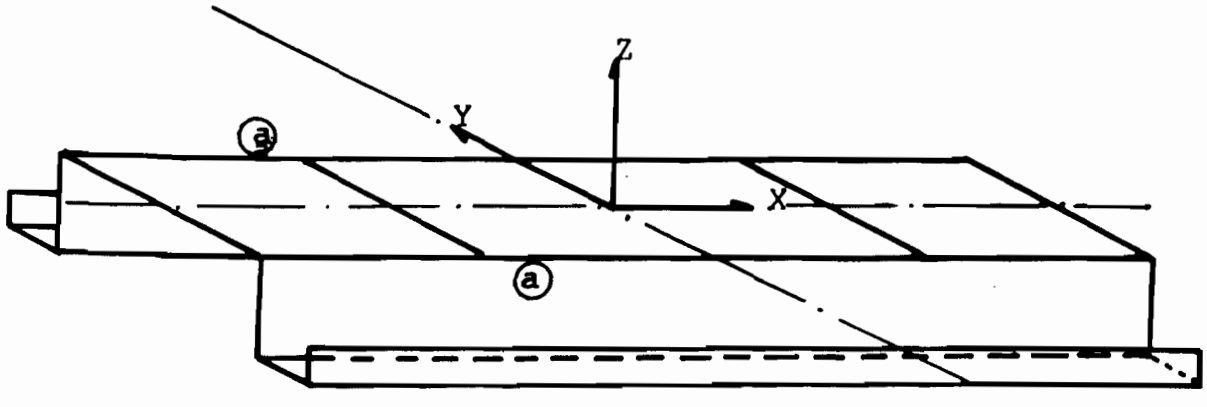

Fig. 4-13 COORDINATE SYSTEM FOR WAVING MEASUREMENTS

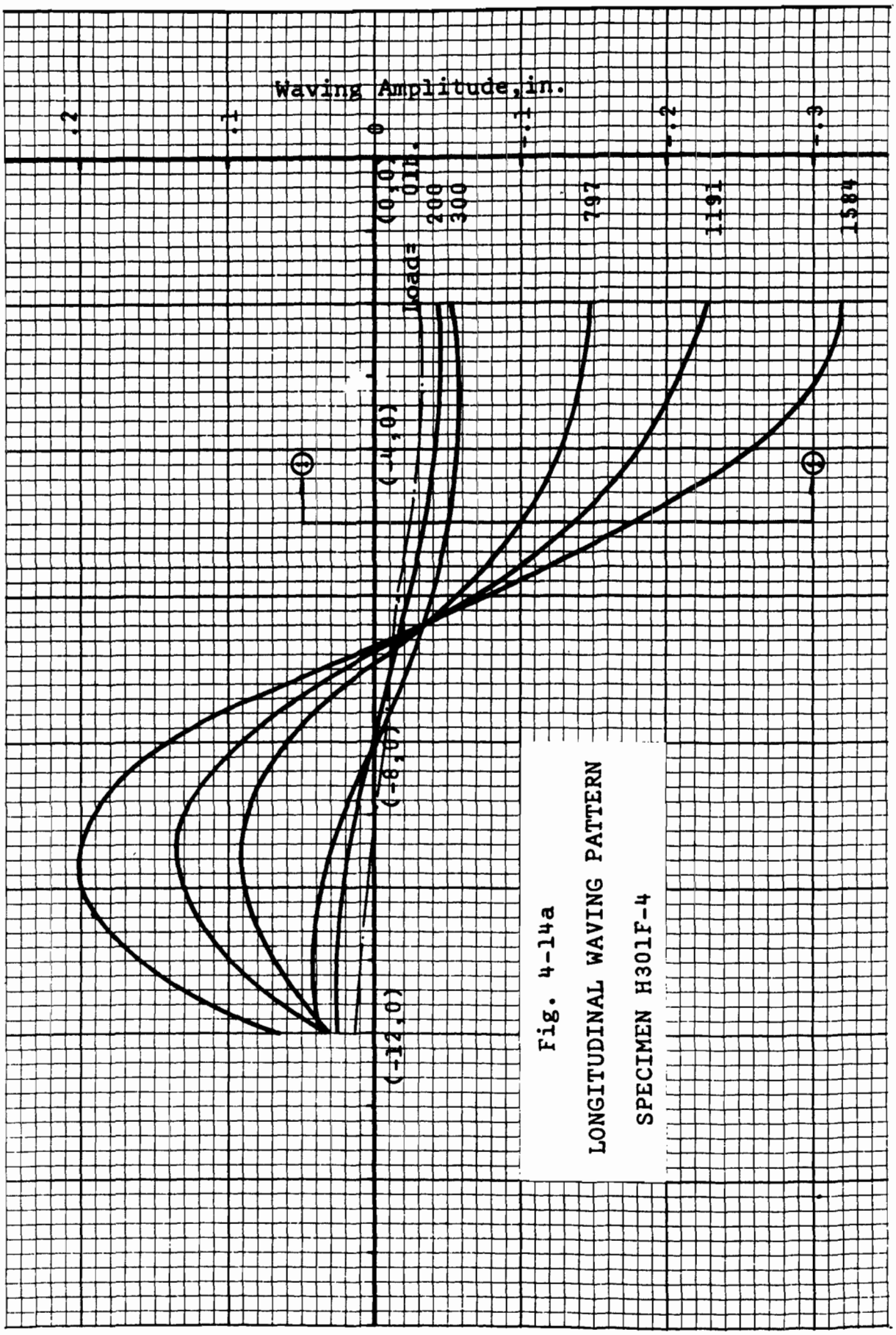

Fig. 4-14a

LONGITUDINAL WAVING PATTERN

SPECIMEN H301F-4

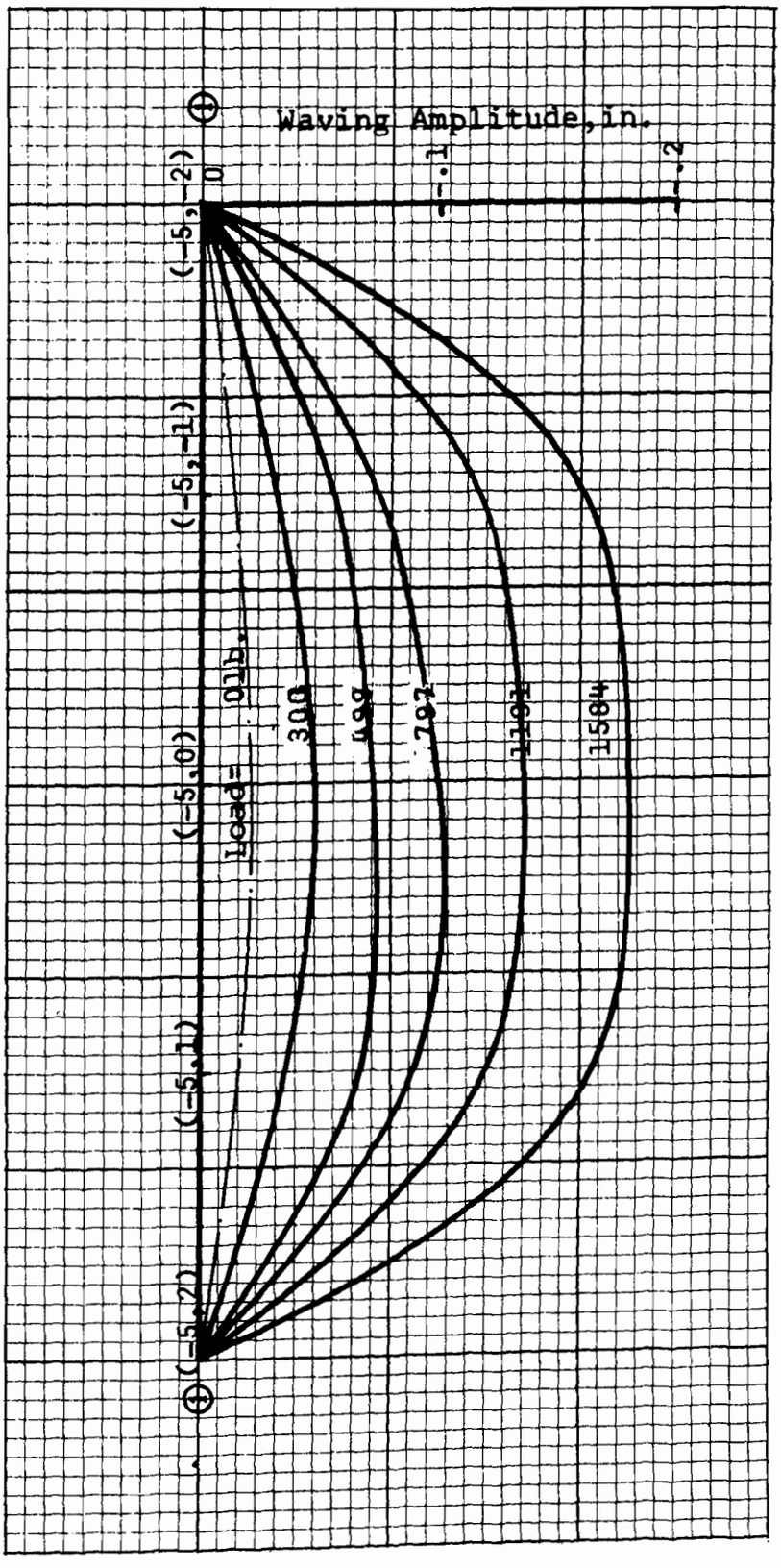

Fig. 4-14b TRANSVERSE WAVING PATTERN (CROSS SECTION ① - ①), SPECIMEN H301F-4

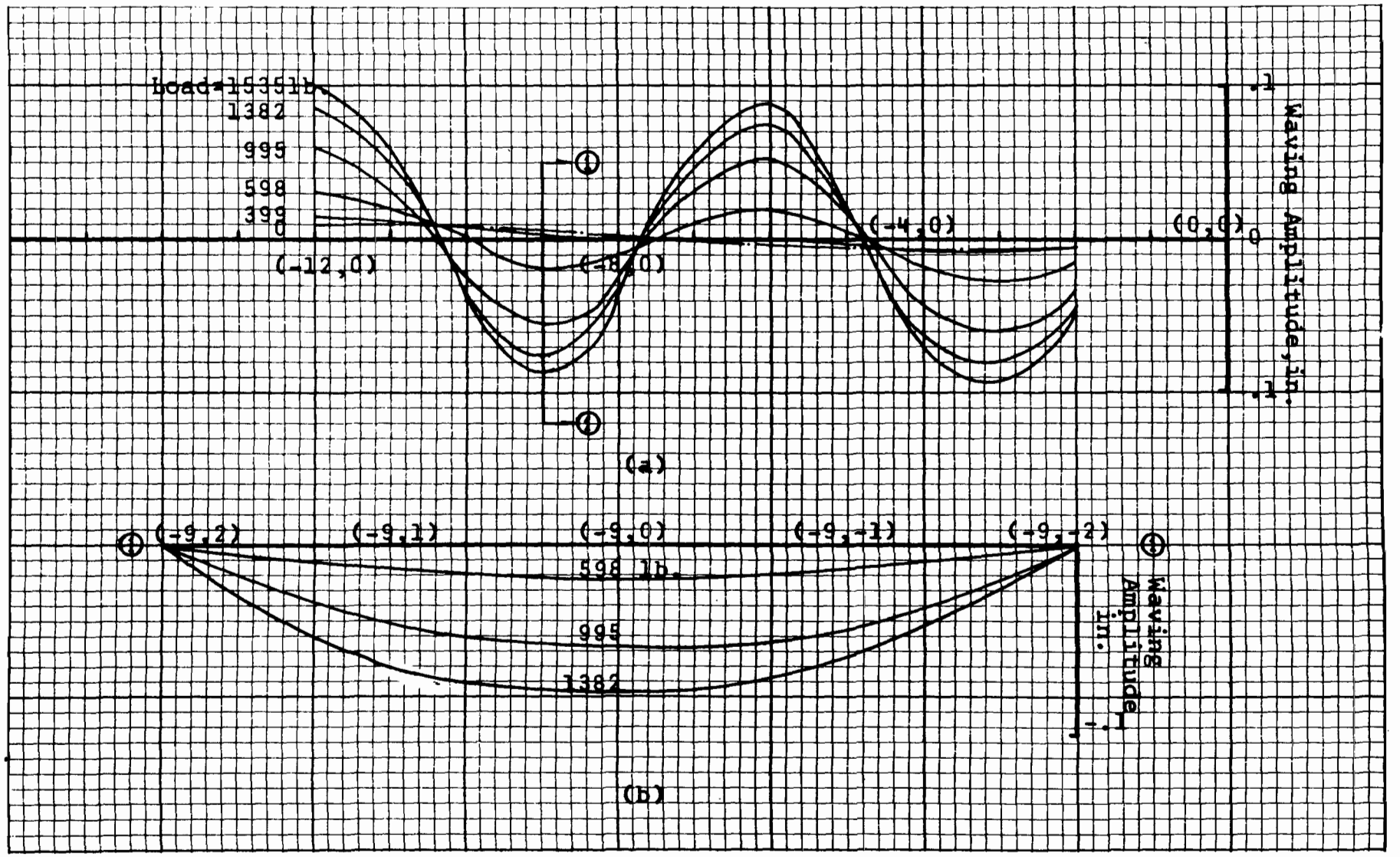

Fig. 4-15a LONGITUDINAL WAVING PATTERN, SPECIMEN H301F-3

Fig. 4-15b TRANSVERSE WAVING PATTERN, SPECIMEN H301F-4 (CROSS SECTION ① - ①)

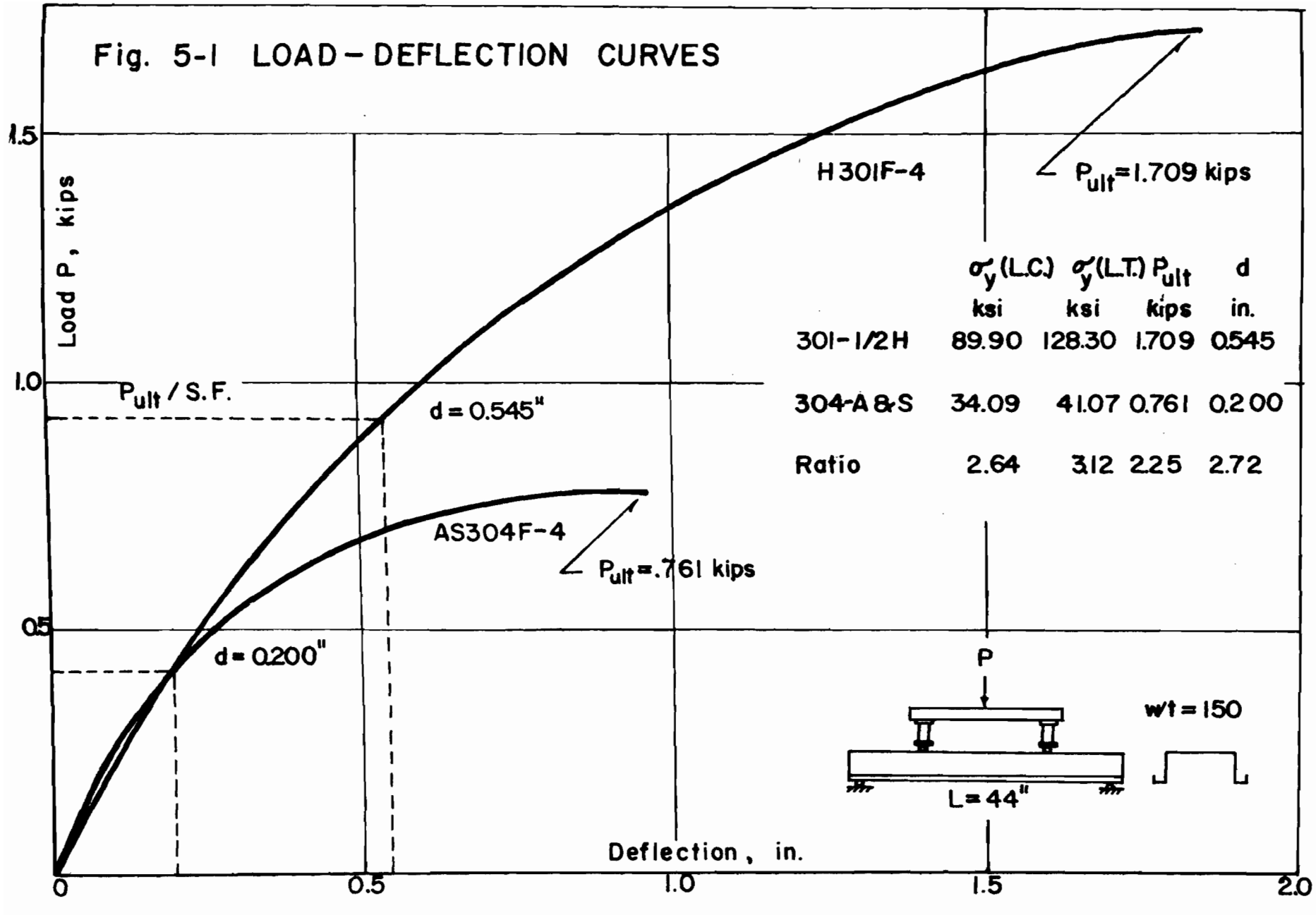

	σ_y (L.C.) ksi	σ_y (L.T.) ksi	P_{ult} kips	d in.
301-1/2H	89.90	128.30	1.709	0.545
304-A 8&S	34.09	41.07	0.761	0.200
Ratio	2.64	3.12	2.25	2.72

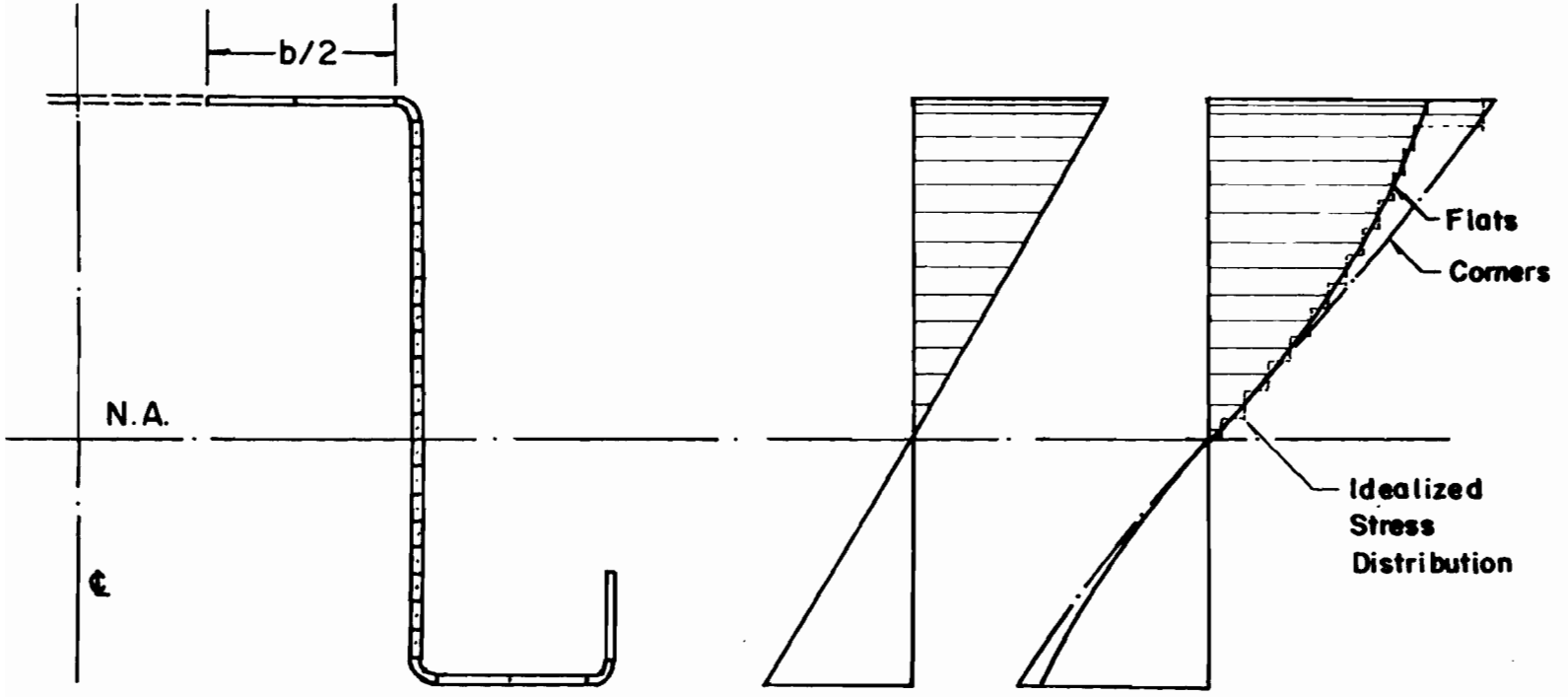

Fig. 5-2 IDEALIZATION OF STRESS DISTRIBUTION

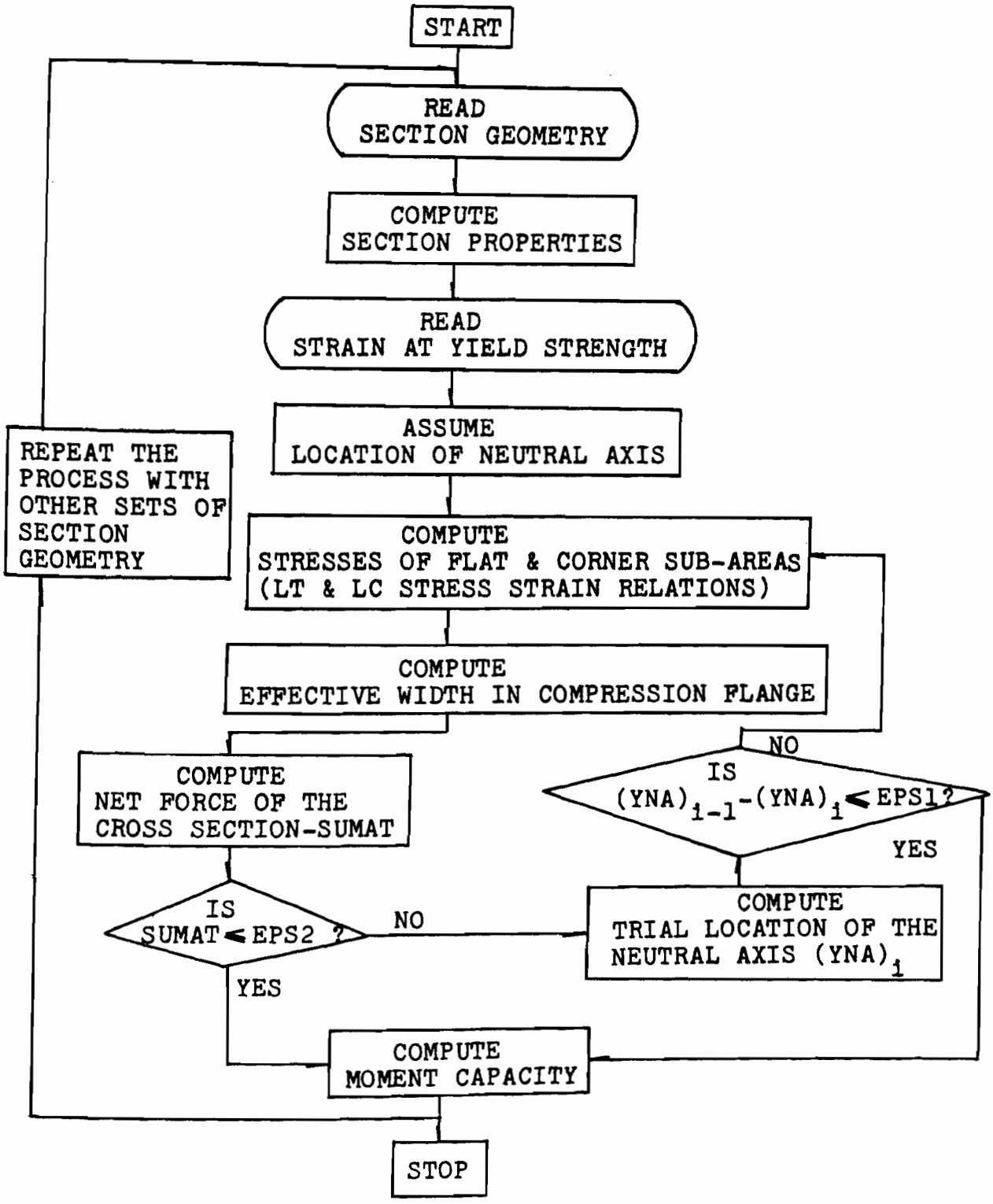

Fig. 5-3 FLOW CHART FOR MOMENT CAPACITY CALCULATIONS

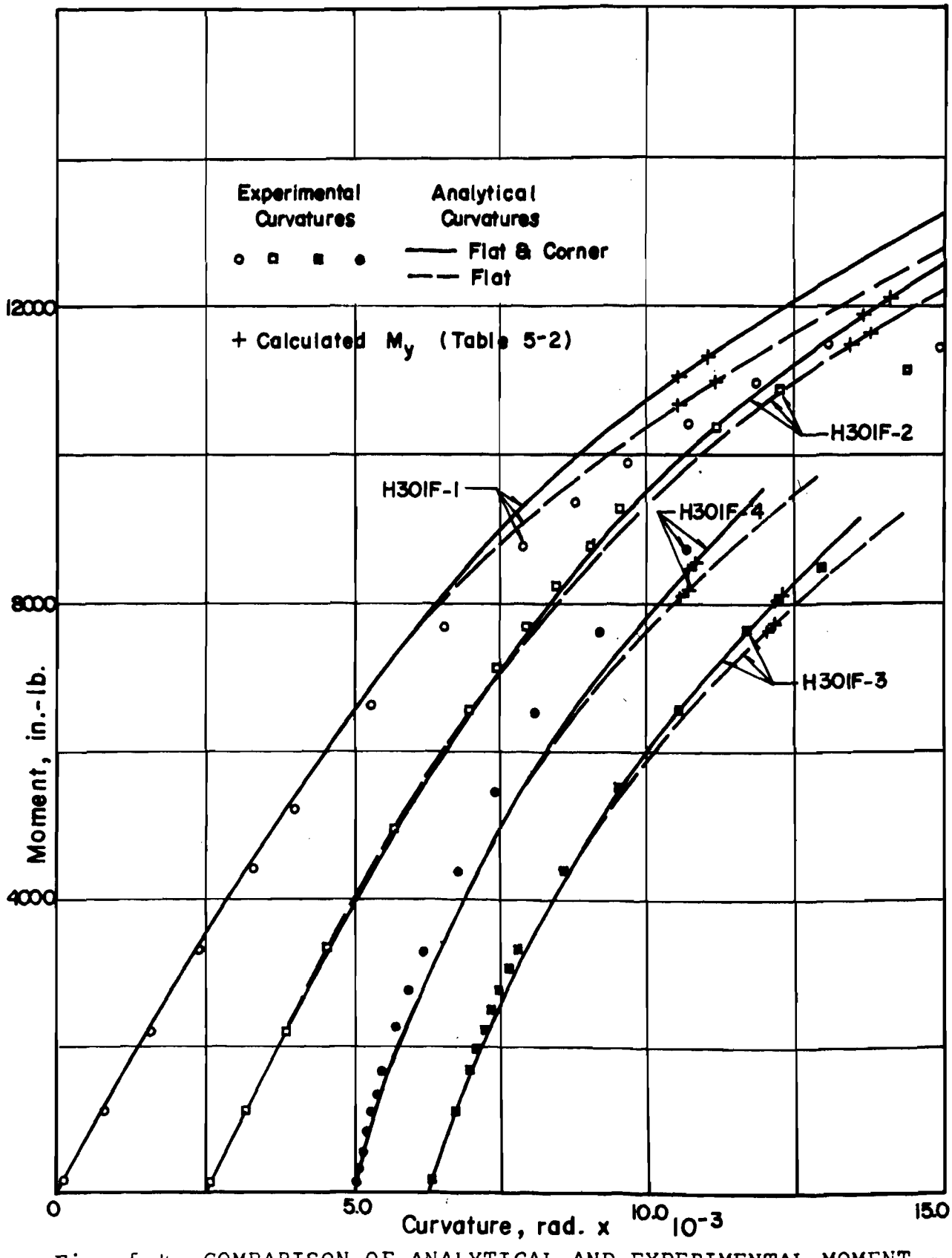

Fig. 5-4 COMPARISON OF ANALYTICAL AND EXPERIMENTAL MOMENT - CURVATURE RELATIONSHIPS, SERIES H301F FLEXURAL MEMBERS

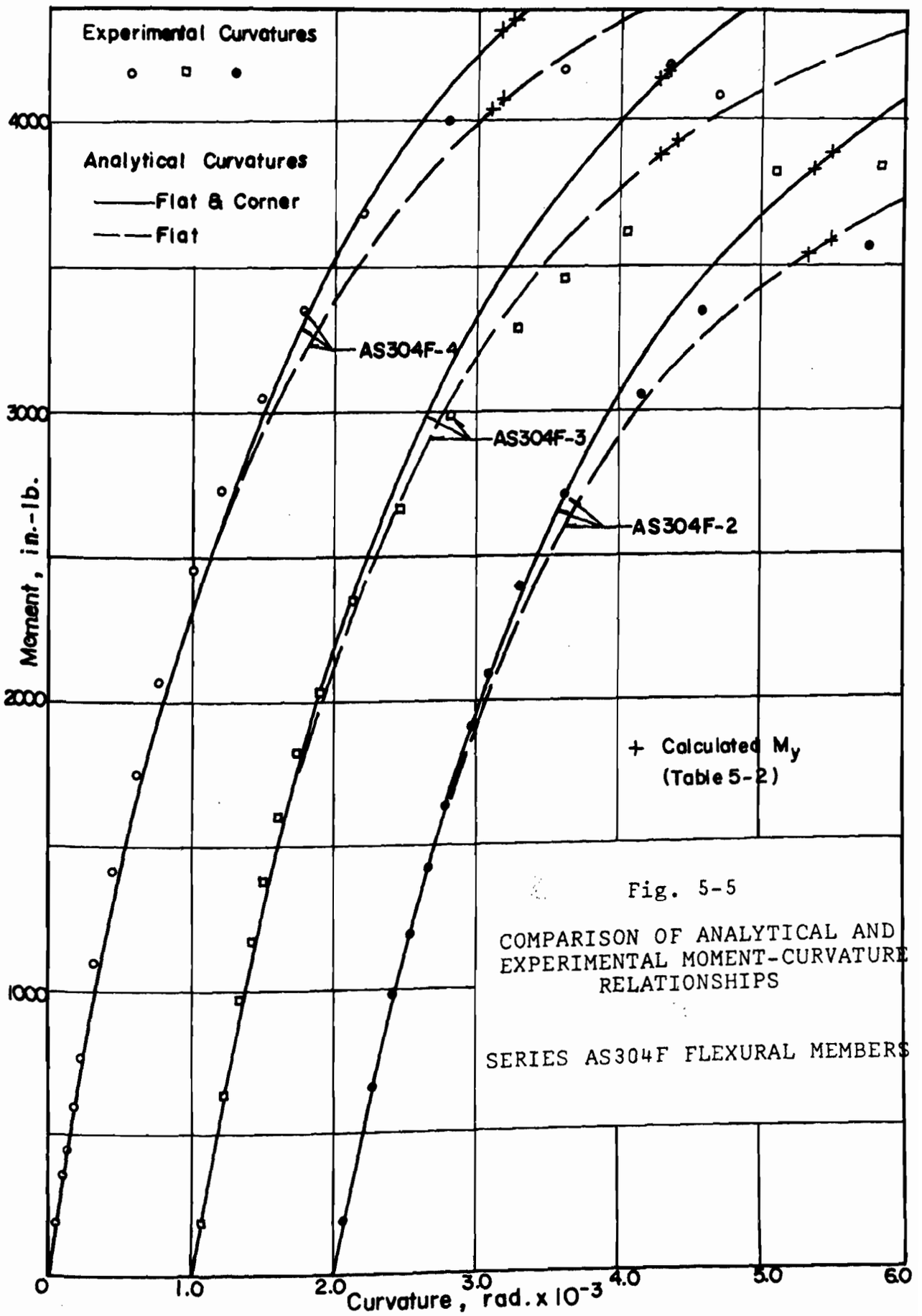

Fig. 5-5

COMPARISON OF ANALYTICAL AND EXPERIMENTAL MOMENT-CURVATURE RELATIONSHIPS

SERIES AS304F FLEXURAL MEMBERS

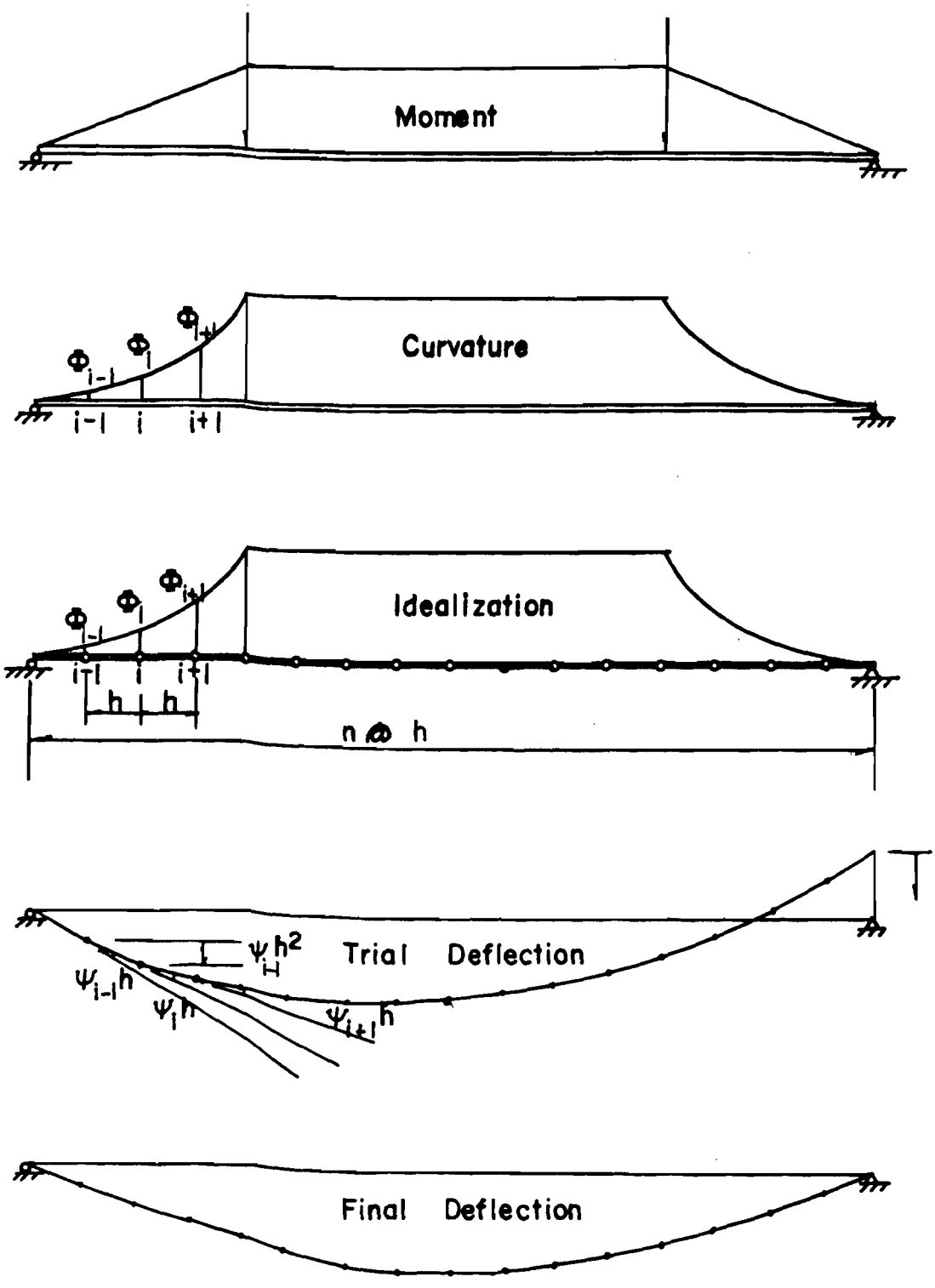

Fig. 5-6 DISCRETE SYSTEM AND INELASTIC DEFLECTION CALCULATIONS

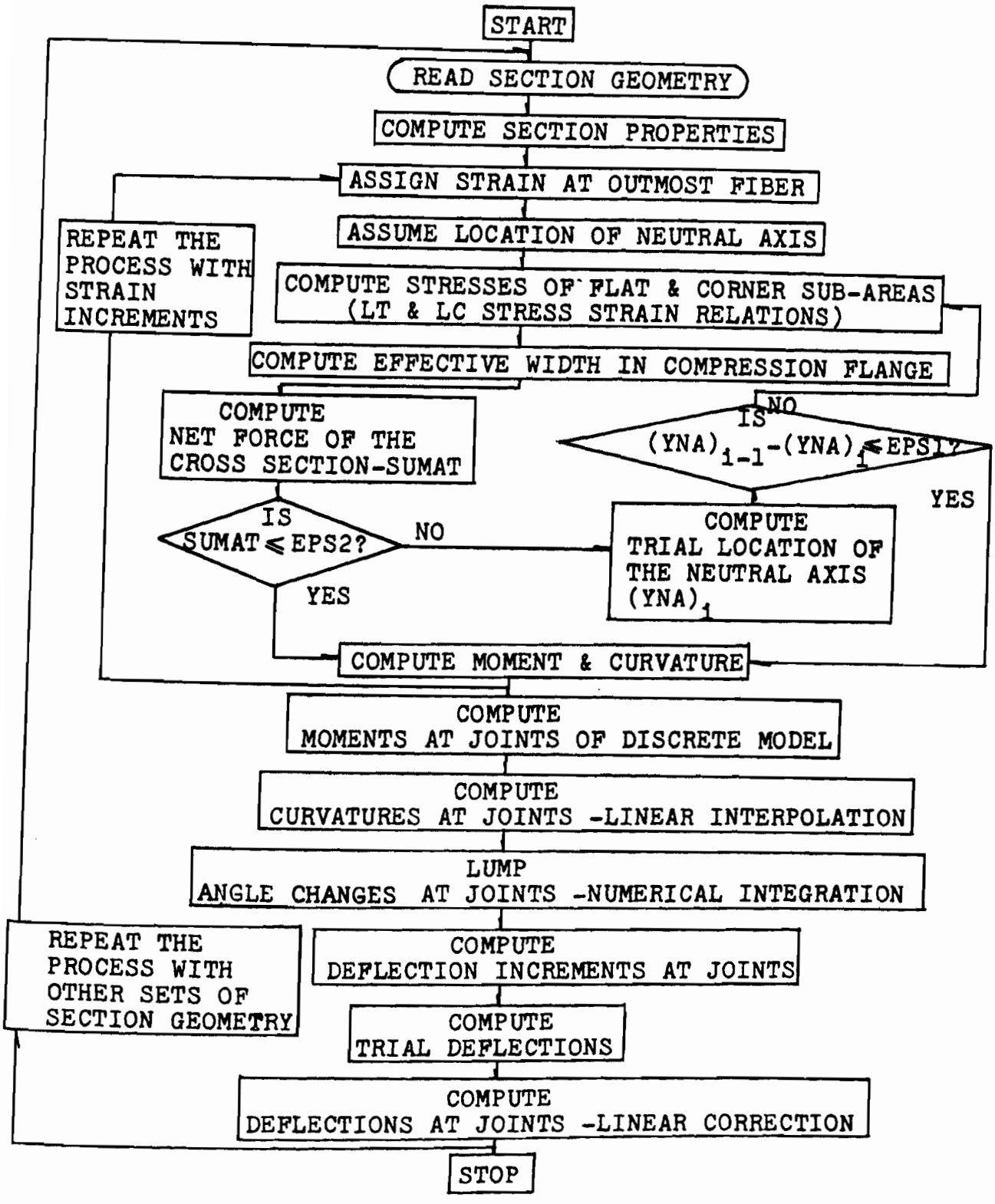

Fig. 5-7 FLOW CHART FOR INELASTIC DEFLECTION CALCULATIONS

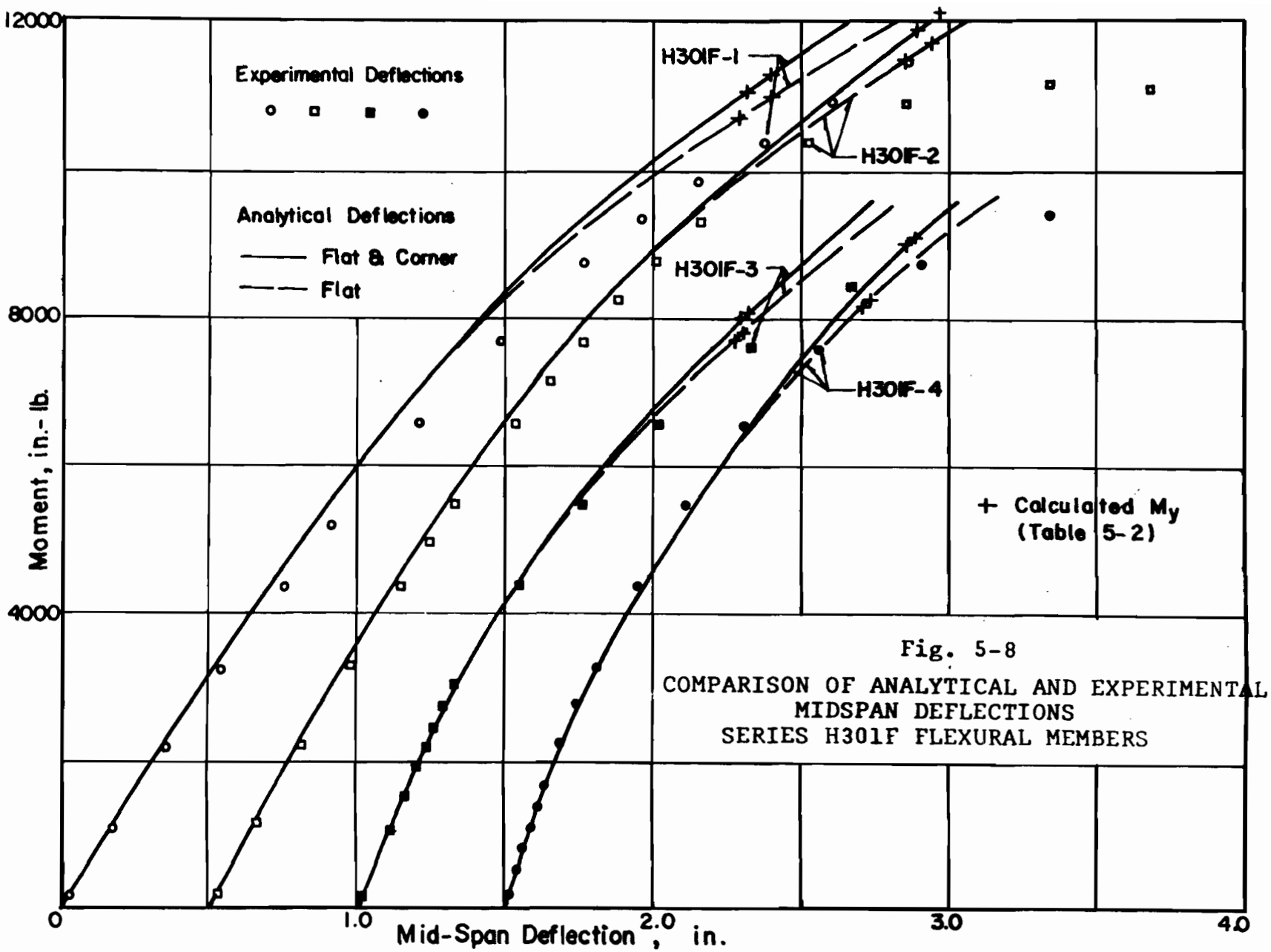

Fig. 5-8

COMPARISON OF ANALYTICAL AND EXPERIMENTAL MIDSPAN DEFLECTIONS SERIES H301F FLEXURAL MEMBERS

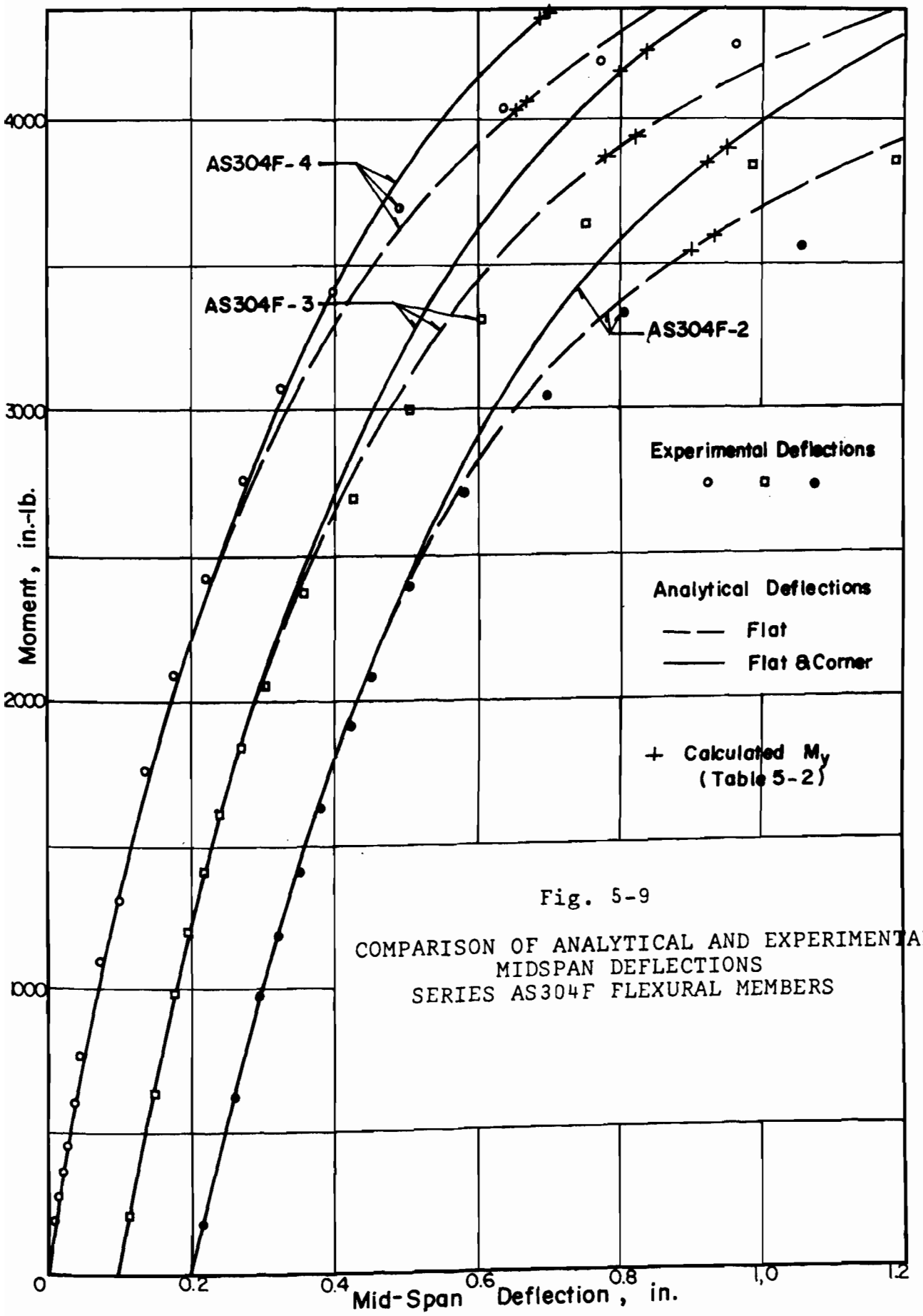

Fig. 5-9

COMPARISON OF ANALYTICAL AND EXPERIMENTAL MIDSPAN DEFLECTIONS SERIES AS304F FLEXURAL MEMBERS

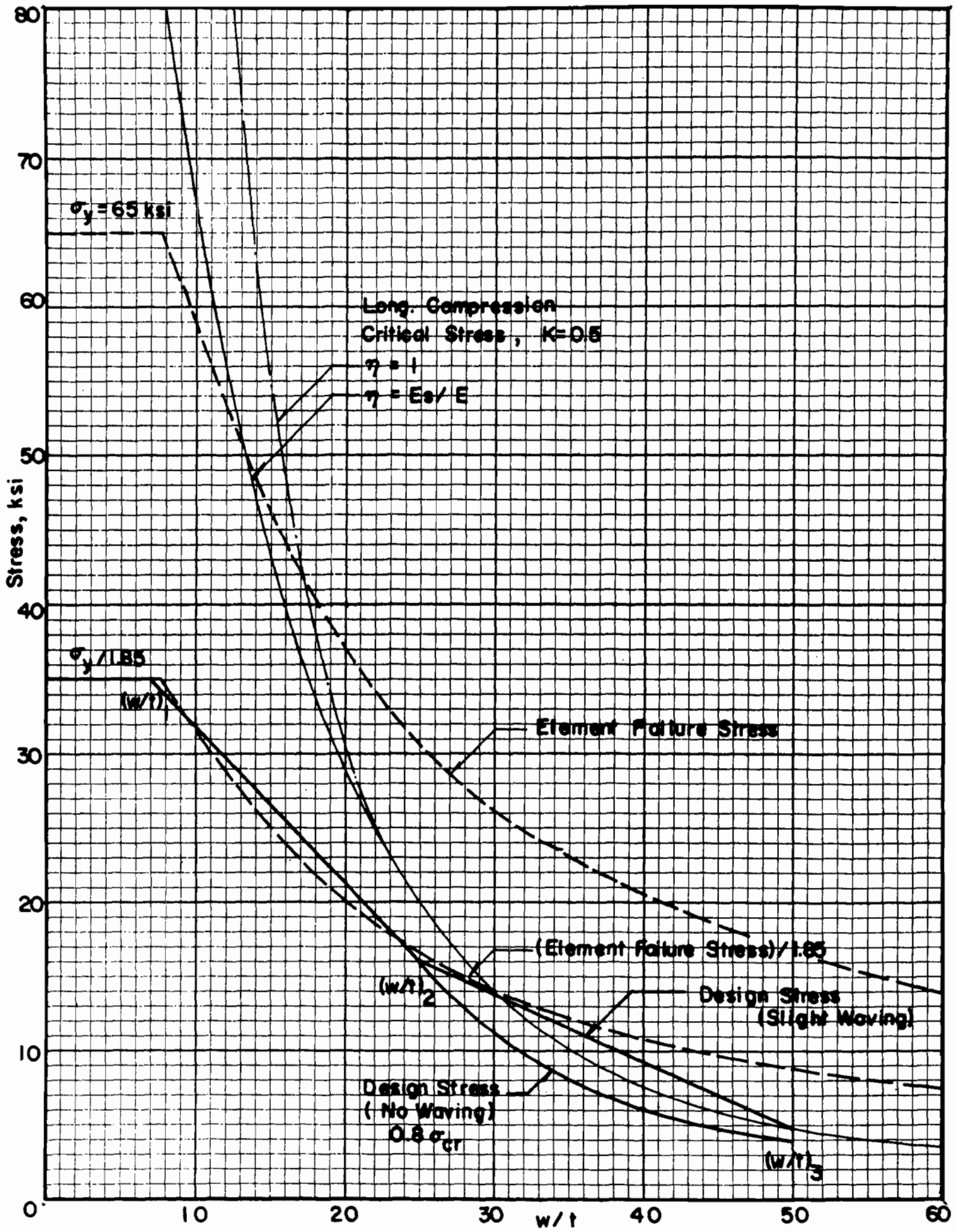

Fig. 6-1 STRESS VS. w/t RATIO - UNSTIFFENED ELEMENTS, TYPE 301 STAINLESS STEEL-1/2 HARD

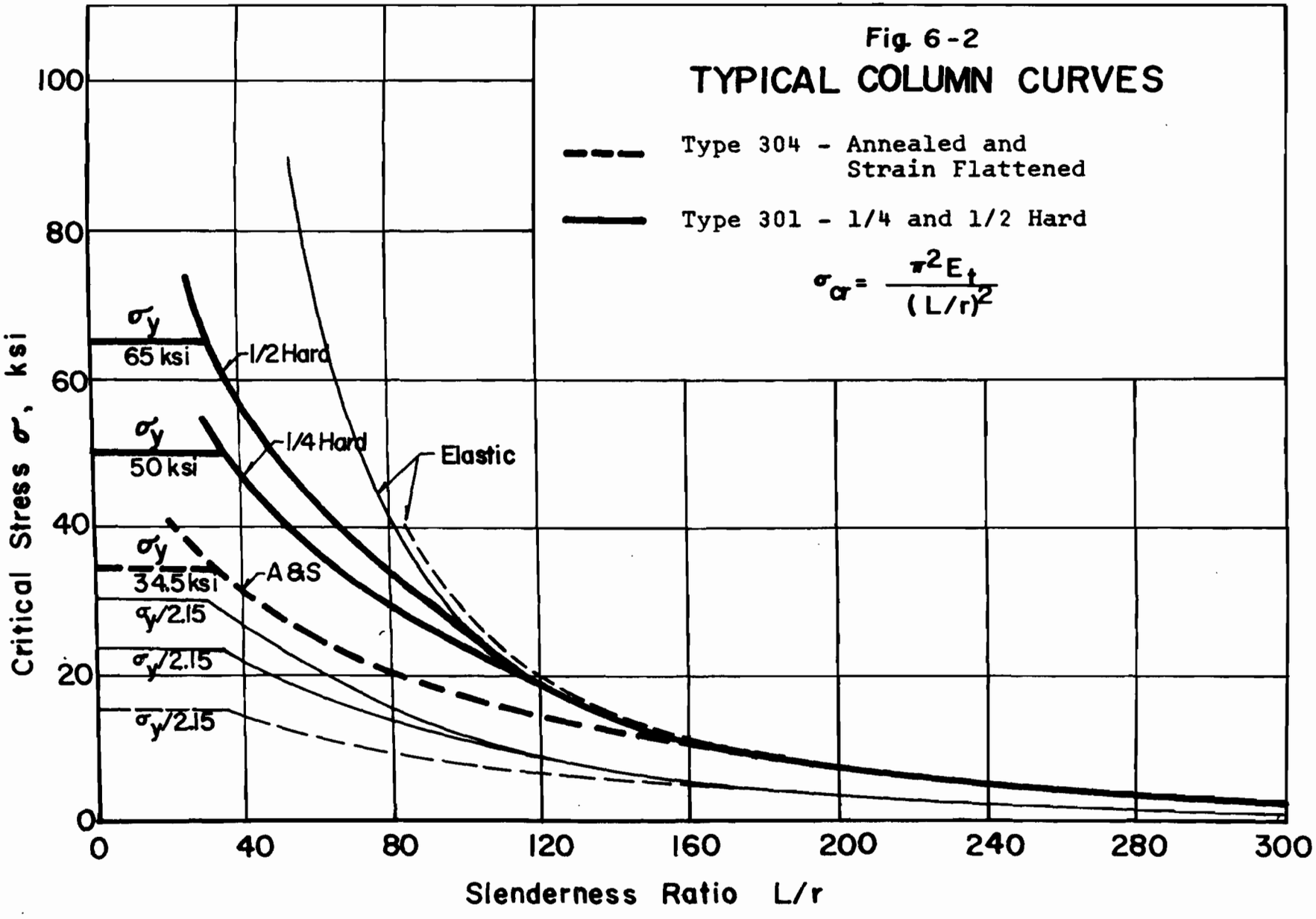
Fig. 6-2
TYPICAL COLUMN CURVES
Type 304 - Annealed and Strain Flattened
Type 301 - 1/4 and 1/2 Hard
$\sigma_{cr} = \frac{\pi^2 E_t}{(L/r)^2}$
Critical Stress σ, ksi
Slenderness Ratio L/r
0
20
40
60
80
100
0
40
80
120
160
200
240
280
300
σy 65 ksi
σy 50 ksi
σy 34.5 ksi
σy/2.15
σy/2.15
σy/2.15
1/2 Hard
1/4 Hard
Elastic
A&S